THE ROLE OF TFEB AND TFE3 IN MEDIATING MITOCHONDRIAL AND LYSOSOMAL ADAPTATIONS IN SKELETAL MUSCLE

ASHLEY N. OLIVEIRA

A DISSERTATION SUBMITTED TO THE FACULTY OF GRADUATE STUDIES IN PARTIAL FULFILLMENT

OF THE REQUIREMENTS FOR THE DEGREE OF

DOCTOR OF PHILOSOPHY

GRADUATE PROGRAM IN KINESIOLOGY AND HEALTH SCIENCE

YORK UNIVERSITY, TORONTO, ONTARIO

OCTOBER, 2022

ABSTRACT

Skeletal muscle adapts to external stimuli to meet metabolic and energetic needs imposed on it. As a highly metabolic tissue, mitochondria are the energetic cores of the cell and are central to the adaptive nature of muscle. Essential to the maintenance of mitochondria is the process of mitophagy, a selective form of autophagy through which damaged mitochondria are removed and degraded via the lysosome. Lysosomes and autophagy machinery are regulated by transcription factors, TFEB and TFE3, that are responsive to cellular stresses including exercise, disuse and starvation. Our work aimed to address the role of TFEB and TFE3 in mediating the adaptability of mitochondria in response to exercise and disuse.

To understand the role of TFEB and TFE3 in mediating the effects of exercise, we employed an *in vitro* model and silenced the expression of TFEB and TFE3. While the absence of TFEB or TFE3 alone impacted the mitophagic response to a single bout of contractile activity, mitochondrial and lysosomal function improved with repeated bouts. These data support the notion that exercise stimulates multifaceted and often redundant signaling pathways to promote adaptations. However, the absence of TFEB and TFE3 together abolished functional mitochondrial and lysosomal adaptations to contractile activity, indicating that both TFEB and TFE3 together are required for adaptations.

We also sought to evaluate the role of TFE3 in atrophic conditions using denervation of the sciatic nerve as a model of disuse in both males and females. Basally, females exhibited increased lysosomal content, higher mitophagy flux and improved mitochondrial function. In response to denervation however, females appeared to preferentially preserve mitochondrial content at the expense of function by reducing mitophagy flux. Curiously, the absence of TFE3

in vivo preserved muscle mass in males and mitochondrial content in both sexes following denervation but this in turn increased mitochondrial dysfunction similar to wildtype females.

The significance of this work is that we provide further evidence of how lysosomes and mitochondrial turnover mediate mitochondrial adaptations to both positive and negative stimuli. Our data also highlight the importance of investigating the effect of biological sex, revealing distinct mitochondrial and lysosomal phenotypes in males and females.

ACKNOWLEDGEMENTS

"The more that you read, the more things you will know. The more that you learn, the more places you will go." - Dr. Seuss

7 years of learning. 7 years of hard work. 7 years of growth. 7 years of memories.

7 years that all began in a fourth-year course on mitochondria. 7 years that all began with one person believing in the potential of a young student. That person was Dr. David Hood. I am forever grateful for that invitation, that opportunity, that leap of faith. You have taught me so much, provided me with so many opportunities, and helped me grow into who I am. Thank you feels insufficient, I just hope I met the potential you saw in me all those years ago.

These 7 years have not always been easy, but I have had the honour and privilege to share that road with great colleagues and even better friends. Jon, you built my foundation, supported me when I stumbled, and I literally could not have done this without you. I am eternally grateful to you and even more grateful that I get to call you a friend. Avi, the friendship we have built over these years is one I will cherish for my lifetime. You are the most supportive, thoughtful and kind person and I only hope I can be the same friend to you that you are to me. Matt, to follow in your footsteps was incredibly motivational and inspiring, you are so brilliant and talented and I am thankful for everything you taught me.

Thank you to all the talented, dedicated and hardworking people I have had the pleasure of working with in the lab both past and present. Thank you for all your help, support and input over the years.

Thank you to my friends and family that have supported me throughout the years. Without each and every one of you, I surely would have failed long ago. Lastly, I would like to thank Ryan. Of all the ways my academic experience has changed my life, the one I am most thankful for is that it brought me to you. You have been my greatest supporter, my greatest friend, a partner in the truest sense. You pick me up when I fall, you cheer me on when I succeed, and you love me for me. You push me to be better each and every day and I hope that I make you proud.

I love you and I dedicate this work to you.

TABLE OF CONTENTS

LIST OF TABLES

LIST OF FIGURES

LIST OF ABBREVIATIONS

	#
ΔΨ	Mitochondrial membrane potential
	A
AA	Amino acid
Ach	Acetylcholine
ADP	Adenosine diphosphate
AICAR	5'-Aminoimidazole-4-carboxamide ribonucleotide
AIF	Apoptosis-Inducing Factor
AKT	Protein kinase B
AMBRA1	Autophagy and beclin 1 regulator 1
AMP	Adenosine monophosphate
AMPK	AMP-activated protein kinase
ANOVA	Analysis of variance
AR	Androgen receptor
ARE	Antioxidant response element
ATF4 / 5	Activating transcription factor 4 and 5
ATFS-1	Activating transcription factor associated with stress-1
Atg	Autophagy related protein
Atgl	Adipose triglyceride lipase
ATP	Adenosine triphosphate
	B
BafA	Bafilomycin A
BCL-2	B-cell lymphoma 2
BDNF	Brain-derived neurotrophic factor
bHLH	Basic helix loop helix
BNIP3L/NIX	BCL2/adenovirus E1B 19-kDa protein-interacting protein 3-like
	C
CAMKII	Ca2+/calmodulin-dependent protein kinase
CARM1	Coactivator-associated arginine methyltransferase 1
CCA	Chronic contractile activity
CHOP	C/EBP homologous protein
CLEAR	Coordinated lysosomal expression and regulation
ClpP	Caseinolytic mitochondrial matrix peptidase proteolytic subunit
COX	Cytochrome c oxidase
COX I / IV	Cytochrome oxidase subunit I and IV
CPN10	10kDa chaperonin, mitochondrial
CREB	cAMP response element binding protein
CS	Citrate synthase
CSA	Cross-sectional area
CtsB	Cathepsin B
CtsD	Cathepsin D
Cyto C	Cytochrome c
	D

DEN	Denervation
Deptor	DEP domain-containing mTOR-interacting protein
DNA	Deoxyribonucleic acid
DRP1	Dynamin-realted protein 1
	E
E1	Estriol
E2	17β-estradiol
E3	estrone
E-box	Enhancer box
EDL	Extensor digitorum longus
eIF2α / B	Eukaryotic initiation factor 2 alpha and B
EM	Electron microscope
ER	Endoplasmic reticulum
ERE	Estrogen response element
ERK	Extracellular signal-regulated kinase 1/2
ERR (α, β, γ)	Estrogen-related receptors (alpha, beta, gamma)
ETC	Electron transport chain
	F
FAD+	Flavin adenine dinucleotide - oxidized
FADH2	Flavin adenine dinucleotide - reduced
FoxO1 / 3	Forkhead box O 1 and 3
FUNDC1	FUN14 domain containing 1
	G
GABARAP	Gamma-aminobutyric acid receptor-associated protein
Gadd45a	Growth arrest DNA damage inducible alpha
GAPDH	Glyceraldehyde-3-Phosphate Dehydrogenase
GATE16	Golgi-associated ATPase enhancer of 16kDa
GCN2	General control nonderepressible 2
GFP	Green fluorescent protein
GLUT(1/ 4)	Glucose transporter (1 and 4)
GPER	G protein-coupled estrogen receptor
Gp78	Glycoprotein 78
GSK	Glycogen synthase kinase
GSK3β	Glycogen synthase kinase-3 beta
GTP	Guanosine triphosphate
	H
H_2O_2	Hydrogen peroxide
HO-1	Heme oxygenase 1
HRP	Horseradish peroxidase
Hsl	Hormone-sensitive lipase
HSP 60 / 70	Heat shock protein 60 and 70
HUWE1	HECT, UBA and WWE domain containing E3 ubiquitin ligase 1
	I
ICU	Intensive care unit
IGF-1	Insulin-like growth factor 1

IL-1	Interleukin-1
IMF	Intermyofibrillar
IMJ	Intermitochondrial junction
IMM	Inner mitochondrial membrane
IMS	Intermembrane space

K

KD	Knockdown
KO	Knockout

L

LAMP	Lysosomal-associated membrane protein
LC3 (I/II)	Microtubule-associated proteins 1a/1b light chain 3 (I and II)
LonP	Lon protease homolog, mitochondrial

M

MAFbx	Muscle atrophy F-box / Atrogin-1
MCAT	Mitochondrial catalase
MCOLN1	Mucolipin 1
MEF2	Myocyte enhancer factor 2
MFF	Mitochondrial fission factor
MFN 1 / 2	Mitofusin-1 and 2
MHC	Myosin heavy chain
MiT	Micropthalmia family of bHLH transcription factors
MITF	Melanocyte inducing transcription factor
MnSOD	Manganese Superoxide Dismutase
MPP	Mitochondrial processing peptidase
MPR	Mannose-6 phosphate receptor
MQC	Mitochondrial quality control
mRNA	Messenger RNA
mt	Mitochondria(l)
MTCO1	Mitochondrially encoded cytochrome c oxidase 1
mtDNA	Mitochondrial DNA
mTORC1	Mechanistic/Mammalian target of rapamycin complex 1
mtPTP	Mitochondrial permeability transition pore
MTS	Mitochondrial targeting sequence
Mul1	Mitochondrial E3 ubiquitin ligase 1
MuRF1	Muscle ring finger 1

N

NAD+	Nicotinamide adenine dinucleotide - oxidized
NADH	Nicotinamide adenine dinucleotide – reduced
NADPH	Nicotinamide adenine dinucleotide phosphate
NDP52	Calcium binding and coiled-coil domain 2 (also known as Calcoco2)
NF-κB	Nuclear factor kappa-light-chain-enhancer of activated B cells
NLRX1	Nod-like receptor X-1
NLS	Nuclear localization signal
NMJ	Neuromuscular junction
NOX	NADPH oxidase

NRF-1 / 2	Nuclear respiratory factor-1 and 2
NuGEMPs	Nuclear genes encoding mitochondrial proteins
	O
$O_2^{\bullet-}$	Superoxide
Ob/Ob	Genetically obese (leptin deficient mouse model)
OCR	Oxygen consumption rate
OE	Overexpress
OMM	Outer mitochondrial membrane
OPA1	Optic atrophy 1
OXPHOS	Oxidative phosphorylation
	P
p38 MAPK	38kDa mitogen-activated protein kinase
p53	Tumor Suppressor protein 53
p62/SQSTM1	Sequestosome 1
P70S6K1	Ribosomal protein S6 kinase beta 1
PARL	Presenilins-associated rhomboid-like protein
PDK1	Pyruvate dehydrogenase kinase isoform 1
PE	Phosphatidylethanolamine
PGC-1α / β	PPAR gamma coactivator 1 alpha and beta
P_i	Inorganic phosphate
PI(3)P	Phosphatidylinositol 3-phosphate
PI3K	Phosphatidylinositol-4,5-bisphosphate 3-kinase
PIM	Protein import machinery
PINK1	PTEN-induced kinase 1
PPAR(α/ β/ γ)	Peroxisome proliferator-activated receptor (alpha, beta, gamma)
PTEN	Phosphatase and tensin homolog
	Q
qPCR	Quantitative polymerase chain reaction
	R
REDD1/2	Regulated in development and DNA damage responses 1 and 2
RNA	Ribonucleic Acid
ROS	Reactive oxygen species
RyR	Ryanodine receptor
	S
Scr	Scrambled siRNA
SDH	Succinate dehydrogenase
SDS-PAGE	Sodium dodecyl sulfate polyacrylamide gel electrophoresis
SERCA	Sarco/endoplasmic reticulum Ca^{2+}-ATPase
SirT1 / 3	Sirtuin 1 and 3
SNARE	SNAP receptor
SOD2	Superoxide dismutase 2, mitochondrial
SR	Sarcoplasmic reticulum
SS	Subsarcolemmal
SS-31	Szeto-Schiller peptide, aka Elamipretide, or Bendavia

STAT3	Signal transducers and activators of transcription 3
	T
TA	Tibialis anterior
TBC1D1	TBC1 domain family member 1
TCA	Tricarboxylic acid cycle
TD	Transactivation domain
TFAM	Mitochondrial transcription factor A
TFB2M	Transcription factor B2, mitochondrial
TFE3	Transcription factor E3
TFEB	Transcription factor EB
TFEB-S	Small transcription factor EB
TFEC	Transription factor EC
TGN	Trans-Golgi network
TIM	Translocase of the inner membrane
TOM	Translocase of the outer membrane
TNFα	Tumor necrosis factor alpha
TSC1 / 2	Tuberous sclerosis proteins 1 and 2
TT	Transverse tubule
TTX	Tetrodotoxin
TWEAK	TNF-like weak inducer of apoptosis
	U
Ub	Ubiquitin
ULK1/2	Unc-51 like kinase 1/ 2
uORF	Upstream open reading frame
UPR	Unfolded protein response
UPRmt	Mitochondrial unfolded protein response.
UPS	Ubiquitin proteasome system
UQCRC2	Ubiquinol-cytochrome c reductase core protein 2
USF-1	Upstream stimulatory factor 1
	V
vATPase	Vacuolar-type ATPase
VDAC	Voltage dependent anion channel
VEH	Vehicle
	Z
ZIP	Leucine zipper

CHAPTER ONE:

INTRODUCTION

With ever growing advancements in technology and medicine, we as a population are experiencing longer and less labour-intensive lives. However, some argue that the cost of this lifespan extension is the increasing prevalence of metabolic diseases such as cardiovascular disease, cancer, type 2 diabetes, and neurodegenerative diseases. While inevitable, aging is a major risk factor for many of these, and it is estimated that by 2068, up to 30% of the Canadian population will be 65 or older[1]. This is compounded by a rise in obesity, as StatsCan postulates that 27% of the Canadian population currently is clinically obese[2]. Advancements in automation and overall declines in the labour sector contribute to the prevalence of sedentarism, and feed into the pervasiveness of obesity within our society. As such the maintenance of health and vitality throughout the lifespan is critical. While keeping an active lifestyle is an excellent way to promote healthspan, this positions skeletal muscle as an intriguing target tissue in the prevention of metabolic diseases.

Skeletal muscle comprises roughly 30-40% of body mass in a lean individual and is a highly metabolic tissue[3]. While often reduced to its role in locomotion, skeletal muscle is integral to the maintenance of whole-body metabolism and is critical to the preservation of quality of life[4]. A key feature of skeletal muscle is its plasticity, which allows it to adapt to external stimuli and meet metabolic demands. The adaptability of skeletal muscle underlies the beneficial effects of exercise, but also contributes to the negative repercussions of sedentarism and aging. While regular exercise promotes an oxidative phenotype within muscle that supports

positive changes in whole body metabolism, chronic disuse leads to losses in muscle mass and function and declines in metabolism. Central to the adaptive nature of skeletal muscle are mitochondria, the metabolic hub within the cell.

Similar to skeletal muscle, mitochondria are highly dynamic organelles that adapt to meet the needs of the cell. While mitochondria are fundamentally sites of energy production, they also participate in cellular signaling, oxidative stress, Ca^{2+} handling and apoptosis or cell death[5]. Mitochondrial content and function are maintained through the collaboration of processes that are collectively known as mitochondrial quality control (MQC). Essential to MQC is the process through which damaged organelles are removed and degraded, which is known as mitophagy, a selective form of autophagy. As dysfunctional mitochondria negatively impact cellular health through poor energy production and augmented oxidative stress, mitophagy is a pro-survival mechanism that recycles damaged organelles into their basic components to support future protein synthesis. Essential to the process of mitophagy are lysosomes, the degradative site within the cell. Lysosomes are highly acidic organelles replete with enzymes capable of breaking down proteins, lipids, carbohydrates and DNA. These organelles are regulated by a family of transcription factors, including TFEB and TFE3[6,7]. TFEB and TFE3 also participate in the regulation of autophagy machinery, and are highly sensitive to a variety of cellular stresses including exercise, disuse and starvation[8]. These transcription factors are essential for mounting a pro-survival response to starvation. The role of TFEB and TFE3 in mediating the adaptability of mitochondria in response to stress remains to be examined.

In the event that poor quality mitochondria are not turned over, they can trigger apoptosis or cell death. Exercise is known to improve mitochondrial function, not only through an increase in the synthesis of mitochondria (mitochondrial biogenesis), but also through the

culling of damaged organelles through mitophagy to optimize the existing pool. In contrast, chronic disuse results in mitochondrial dysfunction which contributes to muscle wasting or atrophy. Thus, understanding the mechanisms involved in the mitochondrial turnover both in positive (exercise) and negative (disuse) conditions can provide valuable insight into skeletal muscle health, and how this contributes the maintenance of healthspan, rather than lifespan.

CHAPTER TWO:

REVIEW OF LITERATURE

1.0 MITOCHONDRIA IN SKELETAL MUSCLE

Skeletal muscle is the largest organ system of the human body comprising roughly 30-40% of a healthy young adult's total body mass[3]. Besides its most obvious role in maintaining posture and locomotion, skeletal muscle is a major contributor to whole body metabolism[9]. It serves as a site for glycogen storage, glucose uptake and utilization, and fat oxidation especially during exercise[4]. Furthermore, the ability of skeletal muscle to respond not only to acute demands, such as during exercise, but also to adapt to chronic stimuli, such as training or disuse, makes skeletal muscle a highly plastic tissue. The dynamic nature of skeletal muscle contributes to the benefits of exercise, but is also a major concern during sedentarism, aging, cancer and various other diseases as deconditioning can occur quite rapidly leading to poor quality of life and health outcomes[5,10]. Central to the overall health of skeletal muscle, as well as its ability to adapt are mitochondria, as these organelles are metabolic cores, signaling hubs, and can even contribute to the regulation of muscle mass. Thus, understanding how mitochondria respond and adapt to stimuli offers insight into the plasticity of skeletal muscle.

1.1 SKELETAL MUSCLE STRUCTURE AND FUNCTION

Skeletal muscle is a highly organized tissue, that is attached to bone through tendons to maintain posture and enable locomotion. As a "layered" tissue, skeletal muscle is bundled into multiple fascicles that house many myofibers (muscle cells), each muscle cell has its own membrane known as the sarcolemma. Beneath the sarcolemma, muscle is organized into

subunits known as myofibrils, which contain the contractile apparatus that is organized into sarcomeres, that repeat along the length of the myofibril[11]. While myofibrils are often depicted as a singular long structure, recent work has actually revealed that they exist in a mesh-like matrix whereby sarcomeres actually split or branch[12,13]. Intriguingly, it appears that the degree of branching is not uniform across all muscles, as more oxidative muscles exhibit branching in over 40% of sarcomeres, while more glycolytic fibers have less[12]. Tightly woven into muscle is a dense network of capillaries which supply the highly metabolic tissue with substrates.

Closely associated with the sarcomere are transverse tubules (TT), and the sarcoplasmic reticulum (SR) which propagate action potentials to elicit contraction. Briefly, muscle contraction is dictated by motor neurons, which innervate hundreds to thousands of fibers, and is referred to as a motor unit. Here, depolarization of the motor neuron leads to the release of the neurotransmitter acetylcholine (Ach), at the neuromuscular junction (NMJ)[14]. Release of Ach, leads to the activation and opening of Na^+ channels allowing the action potential to be propagated along the TT to stimulate the release of Ca^{2+} from the SR through ryanodine receptors (RyR). The influx of Ca^{2+} binds to troponin C, exposing the myosin-binding site on actin, allowing myosin and actin interaction thereby eliciting contraction through a process known as cross-bridge cycling. Ca^{2+} is then taken up by the sarco/endoplasmic reticulum Ca^{2+}-ATPase pump (SERCA) into the SR to allow relaxation[15].

Within skeletal muscle there are different fiber types that are generally classified by the expression of myosin ATPase isoform, and vary in contraction kinetics, and their metabolic characteristics[16–18]. Type I fibers are typically the smallest in cross-sectional area, are easily recruited/excited, possess slow shortening velocities, and are generally fatigue-resistant[19]. Type I fibers are also highly oxidative and possess an abundance of mitochondria (~10%) to support

ATP production, that are organized perpendicular and parallel to the myofibrils[20]. Type II fibers are subdivided into type IIa and type IIx. Type IIx are generally much larger in cross-sectional area, require a large stimulus for depolarization or recruitment, have very fast twitch kinetics, and produce the most force, but are highly susceptible to fatigue. Type IIx fibers largely rely on glycolysis for energy production and have a very low mitochondrial content (~2-3%) and are primarily organized perpendicular to the myofibril[20]. Type IIa fibers are intermediates between type I and type IIx and are generally referred to as fast oxidative fibers.

1.2 Mitochondrial Structure and Function

Within skeletal muscle, mitochondria exist in two distinct subcellular locations; interspersed between the myofibrils are the intermyofibrillar (IMF) mitochondria, and beneath the sarcolemma and adjacent to the nuclei are the subsarcolemmal (SS) mitochondria[21,22]. These pools are morphologically and biochemically different, and support different functions in part due to their location, as SS mitochondria provide energy for membrane and nuclear events, while IMF largely contribute fuel for contraction[23]. It has long be understood that mitochondria exist in a dynamic reticulum, and with recent technology providing the possibility of 3D reconstructions, it is possible to fully appreciate how extensive and complex the reticulum is[24–27]. It has also been revealed that although the two pools are morphologically and biochemically distinct there are connections between SS and IMF mitochondria indicating that these subpopulations are capable of mixing[25].

Mitochondria are double-membranous structures which subdivide the organelle into two separate compartments. The innermost compartment is the matrix, which contains several copies of mitochondrial DNA (mtDNA), transcriptional and translational machinery, TCA cycle enzymes, ATP production enzymes, antioxidants, as well as various chaperones and

proteases to ensure that proteostasis is maintained. The matrix is surrounded by a highly convoluted membrane known as the inner membrane (IMM), and the tight cardiolipin-rich folds of the IMM are termed cristae and help densely pack the complexes of the electron transport chain (ETC) through which oxidative phosphorylation is carried out. The electrochemical gradient, also known as the proton motive force (PMF) is built up through the pumping of protons (H^+) through complexes of the ETC into the intermembrane space (IMS)[28]. This energy is harnessed to produce ATP, but can also impose back-pressure on the ETC driving electron slippage and ROS generation within mitochondria[29]. Encapsulating the IMS is the outer mitochondrial membrane (OMM). Despite being permeable to ions and certain substrates, the OMM houses a number of receptors and channels to help regulate protein import into the mitochondria which is essential as mitochondria heavily rely on the nuclear genome despite having their own genomic material[30,31].

Energy production in the mitochondrion begins with the breakdown of macromolecules into acetyl coenzyme-A, which feeds the tricarboxylic acid (TCA) cycle. The TCA cycle is capable of producing a minimal amount of adenosine triphosphate (ATP), but more importantly provides the reduced substrates nicotinamide adenine dinucleotide (NADH) and flavin adenine dinucleotide ($FADH_2$). NADH is then oxidized into NAD^+ by Complex I, which pumps protons into the IMS and shuttles electrons to Complex III through Coenzyme Q. Complex II oxidizes $FADH_2$ into FAD^+ and shuttles electrons to Complex III in a similar fashion. Complex III then continues to shuttle electrons over to Complex IV through Cytochrome c but is also capable of pumping H^+ into the IMS. Complex IV then oxidizes Cytochrome c, while pumping H^+ into the IMS, and donating the free electron to the final electron acceptor, oxygen to produce water. As such, oxygen consumption is often used as a surrogate for oxidative phosphorylation or

mitochondrial function in general[32,33]. The PMF built up in the IMS is then harnessed by Complex V, which in the presence of ADP dissipates the gradient by allowing protons to flow back into the matrix and produces ATP by combining its precursors ADP and P_i[28,34]. In the absence of ADP, the PMF can exert back pressure on the ETC and cause electrons to prematurely slip off and generate free radicals known as reactive oxygen species (ROS)[29,35,36]. For this reason, mitochondrial ROS production is inherently tied to oxygen consumption and the function of the ETC (Fig. 1). Mitochondria are equipped with antioxidant machinery to convert superoxides into less harmful H_2O_2, namely superoxide dismutase 2 or manganese superoxide dismutase (SOD2) which effectively buffer free radicals in mitochondria[37,38]. Therefore, H_2O_2 is the most common free radical in the matrix, and is often used as a measure of ROS emission[38,39].

1.3 Mitochondrial Life Cycle

Mitochondria are highly dynamic organelles that undergo constant remodeling of the reticulum and undergo turnover once the organelle is no longer viable. Mitochondria are not formed through a *de novo* process but rather are generated through the expansion of the existing reticulum. Through mitochondrial biogenesis, signals largely impinge on the activation of peroxisome proliferator-activated receptor (PPAR)-γ coactivator -1α (PGC-1α), the master regulator of mitochondrial biogenesis (Fig. 1). PGC-1α co-activates a variety of transcription factors including but not limited to nuclear respiratory factor (NRF1; NRF2), PPAR family, and estrogen-related receptors (ERRα/β/γ) to upregulate the expression of nuclear genes encoding mitochondrial proteins (NuGEMPs)[40–43]. Despite containing its own genomic material, mtDNA only encodes 13 proteins, thus mitochondria largely rely on the nuclear genome and these products must then be imported into the organelle in a highly regulated manner[44–46]. Two of the

downstream targets of PGC-1α are mitochondrial transcription factor A and B2, Tfam and TFB2M, which transcriptionally regulate mtDNA[47–49]. Tfam facilitates the recruitment of mtDNA transcription and replication factors thereby upregulating mitochondrially-encoded genes[49–52]. Tumor suppressor protein 53 (p53) has also been shown to play a dual role in regulating both the nuclear and mitochondrial genomes and can further stabilize mtDNA in cooperation with Tfam[53–59]. The expression of the two genomes must be coordinated to achieve stoichiometry and form functioning holoenzymes[60–62].

Mitochondrial biogenesis is an energetically sensitive process. Signals that stimulate mitochondrial biogenesis include the ADP:ATP ratio, NAD^+ levels, ROS and calcium[63–67]. During situations of increased energy demand, such as exercise, ADP:ATP will increase, as will the availability of AMP, causing the activation of AMP-activated protein kinase (AMPK) which has been shown to phosphorylate and stimulate nuclear action of PGC-1α[68–70]. Pharmacological agents such as AICAR and Metformin have been touted as "exercise-mimetics" as these activate AMPK and have been shown to improve mitochondrial quality[71–75]. NAD^+ also serves as a signal for mitochondrial biogenesis, which is sensed by sirtuins (SIRT1, SIRT3) and can deacetylate PGC-1α allowing it to translocate into the nucleus[76–78]. Through SIRT action, resveratrol and nicotinamide riboside, the precursor for NAD^+, have been shown to improve mitochondria, but so far these agents have fallen short of the panacea that is exercise with its wide range of whole-body benefits[76,79–81]. ROS can also stimulate mitochondrial biogenesis in a multi-faceted way through p38 mitogen-activated protein kinase (MAPK) and AMPK[64,82–85] It is highly controversial whether or not the use of supplemental antioxidants prevents exercise-induced benefits, however some groups have shown that external antioxidant intake blunts adaptations to exercise as ROS are major signaling molecules within the cell[86,87]. During muscle

contraction, Ca^{2+} is released to support myosin-actin crossbridge cycling, and these influxes of Ca^{2+} have been shown to activate Ca^{2+}/calmodulin-dependent protein kinase, CaMK, and Calcineurin, and in turn PGC-1α[88–92]. Despite the fact that many of the signaling cascades described here converge on PGC-1α, it is not actually required for mitochondrial biogenesis. While basally, animals lacking PGC-1α do exhibit mitochondrial impairments, young mice are capable of improving both mitochondrial content and function following exercise training[93–99].

The mitochondrial reticulum is in constant flux, as the network continuously undergoes events of fusion and fission (Fig. 1). Fusion is the process through which mitochondria can be added to the reticulum. This is largely carried out by mitofusin-1 and -2, (Mfn1, Mfn2) and optic atrophy 1 mitochondrial dynamin-like GTPase (OPA1) which aid in the fusion of the outer and inner membranes respectively[100,101]. A large network with a high level of branching is indicative of healthy mitochondria and is a common characteristic following exercise training.

This allows for substrate sharing, energy distribution, effective communication, and can also help buffer transient defects[102–105]. Fission on the other hand is the process through which portions of the mitochondrial reticulum are excised and carried out by dynamin-related protein 1(Drp1) encircling the mitochondria and recruiting factors such as mitochondrial fission protein 1 (Fis1) and mitochondrial fission factor (Mff) to constrict and pinch the organelle from the reticulum. These events can occur in healthy portions of the network, or in damaged areas, ultimately facilitating their removal and degradation[106,107]. Fission events that occur in healthy portions of the reticulum are carried out by Drp1 and Mff and occur in contact with the ER[107–110]. While fission events that take place in dysfunctional areas are dependent on Drp1 and Fis1 and happen in close proximity to the lysosome. This is usually an asymmetrical division, in which the smaller damaged portion is excised to limit the spread of free radicals and membrane

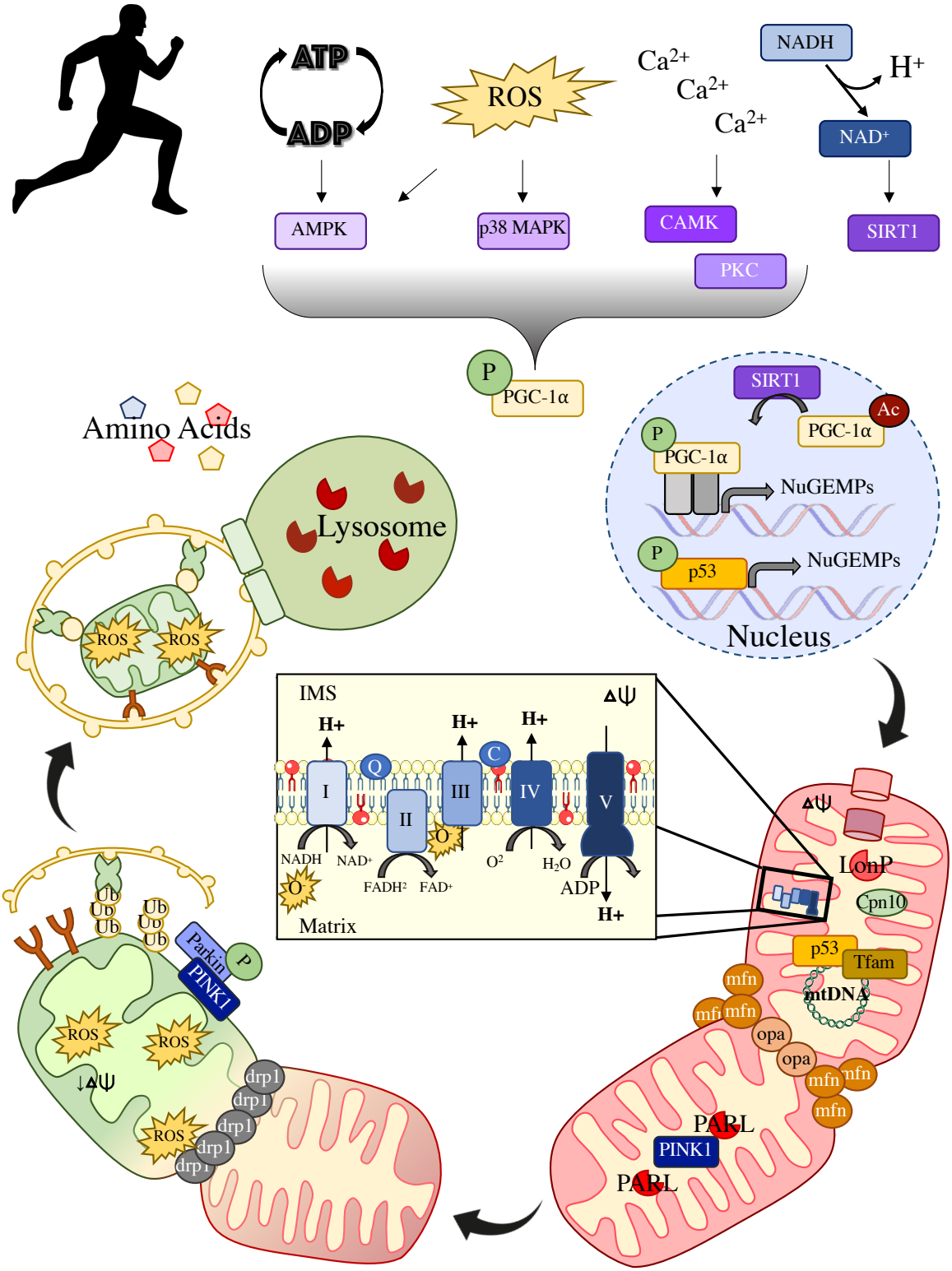
ATP
ADP
ROS
Ca2+
Ca2+
Ca2+
NADH
H+
NAD+
AMPK
p38 MAPK
CAMK
PKC
SIRT1
P
PGC-1α
Amino Acids
Lysosome
SIRT1
Ac
PGC-1α
P
PGC-1α
NuGEMPs
P
p53
NuGEMPs
Nucleus
ROS
ROS
IMS
ΔΨ
H+
H+
H+
Q
C
I
II
III
IV
V
NADH
NAD+
FADH2
FAD+
O2
H2O
ADP
H+
Matrix
ΔΨ
LonP
Cpn10
p53
Tfam
mtDNA
mfn
mfn
mfn
opa
opa
mfn
mfn
mfn
PARL
PINK1
PARL
Ub
Ub
Ub
Ub
Ub
Ub
Parkin
P
PINK1
ROS
ROS
↓ΔΨ
ROS
drp1
drp1
drp1
drp1
drp1

Figure 1: Mitochondrial life cycle. Mitochondrial biogenesis is the process through which mitochondria are synthesized, and is stimulated though a variety of signals, often seen with exercise, such ATP turnover, reactive oxygen species, influxes of calcium, and increases in NAD+. These signals all converge on PGC-1α, widely regarded as the master regulator of mitochondrial biogenesis, as PGC-1α co-activates a number of transcription factors that upregulate nuclear genes encoding mitochondrial proteins. However, PGC-1α is not the sole regulator as other transcription factors have been shown to regulate NuGEMPs as well such as tumor suppressor protein, p53. Since mitochondria also contain their own genomic material, mtDNA, transcription factors such as Tfam and p53 can bind to the D-Loop to upregulate the expression of mitochondrial-encoded proteins. Since mitochondrial biogenesis is not a *de novo* process, but rather an expansion of the existing reticulum, nascent mitochondrial proteins need to be imported into mitochondria and incorporated with mitochondrial encoded proteins to form holoenzymes. For this reason, import and proteostasis are highly regulated within mitochondria. In instances of proteotoxic stress such as protein misfolding or orphaned subunits, mitochondria are equipped with chaperones and proteases, like LonP and Cpn10 to maintain stoichiometry and proteostasis. The reticulum can also be expanded through events of fusion, whereby mitofusins tether and ligate outer membranes, while OPA1 fuses the inner membrane. A highly fused and interconnected reticulum allows for substrate sharing, and efficient ATP production. ATP production is carried out primarily through oxidative phosphorylation via the electron transport chain found on the inner mitochondrial membrane. Here substrates are oxidized, and protons are pumped through the inner membrane to the IMS, building up an electrochemical gradient. Electrons flow through the complexes of the ETC, to meet the final electron acceptor, oxygen, forming water. Complex V, or ATP synthase, harnesses the energy of the electrochemical gradient and allows protons to flow back into the matrix and this energy is used to generate ATP. A consequence of the ETC is the production of reactive oxygen species (ROS), as electrons can prematurely slip and generate superoxides, which can damage the organelle if ROS are produced in excess or not scavenged. Dysfunctional portions of the reticulum can be excised from the network through fission. Fis1 on the mitochondrial membrane recognizes and binds Drp1, which encircles and constricts the mitochondrion to separate the dysfunctional organelle from the network. Under basal conditions, PINK1 is imported into the matrix and degraded by PARL, thereby constantly monitoring mitochondrial health. As damaged mitochondria often exhibit a loss in membrane potential, increased ROS emissions, and ATP depletion, these signals inhibit import, thus causing PINK1 to accumulate on the outer membrane. PINK1 can then activate Parkin, which polyubiquitinates outer mitochondrial proteins which serve as a signal and recruit an autophagosome. The autophagosome is tethered to the ubiquitin chains through adaptor proteins and encircles the damaged organelle. Once fully engulfed, the autophagosome travels along microtubule tracts to the lysosome where the cargo is degraded into basic cellular constituents, this process is known as mitophagy. Amino acids are then exported back into the cytosol to support future protein synthesis.

depolarization, and then targeted for degradation via the lysosomes, through the process of mitophagy[107,111,112].

Mitophagy is a selective form of autophagy, which is a broad term for the cellular recycling of damaged components into basic constituents carried out by the lysosomes. Most autophagy-related pathways share similar initiation, nucleation and elongation steps to generate an autophagosome, which is a membranous structure that engulfs dysfunctional cargo (Fig. 4, discussed further in Section 2.2). Initiation requires the activation of the Unc-51 like autophagy activating kinase (ULK1) complex which in turn activates the Beclin-1 complex[113,114]. Nucleation involves the production of the phospholipid, phosphatidylinositol phosphate (PI(3)P), which is a major component of the lipid membrane of the autophagosome[114–116]. The autophagosome is then elongated through a series of autophagy-related gene (ATG) mediated steps to lipidate and activate microtubule-associated proteins 1A/1B light chain (LC3) into LC3-II, as well as gamma-aminobutyric acid receptor-associated protein (GABARAP) and golgi-associated ATPase enhancer of 16kDa (GATE16)[117–120]. The autophagosome engulfs the damaged cargo and is transported to the lysosome via microtubule tracts. Fusion of the autophagosome to the lysosome is supported by SNARE proteins and lysosomal-associated membrane protein, LAMP, to allow the contents of the autophagosome to be degraded by the lysosome. The process of autophagy is critical for the maintenance of a healthy skeletal muscle.

1.4 Mitochondria as Regulators of Skeletal Muscle

As skeletal muscle is a highly metabolic tissue it relies heavily on the energy provided by mitochondria to support its function. This is evident in models of severe mitochondrial dysfunction, such as that in animals lacking PGC-1α, which exhibit poor exercise performance and are prone to fatigue[121]. Mitochondrial dysfunction, if not addressed can lead to

mitochondrially-mediated apoptosis or cell death. Events such as influxes of mitochondrial Ca^{2+} and oxidative stress can promote the opening of the mitochondrial permeability transition pore (mtPTP) resulting in the release of apoptotic factors such a apoptosis inducing factor (AIF) and cytochrome c into the cytosol[122–126]. The presence of these factors outside of mitochondria can initiate caspase cascades which culminate in DNA fragmentation and nuclear decay. Since skeletal muscle cells are multinucleated, this may not result in the death of the entire fibre but will cause localized atrophy which can expand and cause apoptosis and necrosis of the rest of the cell, contributing to muscle atrophy commonly seen with disuse and aging[127,128]. Thus, the maintenance of mitochondria within skeletal muscle has implications for function, as well as muscle mass[129].

1.5 Estrogen as a Mitochondrial Regulator

Recently there has been a significant shift in the literature towards understanding the role of biological sex in physiological and pathological conditions, as biological sex, and perhaps estrogen specifically, have significant implications. Perhaps the most striking is that the incidence of stroke and cardiovascular disease are more prevalent in men than women, but only until menopause, after which the incidence rate is much higher in females. Although not the focus of this review of literature, it provides an example of the importance of understanding the role of sex and sex hormones in physiology.

Estrogen, the dominant sex hormone present in females, is a category of 18-carbon corticosteroids released by the ovaries in females, and to a lesser extent by the testes in males[130]. 17β-estradiol (E2) is the most common and most potent, while estriol (E1) and estrone (E3) are present at lower levels[130]. As the majority of the literature focuses on 17β-estradiol this will be interchangeably referred to as estrogen. There are 3 main estrogen receptors (ER), including

ERα, ERβ and G protein-coupled estrogen receptor (GPER), which dimerize upon ligand binding to transcriptionally regulate estrogen response elements (ERE) in the genome[131]. Estrogen is critical for skeletal muscle homeostasis and mitochondrial maintenance as ERα can transcriptionally regulate NuGEMPS, PGC-1α, and can translocate into the mitochondrial matrix to regulate mtDNA[131]. As such it has been previously shown that females have increased mitochondrial mass, oxidative capacities, lipid oxidation, and better Ca^{2+} handling, contributing to improved endurance capacity and fatigue resistance in comparison to males [132–140]. Although, this increased oxidative capacity is not always observed in humans[141–143], which may be attributed to other confounding variables. Muscle specific deletion of ERα results in mitochondrial dysfunction, characterized by reduced oxygen consumption, increased ROS, impaired morphology and poor mitochondrial turnover[144]. Thus, this illustrates the importance of estrogen and ER in the maintenance of mitochondria in skeletal muscle.

Aside from its role in mediating gene expression, estrogen can also regulate mitochondria in other ways. Estrogen is heavily implicated in oxidative stress and ROS generation, and females exhibit less ROS emission in comparison to males, a phenomenon which is also seen in humans[130,143–145]. Transcriptionally, estrogen can promote the expression of antioxidants such as MnSOD and HO-1, through the activation of CREB[145]. Moreover, estrogen itself acts as an antioxidant by scavenging free radicals[130,146,147]. There is also evidence that upon translocation into the mitochondrial matrix, ERs can interact with ETC subunits to reduce ROS production[145,148–150]. Furthermore, due to its cholersterol-like structure, 17β-estradiol can imbed itself into mitochondrial membranes[151,152] thereby improving the integrity of the membrane and reducing H_2O_2 emission[152]. Thus, it is clear that the role of sex, and

specifically estrogen, is critical in the maintenance of mitochondria basally and understanding the impact of sex in pathological conditions may be key in sex-specific therapeutic approaches.

2.0 Mitochondrial Turnover and Lysosomes

2.1 Lysosome Structure and Function

Lysosomes are membrane-bound organelles that are highly acidic with a typical pH 4.5-5.5, which is required for proper lysosome function[153]. Vacuolar-type ATPase, v-ATPase, hydrolyzes ATP to pump protons against their gradient into the lysosomal lumen to maintain this acidic environment[154,155]. Ca^{2+} is also critical for the acidification of the lysosome, but also has other roles in mediating the fusion with endosomes, autophagosomes and the plasma membrane, as well as the formation of ER-contact sites[8]. The lysosomal lumen contains a heterogenous array of >60 acid hydrolases that enable the breakdown of macromolecules, including proteins, lipids, carbohydrates and nucleic acids[8,156,157]. These cellular components are degraded into building blocks, such as amino acids, to maintain cellular homeostasis.

Lysosomal biogenesis is a coordinated process that requires both the synthesis of lysosomal proteins, as well as endosome-lysosome trafficking (Fig. 2). Most lysosomal hydrolases are tagged with mannose-6-phosphate in the ER, and trafficked to the Golgi[158]. Here, the mannose-6-phosphate is phosphorylated and recognized by mannose-6-phosphate receptors (MPR) and packaged into vesicles in the *trans*-Golgi network (TGN) to be delivered to early endosomes[158,159]. Within the early endosome, the MPR complex is removed and recycled back to the TGN. The early endosome matures into a late endosome and the hydrolases are delivered to the lysosome through brief interactions known as the "kiss and run" mechanism[159,160]. Alternatively, fusion of the endosome and lysosome can also occur through SNARE proteins and the release of Ca^{2+}, generating a hybrid organelle in which the majority of the cargo is

degraded[8,161]. Lysosomal hydrolases can also be delivered in an indirect method, which involves them being taken to the plasma membrane and undergoing endocytosis and delivery to an early endosome[158]. Moreover, the composition of the lysosomal membrane is even more diverse, as it houses 1) an array of transporters that facilitate the export of cholesterols, sugars, nucleosides, and amino acids; 2) proteins that facilitate organelle fusion and contact such as SNARE proteins, tethering factors and GTPases; 3) motor adaptors that facilitate lysosomal movements; and 4) signaling complexes[8].

2.1.1 Transcriptional Regulators: MiT Family

The microphthalmia (MiT) family are basic helix-loop-helix leucine zipper transcription factors comprised of TFEB, TFE3, MITF and TFEC[162]. The members of the MiT family are structurally very similar, except TFEC which lacks a transactivation domain, and acts as a transcriptional repressor of its dimerization partner[163]. Dimerization is required for the recognition of the palindromic E-box elements (CANNTG)[162]. TFEB is often regarded as the master regulator of lysosomal biogenesis as it was first discovered to regulate lysosome- and autophagy-related genes in response to starvation, by binding coordinated lysosome expression and regulation (CLEAR) elements (GTCACGTGAC) on the genome[6,164]. Indeed, the overexpression of TFEB is sufficient to increase lysosomal content and promote autophagy[165,166]. In contrast, lack of TFEB does reduce lysosomes, but this does not have an impact on autophagosome formation or on autophagy basally. However, it is required for stress-induced responses specifically in the context of starvation[167]. In line with these findings, redundant roles have been described for TFE3 and MITF in binding the same CLEAR network supporting the idea of compensation amongst the MiT family[168–170]. Similar to TFEB, the loss of TFE3 does not result in a lysosomal or autophagy impairment basally but is required for

stress-induced lysosomal and autophagic responses and its overexpression is sufficient to stimulate autophagy and lysosomal biogenesis[169] Despite being expressed in all human tissues, MITF is predominantly found in retinal pigment epithelium (RPE), osteoclasts, melanocytes and a variety of immune cells[170–173]. Thus, TFEB and TFE3 have been the focus of the majority of emerging literature with respect to autophagy and lysosomes.

2.1.2 Regulation of TFEB and TFE3

Basally both TFEB and TFE3 are kept inactive in the cytosol but are responsive to a variety of cellular stresses (Fig. 2). Mechanistic target of rapamycin complex 1 (mTORC1) links nutrient deprivation to lysosomal biogenesis and the stimulation of autophagy, as it is optimally positioned on the lysosomal membrane to sense amino acid availability[174–176]. Under nutrient rich conditions, mTORC1 is activated by small Rag GTPases and Rheb present on the lysosomal membrane, allowing mTORC1 to phosphorylate TFEB on Ser^{142} and Ser^{211}, and Ser^{321} on TFE3[177–181]. The Rag GTPases can also recruit the MiT family to the lysosomal membrane to facilitate mTORC1 phosphorylation, which provides a docking/binding site for chaperone 14-3-3 thereby masking their nuclear localization signal[167,182]. Following starvation, mTORC1 is inhibited and TFEB is released from the lysosomal membrane[168,175]. During nutrient-rich conditions, mTORC1 is not the only regulator of TFEB, as ERK2 is also capable of phosphorylating TFEB on Ser^{142} favouring cytosolic localization[183]. However, it should be noted that the relationship between mTORC1 and TFEB is far more complex, as studies in renal cells have demonstrated that mTORC1 can phosphorylate TFEB on its C-terminus and this in contrast promotes nuclear localization[176]. Similarly, in osteoclasts PKCβ has also been shown to phosphorylate serine residues (Ser^{461}, Ser^{466}, Ser^{468}) on the C-terminus to promote

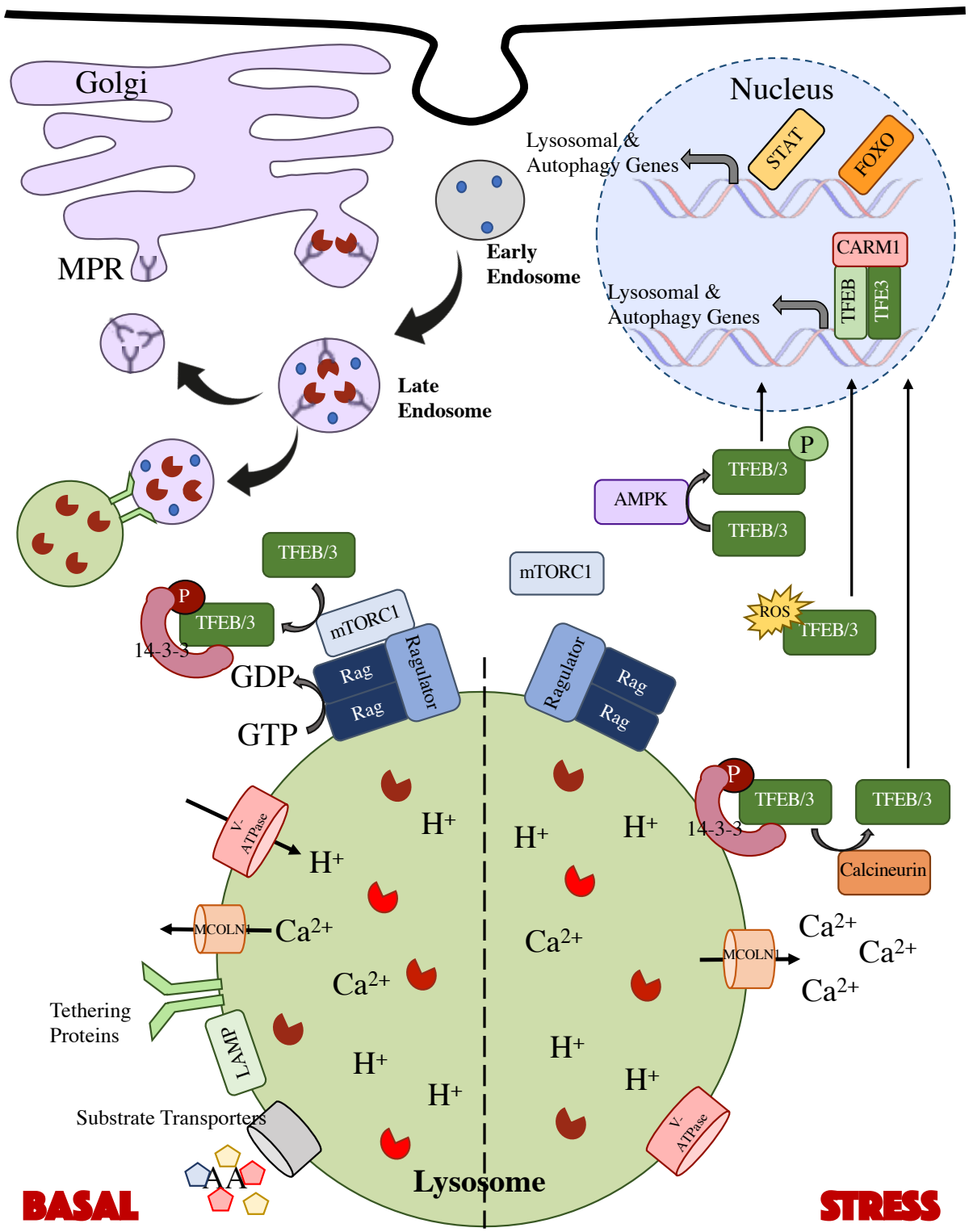
Golgi
MPR
Early Endosome
Late Endosome
Nucleus
Lysosomal & Autophagy Genes
STAT
FOXO
CARM1
TFEB
TFE3
Lysosomal & Autophagy Genes
P
TFEB/3
AMPK
TFEB/3
ROS
TFEB/3
TFEB/3
mTORC1
P
TFEB/3
14-3-3
mTORC1
Ragulator
Rag
Rag
GDP
GTP
Ragulator
Rag
Rag
P
TFEB/3
TFEB/3
14-3-3
Calcineurin
V-ATPase
H+
H+
H+
H+
H+
MCOLN1
Ca2+
Ca2+
Ca2+
MCOLN1
Ca2+
Ca2+
Ca2+
Tethering Proteins
LAMP
H+
H+
H+
H+
Substrate Transporters
AA
V-ATPase
Lysosome
BASAL
STRESS

Figure 2: Regulation of lysosomal biogenesis. Lysosomes are a major degradative organelle within the cell, which are highly acidic and replete with hydrolases capable of degrading protein, lipids, carbohydrates and DNA into basic cellular constituents that can be reused by the cell. The lysosomal membrane is highly diverse and houses an array of transporters that facilitate the export of these components back into the cytosol. There are also a number of proteins that enable the fusion of lysosomes to other organelles, such as SNARE and LAMP proteins. Also present on the lysosomal membrane is v-ATPase, which pumps protons into the lysosomal lumen, to maintain the low pH (4.5-5.5) necessary for proper lysosomal function. Ca^{2+} is also thought to play a role in the acidification of the lysosomes, although this is still poorly understood. Proper Ca^{2+} handling is essential for lysosomal function, and MCOLN1 facilitates the export of Ca^{2+} from the lysosomal lumen. mTORC1, a cellular rheostat that promotes protein synthesis and inhibits protein breakdown is highly associated with lysosomes. Under nutrient rich conditions, Ragulator and Rag proteins, found on the lysosomal membrane, recruit and activate mTORC1, which then can phosphorylate and inhibit MiT family members such as TFEB and TFE3. This phosphorylation promotes the binding of chaperone 14-3-3 and sequesters MiTs in the cytosol. However, under conditions of stress such as starvation, mTORC1 is inactive and Ca^{2+} is released from the lysosomal lumen through MCOLN1. This influx of cytosolic Ca^{2+} activates Ca^{2+}-dependent phosphatase Calcineurin, which dephosphorylates TFEB and TFE3, and promotes the dissociation of 14-3-3, thus allowing nuclear translocation of TFEB and TEF3. Recently it has also been shown that TFEB and TFE3 are sensitive to ROS and AMPK which can independently promote their nuclear localization. Once in the nucleus, TFEB and TFE3 can homo- and hetero-dimerize and bind CLEAR sites found primarily in promoter regions of genes associated with autophagy and lysosomes. TFEB and TFE3 are widely referred to as the master regulators of lysosomal biogenesis and they exhibit a high level of redundancy. However, other transcription factors have been shown to regulate autophagy and lysosomal genes such as FOXO and STAT. Lysosomal biogenesis relies on the upregulation of the expression of lysosomal genes and also an endocytotic pathway. Many nascent lysosomal hydrolases are tagged with mannose-6-phosphate, recognized by mannose-6-phosphate receptors and packaged by the trans-Golgi network. These vesicles fuse with early endosomes forming late endosomes which share many characteristics as lysosomes but differ in that they contain mannose-6-phosphate receptors and their membranes are not as complex as lysosomes. Within the endosome, the mannose-6-phosphate and receptor complex is removed and shuttled back to the Golgi. Late endosomes can then fuse, or transiently link, to lysosomes to donate the lysosomal enzyme. It should be noted that while many lysosomal hydrolases rely on this pathway, many are actually shuttled to the plasma membrane and incorporated through endocytosis. However, these mechanisms remain poorly characterized.

stabilization and nuclear localization, and this is required for normal osteoclast function *in vivo*[184]. Thus, TFEB regulation may be highly nuanced and tissue-specific (Fig. 3).

Following starvation, Ca^{2+} is another major regulator of the MiT family. Ca^{2+} is released from the lysosome via mucolipin-1 (MCOLN1), which activates Calcineurin, a Ca^{2+}-dependent phosphatase, capable of dephosphorylating TFEB and TFE3 thereby allowing their nuclear translocation[185]. MCOLN1 is also sensitive to oxidative stress as increased ROS can trigger the release of Ca^{2+} from the lysosome and subsequent activation of Calcineurin and CAMK independent of nutrient status[186,187]. Furthermore, ROS can also trigger the release of Ca^{2+} from the SR by oxidizing the ryanodine receptors[188]. Interestingly, the MiT family possesses a highly conserved exposed cysteine residue, Cys^{212} on TFEB and Cys^{322} on TFE3, that can become oxidized, resulting in their nuclear localization[189]. Furthermore, AMPK has recently been shown to be a key regulator of TFEB and TFE3 as it phosphorylates the transcription factors on a triple serine residue found on the C-terminus[190]. This post-translational modification was shown to be required for their ability to regulate gene expression, but not necessary for nuclear localization. Interestingly, AMPK also regulates coactivator-associated arginine methyltransferase 1, CARM1, which has recently been shown to act as a transcriptional coactivator of TFEB in the regulation of lysosomal and autophagy genes[191]. Thus, TFEB and TFE3 are responsive to nutrient deprivation, influxes of intracellular Ca^{2+}, oxidative stress and energetic stress.

Moreover, TFEB is known to participate in an autoregulatory loop during starvation. The TFEB promoter contains six CLEAR elements and following starvation TFEB can bind to four of these CLEAR domains to regulate its own expression[183]. It remains unknown whether other MiT family members can regulate the CLEAR elements on the TFEB promoter. To date,

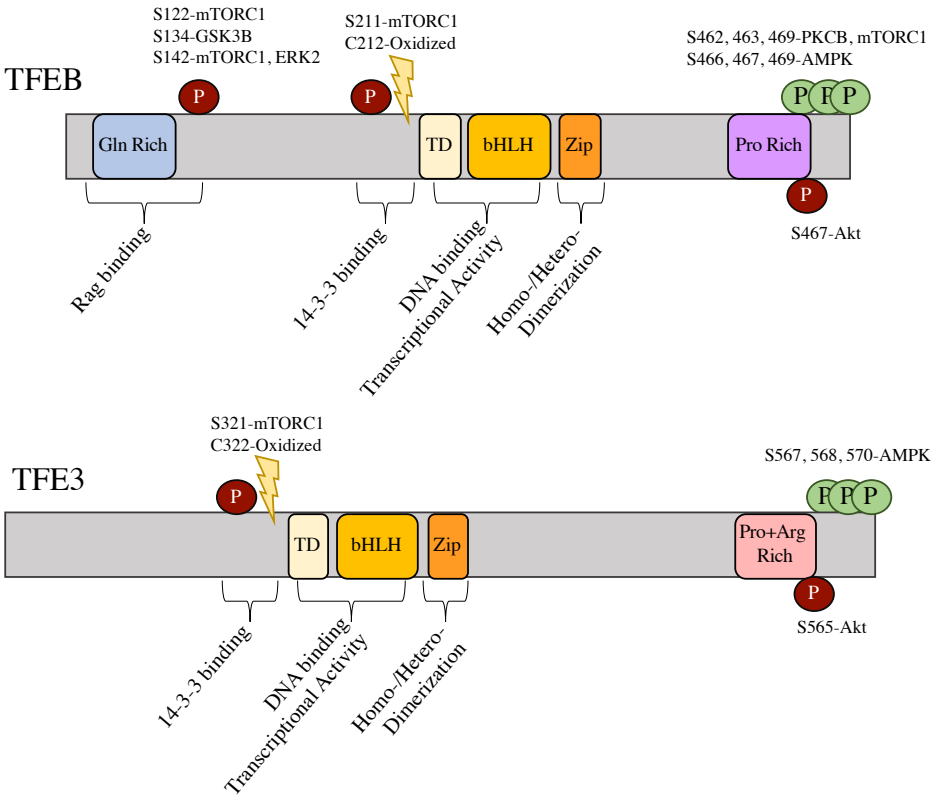

Figure 3: Structure and post-translational modifications of TFEB and TFE3. The two transcription factors share a high level of homology, as both proteins are basic helix loop helix (bHLH) leucine zipper (Zip) transcription factors. This structure allows members of the MiT family to homo- and hetero-dimerize and bind to DNA. Their transactivation domain (TD) resides in close proximity to the bHLH motif, and this allows TFEB and TFE3 to regulate transcription. The main differences in structure are that TFEB contains a glutamine-rich region, while TFE3 does not, and TFE3 contains a proline and arginine rich region, while TFEB is just proline rich. Due to their structural similarities, many post-transcriptional modifications are shared by the two transcription factors. The canonical mode of regulation is through mTORC1, which phosphorylates Ser^{211} on TFEB and Ser^{321} on TFE3 which allows for the binding of chaperone 14-3-3, leading to their cytosolic retention. It has also been shown that mTORC1 can further regulate TFEB through inhibitory phosphorylation events at Ser^{122} and Ser^{142}, however in a hyperactive mTORC1 model it was also shown that mTORC1 phosphorylation of TFEB at $Ser^{462, 463, 469}$ can actually activate the transcription factor. Moreover, Akt has been shown to negative regulate both TFEB and TFE3 through phosphorylation events of Ser^{467} and Ser^{565} respectively. Recently, it has been shown that Cys^{212} on TFEB and Cys^{322} on TFE3 are sensitive to oxidation and this actually promotes their nuclear translocation. Furthermore, AMPK has been shown to phosphorylate triple serine residues on TFEB and TFE3 (466, 467, 469 and 567, 568, 570 respectively) to promote their nuclear translocation and this modification is required for their transcriptional activity. While TFEB has been the more extensively studied thus far, other kinases have been shown to participate in the regulation of TFEB such as GSK3β, ERK2, and PKCβ but it is unclear if TFE3 is also subject to the same regulatory modifications.

seven distinct TFEB transcripts have been described and exhibit tissue-specific expression patterns, although these variants only vary in a non-coding region in their 5'-end[171]. Despite these variations in pre-mRNAs there has only been one protein isoform of TFEB described, until very recently. In a wide array of tissues, a small 281 amino acid splice variant of TFEB was discovered that lacks the basic helix-loop-helix leucine zipper motif[192]. It was found that this splice-variant, named small TFEB or TFEB-S, is highly unstable but actually represses known targets of TFEB such as genes containing CLEAR elements and antioxidant response elements (ARE)[192]. Thus, it is thought that TFEB-S acts as a transient negative regulator of TFEB to fine-tune the autophagy and lysosomal response.

2.1.3 TFEB and TFE3, More Than Lysosomal Regulators

Although TFEB and TFE3 are most known for their roles in lysosomal biogenesis and the regulation of autophagy, these transcription factors are involved in a number of other cellular processes. Intriguingly, whole body deletion of TFEB is embryonic lethal as TFEB is required for the vascularization of the placenta[193]. This function has not been described for other MiT members and deletion of TFE3 produces a viable offspring with no overt phenotype. In this vein however, TFE3 has been shown to be important in the maintenance of pluripotency, as cytosolic sequestering of TFE3 is required for embryonic stem cells to exit their naïve pluripotent state and commit to cellular differentiation[194]. Furthermore, it has been shown that in culture TFE3 negatively regulates myotube differentiation by downregulating the expression of myogenin[195]. Mutation of MITF is associated with Waardenburg syndrome type II, in which patients present with hypopigmentation, deafness and defects in ectodermal development[196]. Thus, despite being most known for their roles in autophagy and lysosomal biogenesis, the MiT family is important in diverse pathways relating to organism development.

Recent work has also highlighted a key role for TFEB and TFE3 in whole-body metabolism. In 2013, Dr. Ballabio's group was the first to describe a role for TFEB in lipid metabolism during starvation, as they showed that TFEB transcriptionally regulates PGC-1α and PPARα to upregulate lipid breakdown. In the liver, TFEB overexpression increased PGC-1α and PPARα, and enhanced fatty acid oxidation, while the loss of TFEB in the liver reduced lipophagy (breakdown of lipid droplets via the lysosomes) leading to an accumulation of fatty deposits in the liver, and decreased circulating ketone bodies following starvation[183]. Similarly, TFE3 whole body knockout animals are more susceptible to obesity following a high-fat diet as they gain significantly more weight, and exhibit impaired lipolysis[197,198]. It was specifically shown that TFE3 transcriptionally regulates lipases such as Atgl and Hsl in adipose tissue and also regulates PGC-1α in adipocytes[198,199]. Interestingly, liver-specific overexpression of TFEB and TFE3 is protective against obesity by preventing weight gain and maintaining insulin sensitivity following a high-fat diet and in the *Ob/Ob* mouse model of obesity[183].

TFEB and TFE3 have also been implicated in glucose metabolism. Overexpression of TFEB results in improved glucose uptake by skeletal muscle likely due to increased expression of glucose transporters (GLUT1, GLUT4 and TBC1D1) and hexokinase 1 and 2[200]. Skeletal muscle-specific deletion of TFEB impairs glucose uptake and decreases glycogen stores leading to insulin-resistance. TFE3 whole body knockout animal, also present with perturbed glucose metabolism, but this appears to be more linked to impaired glycogen synthesis leading to reduced glycogen storage as the expression of glycogen synthase kinase (GSK) is decreased[197,199,201]. In fact, when challenged with a bout of exercise, these animals are unable to replenish their glycogen stores post-exercise[197].

Notably, important roles for TFEB and TFE3 in mitochondrial homeostasis have also been described that go beyond their role in regulating the autophagy machinery, and thereby mitochondrial turnover. Skeletal muscle-specific deletion of TFEB resulted in mitochondrial dysfunction characterized by loss of membrane potential and elevations in ROS emission[200]. This was deemed to be independent of impaired mitochondrial clearance as no changes in autophagy flux were observed[200]. Similarly, TFE3 KO animals showed reduced expression of a number of mitochondrial markers, and impairments in oxygen consumption were observed in the liver along with evidence of increased oxidative stress[197]. Furthermore, it was shown that overexpression of TFEB increased mitochondrial content and function, and although TFEB has been shown to regulate PGC-1α this effect was independent of the coactivation of PGC-1α[200,202]. Interestingly, TFE3 directly regulates Fis1, a key fission protein, and as Fis1-dependent fission is key for mitophagy it remains to be known what role mitophagy, plays in the phenotype[197].

2.1.3 Other Regulators of Lysosomes and Autophagy Machinery

Aside from the MiT family, the forkhead box O (FoxO) family of transcription factors are also key regulators of the autophagy pathway. In the context of muscle atrophy, which will be covered in greater detail in a later section, FoxO3 has been shown to regulate the ubiquitin-proteasome system as well as autophagy, contributing to muscle atrophy[203–206]. Importantly, FoxO3 is required and sufficient to induce autophagy in skeletal muscle and this is independent of mTOR as the addition of rapamycin did not effect the induction of autophagy[207–209]. FoxO3 was shown to directly regulate autophagy-related genes LC3 and BNIP3, and BNIP3-mediated autophagy appears to be the main mitophagic mechanism regulated by FoxO3[207]. Since then, similar roles have been described for the other members of the FoxO family[210].

Recently, another MiT-independent pathway is emerging that appears to be specifically responsive to lysosomal status. In renal tissue, the loss of asparagine endopeptidase or other lysosomal cysteine proteases triggers the activation of STAT3[211]. The activation of STAT3 appears to be in response to lysosomal oxidative stress[211]. In this vein, STAT3 has also been shown to act in concert with v-ATPase to maintain lysosomal pH by enhancing its enzymatic activity[212]. More work is required to understand the full extent of STAT3 signaling with respect to the lysosome across tissues, but it appears to be a key factor in the maintenance of lysosomes and their function.

2.1.5 Sex, Lysosomes and Autophagy-Emerging Evidence

The impact of sex on lysosomes and autophagy has been largely overlooked, however recently research in this area has revealed striking sex differences. Intriguingly, it appears that both androgen receptors (AR), as well as ERs can regulate a wide host of autophagy genes. While AR have been shown to mediate *Ulk2, Bcl2, Atg3, Atg4b, Atg5, Atg7, Lc3b, p62, Ambra1, PI3K3* and *Tfeb* mRNA expression, ER can regulate *Ulk1, Ulk2, Bcl2, Atg5, Atg7, Atg13, Atg14, Atg16l1, Uvrag, Ambra1, Lc3b, p62, PIK3C3* and *CtsD*[213–217]. Despite the apparent overlap, growing evidence suggests that females have increased lysosomal content and augmented autophagy in skeletal muscle[218–222] and neurons[223]. However, this may be highly tissue dependent as an increase in autophagolysosomes was observed in male cardiac tissue, and no differences were observed in renal tissue[224]. Furthermore, it has been shown that 17β-estradiol upon binding to ERα induces autophagy via AMPK and thus promotes phagophore formation through ULK1 in neurons[225]. In the brain, it has been proposed that estrogen can also further activate autophagy through the activation of Akt, which normally inhibits mTORC1 and GSK3β, thereby removing their repression on autophagy[226]. However, following ischemic stroke males

actually increase autophagy, while females reduce autophagy and have better outcomes[226]. Thus, it is evident that the modulation of autophagy through estrogen may be highly tissue- and stress-specific.

2.2 Mitochondrial Turnover

As previously mentioned, mitophagy is a selectively form of autophagy through which dysfunctional mitochondria are recycled. This section will cover mitophagy specific-signaling and mechanisms but important to note is that as a subset of autophagy, mitophagy is still subject to the same initiation, nucleation and elongation steps required for the formation of the autophagosome as described earlier.

2.2.1 Ubiquitin-Dependent Mitophagy Pathways

Of the mitophagy pathways that have been described, the most well characterized is the PTEN-induced putative kinase 1 (PINK1) and Parkin pathway (Fig. 4). PINK1 is regularly imported into the mitochondrial matrix and degraded by mitochondrial proteases, PARL and MPP[227,228], although seemingly inefficient this positions PINK1 to be acutely sensitive to the status of the mitochondria as the import pathway is dependent on membrane potential, oxidative stress and ATP availability. Following membrane depolarization, the import of PINK1 is arrested, causing PINK1 to accumulate on the OMM[229–231]. Recent data suggest that mitochondrial nod-like receptor, NLRX1, functions in a similar fashion, in that it too is regularly imported, but following an import defect it localizes to the cytosol to promote LC3 lipidation and autophagosome formation[232]. Importantly it appears that this occurs independent of PINK1, and it is a key mitophagic regulator in muscle[232]. PINK1 appears to also sense proteotoxic stress, as an accumulation of misfolded proteins can trigger PINK1-dependent mitophagy[233]. Recently, it has also been shown that the import machinery itself can trigger mitophagy in response to

proteotoxic stress, as this causes the PAM to dissociate from the translocase of the inner membrane and initiate mitophagy independent of membrane depolarization[234]. Thus, it appears that import is a key monitor of mitochondrial status and is primely positioned to initiate mitophagy through a multi-faceted manner.

PINK1 on the outer membrane undergoes autophosphorylation, activating the kinase, to then phosphorylate both Parkin and ubiquitin to prime ubiquitination of various OMM proteins[235–238]. In a feed-forward mechanism, more Parkin and ubiquitin are recruited to mitochondria to amplify the mitophagic signal[235,237,239]. The absence of Parkin leads to fragmented mitochondria, impaired oxidative capacity, but surprisingly does not diminish mitophagy flux[240,241]. Other E3 ubiquitin ligases have been shown to localize to mitochondria following stress to ubiquitinate OMM proteins including Mul1, Gp78, and HUWE1[242–244]. These ubiquitin chains serve as a flag to help target and guide the autophagosome to the dysfunctional mitochondria. The autophagosome is then linked to the ubiquitin chains via adaptor proteins such as p62, Optineurin, and Ndp52 which possess both a ubiquitin-binding motif as well as an LC3-interacting region[245–247]. Once the cargo is fully engulfed, the autophagosome will then travel along microtubule tracts to the lysosome where the two will fuse and the cargo will be degraded via the lysosome.

2.2.2 Ubiquitin-Independent Mitophagy Pathways

Ubiquitin-independent pathways are largely receptor-mediated and these are relatively less studied mechanisms in comparison to the PINK1-Parkin pathway. In response to various mitochondrial stress, receptors already present on the OMM are activated and can directly bind to LC3-II, or to any of the other Atg8 proteins (i.e. GABARAP) (Fig. 4). For example, FUNDC1 has been shown to directly respond to hypoxia, and can even activate ULK1 to promote

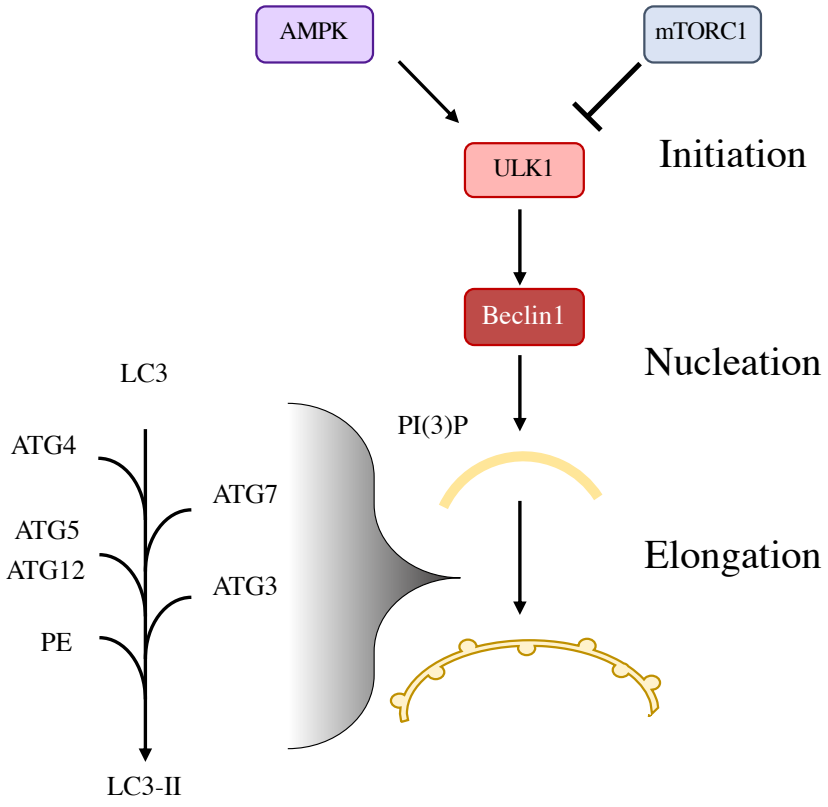
AMPK
mTORC1
Initiation
ULK1
Beclin1
Nucleation
LC3
ATG4
ATG7
ATG5
ATG12
ATG3
PE
PI(3)P
Elongation
LC3-II

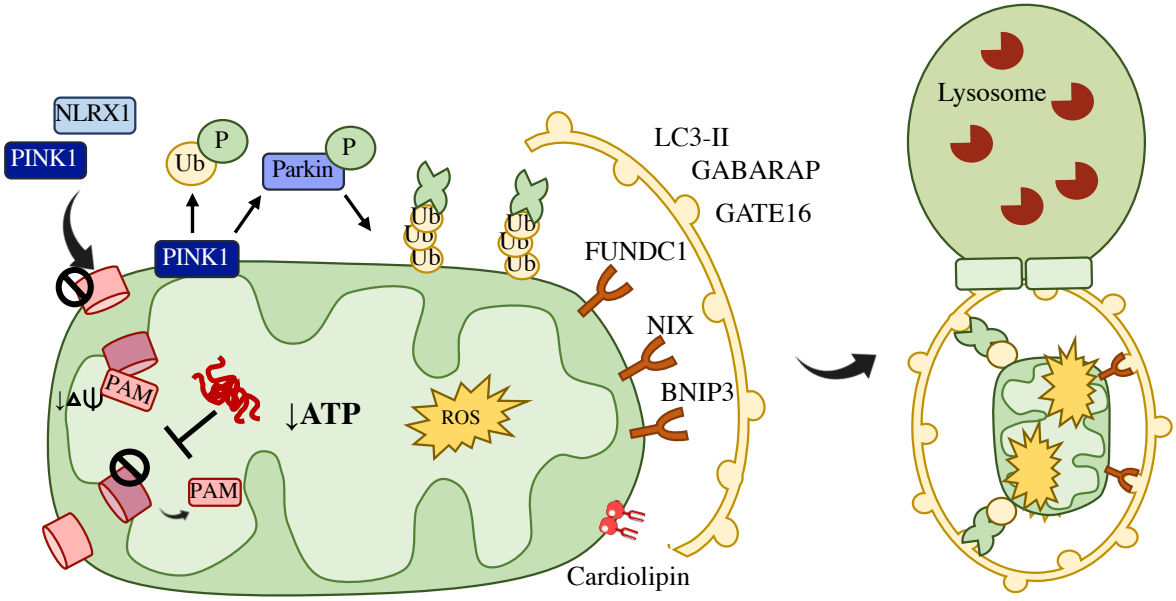
NLRX1
PINK1
Ub
P
Parkin
P
PINK1
PAM
↓ΔΨ
↓ATP
ROS
PAM
Ub
Ub
Ub
Ub
Ub
Ub
LC3-II
GABARAP
GATE16
FUNDC1
NIX
BNIP3
Cardiolipin
Lysosome

Figure 4: Mitophagy mechanisms. Mitophagy is a selective form of autophagy that enables the degradation of dysfunctional mitochondria via the lysosome. Damaged mitochondria are engulfed in an autophagosome which then travels along microtubule tracts to the lysosome. The initiation of the phagophore is regulated by the ULK1 complex. ULK1 is generally negatively regulated by mTORC1, however under conditions of stress mTORC1 is inactivated and AMPK can also activate ULK1. ULK1 then activates Beclin1 and commences the nucleation phase of the phagophore formation, generating phosphatidylinositol phosphate (P1(3)P), a major component of the autophagosome. The growing autophagosome is then elongated through a series of conjugation steps involving autophagy-related proteins (ATG) and phosphatidylethanolamine (PE) in the formation of the mature lipidated form of LC3, LC3-II. Alternatively, GABARAP and GATE16 can also aid in the elongation of the phagophore. Damaged mitochondria can signal for their degradation through a variety of mechanisms. The most well documented is the PINK1-Parkin pathway, whereby losses in membrane potential will arrest the import of PINK1 into the mitochondrial matrix leading to its accumulation on the outer mitochondrial membrane (OMM). PINK1 is not the only protein that exploits the import machinery as a mechanism of sensing mitochondrial health, as NLRX1 behaves in a similar fashion and can trigger mitophagy when in the cytosol by promoting phagophore formation. PINK1 on the OMM can recruit and phosphorylate Parkin, and also prime ubiquitin through its phosphorylation. Parkin can then polyubiquitinate various OMM proteins to signal mitophagy. Furthermore, it has been shown that the PINK1-Parkin pathway is sensitive to misfolded proteins, and recently this has been shown to cause the dissociation of the protein-associated motor (PAM) complex of the import machinery, causing PINK1 to accumulate on the OMM and initiate mitophagy. Independent of PINK1 and Parkin, mitophagy can be initiated through receptors present on the OMM. Receptors such as FUNDC1, NIX and BNIP3 have been shown to respond to various stresses such as hypoxia, and oxidative stress. Cardiolipin, the mitochondrial phospholipid has also been shown to externalize following mitochondrial stress and directly bind to LC3-II present on the autophagosome. While ubiquitin chains require an adaptor protein such as p62 to tether ubiquitin to LC3-II, receptors can bind directly to LC3-II and are usually referred to as ubiquitin-independent. Once the autophagosome completely engulfs the damaged organelle it travels along microtubule tracts to the lysosome where the two fuse and the contents are degraded by the lysosome.

autophagosome formation[248–250]. Other receptors such as NIX play dual roles in mitophagy and in apoptosis, so it is possible that this signaling cascade can tip the scales between cell-survival or cell-death[251–255]. Interestingly in neurons, cardiolipin, a mitochondrial specific phospholipid, has also been shown to externalize in response to stress and can directly bind LC3 to anchor the autophagosome[256]. Several other receptors such as BNIP3 and AMBRA1 have also been implicated in mitophagy[244,257,258]. Currently it is unclear whether these mechanisms are mutually exclusive or act in concert with each other. Recent data suggest that the initial signal or type of dysfunction may dictate which pathway is activated, as many of these pathways are triggered by distinct characteristics like membrane depolarization, import inhibition, ROS or hypoxia[232].

2.2.3 Impact of Sex on Mitophagy

There is very little known about the influence of sex on mitophagy, and while deductions can be made based on the overall evidence of increased autophagy in females, mitophagy relies on its own signaling cascades and thus specific investigations are warranted. Currently, there are very few reports on sex-differences in mitophagy, however one report suggested that testosterone was positively correlated with PINK1 and Parkin protein, thus potentially implying higher mitophagy in male skeletal muscle[259]. However, in other reports increased Parkin expression was found in female skeletal muscle in comparison to males[218]. Furthermore, deletion of ERα in skeletal muscle impairs mitochondrial turnover, but the mechanism is unclear as fission is also impaired, thus this may be an indirect consequence[144]. As estrogen is a known regulator of mitochondria and has been shown to improve oxidative capacity and reduce ROS, it is possible that this improved function is in part driven by the ability of estrogen to increase mitochondrial turnover through mitophagy. However, one could also argue that the

improved mitochondrial pool negates the need for turnover and thus less mitophagy would be expected in female. Thus, further research is required to understand the role of sex and estrogen in mitophagy and mitochondrial maintenance.

2.3 Mitochondrial and Lysosomal Coordination

Emerging literature has begun to provide evidence of intra-organellar communication between mitochondria and lysosomes that seems to go beyond mitophagy. Firstly, mitochondrial dysfunction is apparent in a number of lysosomal storage disorders, and morphological and functional impairments have been documented in the absence of the lysosomal regulators TFEB and TFE3[197,200,260–262]. Notably, in the absence of TFE3, the appearance of swollen mitochondria is observed in skeletal muscle and defects in oxidative capacity are observed in liver tissue[197]. Alternatively, overexpression of TFEB increases mitochondrial content and ETC complex activity, and despite being a known regulator of PGC-1α, this is apparently independent of PGC[200,202]. Surprisingly, impairing mitochondrial function pharmacologically leads to the appearance of large vacuoles and impairs lysosomal function[263,264]. While acute mitochondrial stress promotes the activation of the MiT family, prolonged stress inhibited lysosomal biogenesis[265,266]. Physiologically, lysosomes and mitochondria form contact sites and these connections are important for regulating mitochondrial fission[111], and Ca^{2+} flux from the lysosome to the mitochondria through MCOLN1[267]. Thus, a reciprocal role in the maintenance and homeostasis of these organelles is beginning to be uncovered and further work in skeletal muscle is warranted.

3.0 Mitochondrial Plasticity

3.1 Adaptations to Endurance Exercise

Exercise is often referred to as mitochondrial medicine as it stimulates a multi-faceted approach to rejuvenating the mitochondrial pool contributing to the maintenance and improvement of skeletal muscle health[10]. While exercise has been shown to positively effect almost every tissue in the body, the following section will focus on mitochondrial adaptations within skeletal muscle.

3.1.1 Structural and Functional Adaptations to Skeletal Muscle

Since 1967, thanks to the pioneering work of John Holloszy, it has been known that endurance exercise training shifts the metabolic profile of the muscle towards a more oxidative phenotype (Fig. 5)[268]. Glycogen is spared as an energy source, and there is a greater reliance on fat oxidation resulting in less lactate being produced at a given workload[269]. While fiber type switching does not commonly occur in humans, endurance training does promotes a shift towards a more oxidative phenotype that is reminiscent of type I fibers[270]. Increased mitochondrial content is observed even in type IIx and IIa fibers, so long as intensity is sufficient to recruit these fibers[271]. Notably, greater adaptations are generally reported in SS fractions, compared to IMF mitochondria, as this pool is thought to be more labile[271]. Another important consequence of endurance training is the induction of angiogenesis, which increases capillarization to the muscle to improve nutrient delivery and exchange.

3.1.2 Structural and Functional Adaptations to Mitochondria

Mitochondrial Biogenesis. As the muscle becomes more oxidative with training, the mitochondrial reticulum is not only expanded, but also remodeled and functionally improved (Fig. 5). A single bout of exercise is capable of initiating the signal cascades, but repeated bouts

are required for altered protein expression and functional changes[272]. As muscle contracts, ATP is continuously broken down and resynthesized, this is reflected by a reduction in the energy charge ratio and serves as an indication of the energetic status of the cell. AMP binds to the γ subunit of AMPK to induce a conformational change and its activation[273,274]. AMPK then phosphorylates PGC-1α thereby promoting its nuclear translocation[68,70,72,275]. Concurrent with the breakdown of ATP, NADH is also oxidized into NAD^+ which activates SIRT1 to deacetylate PGC-1α to increase its activity[76,78,276,277]. Ca^{2+} plays a key role in myosin-actin crossbridge cycling and is in constant flux during muscle contraction. Increased intracellular Ca^{2+} activates CAMK and protein kinase C (PKC) to again activate PGC-1α, as well as the transcription factors MEF2 and CREB[88,278,279]. Exercise also stimulates the production of ROS, while it has long been thought that the major contributor of ROS during exercise was derived from mitochondria, it is now believed that cytosolic sources, such as NAD(P)H oxidases (NOX) are the major drivers of exercise-induced oxidative stress[280,281]. Regardless of the source, ROS are sensed by p38 MAPK to activate PGC-1α as well as transcription factors USF and ATF2[64,83,85,86]. An important downstream target of PGC-1α is TFAM, which is upregulated with exercise, and this in turn helps promote transcription of mitochondrially-encoded genes[40,52]. While PGC-1α appears to be at the crux of these signals, animals lacking PGC-1α are still able to positively adapt to training. It appears that only with advancing age does PGC-1α become required for exercise-induced adaptations[97,282]. Indeed, numerous regulators have been shown to control mitochondrial maintenance including p53, SIRT1, TFEB and mTORC1. The tumor suppressor protein, p53, is stabilized and activated in response to exercise via phosphorylation at Ser^{15}, stimulating its subcellular redistribution[58,283,284]. In the nucleus, p53 regulates NuGEMPs, including TFAM, and has even been shown to regulate the transcription of PGC-

1α[55,285–287]. In mitochondria, p53 can directly bind the D-loop region of mtDNA, or bind to TFAM, to regulate mtDNA expression and integrity[56,58,288]. Again, while the loss of p53 results in reductions in mitochondrial content and function, these animals are still able to adapt to exercise[287]. Thus, exercise stimulates a diverse, multi-faceted and likely highly redundant signaling program to ensure that mitochondrial homeostasis is achieved even in the face of genetic mutations, metabolic deficiencies, and disease.

Import and the Unfolded Protein Response. Protein import kinetics are also increased following exercise to support the translocation and incorporation of nuclear-encoded mitochondrial proteins[289,290]. Exercise-induced mitochondrial biogenesis while beneficial, presents a proteotoxic challenge as the influx of imported proteins must be processed, refolded, and in many instances, combined with other subunits either nuclear- or mitochondrially-encoded to form holoenzymes[45]. Every complex of the ETC, except complex II, is comprised of both mitochondrial and nuclear-encoded subunits, highlighting the importance of achieving stoichiometry in order to maintain proper ETC function. As such, to accommodate the influx of nuclear genes encoding mitochondrial proteins (NuGEMPs), increased expression of the protein import machinery is commonly seen with exercise training[290].

Mitochondria are equipped with various chaperones and proteases to handle protein misfolding and orphaned subunits[291], however exercise stimulates such a vast array of genes that this typically exceeds the capacity of the organelle. In order to maintain proteostasis the mitochondrial unfolded protein response (UPR^{mt}) has been shown to be activated following an acute bout of exercise[292–295]. Through retrograde signals that are still poorly understood in mammalian systems, chaperones such as HSP60, and CPN10, and proteases such as LonP and ClpP are upregulated (Fig. 5)[293,294]. The initial signal that triggers the UPR^{mt} may be ROS, as

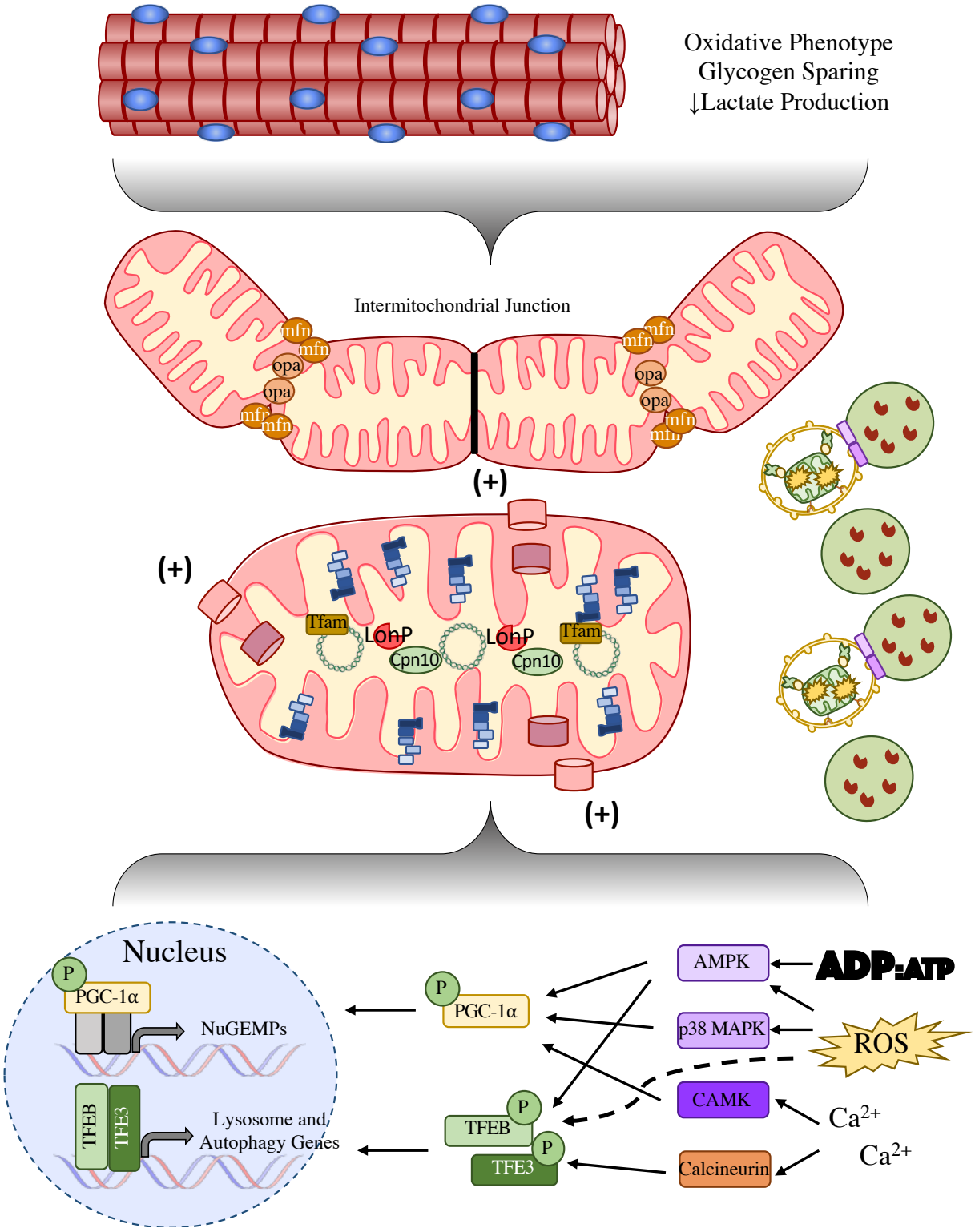
Oxidative Phenotype
Glycogen Sparing
↓Lactate Production
Intermitochondrial Junction
mfn
opa
(+)
Tfam
LOhP
Cpn10
Nucleus
P
PGC-1α
NuGEMPs
TFEB
TFE3
Lysosome and
Autophagy Genes
AMPK
ADP:ATP
p38 MAPK
ROS
CAMK
Ca2+
Calcineurin

Figure 5: Adaptations to exercise training. Exercise training promotes an oxidative phenotype of the skeletal muscle, as mitochondrial content is increased, glycogen is spared, and lactate production is reduced following a subsequent exercise challenge. However, mitochondrial content is not merely increased but rather the pool of organelles becomes more optimal. Fusion is favoured, thereby allowing the expansion of the mitochondrial reticulum which promotes substrate sharing and efficient energy production. While a highly interconnected reticulum may also allow for dysfunction to spread, intermitochondrial junctions provide a "circuit break" to electrically disconnect portions of the reticulum thereby limiting the contamination of damaged areas. Exercise elicits a number of signals such as ATP turnover, ROS emissions, and Ca^{2+} influxes that activate signaling kinases that converge on PGC-1α to upregulate nuclear genes encoding mitochondrial proteins (NuGEMPs) which includes TFAM to regulate mtDNA, import machinery to support the influx of nascent proteins, and ETC components to increase the oxidative capacity. Through the mitochondrial unfolded protein response, which is active following exercise, the protein-handling capacity of the organelle is increased. Chaperones and proteases such as cpn10 and LonP, are upregulated to meet the surge of incoming nascent proteins. Concomitantly, the same signals that promoted mitochondrial biogenesis also promote mitophagy, which culls dysfunctional organelles from the reticulum. Here the signals impinge on TFEB and TFE3 which regulate lysosomal and autophagy-related genes. Thus, exercise not only promotes the synthesis of new mitochondria, but also the removal of damaged ones to foster an optimal pool of organelles.

these have been shown to activate general control nonderepressible 2 (GCN2) which phosphorylates eukaryotic initiation factor alpha (eIF2α), subsequently arresting protein translation and reducing the volume of nascent proteins[296,297]. However, eIF2α phosphorylation does selectively upregulate the translation of proteins that contain upstream open reading frames (uORF) in their 5'-UTR, such as CHOP, ATF4 and ATF5[298,299]. These transcription factors are responsible for increasing the expression of chaperones and proteases and have even been implicated in the regulation of other quality control genes, such as biogenesis and mitophagy[291,295,300,301]. Based on work in *C. elegans*, it appears that misfolded proteins can directly initiate the UPR^{mt} as the peptides from their proteolytic cleavage are exported from the mitochondrion and directly inhibit the mitochondrial translocation of ATFS-1 forcing it to go into the nucleus[302–304]. The mammalian homologue for ATFS-1 was recently discovered to be ATF5, which also possesses both a mitochondrial targeting sequence (MTS) as well as a nuclear

localization signal (NLS), but it remains unclear if it is regulated through the same mechanism as its counterpart ATFS-1[298].

Mitochondrial Morphology. The mitochondrial reticulum is in constant flux, as mitochondria fuse and bud off from the network constantly. Through events of fusion and fission, which were described previously, the reticulum can undergo remodeling and respond to cellular stress and mitigate dysfunction[305,306]. Exercise promotes a more fused network with a high degree of branching, this is generally reflected in a shift in the ratio of fusion to fission proteins to favour fusion[307]. Deletion of both Mfn1 and Mfn2 in adult skeletal muscle impairs mitochondrial function, and is required for exercise adaptations[308]. This emphasizes the importance of fusion in mediating mitochondrial maintenance and its adaptability to exercise. While a highly interconnected reticulum allows for content mixing and substrate sharing, theoretically this would also allow for damaged segments to adversely compromise the entire network[103,309]. Work by Glancy and colleagues identified these electron-dense structures between adjacent mitochondria, which they termed intermitochondrial junctions (IMJ)[103,310]. IMJs serve as a "circuit breaker" to rapidly limit the spread of local dysfunction, as the IMJ closes it electrically dissociates the two portions, effectively quarantining the damaged organelle[103]. Along with morphological changes to the reticulum, mitochondria themselves appear to change with long-term training. The IM is folded into cristae, thanks to the presence of cardiolipin, and in long-term trained athletes an increase in cristae density is observed, supporting more OXPHOS machinery within a given organelle[311]. Thus, not only does the reticulum expand and fuse to become more energetically efficient following training, so too do the organelles themselves (Fig 5).

Lysosomes and Mitophagy. A single bout of exercise stimulates the synthesis of new mitochondria and concurrently promotes the removal of damaged organelles[312,313]. Laker et al. showed using a fluorescent reporter model, pMitoTimer, that mitophagy is induced 6 hrs post exercise and this was dependent on AMPK[314,315]. Indeed, acute treadmill exercise has been shown to promote Parkin localization to the mitochondria, along with increased LC3-II and p62 mitophagy flux up to 90 mins post exercise[94,241]. Acute exercise has also been shown to increase mitochondrial Drp1, likely to promote fission and allow mitophagy. Interestingly, while Parkin is not required for basal mitophagy, the absence of Parkin results in a blunted exercise-induced mitophagic response indicating the importance of the PINK1/Parkin pathway following exercise[241]. Interestingly, training appears to reduce mitochondrial turnover basally and blunts the exercise-induced mitophagy[240,316]. As training improves the mitochondrial pool, this negates the need for a high level of turnover. To support this notion, attenuated metabolic signaling (i.e. AMPK, CAMK) is also seen in muscle with improved mitochondrial content[317,318]. However, there is some conflicting data that suggests that mitophagy is elevated following 5 weeks of swimming as shown by an increase in LC3-II/LC3-I ratio, decrease in p62 and increase in BNIP3 in mitochondrial fractions[319]. Despite the discrepancies in the literature this stresses the importance of methodology in mitophagy measurements.

Static measurements of autophagosomal components are challenging to interpret as these are degraded by the lysosome, so opposing arguments can be made regarding an observed increase in LC3-II for example[7]. As such the use of pharmacological inhibitors such as colchicine, chloroquine and bafilomycin have been used to block the transport of the autophagosome, the fusion of the lysosome with the autophagosome or lysosomal acidification to truly capture the degree of mitophagy or autophagy "flux". Another method of accurately

measuring flux is through the use of fluorescent reporters, such as pMitoTimer, mtKeima, and MitoQC. pMitoTimer fluoresces green and over time shifts to red providing an indication of mitochondrial turnover, however it should be noted that MitoTimer will inherently shift to red within 48 hrs[320]. While disrupting mitochondria with rotenone, antimycin A and paraquat results in more red to green fluorescence[314], this reporter construct is providing an indication of mitochondrial lifespan not mitophagy per say. This becomes especially difficult to interpret in tissues in which the lifespan of mitochondria is longer than two days such as cardiac tissue. Keima is a coral derived fluorophore that is pH sensitive, by targeting Keima to mitochondria through the addition of a mitochondrial targeting sequence, this provides an *in vivo* method of measuring mitophagy[321]. mtKeima fluoresces green under neutral pH, such as within the mitochondria, and fluoresces red under acidic environments, such as within the lysosome. The caveats to mtKeima is that the tissues cannot be fixed as this disrupts the lysosomal pH, and the fluorescent spectrums of Keima partially overlap occasionally producing an orange colour[322]. Finally, MitoQC is a tandem tag reporter in which mCherry and GFP are linked to a mitochondrial targeting sequence[323]. Similar to mtKeima, MitoQC is pH-dependent, as GFP is quenched by the lysosome but mCherry is not, thus under normal conditions mitochondria will fluoresce both red and green, but in acidic environments will only fluoresce red. Strengths of the MitoQC model is that the tissues can be fixed and there is little overlap of the spectra[322]. Thus, tools that fully capture mitophagy flux are required for accurate understanding of how this dynamic process is regulated in different conditions.

Shifting back to the benefits of exercise, a relatively new area of research has demonstrated that not only does acute exercise stimulate mitophagy but it also activates lysosomal biogenesis to ensure that the cell is capable of supporting increased

turnover[197,262,324,325]. Many of the signals described that activate PGC-1α are also involved in activating TFEB and TFE3. First, as AMPK is activated by increased ATP turnover, AMPK has been shown to phosphorylate TFEB and TFE3 on a triple serine residue on the C-terminus following exercise[190]. While Ca^{2+} and ROS are known regulators of TFEB and TFE3 (described in section 1.2.3) it is highly likely that these mechanisms are also at play during exercise, however this has not been confirmed. Interestingly, there is evidence to suggest that nuclear translocation of TFEB following exercise is dependent on PGC-1α expression[324], however others have shown that the beneficial effects of TFEB on mitochondria are independent of PGC-1α[325]. Both are capable of regulating each other's expression[202,324,325], as such it appears that the relationship between PGC and TFEB may be reciprocal and highly complex. Nevertheless, training has been shown to increase lysosomal content and intriguingly these adaptations precede mitochondrial adaptations[326].

3.2 Adaptations to Disuse

Periods of physical inactivity, or sedentarism, result in significant losses in muscle mass and strength, but are also compounded by metabolic and biochemical changes that impact the health and function of muscle[327]. It is valuable to understand how disuse can be modeled experimentally and the implications/considerations for each model[327]. Two of the most common animal models are hindlimb suspension, and hindlimb immobilization. Hindlimb suspension involves fixing the tail to a swivel at the top of the cage, allowing rodents to locomote on their forelimbs and closely simulates microgravity[328]. Hindlimb immobilization involves fixing one limb in a plastic brace or tube, and the position of the ankle dictates which muscles will atrophy: dorsiflexion would affect the tibialis anterior and extensor digitorum longus, while plantar flexion would affect the gastrocnemius, plantaris and soleus muscle[329,330]. This method closely

resembles immobilization or casting in humans and allows the contralateral limb to serve as an intra-animal control. Confined housing is a method that would more closely reflect sedentarism as the animal can still move around freely but total energy expenditure is decreased, this model is valuable as it provides whole-body effects that are commonly seen in humans such as insulin resistance[331]. More invasive techniques are also frequently used in the literature and include denervation, nerve crushing and tetrodoxin (TTX) cuffing[332]. Denervation is a surgical procedure in which a small portion of the nerve (sciatic for experiments done in mice, tibial for rat models) is excised in one limb, and the other is sham operated, removing all neural input to the muscles of the lower hindlimb[333,334]. Animals can still locomote freely, and again the contralateral limb serves as an internal control, this model produces muscle atrophy more rapidly than hindlimb suspension or immobilization and can also be applied to an aging context as denervation is commonly seen[327]. Nerve crushing is also a surgical procedure that involves applying enough force to completely ablate the neural input, but given enough time can also model re-innervation[335]. Finally, TTX is a sodium channel blocker which is a chemical approach causing paralysis, application of a TTX cuff around the nerve blocks impulse conductance while maintaining neuromuscular connection, and the flow of trophic factors that are lost with denervation[336].

3.2.1. Structural and Functional Adaptations to Skeletal Muscle

Loss of muscle is a hallmark of disuse, not only is lean mass reduced but this is also reflected in reductions in cross-sectional area of the myofibers. This is accompanied by losses in strength and muscle function, and physiologically manifests as decreased quality of life (Fig. 6). Muscle wasting is commonly seen with aging, cancer, metabolic disease, and prolonged bed rest or hospitalization and in these clinical settings has severe ramifications on patient

outcomes[337]. In the context of disuse and denervation, type I fibers are most affected, however with respect to sarcopenia and cachexia it appears to be type II predominantly[338,339]. Losses in muscle mass can be seen as early as two days following immobilization with the greatest decline occurring in the first 7 days, however denervation results in accelerated atrophy[340]. The loss in muscle mass is in part due to a shift towards catabolism over anabolism. During disuse, protein synthesis is largely downregulated due to inhibition of Akt and mTORC1 which normally promote anabolism[341–345]. It should be noted however that with denervation mTORC1 activity is increased, which illustrates the importance or reliance on catabolism during disuse which results in a net loss of protein[346,347].

Declines in protein synthesis rates occur rapidly following disuse and have been observed as early as 6hrs following immobilization[348,349]. Furthermore, not only do rates decline, but this is further compounded by anabolic resistance, as stimulating protein synthesis via amino acid infusions is blunted in comparison to non-immobilized limbs[350,351]. The mechanisms behind this anabolic resistance are still relatively unclear but may be in part due to mTORC1 and insulin/insulin growth factor 1 (IGF-1) signaling (Fig. 6). Inhibitors of mTORC1 including REDD1/2 (regulated in development and DNA damage-1 and -2) are upregulated with disuse[352,353]. Furthermore, as insulin resistance is commonly seen with disuse it is proposed that this perturbs pyruvate dehydrogenase kinase 1 (PDK1) which normally mediates mTORC1 phosphorylation of its downstream target p70S6K1 to promote protein synthesis[343,350,352]. IGF-1 resistance is also commonly seen with disuse and is normally a regulator of Akt. Akt is an upstream regulator of mTORC1, as such attenuated Akt signaling would result in mTORC1 inhibition[343,354,355]. Notably, increased p38 MAPK expression and activation has also been shown in disuse conditions, as early as 24 hr of hindlimb suspension, which has been associated

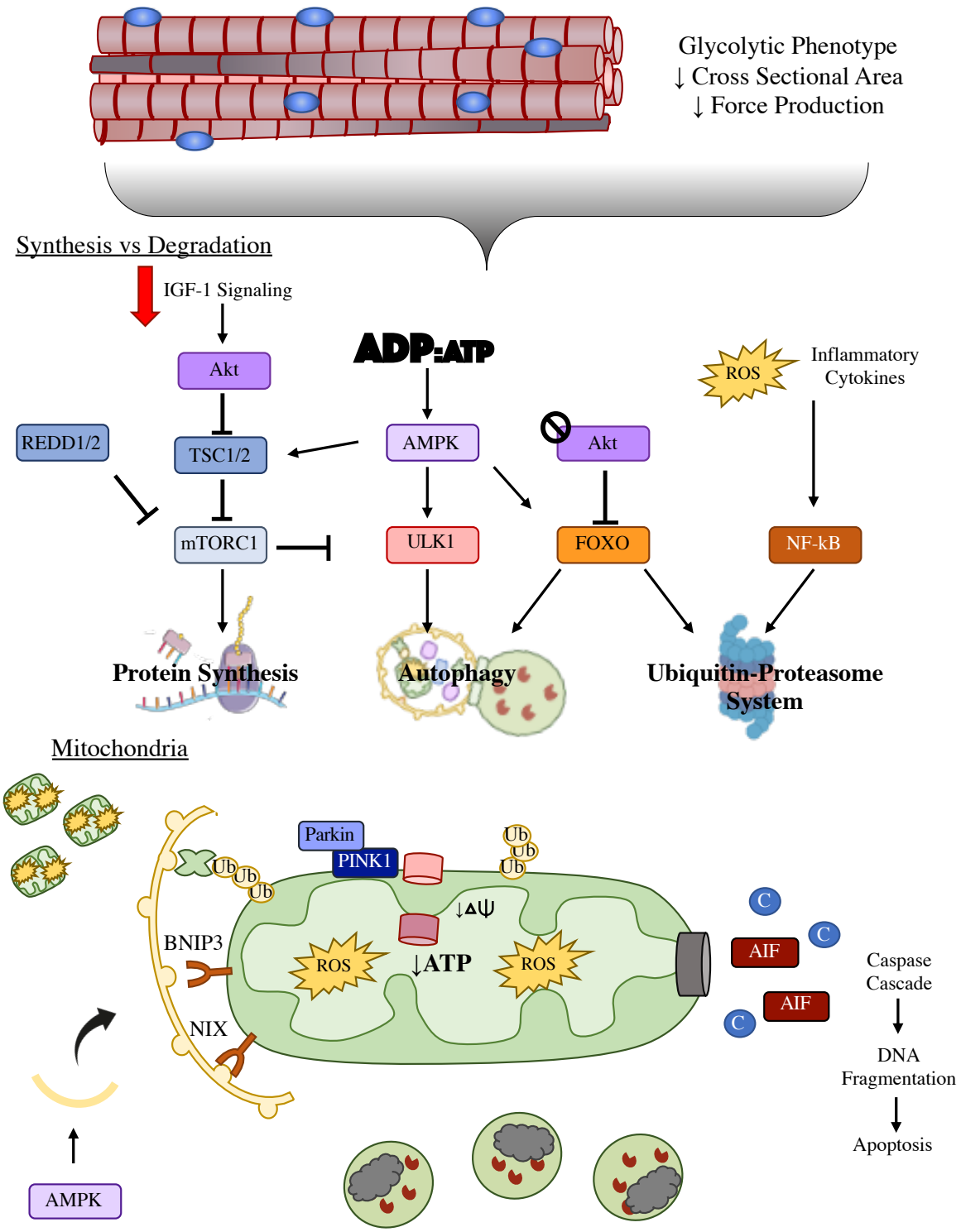
Glycolytic Phenotype
↓ Cross Sectional Area
↓ Force Production
Synthesis vs Degradation
IGF-1 Signaling
Akt
ADP:ATP
ROS
Inflammatory Cytokines
REDD1/2
TSC1/2
AMPK
Akt
mTORC1
ULK1
FOXO
NF-kB
Protein Synthesis
Autophagy
Ubiquitin-Proteasome System
Mitochondria
Parkin
PINK1
Ub
BNIP3
NIX
ROS
↓ΔΨ
↓ATP
C
AIF
Caspase Cascade
DNA Fragmentation
Apoptosis
AMPK

Figure 6: Adaptations to muscle disuse. Chronic disuse results in atrophy of skeletal muscle, which is characterized by a decrease in cross-sectional area of the muscle fibers and muscle weakness. This is also accompanied by a metabolic shift towards a more glycolytic phenotype of the muscle. Atrophy is largely attributed to a shift in the balance between protein synthesis and protein degradation, whereby mTORC1 is inhibited and cannot promote protein synthesis. mTORC1 is inhibited in a multi-faceted way during atrophy. First, anabolic inhibitors such as REDD1 and REDD2 are upregulated during disuse to negatively regulate mTORC1. Second, impaired insulin signaling through IGF-1 limits the activation of Akt, which normally removes the suppression from TSC1/2 on mTORC1. Third, as ATP production is reduced, AMPK is active and can activate TSC1/2 to inhibit mTORC1. Concomitant with the anabolic inhibition, catabolic pathways are largely upregulated. As mTORC1 normally serves as a negative regulator of ULK1 and the autophagy pathway, inhibition of mTORC1 promotes autophagy, and AMPK can actually phosphorylate ULK1 to activate the complex. Another target of AMPK is FOXO, a major regulator of catabolism and is largely upregulated during disuse. Akt is also usually a negative regulator of FOXO but as Akt itself is inhibited, FOXO is able to upregulate genes involved in autophagy and the ubiquitin proteasome system (UPS) to promote protein breakdown. Moreover, in many instances of atrophy, inflammation is accompanied with the release of inflammatory cytokines and ROS that activate NF-κB, which can also transcriptionally regulate a host of E3 ubiquitin ligases involved in UPS. Mitochondrial dysfunction is common consequence of prolonged disuse and is implicated in the atrophy phenotype. Damaged mitochondria produce less ATP, and generate excessive ROS, contributing to the activation of AMPK and NF-κB. If left unchecked, mitochondrial dysfunction can result in the opening of the mitochondrial permeability transition pore and allow the release of cytochrome c and apoptosis inducing factor (AIF). The presence of these in the cytosol trigger apoptosis through the activation of the caspase cascade leading to DNA fragmentation and cell death. The activation of AMPK may help mitigate this, through its activation of autophagy, as damaged mitochondria can be cleared through mitophagy. In fact, PINK1 and Parkin have been shown to accumulate on mitochondria during disuse. Furthermore, mitophagy receptors BNIP3 and NIX are thought to promote mitophagy during disuse. However, the functionality of the lysosomes remains unclear as there is evidence of lipofuscin, an indigestible material, within lysosomes that may mitigate the drive for mitophagy.

with Akt suppression[356]. Thus, in atrophic conditions protein synthesis is reduced in a pleiotropic manner that impinges on mTORC1.

Ubiquitin Proteasome System. The ubiquitin proteasome system (UPS), as the name implies, involves targeting proteins, via the addition of poly-ubiquitin chains, to signal their degradation via the proteasome[357]. The UPS is critical to the maintenance of skeletal muscle, as disruption of the UPS leads to muscle atrophy, and even declines in lifespan[358,359]. Ubiquitination is carried out through a cascade of enzymes that activate (E1 ubiquitin-activating enzyme), conjugate (E2 ubiquitin-conjugating enzyme) and ligate (E3 ubiquitin ligase) ubiquitin to lysine residues on target proteins[360]. MuRF1 and Atrogin1 (also known as MAFbx1) are E3 ubiquitin ligases that are exclusively expressed in muscle and are massively upregulated in atrophic conditions[361–363]. Expression of these E3 ubiquitin ligases closely correlates with losses in muscle mass, as these are most highly expressed during the first 7 days of disuse when the rate of muscle loss is the greatest[364]. Notably, genetic deletion of MuRF1 and Atrogin1 protects against disuse-induced atrophy indicating the importance of the UPS in muscle mass regulation[363,365,366]. Recently it has been shown that MuRF1 targets a number myofibrillar and contractile proteins which contribute to both the loss of muscle mass but also muscle function[360,367]. These findings illustrate the importance of protein breakdown and specifically UPS in atrophic conditions.

There are a number of signals that activate the UPS during disuse (Fig. 6). Inflammatory cytokines such as TNF-α, TWEAK and IL-1 stimulate NF-κB to upregulate atrogenes[362,368–370]. Elevations in ROS are commonly seen with disuse and can further activate NF-κB and FoxO expression[371]. Furthermore as was described, IGF-1 signaling is downregulated during disuse which reduces Akt signaling[355,372,373]. Normally, Akt is responsible for inhibiting FoxO, but as

IGF-1 is downregulated in atrophic conditions, FoxO is upregulated[373,374]. FoxO is generally considered to be one of the most important transcription factors during atrophy as it regulates E3 ubiquitin ligases, UPS-related genes and autophagy-related genes[204,206,208,375–377]. Furthermore, many myofibrillar proteins need to be primed in order to be degraded by the UPS. Calpains and caspases, are Ca^{2+}-dependent proteases, that cleave proteins to be degraded via the UPS and are upregulated following immobilization and denervation[378–381]. While the UPS is a major catabolic process that is heavily implicated in muscle atrophy it is not the only one.

Autophagy and Lysosomes. Autophagy is the process through which protein aggregates and organelles are degraded by the lysosome. Autophagy is a key regulator of muscle mass as inhibition of this pathway leads to muscle atrophy in the absence of any stimulus[207,208]. However, the role of autophagy in muscle wasting conditions may be a bit more nuanced as some have found a protective effect on muscle mass when autophagy is inhibited[382,383] while others have described exacerbated atrophy[384–386]. Reportedly, this was due to an accumulation of damaged and dysfunctional proteins and organelles which impeded muscle performance and accelerated muscle wasting. Thus, it suggests that autophagy is pivotal during atrophy and a balanced autophagic response is required.

During hindlimb immobilization and denervation, an upregulation of FoxO3 is observed and has been shown to regulate both genes involved in the UPS as well as autophagy[208]. Akt is a negative regulator of FoxO3, during immobilization Akt activity is reduced as early as 1 day and remains low throughout the intervention, which coincides with an accumulation of FoxO3 in the nucleus and its subsequent upregulation[206,387–390]. The importance of FoxO3 in atrophic conditions was illustrated upon genetic deletion of the transcription factor which reduced the

extent of muscle wasting[376,391–394]. This was attributed in part to a normalization of autophagy leading to a protective effect on muscle mass and function.

AMPK is another key regulator of the autophagy pathway. Following denervation, AMPK is decreased early on and then elevated following 3 days, at which point it has been shown to phosphorylate FoxO3 to promote its activation[395–397]. AMPK can also directly regulate the autophagy pathway by activating the ULK1 complex which was described earlier to be involved in the induction step of autophagy[389,397–400]. Furthermore, AMPK can directly inhibit mTORC1 by phosphorylating two of its subunits, Raptor and TSC2, thus not only can AMPK regulate autophagy it can also do so indirectly through mTORC1[191,401,402].

Following denervation, decrements are observed in LC3-II autophagy flux following 7 days of denervation[334,403]. Others have also noted that while autophagy flux decreased following 7 days, increases were observed 14 days and onwards[389]. Since there is evidence of TFEB and TFE3 activation following denervation[334], it is possible that this decline in autophagy flux is reflective of insufficient capacity which is subsequently met at later timepoints. Our group and others have shown a marked elevation in lysosomal markers following disuse, which coincides with increased TFEB and TFE3 expression as well as increased TFEB in the nucleus[334,403–406]. This would suggest a drive for lysosomal biogenesis that is likely stimulated to meet the autophagic demands brought on by disuse. However, we and others have reported evidence of lysosomal impairments with disuse such as the presence of lipofuscin in skeletal muscle that is indicative of lysosomal dysfunction[334,407]. This could then suggest that the elevation in lysosomal markers does not in fact represent a functional drive for lysosomal biogenesis but rather an accumulation of ineffective lysosomes. This is a critical point to address in future work, however the methodologies for assessing lysosomal function *in vivo* are still lacking. The

relevance of this is that dysfunctional lysosomes can undergo lysosomal membrane permeabilization (LMP) which results in the release of cathepsins and triggers cell death[408].

3.2.2 Structural and Functional Adaptations to Mitochondria

Declines in mitochondrial content and function in skeletal muscle are hallmark characteristics of the disuse phenotype ultimately shifting the muscle towards a glycolytic profile. Similar to the biphasic response of muscle atrophy, the most rapid and severe declines in mitochondrial content are observed early on following denervation (1-5 days), with more gradual decrements occurring thereafter[409]. Importantly, losses in content and mitochondrial dysfunction precede losses in muscle mass, indicating that mitochondria dysregulation contributes and potentially drives the atrophy phenotype in muscle.

Of the mitochondria that remain, this pool exhibits hallmark signs of dysfunction[409–411]. First, fission is favoured over fusion, resulting in a highly fragmented reticulum, characterized by small often circular mitochondria. Increased expression of Drp1 and Fis1, alongside declines in Mfn1 and Mfn2 have been reported with denervation and immobilization[412]. Interestingly, it has been shown that overexpression of fusion markers such as Mfn1 and Opa1 protect against mitochondrial loss and preserve mitochondrial homeostasis[413]. Furthermore, promoting fission alone induces muscle atrophy, indicating the destructive potential of fragmented mitochondria on skeletal muscle. These small fragmented mitochondria produce more ROS, and contribute significantly to increased oxidative stress within the cell. Increased oxidative stress causes mitochondrial membrane instability, promotes mitochondrial permeability transition pore (mtPTP) opening, contributes to a loss of membrane potential, inhibits protein synthesis, and can oxidize proteins, lipids and nucleic acids promoting proteolysis and cell death[409,414,415]. Membrane instability and mtPTP opening is critical as this promotes the release of apoptosis-

inducing factors from the mitochondrion which include cytochrome c and AIF[409,414,416,417]. The presence of these factors in the cytosol initiates the caspase cascade resulting in myonuclear decay and cell death. Thus, targeting mitochondrial ROS specifically is a viable approach to mitigating atrophy. Treatment with SS-31, a mitochondrial-targeted antioxidant prevented muscle atrophy following 7 days of casting by normalizing the expression and activity of the autophagy and UPS pathways[410,418].

Although fission often has a negative connotation as it causes mitochondrial fragmentation, it is required for mitochondrial clearance[419]. As elongated mitochondria cannot undergo mitophagy, fission is required to maintain mitochondrial homeostasis. Increased ROS emission, inhibition of protein import, losses in membrane potential and poor ATP production are all commonly seen with disuse and are all signals for mitophagy[337]. As such it is not surprising that increased expression of PINK1 and Parkin and mitochondrial localization are observed with denervation[397,403,407,412]. Increases in BNIP3 are also observed and thought to contribute to receptor-mediated mitophagy[368,420]. As such increased mitophagy flux is observed 7 days post denervation, however others have reported declines following 10 day, this suggests that mitophagy flux may exhibit time-dependent changes during the course of disuse[397,403]. Furthermore, it has been suggested in models of autophagy inhibition, that atrophy is exacerbated following denervation due to the accumulation of damaged organelles, namely mitochondria[384]. It is thought that these dysfunctional mitochondria continue to produce ROS leading to enhanced oxidative stress and induce apoptosis thereby resulting in an exacerbated atrophy phenotype.

3.2.3 Impact of Sex on Skeletal Muscle Atrophy

Aside from its role in mitochondrial regulation, estrogen also appears to be involved in skeletal muscle maintenance. While counterintuitive as females have less muscle mass, estrogen has been positively correlated with muscle mass[133], as estrogen decreases during menopause women typically experience a decline in muscle mass and increased risk of injury[421]. Furthermore, estrogen administration repressed immobilization-induced muscle atrophy in male animals[422]. Despite these findings, in humans, women experience more rapid muscle mass loss and this is associated with increased mortality following ICU stays[423,424]. Studies using hindlimb unloading showed a more rapid loss in muscle mass in females, and following 7 days a greater reduction in CSA, but no differences in the percentage of muscle mass lost[219,353]. While others have reported greater reductions in soleus mass in female mice[425], preservation of muscle mass and function in female rats following 14 days of unloading[426] and studies in humans suggest no differences in CSA between males and females following 14 days of unloading[135]. Thus, there exist discrepancies in the literature regarding the effect of sex on skeletal muscle atrophy. It is possible that this can be attributed to differences in models and durations of intervention, thus more work is warranted to better understand how sex impacts muscle atrophy.

As was described, muscle atrophy is largely attributed to declines in anabolic pathways and a greater reliance on catabolism. While increased inhibitory FOXO3a phosphorylation has been observed in females following disuse, increased ubiquitination was also seen[425] and higher mRNA expression of catabolic factors like *Gadd45a*[353]. Females also exhibit higher mRNA expression of anabolic inhibitors *Deptor* and *Redd14*, and fractional protein synthesis rates were decreased earlier in females in comparison to males[353]. Taken together this suggests that females exhibit a greater shift towards catabolism following disuse.

Furthermore, while males experience higher ROS emission basally, the induction of ROS following unloading is greater in females[220]. As such, overexpression of the mitochondrial antioxidant, MCAT, protected against atrophy in females but not males [219]. BNIP3, a marker of mitophagy, was increased in females throughout 7 days of unloading[220], and increased MitoTimer red fluorescence has also been observed in female mice[219]. However, more stringent methods of assessing mitophagy are still lacking.

Finally, there is evidence to suggest that inflammation-induced atrophy, such as cancer cachexia, is worse in males than it is in females[423]. Following exercise, females exhibit less muscle damage in part due to less neutrophil and macrophage infiltration[130,427]. It has been proposed that estrogen limits inflammation due to its ability to stabilize membranes thereby limiting Ca^{2+} influx and decreasing calpain activation[130,428] which are known to mediate neutrophil invasion[429,430]. Again, this is a proposed mechanism following exercise to limit muscle damage but could potentially in part explain why females are protected in inflammation-induced atrophy models.

5.0 SUMMARY

Skeletal muscle is a highly plastic tissue, capable of responding to external stimuli and adapting to metabolic demands. Mitochondria play a vital role in the maintenance and adaptability of skeletal muscle. Thus, investigating the mechanisms and signals involved in how mitochondria adapt to positive and negative stimuli, such as exercise and disuse, contributes to our understanding of the regulation of skeletal muscle health. Characterising these molecular pathways provides the potential for therapeutic interventions during instances of mitochondrial dysfunction and myopathy, such as aging, metabolic diseases, cancer cachexia, and more.

CHAPTER THREE:

PHD OBJECTIVES & HYPOTHESES

It is clear that the process of mitochondrial recycling, mitophagy, is vital in the maintenance and adaptability of mitochondria and the overall health of skeletal muscle. While mitophagy has been implicated in both exercise-induced and disuse-induced adaptations, this is a rather contradictory finding. This emphasizes the need to understand how lysosomal content and quality is affected in these conditions to fully appreciate how eliciting mitochondrial clearance can result in such opposing phenotypes. Furthermore, as most research has long been male-dominated, the role of biological sex on mitophagy dynamics and lysosomal regulation has yet to be uncovered. Thus, the purpose of this dissertation was to investigate how lysosomes adapt to exercise and denervation-induced disuse, with a particular focus on how mitophagy is impacted in these conditions, and the resulting mitochondrial phenotype. Based on this, my dissertation will have the following objectives and hypotheses:

OBJECTIVE #1:

To investigate how lysosomes adapt, both in content and in function, to exercise using an *in vitro* model to stimulate contractile activity, while also evaluating the contribution of the lysosomal regulators TFEB and TFE3 in mediating both lysosomal and mitochondrial adaptations.

Hypotheses:

1. Lysosomes will adapt to chronic contractile activity (CCA) both quantitatively and qualitatively. As redundant roles have been described for TFEB and TFE3, exercise-induced lysosomal adaptations will occur independent of either transcription factor;

2. Based on the literature, we hypothesize that mitochondrial impairments will be present in the absence of TFEB or TFE3, but CCA will rescue this defect;

3. In the absence of both TFEB and TFE3, exercise-induced mitochondrial and lysosomal adaptations will be abrogated due to declines in mitophagy flux.

OBJECTIVE 2:

To further characterize the sexual dimorphism apparent in lysosomes and mitophagy regulation both basally and in response to denervation-induced disuse.

Hypotheses:

1. Given the limited literature available, we hypothesize that females will have greater lysosomal content which would support increased mitophagy flux rates basally;

2. In response to denervation, both males and females will lose muscle mass, mitochondrial content and exhibit mitochondrial dysfunction;

3. In line with the previous hypothesis, given the postulated higher rates of flux, females will exhibit less mitochondrial dysfunction in comparison to males in response to denervation.

OBJECTIVE 3:

To evaluate the role of TFE3, a lysosomal regulator, in denervation-induced atrophy and mitochondrial impairments, with a continued focus on biological sex differences.

Hypotheses:

1. Denervation will lead to increased lysosomal drive to support increased mitophagy flux to remove dysfunctional organelles;

2. The absence of TFE3 will impact lysosomal content and function following denervation, resulting in greater evidence of mitochondrial dysfunction;

3. Males lacking TFE3 will exhibit the most severe phenotype in response to denervation, as males are hypothesized to have less lysosomes in comparison to females, and the absence of TFE3 will exacerbate this deficit.

CHAPTER FOUR:

ROLE OF TFEB AND TFE3 IN MEDIATING LYSOSOMAL AND MITOCHONDRIAL ADAPTATIONS TO CONTRACTILE ACTIVITY IN MUSCLE CELLS

ASHLEY N. OLIVEIRA[1], YUKI TAMURA[2], JONATHAN M. MEMME[1] & DAVID A. HOOD[1]

[1]Muscle Health Research Center, School of Kinesiology and Health Science, York University, Toronto, ON, Canada M3J 1P3
[2]Graduate School of Health and Sport Science, Nippon Sport Science University, Fukusawa, Setagaya, Tokyo, Japan.

Keywords: Lysosomal biogenesis; lysosomal function; mitophagy; oxygen consumption; mitochondrial biogenesis; C2C12 skeletal muscle cell

Running Head: TFEB and TFE3 in adaptations to contractile activity

Funding: This work was supported by the Canadian Institutes for Health and Research.

Data Availability: Data are available upon request from the authors.

To whom correspondence should be addressed: David A. Hood, PhD
Muscle Health Research Centre,
York University, 4700 Keele St,
Toronto, ON, M3J 1P3, Canada
Tel: (416) 736-2100 ext.66640
Email: dhood@yorku.ca

This manuscript has been submitted to Autophagy Reports (December, 2022).

Abstract

Exercise is potent stimulus for mitochondrial adaptations, serving to activate mitochondrial biogenesis as well as mitochondrial. Through the process of mitophagy, dysfunctional mitochondria are selectively targeted and recycled via the lysosomes, which is activated following a single bout of exercise. The microphthalamia (MiT) family of transcription factors, including TFEB and TFE3, are widely recognized as the master regulators of lysosomal biogenesis, as they homo- and hetero-dimerize to transcriptionally regulate lysosomal and macroautophagy-related genes. It is currently unknown to what extent TFEB and TFE3 regulate mitophagy, and whether these transcription factors mediate mitochondrial adaptations to contractile activity (CA). Here we show that following an acute bout of CA, LC3-II mitophagy flux is induced and the absence of TFEB or TFE3 impairs this acute mitophagic response. However, the loss of either transcription factor alone does not mitigate the improvements in oxygen consumption seen following chronic CA (CCA). CCA also elicited functional improvements in lysosomes including a reduction in size and increased proteolytic activity, evidenced by increased digestion and unquenching of DQ-BSA fluorophore, thereby illustrating a level of redundancy between the two transcription factors in mediating CCA-induced adaptations. However, in the absence of both TFEB and TFE3, lysosomal adaptations were not observed following CCA and CCA-induced mitochondrial adaptations were attenuated. These findings underscore the importance of the lysosomes, and of TFEB and TFE3, in mediating mitochondrial adaptations to chronic contractile activity.

List of Abbreviations

AMBRA1	Autophagy and beclin1 1 regulator 1
AMPK	5'AMP-activated protein kinase
ATG7	Autophagy related 7
ATP5A	ATP synthase F1 subunit alpha
BafA	Bafilomycin A_1
BNIP3	BCL2 interacting protein 3
CA	Contractile activity
CCA	Chronic contractile activity
CLEAR	Coordinated lysosome expression and regulation
COX I	Cytochrome c oxidase subunit 1
COX IV	Cytochrome c oxidase subunit IV
CTSD	Cathepsin D
Drp1	Dynamin related protein 1
FBS	Fetal bovine serum
Fis1	Mitochondrial fission 1 protein
FUNDC1	FUN14 domain containing 1
HS	Horse serum
LAMP1/2	Lysosome membrane associated protein 1/2
LC3	Microtubule-associated protein 1A/1B light chain 3B
MCOLN1/TRPML1	Mucolipin1
MiT	Microphthalmia
MQC	Mitochondrial quality control
mTORC1	Mammalian/Mechanistic target of rapamycin complex 1
NDUFB8	NADH:Ubiquinone oxidoreductase subunit B8
NIX/BNIP3L	BNIP3-like protein
OCR	Oxygen consumption rate
PHB2	Prohibitin 2
PINK1	PTEN-induced kinase 1
PS	Penicillin-streptomycin
ROS	Reactive oxygen species
SCR	Scramble
SDHB	Succinate dehydrogenase complex iron sulfur subunit B
SQSTM1 or p62	Squestosome 1
TFEB	Transcription factor EB
TFE3	Transcription factor E3
UQCRC2	Ubiquinol-Cytochrome c reductase core protein 2
v-ATPase	Vacuolar-type ATPase
VDAC	Voltage-dependent anion channel
VEH	Vehicle

Introduction

Mitochondrial quality control (MQC) comprises a number of mechanisms that aim to maintain a healthy pool of mitochondria. Within MQC, mitochondrial biogenesis governs the synthesis of new organelles, and mitophagy is responsible for degrading dysfunctional mitochondria (reviewed in [5]). Mitophagy is a selective form of autophagy, which is a broad term for the recycling of damaged cellular components via the lysosomes into their basic constituents to support future protein synthesis [431]. Through highly directed events of fission, that are largely governed by dynamin-related protein 1 (Drp1) and mitochondrial fission protein 1 (Fis1), dysfunctional portions of the mitochondrial reticulum are identified, excised and targeted for degradation[107]. Loss of membrane potential[229,432], inhibition of import[228,232,433], accumulation of misfolded proteins[233,234] and elevations in reactive oxygen species (ROS) emission[419,434] are common mitochondrial characteristics that initiate and signal mitophagy. The most well described mechanism is the PTEN induced kinase 1 (PINK1)-Parkin pathway, which stems from a loss of membrane potential leading to the arrest of PINK1 import into the mitochondrial matrix[229,231,432]. The import of PINK1 is also sensitive to misfolded proteins in the matrix, which trigger the dissociation of the protein motor complex from the translocase of the inner membrane and prevent the import of PINK1[233,234]. Accumulation of PINK1 on the outer mitochondrial membrane signals the recruitment and activation of Parkin, an E3 ubiquitin ligase which poly-ubiquitinates outer mitochondrial membrane proteins[230,235,237,239]. The autophagosome, a membranous structure largely comprised of scavenged lipids and the lipidated form of microtubule-associated protein 1A/1B-light chain 3 (LC3), LC3-II, is targeted to the dysfunctional organelle and anchored to the ubiquitin chains through adaptor proteins such as sequestosome1/p62 (SQSTM1) and Optineurin[247,435]. Independent of PINK1 and Parkin,

a number of receptors have been identified that respond to mitochondrial stress to initiate mitophagy including FUNDC1[249], NIX[251], BNIP3[436], AMBRA1[437], PHB2[438] and even cardiolipin has been shown to become externalized following stress and directly binding to LC3[256]. There is no evidence to suggest that each mechanism acts exclusively, rather it is more likely that multiple signaling pathways occur simultaneously. Furthermore, this illustrates the importance of mitophagy and underscores the reliance of the health of the cell on this MQC process as mitophagy can be carried out in a highly multi-faceted way.

Central to mitophagy are the lysosomes, the degradative organelle within the cell. Lysosomes are regulated by the microphthalmia (MiT) family of transcription factors, including transcription factor EB (TFEB) and transcription factor E3 (TFE3), which homo- or hetero-dimerize to bind to coordinated lysosomal expression and regulation (CLEAR) sites on the genome to regulate lysosome- and autophagy-related genes[6,166,167,169,171]. Basally, TFEB and TFE3 are sequestered in the cytosol through mTORC1 phosphorylation of Ser^{122}, Ser^{142}, Ser^{211} for TFEB, and Ser^{321} for TFE3, and bound to chaperone 14-3-3[169,174]. Signals such as mTORC1 inhibition, brought on by starvation, activation of Calcineurin, through the influx of cytosolic calcium, can facilitate the dephosphorylation and dissociation from 14-3-3 of TFEB and TFE3 to allow nuclear translocation[175,439,440]. Recently, it has also been shown that TFEB and TFE3 can be directly oxidized by ROS on a highly conserved exposed cysteine, thereby promoting their nuclear localization[189]. Furthermore, AMPK can directly phosphorylate the triple-serine residue on the C-terminus of TFEB and TFE3 to promote their nuclear localization, and this post-translational modification is required for DNA binding[190].

In skeletal muscle, Ca^{2+}, ROS and AMPK activation are common signals that occur with contractile activity that have been linked to mitochondrial biogenesis. It has been shown

repeatedly that a single bout of exercise can trigger mitophagy and initiate lysosomal biogenesis[241,248,312,315,326,441]. Furthermore, TFEB and TFE3 are activated and translocate to the nucleus following an acute bout of exercise[197,200,324]. Following training, as the mitochondrial pool improves, a decline in mitophagy flux is observed, however the muscle is primed to handle future stress as training increases lysosomal content[240,312,313,316]. Through mitophagy there is a strong link between lysosomes and mitochondria, as the function of one is required for the health of the other, however recent literature has argued that the relationship between the two organelles is far more bidirectional. Dysfunctional lysosomes can impact mitochondrial status and this is commonly observed in lysosomal storage disorders such as Pompe and Danon disease[197,200,261,262]. However, it has been recently shown that disrupting mitochondrial function leads to impaired breakdown within the lysosome and the appearance of large vacuoles[264,442]. Furthermore, while acute mitochondrial stress activates the MiT family, prolonged exposure represses lysosomal biogenesis[265]. In addition, mitochondria and lysosomes form dynamic contact sites, thought to serve as communication points. These sites are important in regulating fission events[111] and the transfer of Ca^{2+} into mitochondria via the lysosomal Ca^{2+} channel, TRPML1/MCOLN1[267]. These findings are beginning to uncover a reciprocal relationship between these organelles, and how coordinated the maintenance of their functions can be.

While exercise is widely accepted as a potent stimulus for improving mitochondrial health, often attributed to the stimulation of mitochondrial biogenesis, the importance of mitophagy and the lysosomes has yet to be fully been explored. TFEB and TFE3 have been identified as key metabolic regulators during exercise as the absence of TFE3 results in poor glucose handling and perturbed lipid oxidation during exercise[197,200]. Recent work *in vivo* has illustrated that lysosomal biogenesis actually precedes increases in mitochondrial content and

function during training[326], which may suggest that lysosomal adaptations are required for mitochondrial adaptations to exercise. To evaluate the role of lysosomal regulators, TFEB and TFE3, in mediating mitochondrial adaptations, the expression of these transcription factors was reduced using siRNA in murine skeletal muscle cells. When differentiated into myotubes, C2C12 cells maintain their contractile properties and can be induced to contract through electrical stimulation, a model of "exercise in a dish". This method is now widely used and reported in the literature, hereby referred to as chronic contractile activity or CCA[443,444]. We hypothesized that the loss of these transcription factors alone would not impact mitochondrial biogenesis, that any impairments would be rescued by CCA, but that the absence of both transcription factors together would blunt mitochondrial adaptations to CCA.

Results

Acute contraction-induced mitophagy flux in siTfeb or siTfe3 conditions. To mitigate discrepancies in myotube formation cells were transfected on day 3 of differentiation (Fig. 1A), at which stage myoblasts have already aligned and begun to fuse with one another. *Tfeb* and *Tfe3* mRNA expression was successfully reduced by 83% and 79% respectively (Fig. 1B-C) following siRNA treatment independently, and in the absence of a compensatory response in the expression of the other transcription factor. Due to the highly dynamic nature of mitophagy, Bafilomycin A (BafA) was administered 24 hr prior to harvesting (Fig. 1A) and mitochondrial isolation to block the degradation of autophagosomes to accurately capture mitophagy flux (Fig. 1A). Cells were subjected to an acute 3 hr bout of electrical stimulation to induce contractile activity (CA) to evaluate the role of TFEB and TFE3 in mediating acute responses to contractile activity (Fig. 1A). Following BafA treatment, SQSTM1 and LC3-II accumulated in all

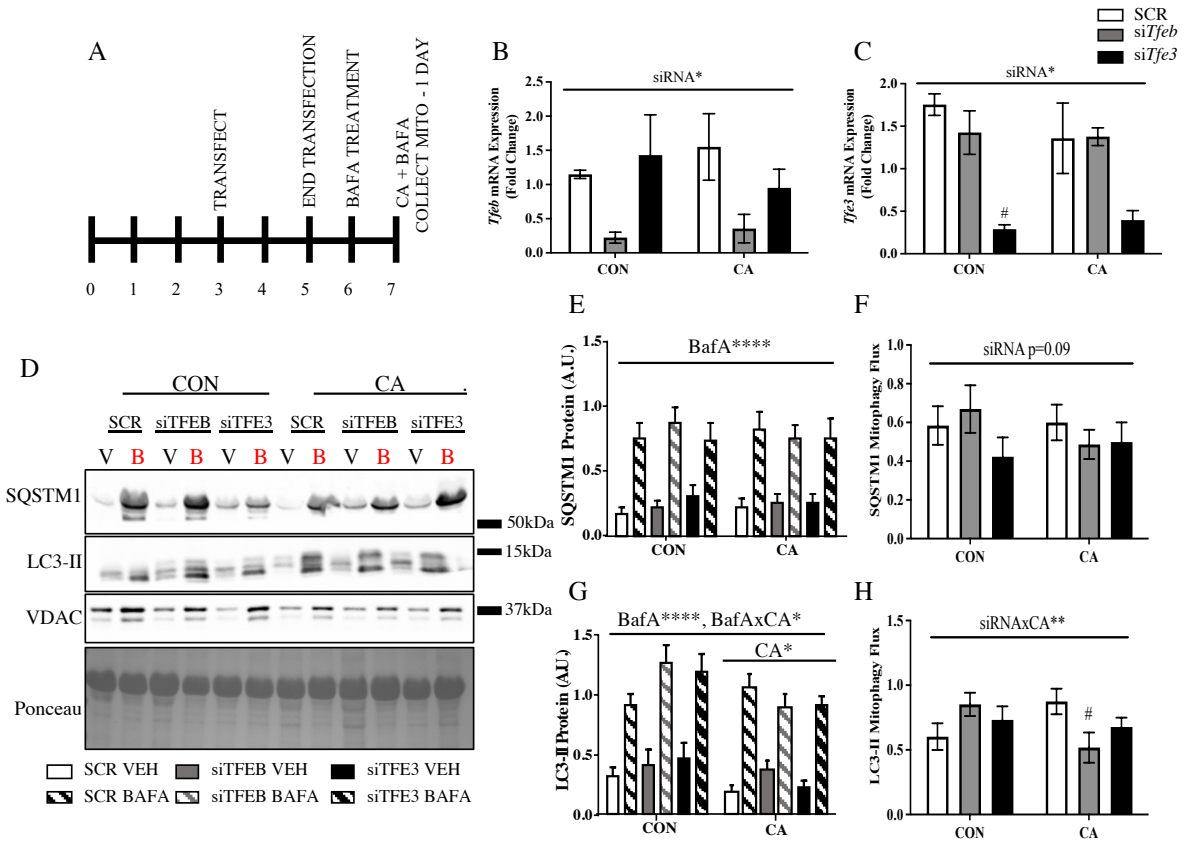

Figure 1: Acute contraction-induced mitophagy flux in si*Tfeb* or si*Tfe3* conditions. Schematic of the experimental design (A). *Tfeb* (B) and *Tfe3* (C) mRNA expression following siRNA treatment and an acute bout of CA normalized to both *Actb* and *B2mg* (n=3). Representative western blots for SQSTM1, LC3-II in mitochondrial fractions (D). Quantification of SQSTM1 protein content in mitochondrial fractions (E). Quantification of SQSTM1 mitophagic flux, calculated as the difference between BafA- and Veh-treated conditions (F). Quantification of LC3-II protein content in mitochondrial fractions (G), Quantification of LC3-II mitophagic flux, calculated as above (H, n=9). Statistics are shown as follows, "siRNA" represents a main effect of KD; "BafA" indicates a main effect of BafA treatment; "CA" denotes a main effect of CA; "BafAxCA" reflects an interaction effect between BafA and CA; "siRNAxCA" represents a main effect of KD and CA; * denotes the p value for each effect, *, $p<0.05$; **, $p<0.01$; ***, $p<0.001$; ****, $p<0.0001$; # reflects post-hoc analyses indicating a significant difference from time-matched SCR conditions, $p<0.05$.

conditions as expected (Fig. 1D, 1E, 1G). SQSTM1 mitophagy flux was modestly increased by acute CA (Fig. 1F), while LC3-II mitophagy flux was increased by 45% in SCR conditions (Fig. 1H). This CA-induced mitophagic response was not observed with the reduction of TFEB where LC3-II mitophagy flux actually decreased by 39%. No changes were observed with the reduction of TFE3 (Fig. 1H).

Chronic contraction-induced mitophagy flux in siTfeb or siTfe3 conditions. We have previously documented that although a single bout of contractile activity induces mitophagy flux, repeated bouts result in reduced flux as the pool of organelles is improved, thereby obviating the need for mitochondrial clearance[313]. To evaluate the role of TFEB and TFE3 in mediating this adaptive response, cells were subjected to four consecutive bouts of electrical stimulation, and were treated with BafA 24 hrs prior to collection (Fig. 2A). Following siRNA transfection, *Tfeb* and *Tfe3* mRNA expression was reduced by 77% and 60% respectively, both basally and following chronic CA (CCA; Fig. 2B-C). Surprisingly, a compensatory effect was observed with the reduction of TFEB following CCA, as *Tfe3* expression was further increased (Fig. 2C). With the reduction TFEB or TFE3, no significant changes were observed in the transcript levels of *Sqstm1*, *Map1lc3b*, *Beclin1* or *Park2*. However, following CCA, *Sqstm1* mRNA trended to increase, and in the absence of TFEB, *Sqstm1* was further upregulated by 57% (Fig. 2D). Similarly, following CCA a reduction in *Map1lc3b* and *Beclin1* mRNA was observed in SCR conditions, however with the reduction of TFEB these were increased in comparison by 66% and 67% respectively (Fig. 2E-F). Reduced *Map1lc3b* and *Beclin1* mRNA (44% and 30% respectively) was observed basally with the reduction of TFE3 and was unchanged following CCA. No effect of CCA or knockdown was observed on *Park2* mRNA (Fig. 2G).

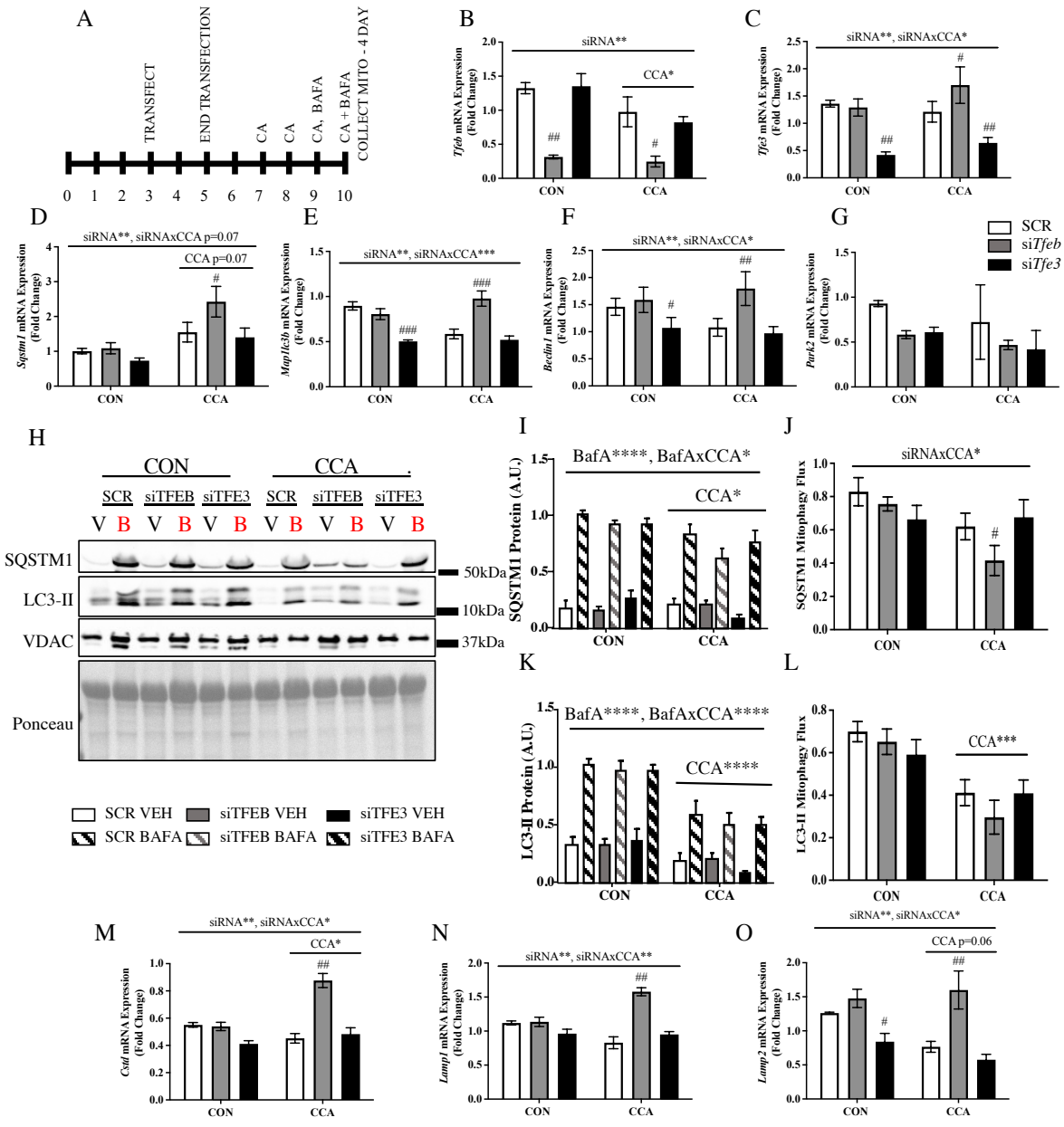
A
TRANSFECT
END TRANSFECTION
CA
CA
CA, BAFA
CA + BAFA
COLLECT MITO - 4 DAY
0 1 2 3 4 5 6 7 8 9 10
B
Tfeb mRNA Expression (Fold Change)
siRNA**
CCA*
CON
CCA
C
Tfe3 mRNA Expression (Fold Change)
siRNA**, siRNAxCCA*
D
Sqstm1 mRNA Expression (Fold Change)
siRNA**, siRNAxCCA p=0.07
CCA p=0.07
E
Map1lc3b mRNA Expression (Fold Change)
siRNA**, siRNAxCCA***
F
Beclin1 mRNA Expression (Fold Change)
siRNA**, siRNAxCCA*
G
Park2 mRNA Expression (Fold Change)
SCR
siTfeb
siTfe3
H
CON
CCA
SCR siTFEB siTFE3 SCR siTFEB siTFE3
V B V B V B V B V B V B
SQSTM1
LC3-II
VDAC
Ponceau
50kDa
10kDa
37kDa
SCR VEH
siTFEB VEH
siTFE3 VEH
SCR BAFA
siTFEB BAFA
siTFE3 BAFA
I
SQSTM1 Protein (A.U.)
BafA****, BafAxCCA*
CCA*
J
SQSTM1 Mitophagy Flux
siRNAxCCA*
K
LC3-II Protein (A.U.)
BafA****, BafAxCCA****
CCA****
L
LC3-II Mitophagy Flux
CCA***
M
Ctsl mRNA Expression (Fold Change)
siRNA**, siRNAxCCA*
CCA*
N
Lamp1 mRNA Expression (Fold Change)
siRNA**, siRNAxCCA**
O
Lamp2 mRNA Expression (Fold Change)
siRNA**, siRNAxCCA*
CCA p=0.06

Figure 2: Chronic contraction-induced mitophagy flux in si*Tfeb* or si*Tfe3* conditions. Schematic of the experimental design (A). *Tfeb* (B) and *Tfe3* (C) mRNA expression following siRNA treatment and CCA normalized to both *Actb* and *B2mg*. Gene expression of *Sqstm1* (D), *Map1lc3b* (E), *Beclin1* (F), and *Park2* (G) normalized to both *Actb* and *B2mg* (n=3). Representative western blots for SQSTM1, LC3-II in mitochondrial fractions (H). Quantification of SQSTM1 protein content in mitochondrial fractions (I). Quantification of SQSTM1 mitophagic flux, calculated as the difference between BafA- and Veh-treated conditions (J). Quantification of LC3-II protein content in mitochondrial fractions (K), Quantification of LC3-II mitophagic flux, calculated as above (L, n=9). Gene expression of *Ctsd* (M), *Lamp1* (N), and *Lamp2* (O) normalized to *Actb* and *B2mg* (n=3). Statistics are shown as follows, "siRNA" represents a main effect of KD; "BafA" indicates a main effect of BafA treatment; "CCA" denotes a main effect of CCA; "BafAxCA" reflects an interaction effect between BafA and CCA; "siRNAxCCA" represents a main effect of KD and CCA; * denotes the p value for each effect, *, $p<0.05$; **, $p<0.01$; ***, $p<0.001$; ****, $p<0.0001$; # reflects post-hoc analyses indicating a significant difference from time-matched SCR conditions, $p<0.05$; ##, $p<0.01$.

Following BafA treatment, SQSTM1 and LC3-II accumulated in mitochondrial fractions as expected (Fig. 2I, 2K). With the reduction of TFEB or TFE3, no significant changes in SQSTM1 or LC3-II mitophagy flux were observed basally (Fig. 2J, 2L). Similarly, autophagy flux in whole cell lysates also did not differ between conditions basally (Fig. S1). In line with previous literature, SQSTM1 mitophagy flux was reduced following CCA in both SCR and si*Tfeb* conditions by 25% and 45% respectively, however no change was observed with the reduction of TFE3 (Fig. 2J). A decline in LC3-II mitophagy flux was observed across all conditions irrespective of TFEB or TFE3 expression following CCA (Fig. 2L).

No differences were observed with the reduction of TFEB or TFE3 on the gene expression of various lysosomal markers under basal conditions (Fig. 2M-O). Following CCA, in SCR conditions *Ctsd*, *Lamp1* and *Lamp2* expression was decreased, in line with the *Map1lc3b* and *Beclin1* mRNA, suggesting less transcriptional drive for autophagy and lysosomal machinery (Fig. 2M-O). However, with the reduction of TFEB, CCA led to increases in *Ctsd, Lamp1* and *Lamp2* mRNA by 63%, 40%, and 10%, respectively (Fig. 2M-O). It should be noted

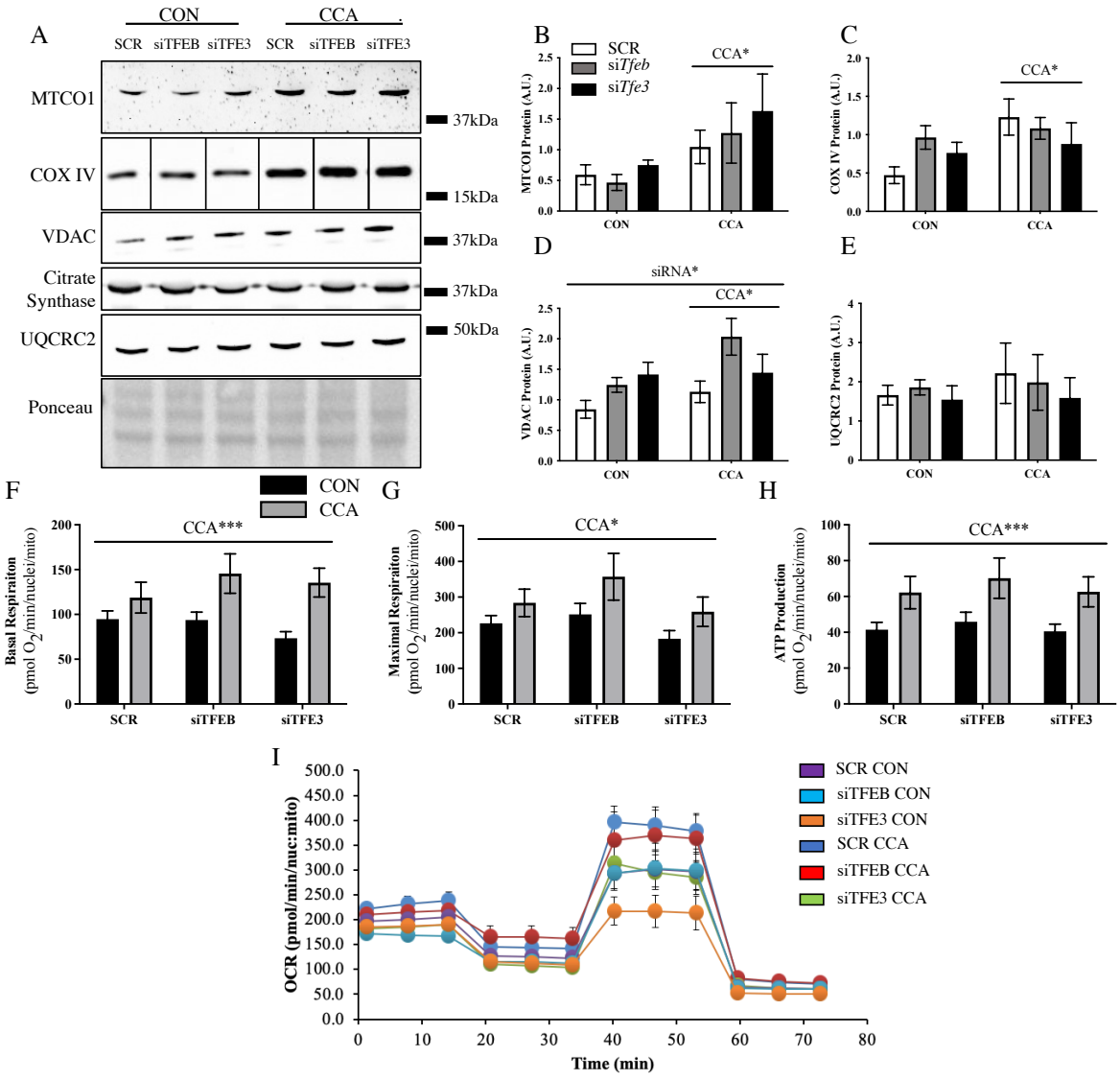

Figure 3: Mitochondrial adaptations to chronic contractile activity in si*Tfeb* or si*Tfe3* conditions. Representative western blots of mitochondrial markers following CCA (A). Graphical representation MTCO1 (B), COX IV (C), VDAC (D), UQCRC2 (E) following CCA. Oxygen consumption rates during basal respiration (F), maximal respiration (G) and coupled respiration, or ATP production (H) assessed using Seahorse corrected for nuclear and mitochondrial content. Experiments were reproduced 3 times, with 12 technical repeats per experiment. Representative tracing of oxygen consumption (I). Statistics are shown as follows, "siRNA" represents a main effect of KD; "CCA" denotes a main effect of CCA; * denotes the p value for each effect, *, $p<0.05$; ***, $p<0.001$.

that a trend for increased *Tfe3* mRNA expression was observed in the absence of TFEB following CCA. This potential compensatory increase may have supported the increased gene expression observed (Fig. 2C).

Mitochondrial adaptations to chronic contractile activity in the absence of TFEB or TFE3. The reduction of TFEB or TFE3 had no impact on the protein levels of mitochondrial markers, COX I, COX IV, VDAC or UQCRC2 basally (Fig. 3A-E). Oxygen consumption was also not different with the reduced expression of TFEB or TFE3, indicating that TFEB or TFE3 are not required individually for the maintenance of mitochondria basally in skeletal muscle cells (Fig. 3.F-I).

Mitochondrial adaptations to CCA have been well documented *in vivo*, as well as *in vitro*. Protein expression of a number of mitochondrial markers including COX I, COX IV, VDAC and UQCRC2 increased irrespective of TFEB or TFE3 expression (Fig 3A-E). Assessment of mitochondrial function revealed significant increases in basal respiration, maximal respiration and ATP production following CCA, and this occurred irrespective of TFEB or TFE3 status (Fig. 3F-I), indicating that TFEB or TFE3 are not required individually for mitochondrial adaptations to CCA.

Lysosomal adaptations to chronic contractile activity in siTfeb or siTfe3 conditions. Unexpectedly, we observed a 2-fold and 1.8-fold increase in lysosomal area basally with the reduced expression of TFEB and TFE3, respectively, based on Lysotracker Green staining (Fig. 4A, 4B). To further appreciate lysosomal morphology, which greatly impacts lysosomal function, cells were stained with Lysoview 405 and imaged live. The reduction of TFEB or TFE3 basally did not result in any changes in lysosomal size (Fig. 4C, 4D). To assess lysosomal function, cells were treated with DQ-BSA, a fluorescent-tagged protein that emits green

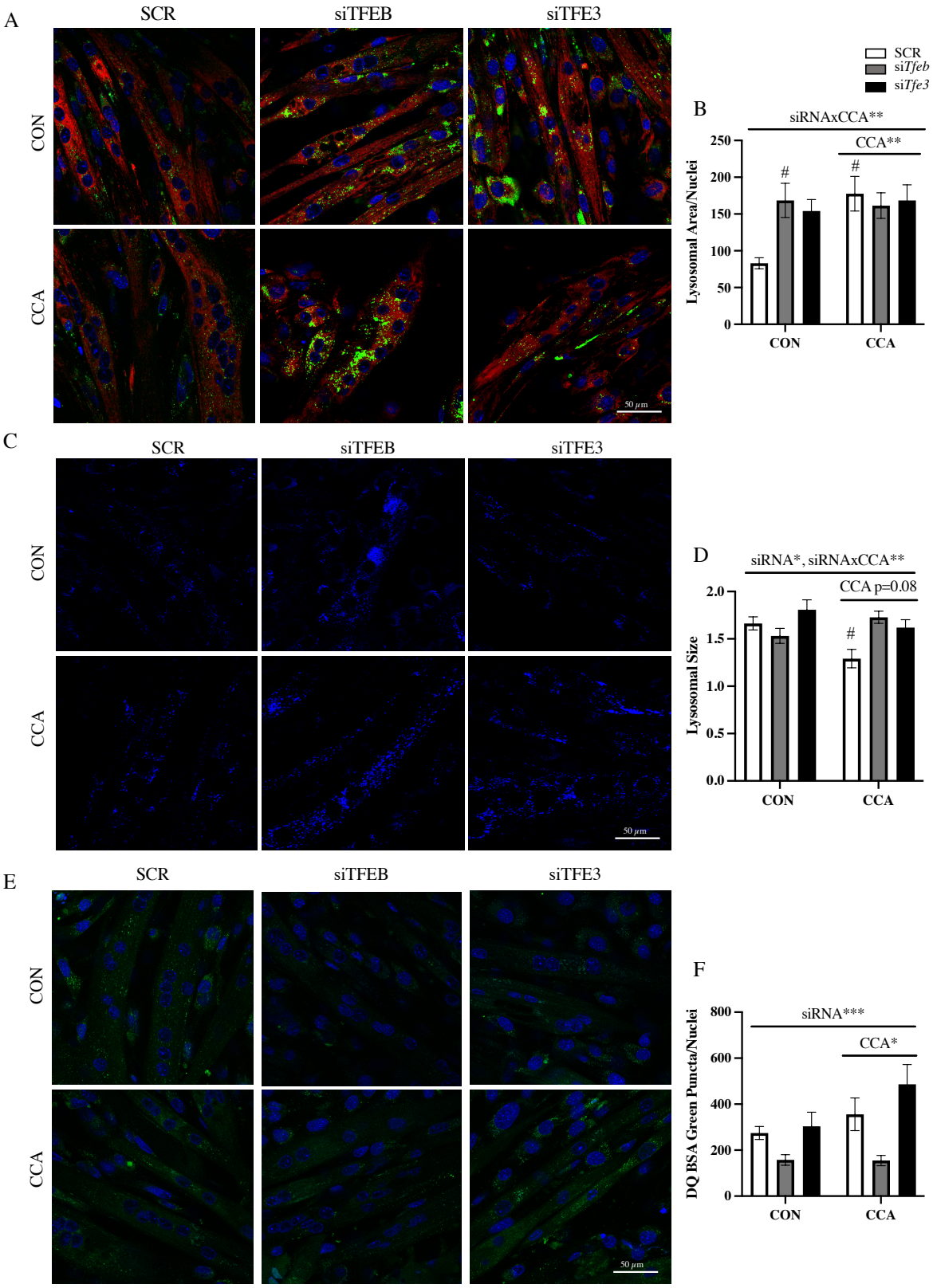
A
SCR
siTFEB
siTFE3
CON
CCA
50 μm
B
SCR
siTfeb
siTfe3
siRNAxCCA**
CCA**
#
#
Lysosomal Area/Nuclei
250
200
150
100
50
0
CON
CCA
C
SCR
siTFEB
siTFE3
CON
CCA
50 μm
D
siRNA*, siRNAxCCA**
CCA p=0.08
#
Lysosomal Size
2.0
1.5
1.0
0.5
0.0
CON
CCA
E
SCR
siTFEB
siTFE3
CON
CCA
50 μm
F
siRNA***
CCA*
DQ BSA Green Puncta/Nuclei
800
600
400
200
0
CON
CCA

Figure 4: Lysosomal adaptations to chronic contractile activity in si*Tfeb* or si*Tfe3* conditions. C2C12 myotubes were stained with Mitotracker Red, Lysotracker Green and Hoescht following CCA and 21 hr recovery (A). Quantification of lysosomal area normalized to nuclei (B). Representative images of cells stained with Lysoview 405 to assess lysosomal size (C). Graphical representation of average size of Lysoview puncta in each field of view (D). Cells were treated with DQ-BSA for 4 hr and stained with Hoescht (E). Graphical representation of DQ-BSA puncta per nuclei (F). Each experiment was repeated 3 times with 2 technical repeats/well, and 4 images were taken per well. Statistics are shown as follows, "siRNA" represents a main effect of KD; "CCA" denotes a main effect of CCA; "siRNAxCCA" represents a main effect of KD and CCA; * denotes the p value for each effect, *, $p<0.05$; **, $p<0.01$; ***, $p<0.001$; # reflects post-hoc analyses indicating a significant difference from SCR conditions, $p<0.05$.

fluorescence when unquenched upon degradation within the lysosomes. Basally si*Tfeb* reduced the number of green puncta, indicating a lysosomal impairment (Fig. 4E, 4F).

Following CCA, lysosomal area increased 2.1-fold in SCR conditions (Fig. 4A, 4B). This was not observed with the reduction of TFEB or TFE3 (Fig. 4A, 4B). A significant 23% reduction in lysosomal size was observed in SCR cells following CCA, but this decrease was not seen in si*Tfeb* or si*Tfe3* conditions (Fig. 4C, 4D). Since enlarged lysosomes, or lysosomal swelling, is often a sign of dysfunction, this decrease in size likely indicates a healthier pool of lysosomes following CCA. Corroborating this, DQ-BSA digestion was increased by 30% following CCA in SCR conditions, indicating improved lysosomal function (Fig. 4E, 4F). However, this adaptation to CCA was not observed in si*Tfeb* conditions, but was present in si*Tfe3* conditions. This suggests that TFEB, but not TFE3, is a key regulator of lysosomal adaptations to CCA in muscle cells.

Reduced contraction-induced mitophagy flux in siTfeb and siTfe3 conditions. To assess the importance of reducing both TFEB and TFE3 together, we then generated a TFEB and TFE3 DKD condition using siRNA and employed the same experimental design (Fig. 5A). *Tfeb* and *Tfe3* mRNA expression was reduced by on average 60% (ranging from 35%-82%) and 27%

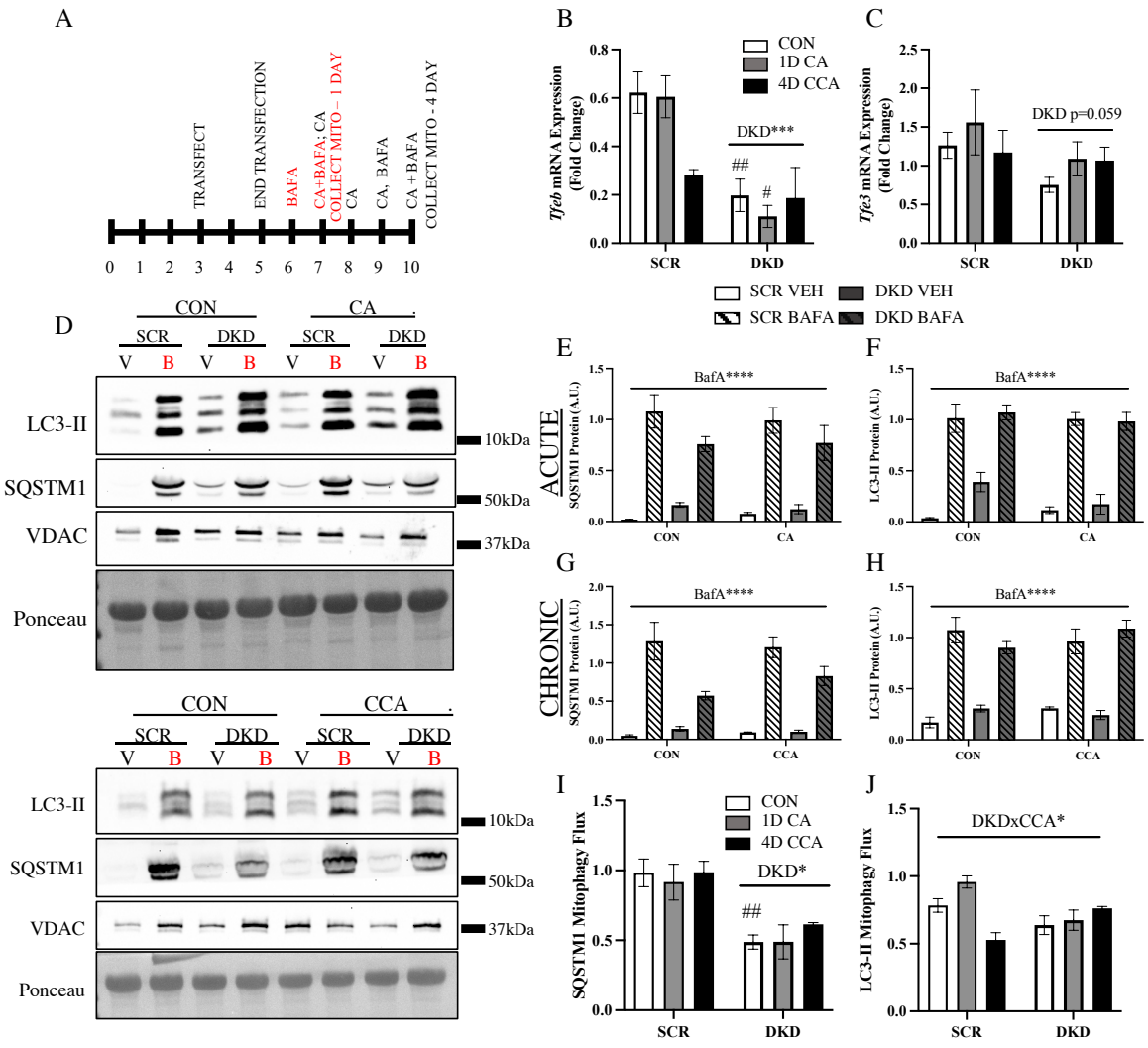

Figure 5: Acute contraction-induced mitophagy flux in si*Tfeb* and si*Tfe3* conditions. Schematic of the experimental design (A). *Tfeb* (B) and *Tfe3* (C) mRNA expression following siRNA treatment, acute CA and CCA normalized to both *Actb* and *B2mg*. Representative western blots for SQSTM1, LC3-II in mitochondrial fractions (D). Quantification of SQSTM1 (E) and LC3-II (F) protein content in mitochondrial fractions following acute CA. Quantification of SQSTM1 (G) and LC3-II (H) protein content in mitochondrial fractions following chronic CCA. SQSTM1 (I) and LC3-II (J) mitophagic flux, calculated as the difference between BafA- and Veh-treated conditions (J, n=3). Statistics are shown as follows, "DKD" represents a main effect of DKD; "BafA" indicates a main effect of BafA treatment; "CCA" denotes a main effect of CCA; "DKDxCCA" represents a main effect of DKD and CCA; * denotes the p value for each effect, *, $p<0.05$; ***, $p<0.001$; ****, $p<0.0001$; # reflects post-hoc analyses indicating a significant difference from time-matched SCR conditions, $p<0.05$; ##, $p<0.01$.

(ranging from 10% to 40%) respectively (Fig. 5B-C). Declines in the expression of *Beclin1* and *Park2* were observed in the DKD basally (Fig. S2 A, D), but no differences in the transcript levels of *Sqstm1, Map1lc3b, Lamp2,* or *Mcoln1* were observed (Fig. S2). BafA treatment induced an accumulation of both SQSTM1 and LC3-II on mitochondrial fractions across all conditions and timepoints (Fig. 5D, 5E, 5F). With the reduced expression of TFEB and TFE3, LC3-II and SQSTM1 mitophagy flux was reduced basally by 20% and 50% respectively (Fig. 5I, 5J). However, autophagy flux assessed in whole cell lysates was not significantly impaired in the DKD condition basally (Fig. S3) illustrating that mitophagy is regulated independently from autophagy. In line with previous results, LC3-II mitophagy flux was increased by 1.2-fold following CA and decreased by 33% following CCA in the SCR condition. This CA-induced increase was dependent on the presence of both TFEB and TFE3 (Fig. 5I). Similar to the previous findings, SQSTM1 mitophagy flux was reduced by 50% across all timepoints in TFEB and TFE3 DKD conditions (Fig. 5J).

Mitochondrial adaptations to chronic contractile activity in siTfeb and siTfe3 conditions. The protein content of a host of mitochondrial markers was assessed, and surprisingly a main effect of DKO was observed for Citrate Synthase, COX I, and SDHB indicating increased mitochondrial proteins in TFEB and TFE3 DKD conditions (Fig. 6A-D). Strong trends were observed in COX I and SDHB to increase following CCA, and NDUFB8 was significantly upregulated by 2-fold (Fig. 6C-E). Further increases in Citrate Synthase (10%), COX I (25%) and SDHB (33%) were observed when TFEB and TFE3 expression was reduced following CCA (Fig. 6A-D). Despite these modest increases in mitochondrial content following CCA, assessment of mitochondrial function revealed a significant increase in maximal respiration and ATP production following CCA (Fig. 6F-I). However, this mitochondrial adaptation was

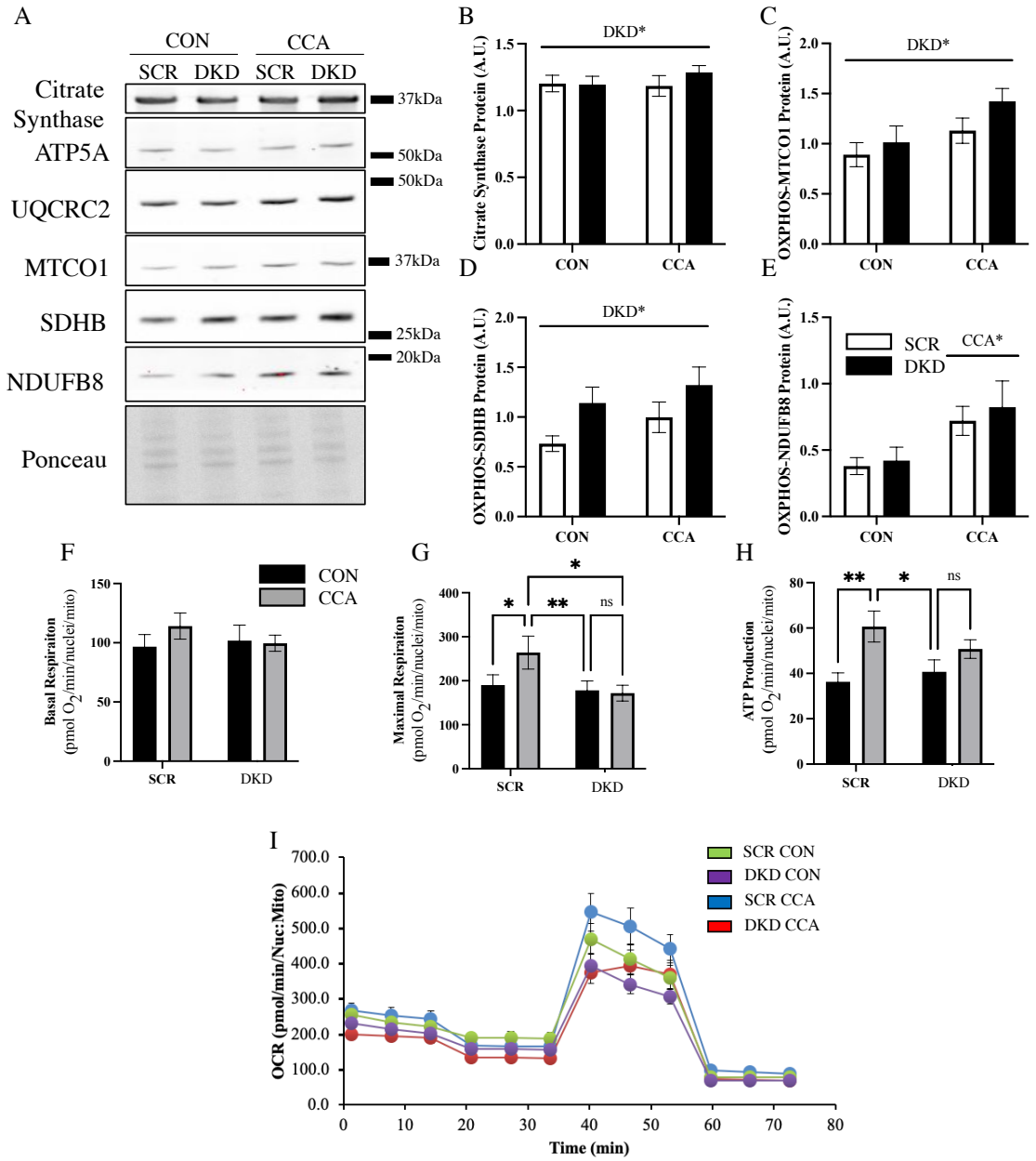

Figure 6: Mitochondrial adaptations to chronic contractile activity in si*Tfeb* and si*Tfe3* conditions. Representative western blots of mitochondrial markers following CCA (A). Graphical representation Citrate Synthase (B), MTCO1 (C), SDHB (D), NDUFB8 (E) following CCA (n=3). Oxygen consumption rates during basal respiration (F), maximal respiration (G) and coupled respiration, or ATP production (H) assessed using Seahorse corrected for nuclear and mitochondrial content. Experiments were reproduced 3 times, with 20 technical repeats per experiment. Representative tracing of oxygen consumption (I). Statistics are shown as follows, "DKD" represents a main effect of DKD; "CCA" denotes a main effect of CCA; * denotes the p value for each effect, *, $p<0.05$; **, $p<0.01$; ***, $p<0.001$; ****, $p<0.0001$.

completely abolished in TFEB and TFE3 DKD conditions(Fig. 6F-I), indicating that the increase in mitochondrial markers observed likely reflected an accumulation of dysfunctional organelles. This further suggests that TFEB and TFE3 are required for mitochondrial adaptations to CCA.

Lysosomal adaptations to chronic contractile activity in siTfeb and siTfe3 conditions. Contrary to our initial hypothesis, a significant increase in LAMP1 was observed in DKD conditions (Fig. 7A, 7C), while MCOLN1 and v-ATPase remained unchanged, indicating some compositional changes at the level of the lysosome (Fig. 7D-E). Cathepsin B, a lysosomal protease, typically undergoes a maturation step within the lysosome and can serve as an indication of lysosomal status/function. We observed a 22% increase in mature Cathepsin B protein content in TFEB and TFE3 DKD conditions(Fig. 7F), however when the ratio of mature:premature was assessed as a functional metric, a significant 20% reduction was observed in the DKD conditions (Fig. 7G). No differences were observed basally in lysosomal content, as measured by Lysotracker Green staining in the absence of both TFEB and TFE3 (Fig. 8A, 8C). However following CCA, lysosomal content increased by 71% in SCR conditions and by 95% in DKD conditions (Fig. 8A, 8C). Lysosomal function assessed using DQ-BSA staining, was decreased by 22% basally in TFEB and TFE3 DKD conditions (Fig. 8D-F). In SCR conditions, lysosomal function increased by 26% following CCA, however in the DKD condition lysosomal function was reduced by 52% (Fig. 8D-F). Taken together these results indicate that TFEB and TFE3 are required for normal lysosomal function, as well as the adaptive response to CCA.

Discussion

Exercise is a potent stimulus for improving mitochondrial quality and quantity, and the mechanisms involved in these adaptations are still being characterized. These changes are a by-

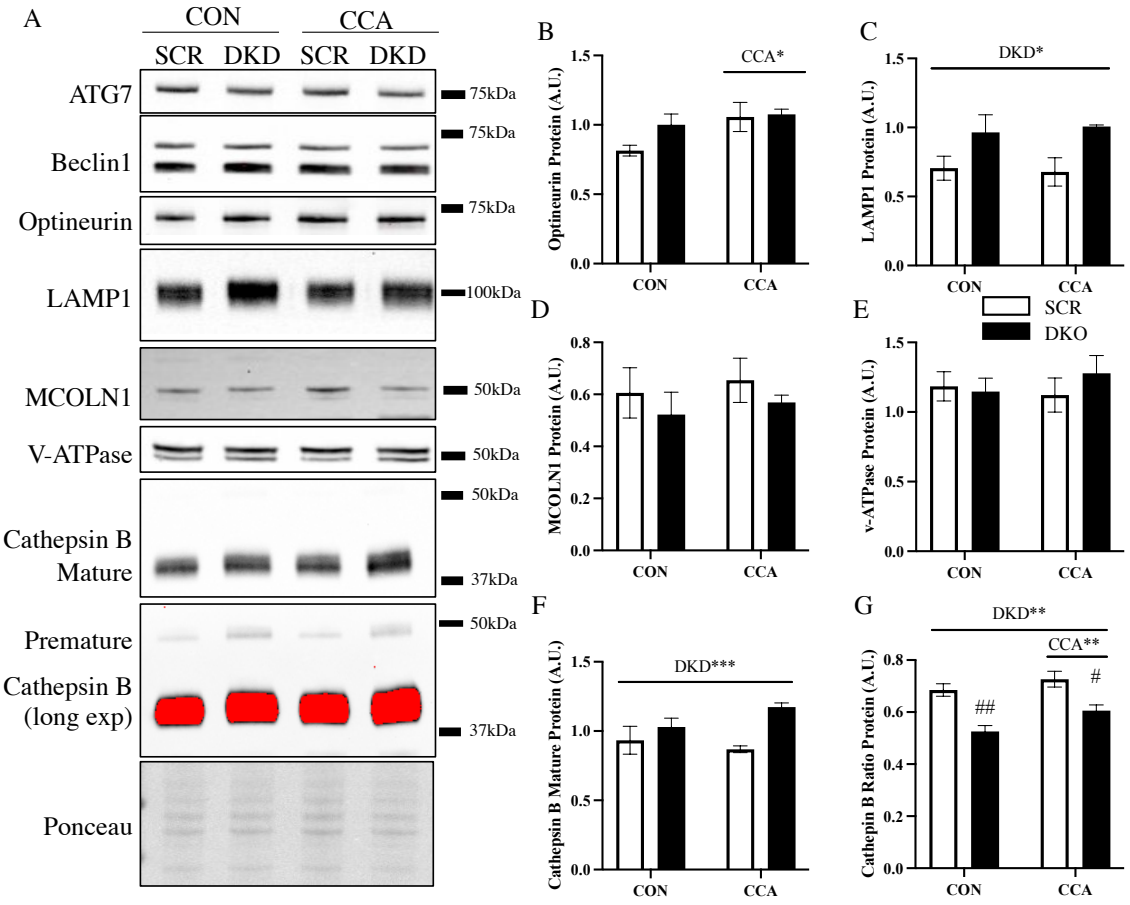

Figure 7: Lysosomal adaptations to chronic contractile activity in si*Tfeb* and si*Tfe3* conditions. Representative western blots of lysosomal markers following CCA (A). Graphical representation Optineurin (B), LAMP1 (C), MCOLN1 (D), v-ATPase (E), and Cathepsin B (F) following CCA (n=3). The ratio of mature Cathepsin B to total was assessed as an indication of lysosomal status (G). Statistics are shown as follows, "DKD" represents a main effect of DKD; "CCA" denotes a main effect of CCA; * denotes the p value for each effect, *, $p<0.05$; **, $p<0.01$; ***, $p<0.001$; # reflects post-hoc analyses indicating a significant difference from time-matched SCR conditions, $p<0.05$; ##, $p<0.01$.

product of not only stimulating mitochondrial biogenesis, but also the clearance of dysfunctional mitochondria through mitophagy[5]. Recent work has suggested that lysosomal adaptations precede mitochondrial adaptations to exercise[326], and a growing body of evidence suggests a high level of coordination between these organelles in maintaining their function[264,265,267]. As such this study aimed to understand the impact of lysosomal regulators on mitochondrial maintenance and adaptations to exercise. Our data show that the reduced

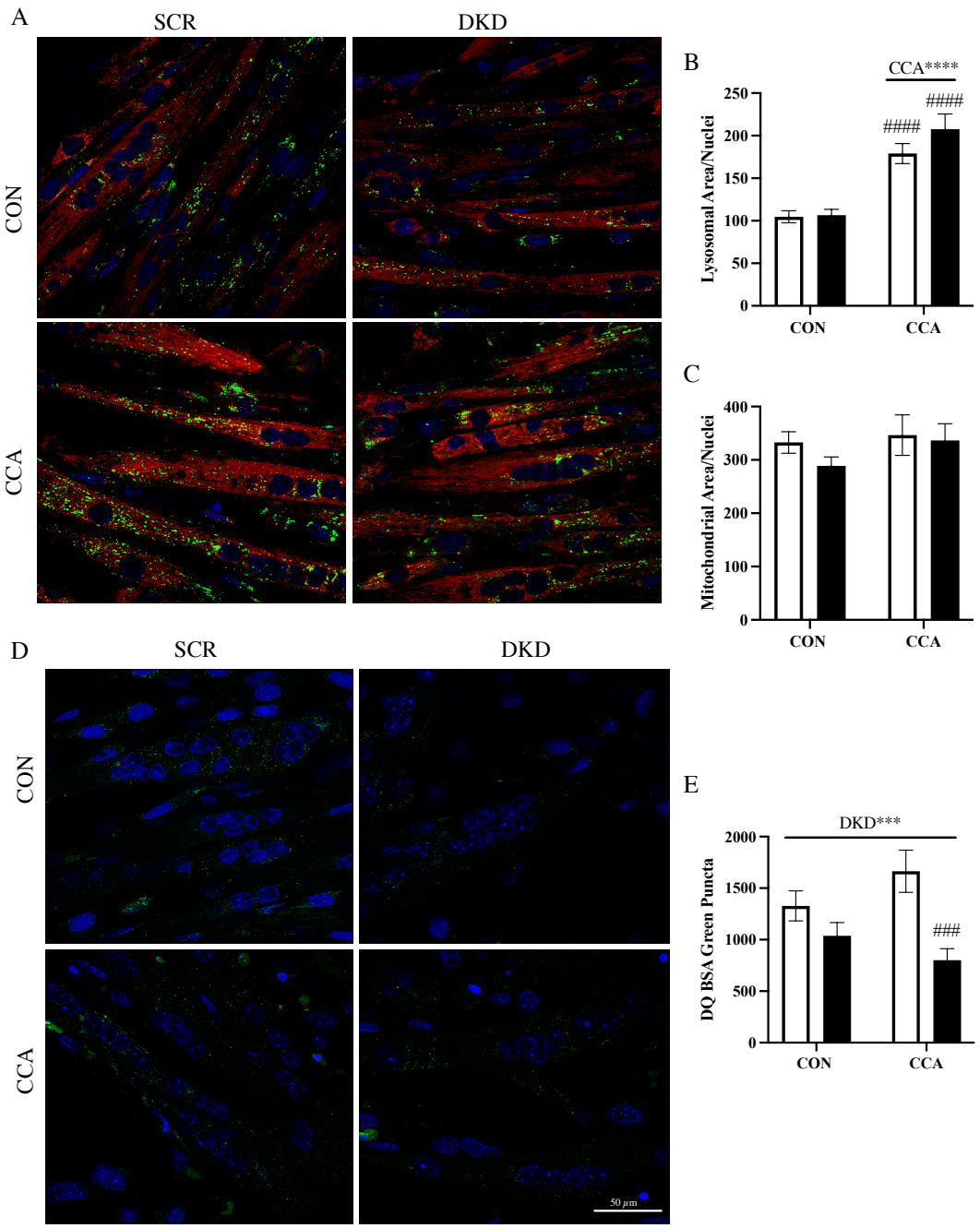

Figure 8: TFEB and TFE3 are required for functional lysosomal adaptations to CCA. C2C12 myotubes were stained with Mitotracker Red, Lysotracker Green and Hoescht following CCA and a 21 hr recovery (A). Quantification of lysosomal area normalized to nuclei (B), and mitochondrial area normalized to nuclei (C). Cells were treated with DQ-BSA for 4 hrs and stained with Hoescht (D). Graphical representation of DQ-BSA puncta per nuclei (E). Each experiment was repeated 3 times with 3 technical repeats/well, and 4 images were taken per well. Statistics are shown as follows, "DKD" represents a main effect of DKD; "CCA" denotes a main effect of CCA; * denotes the p value for each effect, ***, $p<0.001$; ****, $p<0.0001$; # reflects post-hoc analyses indicating a significant difference from SCR conditions, $p<0.05$; ##, $p<0.01$, ####, $p<0.0001$.

expression of TFEB or TFE3 individually may impact acute signaling, but it does not impede mitochondrial adaptations to CCA. However, the reduction of both TFEB and TFE3 together compromised mitochondrial adaptations, likely due to lysosomal impairments and reduced mitophagy flux.

Previous accounts have demonstrated that TFEB or TFE3 are sufficient to upregulate lysosomal- and autophagy-related genes, but they are not required to maintain basal autophagy flux[166,169,445]. This is likely due to the redundant nature of the MiT family, whereby all transcription factors can bind to the CLEAR network and appear to respond to the same activating signals[164,166]. However, TFEB and TFE3 are required for the appropriate autophagic response to stress, the most well documented being starvation[169,445]. Previous reports *in vivo* have demonstrated both morphological and functional mitochondrial impairments in the absence of TFEB or TFE3[197,325]. However, these were not observed in the present study, possibly due to the nature of the experimental design which mimics a conditional knockout, as TFEB and TFE3 were reduced during early maturation to avoid interference with the differentiation process[195].

TFEB and TFE3 have previously been implicated in the process of mitophagy in response to mitochondrial perturbations[446], however this has not yet been assessed in skeletal muscle or in the context of contractile activity or exercise. In line with previous accounts on stress-induced autophagy, the reduced expression of TFEB or TFE3 alone did not impact basal mitophagy flux. However, the acute CA-induced increase in mitophagy flux was blunted in si*Tfeb* or si*Tfe3* conditions. Following repeated bouts of CA, mitophagy was reduced. This is in line with previous literature *in vivo*, which suggests that as the mitochondrial pool improves with CCA, signaling towards mitophagy is reduced. There was no difference in the mitophagic

response following CCA with reduced TFEB or TFE3 expression, indicating that while the acute response may be impacted, there is likely some adaptive compensation with the repeated stress of CA. This was observed in the reduced expression of TFEB, in which a compensatory increase in *Tfe3* mRNA likely contributed to the further upregulation of the autophagy and lysosomal genes, *Map1lc3b*, *Beclin1, Ctsd, Lamp1* and *Lamp2* following repeated bouts of CCA. Previous reports have also suggested that in the absence of TFE3 there is a compensatory increase in MITF expression in primary myoblasts[202], although this was not addressed in this current study. Increased mitochondrial content and improved mitochondrial function were observed following CCA in the silencing of TFEB or TFE3 individually, indicating that the loss of each of these transcription factors alone is not required for mitochondrial adaptations to contractile activity.

Recent reports have illustrated that TFEB and TFE3 are activated *in vivo* following an acute bout of exercise and that this promotes increases in lysosomal content in response to training[190,197,262,324–326]. Even though mitophagy flux is reduced following exercise training or CCA (current study), muscle becomes primed with an increased capacity for autophagy or mitophagy to response to future stress. Our data indicate that lysosomes do adapt to contractile activity, and in response to CCA exhibit morphological and functional changes. Enlarged or swollen lysosomes are a sign of lysosomal impairment[447]. Here we show that CCA reduces lysosomal size, potentially indicating a healthier pool or organelles. Direct evidence for this improvement is provided by the enhanced DQ-BSA fluorescence following CCA. Intriguingly, in TFEB knockdown conditions alone, lysosomal size was not reduced, nor was an improvement in lysosomal function observed following CCA. Despite this lack of lysosomal adaptation, mitochondria were still able to increase in function and content, illustrating the

independent nature of the plasticity of these organelles. It is possible that the increase in TFE3 expression in the absence of TFEB served to help fulfill this compensatory role, as TFE3 has been shown to regulate PGC-1α in skeletal muscle[202] in order to achieve the mitochondrial adaptations to CCA.

In light of the redundancy of these transcription factors, we sought to generate a DKD condition lacking both TFEB and TFE3. The reduced expression of both TFEB and TFE3 greatly impacted mitophagy flux basally and abolished the CA- and CCA-induced fluctuations in mitophagy flux. In line with these results, as CCA tended to increase various mitochondrial markers, the knockdown of TFEB and TFE3 further increased their cellular levels. Taken together with the reduction in mitophagy flux, this likely represents an accumulation of dysfunctional mitochondria instead of the enhanced biogenesis of a nascent pool of healthy organelles. In line with this hypothesis, oxygen consumption rates improved in SCR conditions, but this adaptation was completely lost in TFEB and TFE3 DKD conditions, indicating that TFEB and TFE3 together are required for mitochondrial biogenesis adaptations to CCA. Furthermore, while the current study focused on the role of TFEB and TFE3 in lysosomes, previous work has identified both TFEB and TFE3 as metabolic regulators during exercise[197,200]. The lack of mitochondrial adaptations to CCA are therefore likely attributed to a decline in mitophagy flux, and metabolic impairments that limited mitochondrial substrate availability and utilization. Our data likely illustrate another mode in which TFEB and TFE3 contribute to contractile activity-induced adaptations.

As TFEB and TFE3 are positive lysosomal regulators, we hypothesized that the absence of these transcription factors would result in a reduction of lysosomal content. To our surprise, we observed an increase in a number of lysosomal markers. We reasoned that this must indicate

an accumulation of lysosomes that are dysfunctional. Indeed, we provide evidence of lysosomal dysfunction, seen by ineffective maturation of lysosomal protease Cathepsin B and reductions in DQ BSA fluorescence both basally and following CCA. Recent work has shown that lysosomes also need to be recycled, and blocking this reformation in muscle results in a loss of force production and signs of muscle dysfunction[448]. Some work has shown that lysosomes can undergo exocytosis to expel their contents and also aid in plasma membrane repair, and that this process relies on TFEB expression[449]. There are a number of mechanisms through which lysosomes can undergo turnover but these are still being uncovered[158]. Based on the current findings, as lysosomes accumulate in TFEB and TFE3 DKD conditions following CCA, this suggests that lysosomal recycling is a key mechanism for lysosomal adaptations, which in turn supports mitochondrial adaptations through mitophagy. Thus, more work is warranted to characterize these mechanisms, especially in the context of exercise.

In summary, our findings demonstrate the necessity for the maintenance of lysosomal function, as well as normal mechanisms of mitochondrial turnover (i.e. mitophagy) in mediating mitochondrial adaptations to chronic contractile activity. We also provide evidence of redundancy among the members of the MiT family, as the absence of one transcription factor alone did not impede the ability of skeletal muscle to adapt to contractile activity. There is growing evidence that mitochondria and lysosomes dynamically regulate each other through contact sites. Understanding how these organelles communicate and interact during exercise would provide insight into the interplay of the adaptability of these organelles. We also provide further evidence of the dynamic nature of lysosomes that is akin to that exhibited by mitochondria in response to chronic contractile activity, as well as the necessity for both TFEB and TFE3 in facilitating this response. A greater understanding of how these transcription

factors regulate lysosome recycling will surely provide insight into how skeletal muscle adapts to exercise.

Materials & Methods

Cell culture and siRNA transfection. C2C12 murine skeletal muscle cells (ATCC, CRL 1772) were grown in 6-well plates in Dulbecco's modified Eagle's medium (DMEM; Wisent, 319-015-CL) supplemented with 10% fetal bovine serum (FBS; Gibco, 12-483-020) and 1% penicillin-streptomycin (PS; Wisent, 450-201-EL). Once myoblasts reached ~90% confluency, differentiation was induced by switching the media to DMEM supplemented with 5% horse serum (HS; Gibco, 16-050-114) and 1% PS and replenished daily. On day 2 of differentiation cells were switched to pre-transfection media (DMEM, 5% HS) for 24 hrs. The following day the cells were transfected with either 100nmol of scrambled (SCR), si*Tfeb*, or si*Tfe3* siRNA and equal volumes of lipofectamine RNAiMAX (ThermoFisher, 13778075) in pre-transfection media. Cells were transfected for 48 hrs, following which cells were washed with PBS and replenished with normal differentiation media.

Chronic contractile activity, Bafilomycin A_1 Treatment. Following transfection, cells were given 24hrs to recover in normal differentiation media, and then subjected to electrical stimulation as previously described[262,443]. Briefly, plastic lids for the 6-well plates were retrofitted with two platinum electrodes that run the width of well in parallel at opposite ends, at a depth suitable to be submerged in media once placed on the plate. Electrodes were designed in a parallel circuit and attached to a stimulator unit that would deliver electrical stimulation at a frequency of 5 Hz, 10V intensity eliciting contractile activity of the myotubes. Stimulation was done chronically for 3 hrs per day, for 4 consecutive days allowing a 21hr recovery period between bouts at 37°C and 5% CO_2. Media was replenished before and after stimulation. To assess mitophagy and

autophagy flux, cells were treated 24hrs prior to collection with either vehicle (Veh), DMSO, or 50nM Bafilomycin A_1 (BafA; BioShop, BAF002.1). BafA or Veh, were also supplemented when media was changed prior to stimulation, at which time non-stimulated controls also received replenishment of media and treatment. Flux was then calculated as the difference between BafA-treated conditions and Veh-treated conditions with respect to common markers found within the autophagosome, namely SQSTM1 and LC3-II, as previously described[7,262].

Mitochondrial fractionation. Briefly, cells were scraped using a rubber policeman with ice-cold PBS and centrifuged at 14,000xg for 5 min. Pellets were then resuspended in 200μL of resuspension buffer (1000mM KCl, 10mM MOPS and 0.2% BSA) and homogenized using a glass dounce homogenizer (Canadawide Scientific, 914-900-02) and then centrifuged at 1,000xg for 10 min at 4°C. The supernate was then centrifuged at 14,000xg for 15 min at 4°C to pellet mitochondria, pellets were washed and spun again. Finally, the pellet was resuspended in 25-30μL of resuspension buffer and subjected to 3 freeze-thaw cycles on dry ice to disrupt the membranes and liberate all matrix proteins.

Mitochondrial respiration using Seahorse. 10,000 cells were seeded and grown on seahorse 96-well plates and subjected to the same experimental design described above. 96-well plastic lids were retrofitted with platinum electrodes, whereby each well had two point electrodes on opposite ends that were of sufficient length/depth to be submerged in media. Electrodes were only retrofitted to half the plate, so that control and stimulated conditions could be analyzed in the same experiment. Myotubes were subjected to the same CCA protocol as above using a voltage of 1.5V. The Seahorse XF96 Mito Stress Test Kit (Agilent Biosciences, 103015-100; Seahorse XFe96 Analyzer, Agilent Biosciences, Santa Clara, CA, USA) was performed 21 hrs following the last bout according to manufacturer's instructions. Cells were then washed with

PBS and 10μM Hoescht (ThermoFisher, 62249) and 100nM Mitotracker Green (ThermoFisher, M7514) was applied in phenol-free media for 15 min and subsequently washed. Fluorescence was then measured using Cytation5 plate reader (BioTek Instruments, Winooski, VT, USA) and the ratio of nuclei to mitochondria was used to normalize oxygen consumption rates (OCR) to better represent mitochondrial respiration per mitochondria.

Protein extraction and immunoblotting. Protein extracts were made from frozen pellets of collected myotubes. Briefly, pellets were vigorously resuspended in Passive Lysis Buffer (Promega, E194A) supplemented with protease and phosphatase inhibitors (Roche, 11-697-498-001; Sigma, P0044; Sigma, P5726). Lysates were then subjected to 5 freeze-thaw cycles using liquid nitrogen and then centrifuged at max speed at 4°C and supernate was collected. Protein concentration was then measured using the Bradford method. Whole cell protein extracts or mitochondrial fractions (20μg) were applied to a 10-18% SDS-PAGE gels and subsequently transferred onto a nitrocellulose membrane. Membranes were blocked in 5% skim milk in TBS-T (100 mM TRIS, 100 mM NaCl, 0.1% Tween 20) for 1 hr at room temperature with constant agitation. Primary antibodies were diluted in 5% skim milk in TBS-T directed against ATG7 (1:1000; Sigma-Aldrich, A2856), Beclin1 (1:1000; Cell Signaling Technology, 3738S), Citrate Synthase (1:1000; Abcam, ab96600), MTCO1 (1:500; Abcam, ab14705), COX IV (1:500; Abcam, ab14744), CTSB (1:1000; Cell Signaling Technology, 31718S), GAPDH (1:100,000; Abcam, ab8245), LAMP1 (1:1000; Abcam, ab24170), LC3 (1:500; Cell Signaling Technology, 4108S), MCOLN1 (1:1000; Invitrogen, PA1-46474), Optineurin (1:500; Santa Cruz Biotechnology, SC-166576), SQSTM1(1:1000; Cell Signaling Technology, 5114S), TFE3 (1:500; Sigma-Aldrich, HPA023881), UQCRC2 (1:500; Abcam, AB14745), v-ATPase (1:1000, Santa Cruz Biotechnology, SC-55544), VDAC (1:500; Abcam, AB14734), total OXPHOS:

ATP5A, UQCRC2, MTCO1, SDHB, NDUFFB8 (1:1000, Abcam, STN-19467) and incubated overnight at 4°C and then horseradish-peroxidase (HRP)-linked secondary antibodies (Cell Signaling Technology, 7074S; 7076S) were applied according to the manufacturer's suggestions the following day for 1 hr at room temperature. Blots were then imaged using ECL (BioRad, 1705061) and iBright 1500 imager (Invitrogen, Waltham, MA, USA).

RNA extraction and qPCR. Total RNA was isolated from myotubes using TRIzol (Ambion, 15596018) according to the manufacturer's instructions. RNA concentrations were measured using spectrophotometry (Nanodrop2000; ThermoFisher Scientific, Waltham, MA, USA). Total RNA (2μg) was then reverse transcribed to generate cDNA using Superscript III reverse transcriptase and Oligo(dt)20 (Invitrogen, 18080-044; 18418020) according to the manufacturer's instructions. qPCR was carried out using the StepONE Plus PCR system (Applied Biosystems, Waltham, MA, USA) and Sybr Green Master Mix (Bimake, B21202). Primers were designed, optimized to ensure primer efficiency, and then verified for specificity with dissociation melt curves. Each sample and primer was run in duplicate with a negative control containing no cDNA and normalized to two housekeeping genes, *ActB,* and *B2MG,* (see Table 1 for primer sequences). Data was analyzed using the $2^{-\Delta\Delta Ct}$ method, and statistical analysis was performed on the unlogged ΔCt values using a two-way ANOVA with Bonferroni post-hoc tests.

Confocal microscopy and staining. Cells were cultured on glass-bottom 6-well plates (Cellvis, P06-1.5H-N) and 21 hr following their last bout of CCA were incubated with 10μM Hoescht 33342 (ThermoFisher, P162249), 100nM Mitotracker Red (ThermoFisher, M7512) and 50nM Lysotracker Green (ThermoFisher, L7526) in phenol-free DMEM (Wisent, 319-065-CL) for 15 min at 37° with 5% CO_2 then washed with PBS and phenol-free DMEM was replenished. Live

Table 1: List of primer oligonucleotide sequences in real-time qPCR analysis for *Mus musculus*

Gene	Forward Primer	Reverse Primer
Tfe3	5'-GGAATGGTGGCAAAGGTATAA-3'	5'-GGCTCTGAAACAGGGGTAGT-3'
Tfeb	5'-AGCTCCAACCCGAGAAAGAGTTTG-3'	5'-CGTTCAGGTGGCTGCTAGAC-3'
Sqstm1	5'-TGTGGTGGGAACTCGCTATAA-3'	5'-CAGCGGCTATGAGAGAAGCTAT-3'
Map1lc3b	5'-GCTTGCAGCTCAATGCTAAC-3'	5'-CCTGCGAGGCATAAACCATGTA-3'
Beclin1	5'-AGGCTGAGGCGGAGAGATT-3'	5'-TCCACACTCTTGAGTTCGTCAT-3'
Park2	5'-GTCTGCAATTTGGTTTGGAGTA-3'	5'-GCATCATGGGATTGTCTCTTAAA-3'
Ctsd	5'-TTTGCCAATGCTGTCGTACT-3'	5'-AGCGAGTGTGACTATGTGTGA-3'
Lamp1	5'-CTAGTGGGAGTTGCGGTATCA-3'	5'-AGGGCATCAGGAAGAGTCATAT-3'
Lamp2	5'-GCTGAACAACAGCCAAATTA-3'	5'-CTGAGCCATTAGCCAAATACAT-3'
Mcoln1	5'-TTGCAGCCTACACACAGGAG-3'	5'-AGAGAGCCAAAGCTGATCCA-3'
B2mg	5'-GGTCTTTCTGGTGCTTGTCT-3'	5'-TATGTTCGGCTTCCCATTCT-3'
Actb	5'-TGTGACGTTGACATCCGTAA-3'	5'-GCTAGGAGCCAGAGCAGTAA-3'

cells were then imaged using an inverted Nikon Eclipse TE-2000 confocal microscope equipped with a 60x/1.5 oil-immersion objective lens and a custom-built chamber to maintain temperature and CO_2 levels. Cells were also stained with Lysoview 405 (Biotium, 70066) at a 1x concentration and incubated for 15 min to visualize lysosomal morphology and size. Finally, cells were incubated with 10μg of DQ-BSA green (ThermoFisher, D12050) for 4 hr, cells were then washed with PBS and Hoescht was applied for 5 min and then replenished with phenol-free media. Images were captured and analyzed using the NIS Elements Software (AR 3.1 Version, Nikon, Tokyo, Japan). To selectively quantify mitochondrial or lysosomal parameters within myotubes, regions of interest (ROI) were manually draw around myotubes and analysis

was done within those ROIs. For each stain, 3-5 images were taken per well, 2 wells were devoted to each condition and the experiment was repeated 3 separate times.

Statistical analyses. Data presented are means ± SEM and statistical analyses were performed using Prism 9 (GraphPad, La Jolla, CA, USA). Two-way ANOVAs were conducted for all siRNA and CCA experiments with repeated measures and Bonferroni post-hoc tests. P values less than 0.05 were accepted as significant. Throughout the manuscript a main effect of knockdown is denoted as "siRNA" and later in double knockdown experiments as "DKD" with the asterisk (*) representing the p value. Similarly, a main effect of CCA is represented as "CCA", and any interaction effects are shown as "siRNAxCCA" or "DKDxCCA". Hashtag symbol (#) represents post-hoc analyses illustrating a significant difference from SCR conditions.

Acknowledgments

This work was supported by the Natural Sciences and Engineering Research Council of Canada and funding from the Canadian Institutes of Health Research. D.A. Hood is the holder of a Tier I Canada Research Chair in Cell Physiology. A.N. Oliveira is the recipient of the Natural Science and Engineering Research Council Doctoral Canada Graduate Scholarship. We would like to acknowledge and thank Dr. Yuki Tamura for pilot work and technical assistance in protocol designs. We would also like to thank Sara Keshavari for her assistance in preparing experiments and samples.

Disclosure Statement: No potential conflict of interest.

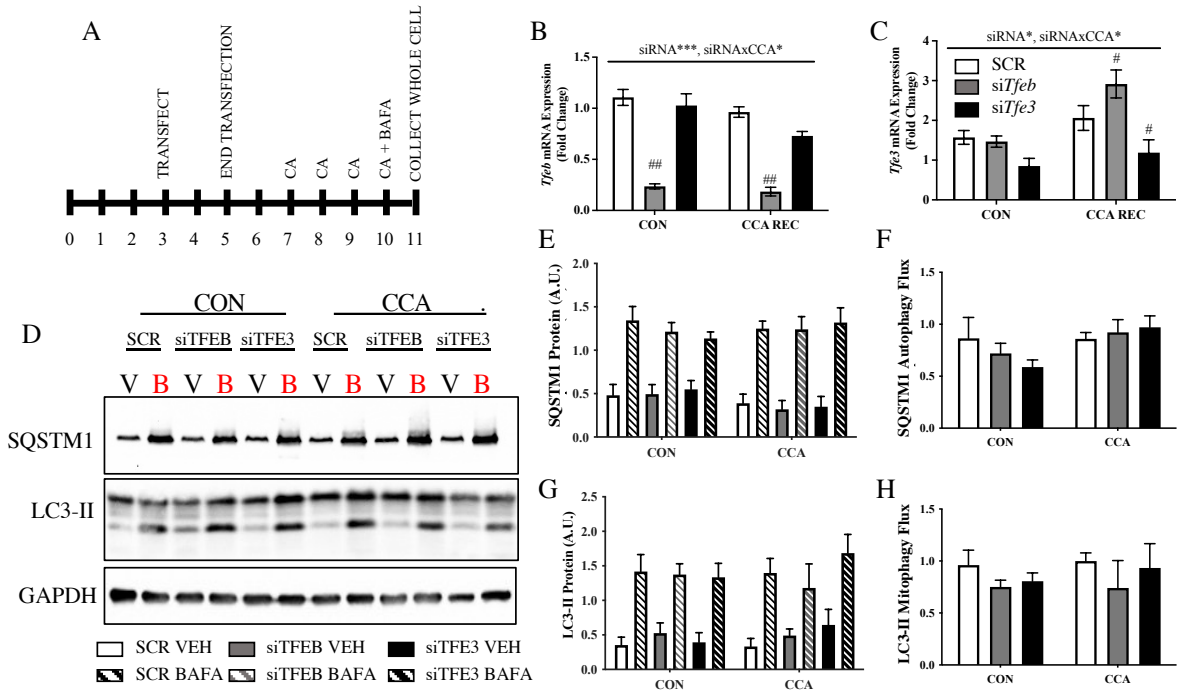

Supplemental Figure 1: Chronic contractile activity-induced autophagy flux in si*Tfeb* or si*Tfe3* conditions. Schematic of the experimental design (A). *Tfeb* (B) and *Tfe3* (C) mRNA expression following siRNA treatment and CCA+21hr recovery normalized to both *Actb* and *B2mg* (n=3). Representative western blots for SQSTM1, LC3-II in whole cell lysate (D). Quantification of SQSTM1 (E) and LC3-II (G) protein content in whole cells lysates following CCA and recovery. SQSTM1 (F) and LC3-II (H) autophagic flux, calculated as the difference between BafA- and Veh-treated conditions (n=9). Statistics are shown as follows, "siRNA" represents a main effect of KD; "siRNAxCCA" represents a main effect of KD and CCA; * denotes the p value for each effect, *, $p<0.05$; ***, $p<0.001$.

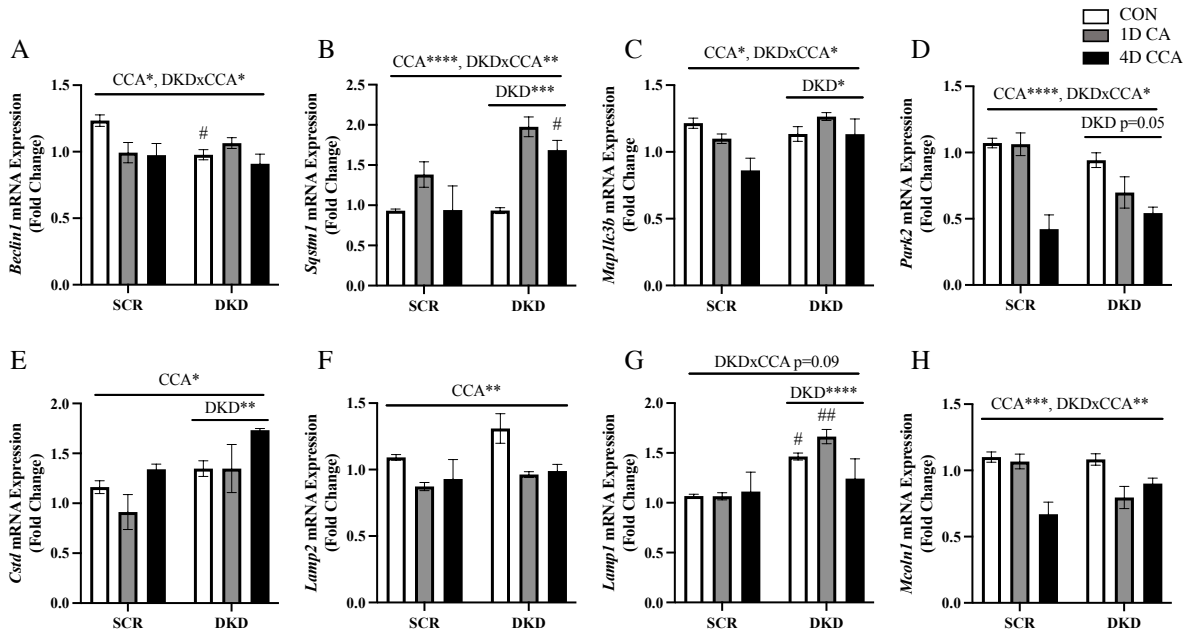

Supplemental Figure 2: mRNA expression in si*Tfeb* and si*Tfe3* conditions following CA and CCA. Gene expression of *Beclin1 (A), Sqstm1* (B), *Map1lc3b* (C), *Park2* (D), *Ctsd* (E), *Lamp2* (F), *Lamp1* (G), and *Mcoln1* (H) normalized to both *Actb* and *B2mg* (n=3) following acute CA and CCA. Statistics are shown as follows, "DKD" represents a main effect of DKD; "CCA" denotes a main effect of CCA; "DKDxCCA" represents a main effect of DKD and CCA; * denotes the p value for each effect, *, $p<0.05$; **, $p<0.01$; ***, $p<0.001$; ****, $p<0.0001$; # reflects post-hoc analyses indicating a significant difference from SCR conditions, $p<0.05$; ##, $p<0.01$.

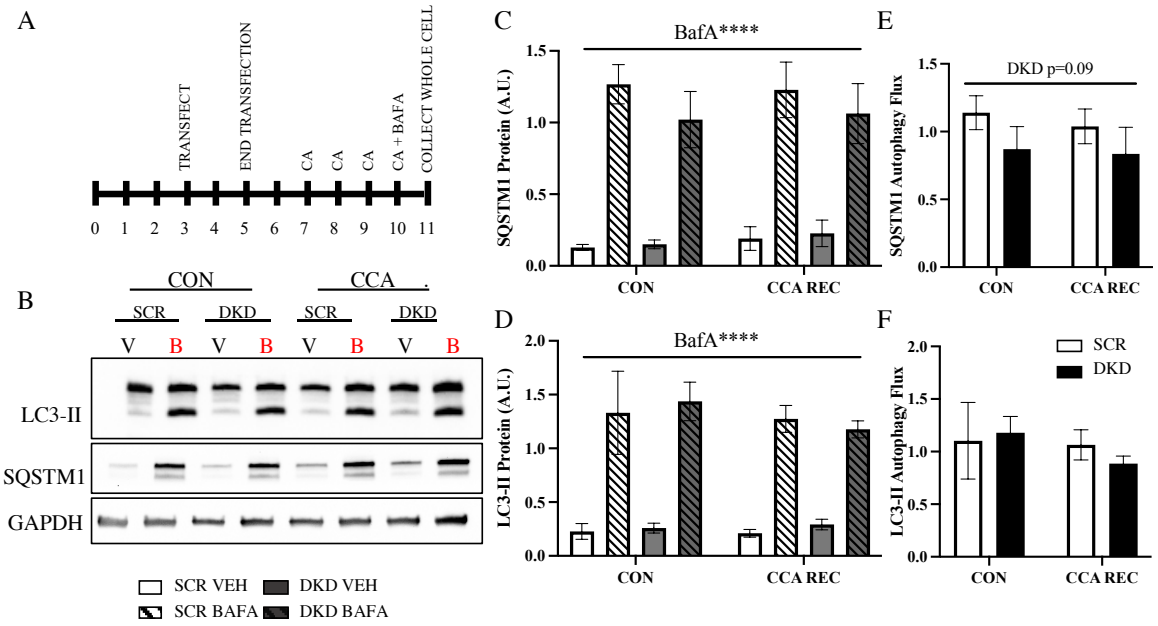

Supplemental Figure 3: Chronic contractile activity-induced autophagy flux in si*Tfeb* and si*Tfe3* conditions. Schematic of the experimental design (A). Representative western blots for SQSTM1, LC3-II in whole cell lysate (D). Quantification of SQSTM1 (C) and LC3-II (D) protein content in whole cells lysates following CCA and recovery. SQSTM1 (E) and LC3-II (F) autophagic flux, calculated as the difference between BafA- and Veh-treated conditions (n=3). Statistics are shown as follows, "DKD" represents a main effect of DKD; "BafA" indicates a main effect of BafA treatment; * denotes the p value for each effect, ****, p<0.0001.

CHAPTER FIVE:

DIMORPHIC EFFECT OF TFE3 IN DETERMINING MITOCHONDRIAL AND LYSOSOMAL CONTENT IN MUSCLE FOLLOWING DENERVATION

ASHLEY N. OLIVEIRA, JONATHAN M. MEMME, JENNA WONG & DAVID A. HOOD

Muscle Health Research Center, School of Kinesiology and Health Science, York University, Toronto, ON, Canada M3J 1P3

Keywords: Mitochondrial respiration, ROS emission, sex differences, lysosomal biogenesis, mitophagy, autophagy

Running Head: Sex-dependent role of TFE3 in muscle denervation

Funding: This work was supported by the Canadian Institutes for Health Research.

Data Availability: Data are available upon request from the authors.

To whom correspondence should be addressed: David A. Hood, PhD
School of Kinesiology & Health Science
Muscle Health Research Centre,
York University, 4700 Keele St,
Toronto, ON, M3J 1P3, Canada
Tel: (416) 736-2100 ext.66640
Email: dhood@yorku.ca

This manuscript has been submitted to the Journal of Cachexia, Sarcopenia and Muscle (October 2022).

Abstract

Background: Muscle atrophy is a common consequence of prolonged inactivity and is accompanied by mitochondrial dysfunction. Damaged mitochondria can be recycled by mitophagy, via the lysosomes. Ineffective clearance of mitochondria can lead to cellular pathology, but the regulation of mitophagy and lysosomes via the transcription factor TFE3 is incompletely understood. In addition, the effect of biological sex is still widely underreported in the context of muscle disuse, and with respect to mitophagy and lysosomes.

Methods: Wild-type (WT) mice, along with mice lacking TFE3 (KO), a transcriptional regulator of lysosomal and autophagy-related genes, were subjected to unilateral sciatic nerve denervation for up to 7 days, while the contralateral limb was sham-operated and served as an internal control. A subset of animals was treated with colchicine to capture autophagy and mitophagy flux. Mitochondrial and lysosomal proteins were assessed along with organelle function.

Results: WT females exhibited increased oxygen consumption rates and decreased ROS emission during active respiratory states, however this was blunted in the absence of TFE3. Surprisingly, females exhibited 40% higher LC3-II mitophagy flux, and increased lysosomal content basally that was independent of TFE3 expression. Following denervation, female mice were modestly protected from muscle atrophy compared to male counterparts. Intriguingly, this sex-dependent protection was lost in the absence of TFE3. Denervation resulted in 45% and 27% losses of mitochondrial content in WT and KO males respectively, however females were completely protected against this decline. Decreases in mitochondrial function were more severe in WT females compared to males following denervation, as ROS emission was 2.4-fold higher. However, TFE3 KO males exhibited a robust 5-fold induction in ROS emission

following denervation in contrast to their WT counterparts. In response to denervation, LC3-II mitophagy flux was reduced by 44% in females likely contributing to the maintenance of mitochondrial content, however this response was dysregulated in the absence of TFE3. While both males and females exhibited increased lysosomal content following denervation, this response was augmented in females in a TFE3-dependent manner.

Conclusions: Females have higher lysosomal content and mitophagy flux basally, likely contributing to the improved mitochondrial phenotype. Denervation-induced mitochondrial adaptations were sexually dimorphic, as females preferentially preserve content at the expense of function, while males display a tendency to maintain mitochondrial function. Our data illustrate that TFE3 is vital for the sex-dependent differences in mitochondrial function basally, and in determining the atrophy phenotype in response to denervation.

List of Abbreviations

ADP	Adenosine diphosphate
ATP	Adenosine triphosphate
ATG7	Autophagy related 7
COL	Colchicine
COX	Cytochrome c oxidase
COX I	Cytochrome c oxidase subunit 1
COX IV	Cytochrome c oxidase subunit IV
CTSD	Cathepsin D
EDL	Extensor digitorum longus
KO	Knockout
LAMP1/2	Lysosome membrane associated protein 1/2
LC3	Microtubule-associated protein 1A/1B light chain 3B
MCOLN1/TRPML1	Mucolipin1
MiT	Microphthalmia
MQC	Mitochondrial quality control
ROS	Reactive oxygen species
SOL	Soleus
SQSTM1 or p62	Squestosome 1
TA	Tibialis Anterior
TFEB	Transcription factor EB
TFE3	Transcription factor E3
UQCRC2	Ubiquinol-Cytochrome c reductase core protein 2
v-ATPase	Vacuolar-type ATPase
VDAC	Voltage-dependent anion channel
VEH	Vehicle
WT	Wildtype

Introduction

Loss of skeletal muscle mass as a result of fiber atrophy is a consequence of prolonged periods of inactivity, but is also commonly seen with age, cancer, among others[S1], the severity of which is a strong predictor of patient outcome and mortality[450]. There remains a large gap in the literature regarding how biological sex influences the mechanisms involved in atrophy. This is problematic as it has been documented that females are more prone to developing muscle weakness during hospital visits requiring intensive care and have a higher incidence of mortality[424]. Therefore, there is an urgent need to better understand muscle atrophy in female subjects.

Muscle atrophy is often preceded by aberrant mitochondrial phenotypes[451,452,S2]. Declines in mitochondrial enzymatic activity, reductions in coupling efficiency, impaired ATP production, and decrements in oxygen consumption rates are observed with prolonged disuse[333,453,S1,S3-S8]. Elevations in reactive oxygen species (ROS) have also been seen and are thought to be a major driver in the muscle atrophy phenotype[410,454,S9]. Recently, it was shown that despite males having higher ROS emission basally, the production of ROS following hindlimb unloading is greater in females[220,455].

Due to the exacerbated mitochondrial dysfunction observed during disuse, there is a greater cellular requirement for mitophagy, the selective removal of damaged mitochondria via the lysosomes[334,456,S10]. Dysfunctional mitochondria are segregated from the reticulum through events of fission and targeted for degradation[229,419,S11,S12]. A variety of mitophagic signaling pathways have been described, which all culminate in engulfment by the autophagosome and trafficking to the lysosome[229,249,251,S13]. The lysosomes are critical sites for catabolism, and are tightly linked to mitochondrial health and cellular homeostasis[S14]. Lysosomes are regulated by

the microphthalamia (MiT) family of transcription factors, namely TFEB and TFE3, which have been shown to respond to various signals including nutrient deprivation, ROS and Ca^{2+} influx [169,185,189,445,S15,S16]. While considerable effort has been devoted to the study of TFEB, much less is known about the impact of TFE3 on lysosome formation.

Increases in the expression of lysosomal markers are seen with disuse, as are the regulators TFEB and TFE3, indicating a greater need for lysosomes during muscle disuse[218]. Recently, reductions in mitophagy flux and increased inclusions found within skeletal muscle thought to be indicative of lysosomal dysfunction were observed in male rats following denervation[334]. Basally there is evidence to suggest that females have increased autophagy machinery and lysosomal content in comparison to males[218,S17]. The would suggest a better maintenance of mitochondria during an imposed stress such as disuse, however some data suggest a worse mitochondrial phenotype[220]. Increased LC3-II and p62 levels have been found in female rodents following hindlimb unloading[220] but formal flux measurements have yet to be done. Thus, the purpose of this study was to investigate the role of lysosomes and the transcriptional regulator TFE3, in a severe model of disuse, sciatic denervation, by utilizing a TFE3 whole body knockout animal and capturing sex differences through the use of both males and females with a specific focus on mitophagy. We hypothesized that females would have some mitophagic impairment leading to a worse denervation-induced mitochondrial phenotype. Similarly, we speculated that TFE3 KO animals would exhibit a paradoxical phenotype whereby mitochondria were preserved due to lysosomal impairments, but that the functionality of these organelles would be poor.

Methods

Animal handling and sciatic denervation surgery C57BL/6 (WT) and B6.129S1-*Tfe3*$^{tm-1Est}$/Mmjax were obtained from Jackson Laboratories and have been used previously[197]. Three month old male and females animals were randomly assigned to either 1- or 7-day experimental groups and subjected to sciatic denervation surgery[333]. During deep anaesthetized using isofluorane, a 2-3 mm section of the sciatic nerve was excised on one hindlimb, while the other was sham-operated serving as an internal control. Animals were given analgesics (Meloxicam, 2μg/g body weight on the day of surgery, and 1μg/g body weight on the subsequent day) and antibiotics (Baytril, 5mg/kg) post-surgery and provided food and water *ad libitum* throughout the treatment. The affected hindlimb muscles were collected for analysis. All procedures were approved by the Animal Care Committee at York University under the Canadian Council of Animal Care.

Colchicine treatment and flux measurements. A subset of animals was treated with either colchicine (0.4mg/kg/day; Col; C9754, Sigma) or 0.9% saline as vehicle (Veh) via intraperitoneal injection for 3 days prior to tissue collection as previously described[334,S18]. Constituents of the autophagosome were measured via immunoblotting in both mitochondrial fractions and whole muscle lysates to accurately capture mitophagy and autophagy. To calculate flux, the Veh values were subtracted from the mean Col value for the corresponding timepoint.

Cytochrome C Oxidase (COX) activity. COX activity was used as an indication of mitochondrial content. Briefly, frozen portions of TA muscle were lysed in enzyme extraction buffer using the Qiagen TissueLyser II and sonicated (3x3 s, at 30% power). A buffered test solution with fully reduced horse heart cytochrome c (C-2506, Sigma) was prepared and combined with enzyme

extracts in a 96-well plate. The maximal oxidation rate of fully reduced cytochrome c was measured by the absorbance at 550nm at 30°C using a microplate reader (Cytation 5, BioTek).

Mitochondrial fractionation. The gastrocnemius muscle was minced on a chilled watch glass on ice immediately after collection. Mitochondrial isolation buffer (67mM sucrose, 50mM Tris, 50mM KCl, 10mM EDTA, 0.2% BSA; pH 7.4) was added to the minced tissue, homogenized and centrifuged at 1,200 xg for 15 min at 4°C. Following, the supernate was centrifuged at 12,000 g to pellet mitochondria and the sample was cleaned with subsequent centrifugation steps.

High-resolution respirometry and ROS emission. High-resolution respirometry (Oxygraph-2K, Oroboros Instruments) was performed on a medial section of the control and denervated TA. As previously described[333], fibers were mechanically teased apart in ice-cold BIOPS (2.77mM CaK_2EGTA, 7.23mM K_2EGTA, 7.55mM Na_2ATP, 6.56mM $MgCl_2 \cdot 6H_2O$, 20mM taurine, 15mM Na_2 phosphocreatine, 20mM imidazole, 0.5mM DTT, 50 mM 2-(*N*-morpholino)ethanesulfonic acid hydrate, and pH 7.1), and permeabilized in BIOPS containing 40µg/µl saponin at 4° C for 30 mins and washed twice with Buffer Z (105mM K-2-(*N*-morpholino)ethanesulfonic acid, 30mM KCl, 10mM KH_2PO_4, 5mM $MgCl_2 \cdot 6H_2O$, 1mM EGTA, 5 mg/ml bovine serum albumin, and pH 7.4). In the chamber, fibers were incubated with oxygenated Buffer Z supplemented with 10µM Amplex-Red(A36006, ThermoFisher) to measure ROS emission, 1µM Blebbistatin (B592500, Toronto Research Chemicals) to prevent tetanus of fiber and 25 U/ml Cu/Zn SOD1 to convert O_2^- to H_2O_2 and 2mM EGTA. Substrates were subsequently titrated in the following order: pyruvate-malate to assess complex I supported respiration, ADP to assess complex I active respiration, and succinate to assess complex I+II active respiration.

Protein extracts and immunoblotting. The distal portion of the TA was lysed in Sakamoto buffer (20mM Hepes, 2mM EGTA, 1% Triton X-100, 10% glycerol, 50mM β-glycerophosphate, 1mM PMSF, 1mM DTT) supplemented with phosphatase and protease inhibitors (11-697-498-001, Roche; P0044, Sigma; P5726, Sigma) using the Qiagen TissueLyser II and centrifuged at 12,000 xg for 10 min. Supernates were collected and protein concentration was measured using the Bradford method. Whole cell protein extracts or mitochondrial fractions (20µg) were applied to a 10-18% SDS-PAGE gels and subsequently transferred onto a nitrocellulose membrane. Membranes were blocked in 5% skim milk in TBS-T (100mM TRIS, 100mM NaCl, 0.1% Tween 20) for 1 hr at room temperature with constant agitation. Primary antibodies were diluted in 5% skim milk in TBS-T and incubated overnight at 4°C and then horseradish-peroxidase (HRP)-linked secondary antibodies were applied the following day for 1 hr at room temperature (See Table 1 for a list of antibodies). Blots were then imaged using ECL (1705061, BioRad) and iBright imager (iBright 1500, Invitrogen).

RNA extracts and qPCR. The frozen proximal portion of the TA was used to isolate total RNA using the Qiagen TissueLyser II and TriZOL (15596018, Ambion) according to manufacturer's instructions. Total RNA (2µg) was then reverse transcribed to generate cDNA using Superscript III reverse transcriptase and Oligo(dt)20 (18080-044, 18418020, Invitrogen). qPCR was carried out using the StepONE Plus PCR system (Applied Biosystems) and Sybr Green Master Mix (B21202, Bimake). Primers were designed, optimized to ensure efficiency and verified for specificity with dissociation melt curves. Each sample and primer were run in duplicate with a negative control and normalized to two housekeeping genes, *ActB,* and *B2MG,* (see Table 2 for primer sequences). Data were analyzed using the $2^{-\Delta\Delta Ct}$ method, and statistical analysis was performed on the unlogged ΔCt values using a two-way ANOVA with Bonferroni post-hoc tests.

Statistical Analyses. Data presented are means ± SEM and statistical analyses were performed using Prism 9 (GraphPad Software). Three-way ANOVAs were conducted with repeated measures and Boneferroni post-hoc tests. Two-way ANOVAs were conducted to assess the response to denervation between genotypes and sex. P values less than 0.05 were accepted as significant.

Results

Females are protected from denervation-induced atrophy, as are male mice lacking TFE3. Phenotypically, TFE3 KO animals are not different from wildtype animals evidenced by similar body weights, and females of both genotypes were about 20% smaller than their male counterparts (Fig. 1A). Similarly, females had smaller TA and gastrocnemius muscle masses irrespective of genotype (Fig. 1B, 1C). However, a modest 8% reduction in gastrocnemius mass was observed in TFE3 KO males in comparison to WT males, while no differences were seen in the females (Fig. 1C). This male-specific reduction was also observed when all hindlimb muscle weights were pooled (Fig. 1D). As body weight did not differ between the genotypes, this decrease in muscle mass observed in the males is likely countered by an increase in adiposity, as reported previously[197]. Notably, our data suggest that females lacking TFE3 do not share this phenotype, as muscle mass and body weight did not differ (Fig. 1A-D). Therefore, this indicates that TFE3 is involved in the maintenance of skeletal muscle mass basally in a sex-dependent manner.

Following 7 days of denervation, significant muscle atrophy occurred across individual muscle groups (Fig. S1) and this was further exemplified when the sum of the hindlimb muscles was calculated (Fig. 1D). Interestingly, WT females appear to be mildly protected against denervation-induced atrophy as these animals lost about 22mg of muscle in comparison to WT

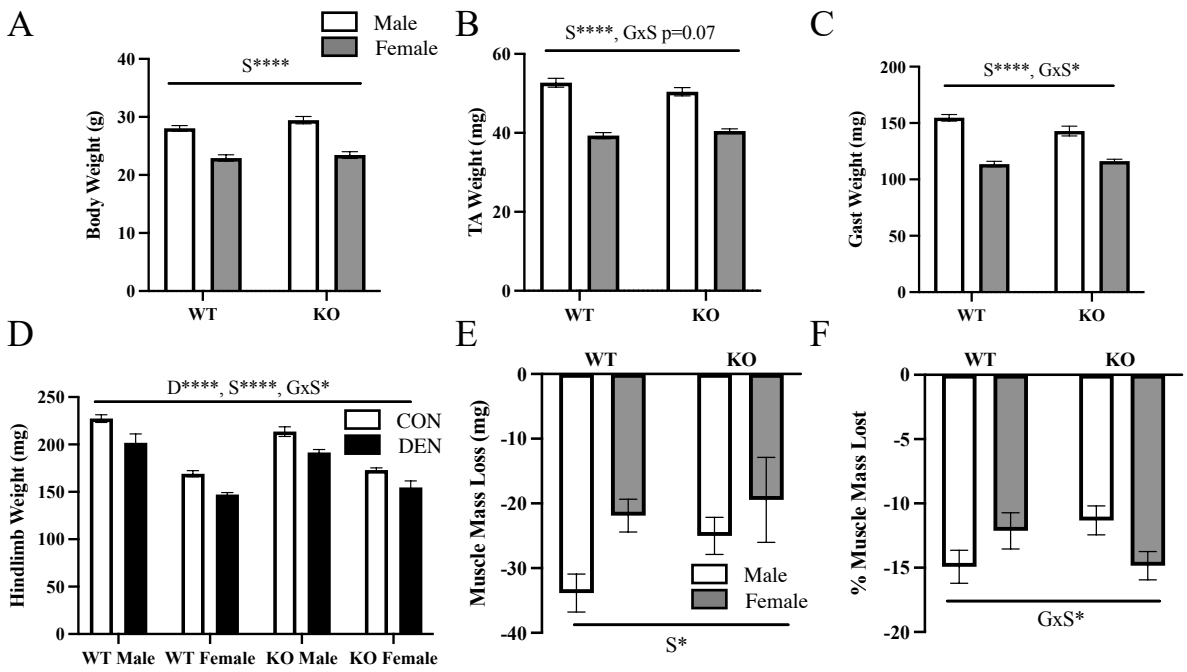

Fig. 1 Females are protected from denervation-induced atrophy, as are mice lacking TFE3. Body weights of WT and TFE3 KO animals stratified by sex (A). TA (B) and gastrocnemius (C) muscle weights basally (n=16). Sum of hindlimb muscle weights, including TA, gastrocnemius, and soleus, in WT and KO animals stratified by sex between control and denervated limbs within the same animal (D). Absolute hindlimb muscle mass lost following 7 days of denervation (E) and expressed as a percentage of control (F; n=8). S, denotes a main effect of sex; D, indicates a main effect of denervation; GxS, represents an interaction between genotype and sex; *, $p<0.05$; **, $p<0.01$; ****, $p<0.0001$.

males that lost about 34mg (Fig. 1D, 1E). Considering the sex-dependent differences in starting muscle mass, this represented a decline of 15% for the males, but only 12% for the females (Fig. 1F). The absence of TFE3 was also associated with a modest protective effect, as KO males lost on average 25mg of muscle mass, which equates to an 11% loss (Fig. 1D-1F). However, the protective effect observed in the WT females appeared to be lost in the absence of TFE3 as these animals lost 19mg of muscle, or 15%, comparable to WT males (Fig. 1D-1F). These data suggest that TFE3 has a dimorphic role in the muscle atrophy phenotype following denervation.

Sex-dependent response in mitochondrial content and function to denervation. No significant differences in COX activity were observed between WT males and females, however the absence of TFE3 resulted in a 20% decline (Fig. 2A), indicating that mitochondrial content is in part maintained by TFE3 basally. Using high-resolution respirometry in permeabilized muscle fibers, increased oxygen consumption across all respiratory states (Fig. 2B), was observed in females in comparison to males, irrespective of genotype. Intriguingly, in the absence of TFE3 in females, reduced complex I active and complex I+II active respiration (20% and 27% lower respectively) was observed in comparison to WT females (Fig. 2B). ROS emission was lower in WT females compared to males across all respiratory states (Fig. 2C), supporting previous work[218,220]. In the absence of TFE3, ROS emission across all respiratory states was reduced in males in comparison to WT males (Fig. 2C), however this was not observed in females, further indicating that TFE3 exerts a differential effect on mitochondrial function in males and females (Fig. 2C).

COX enzyme activity was significantly reduced following chronic denervation in male animals of both genotypes by 45% in WT, but only by 27% in KO animals (Fig. 2D, S1). Quite surprisingly, COX activity was maintained in both WT and KO females (Fig. 2D, S1), indicating that females are protected against denervation-induced declines in mitochondrial content (Fig. 2D). Complex I-supported respiration was significantly reduced across all conditions following 7 days of denervation, although this decrement was not observed during active respiratory states (Fig. 2E, S1). Increased ROS emission was observed across all conditions and during both inactive and active respiratory states (Fig. 2F, S1). However, it should be noted that despite having the highest ROS production basally, WT males showed the least induction of ROS following chronic denervation. This was especially evident during complex I basal and active

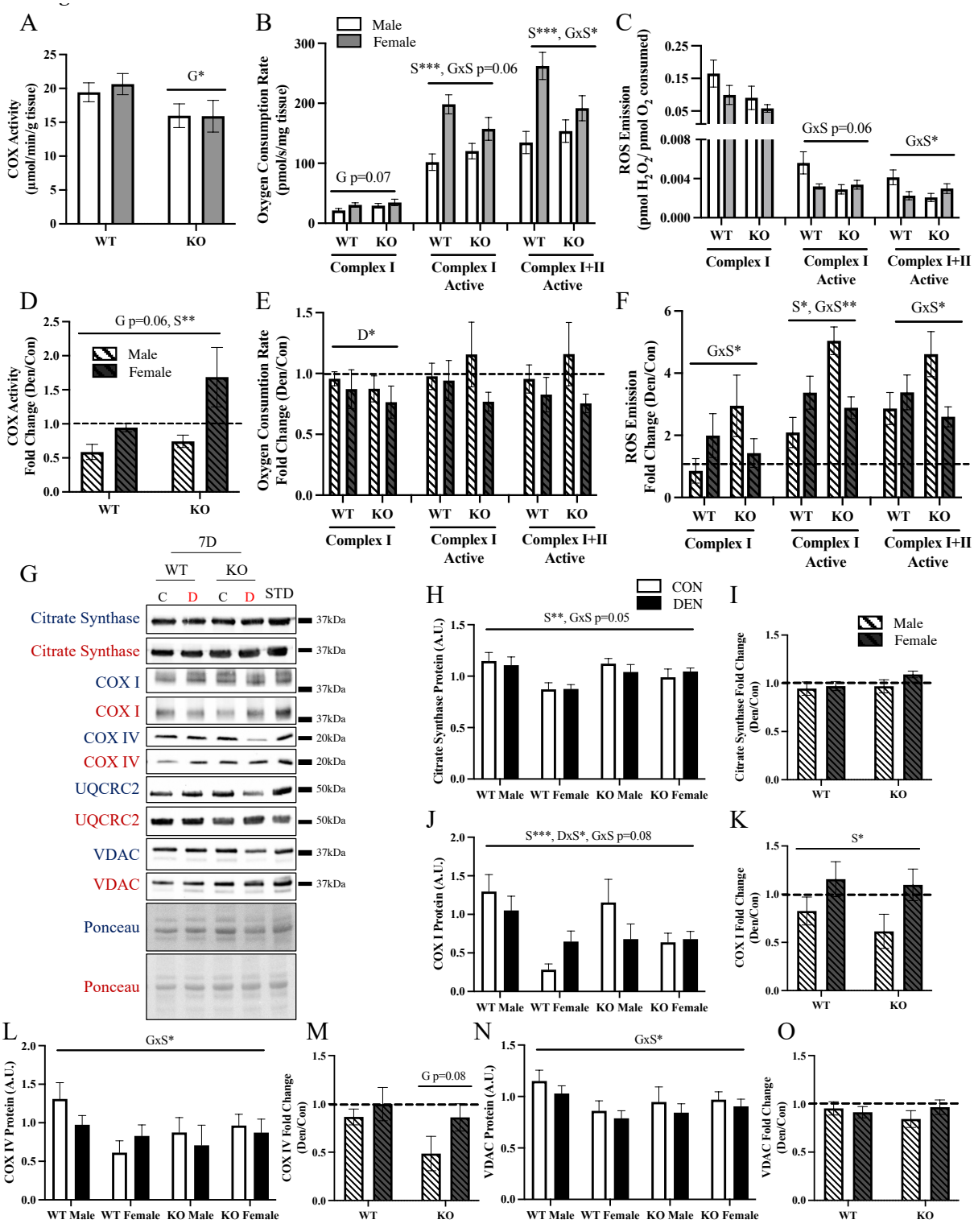
A
COX Activity (µmol/min/g tissue)
G*
WT
KO
B
Male
Female
Oxygen Consumption Rate (pmol/s/mg tissue)
G p=0.07
S***, GxS p=0.06
S***, GxS*
Complex I
Complex I Active
Complex I+II Active
C
ROS Emission (pmol H2O2/ pmol O2 consumed)
GxS p=0.06
GxS*
D
COX Activity Fold Change (Den/Con)
G p=0.06, S**
E
Oxygen Consumption Rate Fold Change (Den/Con)
D*
F
ROS Emission Fold Change (Den/Con)
GxS*
S*, GxS**
7D
G
C D C D STD
Citrate Synthase
COX I
COX IV
UQCRC2
VDAC
Ponceau
37kDa
20kDa
50kDa
H
CON
DEN
Citrate Synthase Protein (A.U.)
S**, GxS p=0.05
WT Male WT Female KO Male KO Female
I
Citrate Synthase Fold Change (Den/Con)
J
COX I Protein (A.U.)
S***, DxS*, GxS p=0.08
K
COX I Fold Change (Den/Con)
S*
L
COX IV Protein (A.U.)
M
COX IV Fold Change (Den/Con)
G p=0.08
N
VDAC Protein (A.U.)
O
VDAC Fold Change (Den/Con)

Fig. 2 Sex-dependent response in mitochondrial content and function to denervation. Cytochrome c oxidase (COX) activity assessed as a measure of mitochondrial content basally (A). Oxygen consumption measured in permeabilized muscle fibers under complex I, complex I active and complex I+II active respiratory states (B), and the corresponding ROS emission (C). COX activity following denervation, expressed as a fold over the contralateral control limb (D). Oxygen consumption rates following 7 days of denervation (E) and corresponding ROS emission (F) expressed relative to intra-animal control. Representative western blot for mitochondrial markers (G). Quantification of Citrate synthase (H), COX I (J), COX IV (L), VDAC (N) following denervation. Effect of 7 days of denervation on citrate synthase (I), COX I (K), COX IV (M), and VDAC (O) expressed as a fold change. G, represents a main effect of genotype; S, denotes a main effect of sex; D, indicates a main effect of denervation; GxS, represents an interaction between genotype and sex; DxS, indicates an interaction effect between denervation and sex *, $p<0.05$; **, $p<0.01$; ***, $p<0.001$.

respiratory states. In contrast, WT females exhibited much more pronounced 2-4-fold elevations in ROS as a result of denervation. While the absence of TFE3 did not further increase these levels of ROS in females, TFE3 ablation led to marked 3-5- fold increases in ROS emission in male mice. Taken together, these data suggest that males are partially spared from denervation-induced mitochondrial dysfunction, but that this protection is dependent on the presence of TFE3.

Mitochondrial markers citrate synthase, COX IV and VDAC protein content were lower in females in comparison to males under basal conditions, however this sex difference was largely not observed in the absence of TFE3 (Fig. 2H, 2L, 2N) suggesting that TFE3 normally contributes to sex differences in the expression of mitochondrial proteins. Following chronic denervation, COX I was reduced in WT males by 20% and by 40% in KO males (Fig. 2J, 2K). In line with the COX activity data (Fig. 2D), COX I expression was actually increased 2-fold in WT females and did not change in KO females (Fig. 2J) supporting a sex-dependent response to denervation. A similar trend was observed for COX IV, whereby males tended to display a

decrease, but WT females exhibited a modest increase while KO females showed no change in COX IV levels (Fig. 2L, 2M).

mRNA expression of TFEB along with lysosomal and autophagy markers in the presence and absence of TFE3. Tfeb mRNA was 54% higher in WT females in comparison to WT males, and in the absence of TFE3, *Tfeb* mRNA was elevated in males by 52% compared to WT animals (Fig. 3A). However, no difference between the sexes were observed in the absence of TFE3 indicating a sexually divergent response. No differences were observed in the mRNA levels of lysosomal markers, including *Ctsb, Ctsd, Mcoln1, Lamp1* and *Lamp2* in the absence of TFE3 basally (Fig. 3B). Furthermore, a similar finding was observed in the mRNA of autophagy-related genes, *Beclin1, Map1lc3b, p62* and *Park2* (Fig. 3C). Intriguingly, despite the increased TFEB mRNA observed in WT females, a main effect of sex was observed in a number of targets including *Ctsb, Lamp1, Beclin1, p62,* and *Park2,* which were all reduced in comparison to their male counterparts (Fig. 3A-C).

Females have higher lysosomal content and mitophagy flux basally and exhibit early changes in lysosomes following denervation. Lysosomal protein content was assessed basally and following 1 day of denervation (Fig. 4A, S4). Standards were used to make comparisons between males and females, visible in the expanded images (Fig. S4). Basally, an increase in a variety of lysosomal markers was observed in females. The lysosomal regulator TFEB was significantly higher in females compared to males irrespective of genotype (Fig. 4B). It is possible that this increased TFEB expression supported the 2.5-3-fold increase in the lysosomal proteins Cathepsin D (Mature form; Fig. 4F) and v-ATPase (Fig. 4E) in females. No evidence of compensatory TFEB protein expression was found in either males or females in the absence of TFE3. In addition, transcription family member TFE3 did not show any sex-dependent

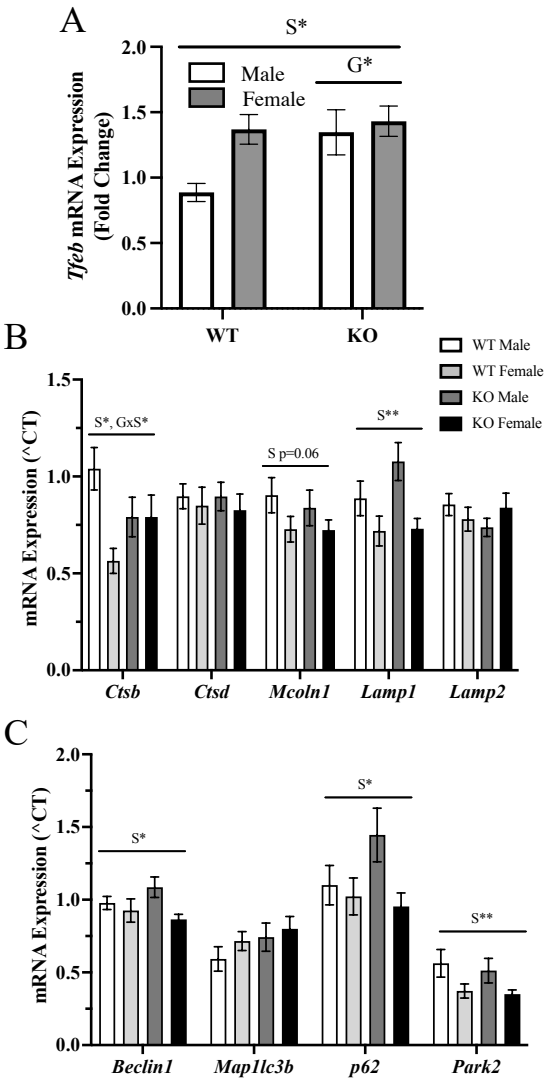

Fig. 3 mRNA expression of TFEB along with lysosomal and autophagy markers in the presence and absence of TFE3. Basal *Tfeb* gene expression in WT and KO animals stratified by sex (A). Lysosomal mRNA levels in male and female WT and KO animals, including *Ctsb, Ctsd, Mcoln1, Lamp1* and *Lamp2* (B), and autophagy-related genes, *Beclin1, Map1lc3b, Sqstm1,* and *Park2* (C) normalized to *Gapdh* and *B2MG*. S, denotes a main effect of sex; GxS, represents an interaction between genotype and sex; *, $p<0.05$; **, $p<0.01$.

differences in WT mice (Fig. 4C). The mitophagy E3 ubiquitin ligase Parkin was 66% higher in females in comparison to male counterparts basally (Fig. 4D). It appears that TFEB, and likely other MiT family members, are sufficient to maintain lysosomes as the loss of TFE3 did not impact lysosomal markers basally. Interestingly, the ratio of mature/total Cathepsin D, which is used as one indicator of lysosomal function, was not different between sexes, genotype or following acute denervation (Fig. 4G). Furthermore, 1 day of denervation did not appear to have a widespread effect as no changes were observed in TFE3, Parkin or v-ATPase protein

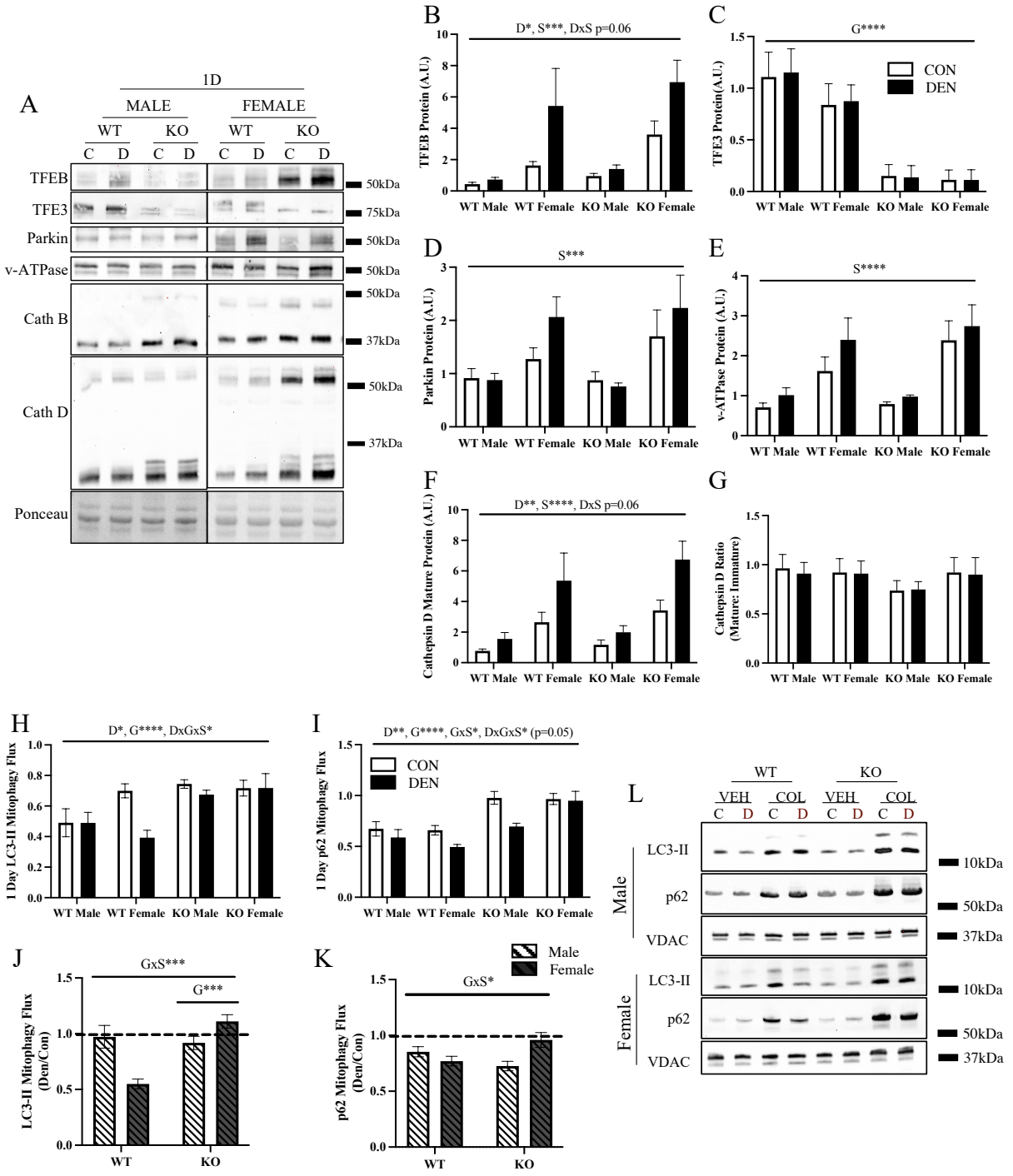
A
1D
MALE
FEMALE
WT
KO
C D
TFEB
TFE3
Parkin
v-ATPase
Cath B
Cath D
Ponceau
50kDa
75kDa
37kDa
B
D*, S***, DxS p=0.06
TFEB Protein (A.U.)
C
G****
TFE3 Protein(A.U.)
CON
DEN
D
S***
Parkin Protein (A.U.)
E
S****
v-ATPase Protein (A.U.)
F
D**, S****, DxS p=0.06
Cathepsin D Mature Protein (A.U.)
G
Cathepsin D Ratio (Mature: Immature)
WT Male
WT Female
KO Male
KO Female
H
D*, G****, DxGxS*
1 Day LC3-II Mitophagy Flux
I
D**, G****, GxS*, DxGxS* (p=0.05)
1 Day p62 Mitophagy Flux
J
GxS***
G***
LC3-II Mitophagy Flux (Den/Con)
K
GxS*
p62 Mitophagy Flux (Den/Con)
Male
Female
L
VEH
COL
LC3-II
p62
VDAC
10kDa
50kDa
37kDa

Fig. 4 Females have higher lysosomal content and mitophagy flux basally and exhibit early changes in lysosomes following denervation. Representative blots of lysosomal markers following 24 hr of denervation (A). Quantification of TFEB (B), TFE3 (C), Parkin (D), v-ATPase (E), and mature Cathepsin D (F) following denervation in both sexes of WT and KO animals. Quantification of the ratio of mature to total Cathepsin D (G), an indication of lysosomal status. A subset of animals were treated with colchicine to assess mitophagy flux. LC3-II (H) and p62 (I) mitophagic flux was calculated by taking the difference between colchicine- and vehicle-treated conditions. The fold change in LC3-II (J) and p62 mitophagy flux (K) following acute denervation. Representative blots for LC3-II and P62 in mitochondrial fractions. G, represents a main effect of genotype; S, denotes a main effect of sex; D, indicates a main effect of denervation; GxS, represents an interaction between genotype and sex; DxS, indicates an interaction effect between denervation and sex; DxGxS, denotes an interaction effect between denervation, genotype and sex; *, $p<0.05$; **, $p<0.01$; ***, $p<0.001$; ****, $p<0.0001$.

levels. However, females appear to be more responsive to acute denervation as TFEB expression increased 3-fold in WT females and 2-fold in KO females, while no changes were observed in males of both genotypes (Fig. 4B). Similarly, although Cathepsin D expression increased following acute denervation, the greatest induction was observed in females of both genotypes (Fig. 4F).

A subset of animals was treated with colchicine 3 days prior to tissue collection to fully capture the dynamic nature of autophagy and mitophagy (Fig. 4L). In line with the increased lysosomal content and Parkin expression observed basally in females, LC3-II mitophagy flux was 40% higher in WT females in comparison to their male littermates under control conditions (Fig. 4H). Following 1 day of denervation, only WT females reduced their LC3-II mitophagy flux by 44%, while all other groups showed no change (Fig. 4H, 4J). This was also seen in p62-mitophagy flux as females decreased p62 mitophagy flux by 25%. This sex-dependent response was largely absent in the TFE3 KO mice (Fig. 4I; 4K). Unexpectedly, an increase in both LC3-II and p62 basal mitophagy flux was observed in both males and females in the absence of TFE3, which remained mostly unchanged following acute denervation (Fig. 4H, 4I). Autophagy flux

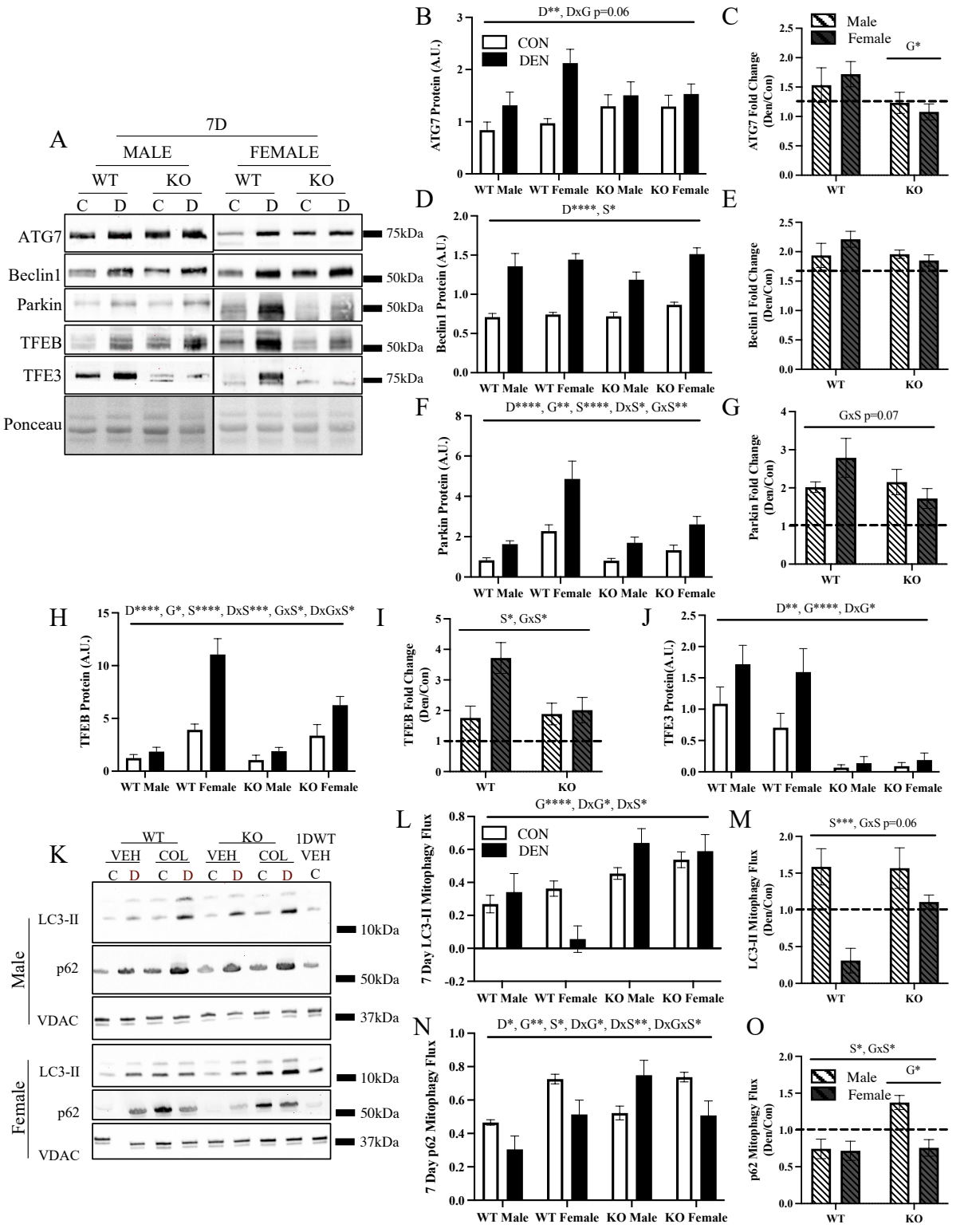
A
7D
MALE
FEMALE
WT
KO
WT
KO
C D C D C D C D
ATG7
Beclin1
Parkin
TFEB
TFE3
Ponceau
75kDa
50kDa
50kDa
50kDa
75kDa
B
D**, DxG p=0.06
CON
DEN
ATG7 Protein (A.U.)
WT Male WT Female KO Male KO Female
C
Male
Female
G*
ATG7 Fold Change (Den/Con)
WT KO
D
D****, S*
Beclin1 Protein (A.U.)
WT Male WT Female KO Male KO Female
E
Beclin1 Fold Change (Den/Con)
WT KO
F
D****, G**, S****, DxS*, GxS**
Parkin Protein (A.U.)
WT Male WT Female KO Male KO Female
G
GxS p=0.07
Parkin Fold Change (Den/Con)
WT KO
H
D****, G*, S****, DxS***, GxS*, DxGxS*
TFEB Protein (A.U.)
WT Male WT Female KO Male KO Female
I
S*, GxS*
TFEB Fold Change (Den/Con)
WT KO
J
D**, G****, DxG*
TFE3 Protein(A.U.)
WT Male WT Female KO Male KO Female
K
WT
KO
1DWT
VEH COL VEH COL VEH
C D C D C D C D C
Male
LC3-II
p62
VDAC
Female
LC3-II
p62
VDAC
10kDa
50kDa
37kDa
10kDa
50kDa
37kDa
L
G****, DxG*, DxS*
CON
DEN
7 Day LC3-II Mitophagy Flux
WT Male WT Female KO Male KO Female
M
S***, GxS p=0.06
LC3-II Mitophagy Flux (Den/Con)
WT KO
N
D*, G**, S*, DxG*, DxS**, DxGxS*
7 Day p62 Mitophagy Flux
WT Male WT Female KO Male KO Female
O
S*, GxS*
G*
Male
Female
p62 Mitophagy Flux (Den/Con)
WT KO

Fig. 5 Females exhibit a profound autophagic and mitophagic response to denervation, and this is blunted in the absence of TFE3. Representative blots for autophagy- and mitophagy-related markers following 7 days of denervation (A). Quantification for ATG7 (B), Beclin1 (D), Parkin (F), TFEB (H), and TFE3 (J) protein content following 7 days of denervation. Effect of 7 days of denervation on ATG7 (C), Beclin1 (E), Parkin (G), TFEB (I) and TFE3 (K) expressed as a fold change. Representative blots of mitophagy flux following 7 days of denervation. Quantification of LC3-II (L) and p62 (N) mitophagy flux, taken as the difference between colchicine- and vehicle-treated conditions. Effect of denervation on mitophagy flux was summarized as a fold change of denervated over control conditions (M, O). G, represents a main effect of genotype; S, denotes a main effect of sex; D, indicates a main effect of denervation; GxS, represents an interaction between genotype and sex; DxS, indicates an interaction effect between denervation and sex; DxG, interaction effect between denervation and genotype; DxGxS, denotes an interaction effect between denervation, genotype and sex; *, $p<0.05$; **, $p<0.01$; ***, $p<0.001$; ****, $p<0.0001$.

was also assessed in whole muscle lysates (Fig. S2). In line with the mitophagy results, a surprising increase in autophagy flux was observed in the absence of TFE3 (Fig. S2). Declines in LC3-II and p62 autophagy flux were seen in WT animals irrespective of sex following denervation. However, the absence of TFE3 altered this denervation-induced response, especially in males where no reduction was observed (Fig. S2, A-C). Thus, female animals maintain a higher lysosomal content basally to support greater flux independent of TFE3. However, following acute denervation females exhibit an inhibition of mitophagy in order to preserve mitochondria, and this response is reliant on TFE3.

Females exhibit a profound autophagic and mitophagic response to chronic denervation, and this is blunted in the absence of TFE3. The upstream autophagy regulator ATG7 was increased by 1.9-fold in WT animals following 7 days of denervation, however this was blunted in the absence of TFE3 (Fig. 5B, 5C). In contrast, the autophagy regulator Beclin1 was increased by 2-fold, irrespective of TFE3 expression (Fig. 5D, 5E). In line with the previous findings, Parkin protein content was twice as high in females in comparison to males and was further increased

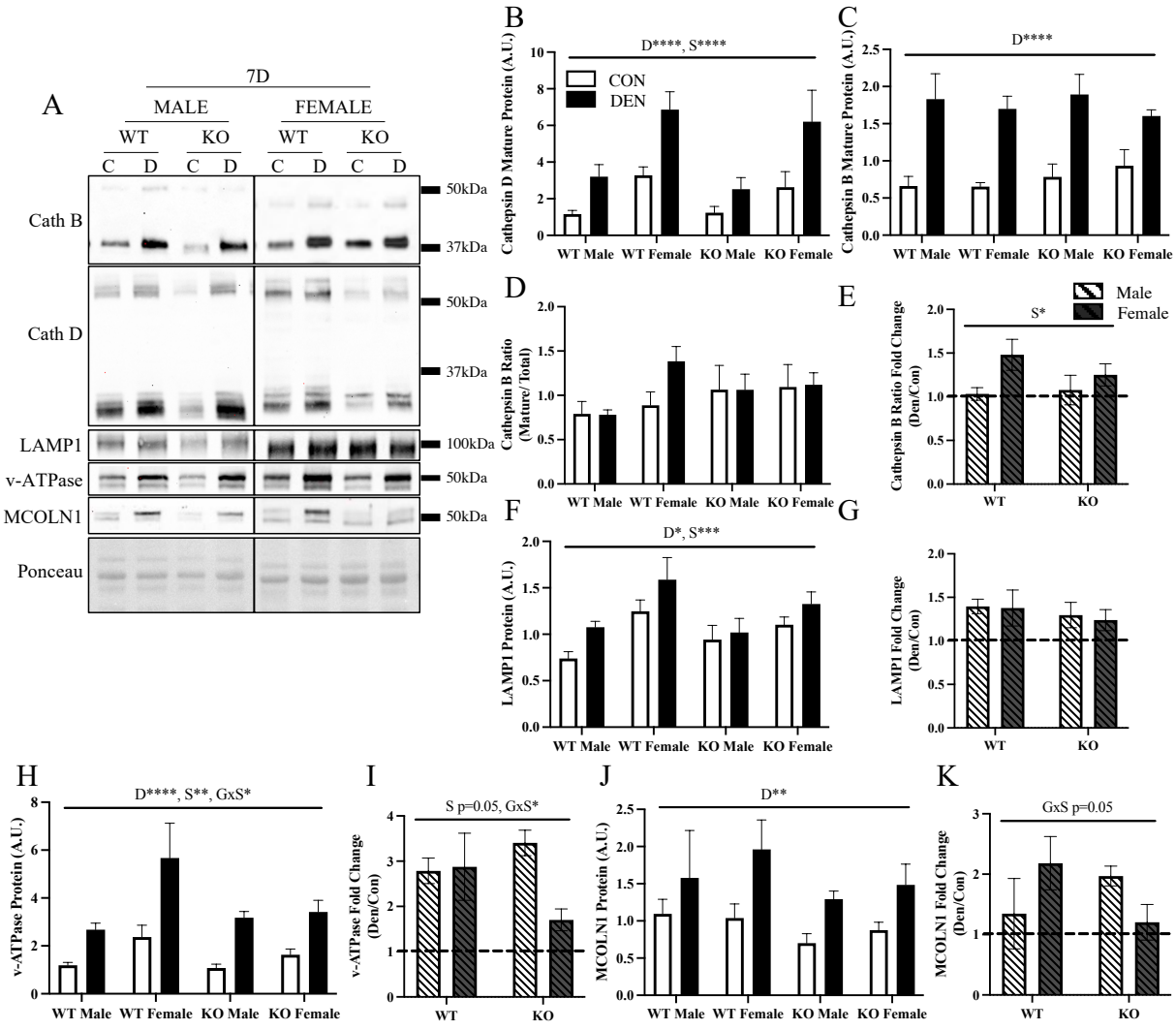

Fig. 6 Increases in lysosomal markers in females following denervation are partially dependent on TFE3. Representative blots of lysosomal markers following 7 days of denervation (A). Quantification of mature Cathepsin D (B), mature Cathepsin B (C), Cathepsin B ratio (D), LAMP1 (F), v-ATPase (H), and and MCOLN1 (J) following denervation in both sexes of WT and KO animals. Effect of 7 days of denervation on Cathepsin D ratio (E), LAMP1 (G), v-ATPase (I), and MCOLN1 (K) expressed as a fold change. S, denotes a main effect of sex; D, indicates a main effect of denervation; GxS, represents an interaction between genotype and sex; *, $p<0.05$; **, $p<0.01$; ***, $p<0.001$; ****, $p<0.0001$.

by chronic denervation (Fig. 5F, 5G). TFEB protein content was also 3-fold higher in females basally (Fig. 5H). Denervation increased TFEB expression further by 2.8-fold in WT females. This large increase was significantly blunted in KO females (1.8-fold; Fig. 5H, 5I). Similarly, TFE3 was also induced by chronic denervation in WT mice, but in contrast to TFEB, no sex differences were observed (Fig. 5J).

Mitophagy flux was assessed and in accordance with the acute findings, higher LC3-II and p62 flux was observed basally in females and in TFE3 KO animals (Fig. 5L, 5N). Furthermore, a sex-dependent response to denervation was noted as WT females decreased both their LC3-II and p62 mitophagy flux, whereas this was less evident in WT males following denervation (Fig. 5L-O). Intriguingly, in the absence of TFE3, males increased both LC3-II and p62 mitophagy flux following chronic denervation, illustrating a divergent response in comparison to WT males. The reduction in mitophagy flux in WT females was attenuated by the absence of TFE3. Taken together, WT females exhibit a reduced mitophagic response following denervation that is presumably supporting the maintenance of mitochondrial content. This is likely reflective of an accumulation of dysfunctional mitochondria, as supported by the exacerbated ROS emission, rather than a beneficial adaptation. Thus, females demonstrate a preference towards mitochondrial preservation at the expense of function, however this inhibition of mitophagy is not as great in females lacking TFE3, potentially indicating an impaired ability to mount a sex-appropriate response in the absence of the transcription factor. In KO males, despite the increase in mitophagy flux, it is clear that this is insufficient clearance, as there remains evidence of mitochondrial dysfunction.

Increases in lysosomal markers in females following denervation are partially dependent on TFE3. In contrast to the protein data, females exhibited lower levels of *p62* and *Park2* mRNA

under basal conditions (Fig. S3). Following 7 days of denervation, the expression of autophagy and mitophagy markers *Beclin1, p62*, *Map1lc3b*, *Park2* mRNA was significantly increased across all conditions, independent of TFE3 (Fig. S3). *Ctsb, Ctsd* and *Lamp2* mRNA were also significantly increased across all conditions independent of TFE3 (Fig. S3). Basally, sex differences were observed for mature Cathepsin D, LAMP1 and v-ATPase protein expression, as females had 2- (Fig. 6B), 1.5- (Fig. 6F), and 1.8-fold higher protein expression, respectively. Chronic denervation resulted in a massive induction of lysosomal proteins, as Cathepsin B, Cathepsin D, MCOLN1, LAMP1 and v-ATPase were all upregulated independent of genotype or sex (Fig. 6A). However, following denervation only females exhibited a 50% increase in the ratio of mature/total Cathepsin B, which serves as an indication of lysosomal function (Fig. 6E), while a more modest increase was observed in females lacking TFE3 (Fig. 6E). Furthermore, while v-ATPase increased across all conditions by 2.8-3.4-fold following denervation, female KO mice exhibited a blunted response as v-ATPase was only increased by 1.7-fold (Fig. 6H, 6I). A similar trend was observed for MCOLN1, as its content increased by 100% in WT females, but only a 20% induction was observed in KO females (Fig. 6J, 6K). Interestingly, WT males showed a modest 30% increase, but KO males exhibited a similar doubling effect as females (Fig. 6J, 6K). Thus, it appears that the loss of TFE3 has a greater impact on the lysosomal adaptations to chronic denervation in females, compared to males.

Discussion

Prolonged periods of physical inactivity have severe ramifications for skeletal muscle mass and function. A common feature that has widely been overlooked until very recently is the impact of sex on muscle atrophy. The purpose of the present study was to explore disuse-induced muscle atrophy between the sexes with a focus on the adaptive roles of lysosomes and

mitochondria. As lysosomes are a major degradative site within the cell, we aimed to better understand the importance of these organelles by genetically deleting a lysosomal regulator, TFE3. Importantly, this transcription factor resides on the X chromosome and thus we speculated that it would be a good candidate to investigate sexual dimorphisms.

Basal sex-dependent phenotypes.

Females exhibited greater mitochondrial function, characterized by increased oxygen consumption and reduced ROS emission compared to males under basal conditions. Our data also indicate that females have higher basal autophagy and mitophagy flux facilitated by an increased lysosomal content, compared to males. We speculate that this elevated mitochondrial turnover likely contributes to the greater mitochondrial function and decreased ROS emission in young female mouse muscle. Also contributing to this reduced oxidative stress may be the antioxidant properties of estrogen[146,147,152,S19], and its ability to imbed into mitochondrial membranes improving the integrity and leading to reduced H_2O_2 emission[152].

TFE3 has been implicated in autophagy and lysosomal regulation since studies have found that the loss of TFE3 negatively impacts lysosomes under stress conditions[169,S15]. Our results indicate that the lack of TFE3 exerts a subtle metabolic phenotype, as mitochondrial content was reduced in both males and females. Intriguingly a reduction in mitochondrial function was observed in females, but not in males. This indicates that mitochondrial function is regulated in part through TFE3 in a sex-dependent manner. Furthermore, as no differences were observed in lysosomal proteins basally in the absence of TFE3, this cannot be attributed to previously described roles of TFE3 in determining lysosomal content. Moreover, despite the marked increase in *Tfeb* mRNA in TFE3 KO animals, we did not observe any compensation in TFEB at the protein level. This indicates that basal levels of TFEB, along with the possible

BASAL		
	WT	KO
MUSCLE MASS	M>F	M>F ↓ M N/C F
MITOCHONDRIAL CONTENT	M<F	M=F ↓M ↓F Overall decrease
MITOCHONDRIAL FUNCTION	M<F	M=F Resp ↓ F
MITOPHAGY	M<F	M=F ↑M N/C or ↑ F Overall increase
LYSOSOMAL CONTENT	M<F	M<F N/A M N/A F
Conclusions: TFE3 regulates muscle mass basally in males. Loss of TFE3 reduces mitochondrial content irrespective of sex. Sexual dimorphism of mitochondrial function is reliant on TFE3. Loss of TFE3 increases mitophagy flux, surprisingly. Lysosomal content is not dependent on TFE3 basally.		
DENERVATION		
	WT	KO
LOSS OF MUSCLE MASS	M>F	M<F
LOSS OF MITOCHONDRIAL CONTENT	M>F	M>F Overall protection
MITOCHONDRIAL DYSFUNCTION	M<F	M>F Similar response as WT F
MITOPHAGY	M>F N/C M ↓ F	M>F ↑M ↑ F
INDUCTION OF LYSOSOMES	M<F	M>F N/A M ↓ F
Conclusions: Females preserve muscle mass following denervation, loss of TFE3 reverses this dimorphism. Females preserve mitochondrial content at the expense of function by reducing mitophagy, loss of TFE3 makes the response to denervation similar to WT females. Lysosomal induction in females is dependent on TFE3, but not in males.		

Fig. 7 Summary of findings.

contribution of other factors such as MITF or FOXO[169,170,376,S20], are sufficient to maintain lysosomal content basally. Further, contrary to our initial hypothesis, an increase in mitophagy flux was observed in the absence of TFE3 irrespective of sex. This increased turnover potentially supports the reduced mitochondrial content observed in these animals. These data indicate that TFE3 participates in the maintenance of mitochondria in a sex-dependent manner.

Sex-dependent denervation-induced phenotypes

Our data verify that female mice have significantly less muscle mass in comparison to male counterparts. However, females exhibited a protective effect following 7 days of denervation, as they lost less muscle in comparison to males. This was surprising as recent work showed no differences between males and females in muscle atrophy following 7 days of hindlimb-unloading in mice[353]. It is likely that the differences can be attributed to the severity of the model, as denervation generally produces losses in muscle mass that are observed with longer periods of hindlimb unloading[S1]. In line with this hypothesis, female rats subjected to 14 days of hindlimb unloading experienced a preservation of muscle mass and function in comparison to males[426]. The mechanisms involved may be related to effects of estrogen, since estrogen administration in male rats has been shown to protect against atrophy following 10 days of immobilization[422].

As has been described in numerous accounts, prolonged denervation leads to mitochondrial dysfunction and declines in mitochondrial content[333,334,409,411,457,S21]. Here we show that this response is also sexually dimorphic, such that males lose mitochondrial content while females do not. However, it appears that females are preserving mitochondria at the cost of function, as females exhibited a greater induction of ROS emission with denervation. This is in line with previous findings that have also observed a greater elevation in ROS emission in

females following hindlimb unloading[219,220]. Females reduce their mitophagy flux in response to denervation thereby maintaining mitochondrial content, but at the expense of increased dysfunction. Interestingly, females exhibited a greater induction of ATG7, Parkin and TFEB, indicating that this preference to preserve mitochondria is not due to a lack of lysosomes or autophagy machinery. Thus, these data indicate that males and females have different priorities during atrophy conditions, but it remains unclear what drives this dimorphism, and which strategy is beneficial in the long run.

We initially hypothesized that in atrophic conditions autophagy and lysosomes would be dysregulated in the absence of TFE3, thereby exacerbating the disuse-induced phenotype. This would be in line with previous reports that have shown that the inhibition of autophagy induces muscle atrophy[S22] and can exacerbate muscle wasting[384,386]. Surprisingly, muscle mass was spared following denervation in the absence of TFE3, an effect that was only observed in males, not females. Further, mitochondrial content was preserved in the absence of TFE3 in females, but similar to their WT counterparts this was accompanied by increased mitochondrial dysfunction. In response to denervation, mitophagy flux did not decline in the absence of TFE3, leading to the maintenance or increase in mitochondrial content markers with denervation. Thus, our data suggest that TFE3 is playing a sex-dependent role, as the decrease in mitophagy flux observed in WT females was lost in the absence of TFE3.

The induction of autophagy and lysosomal proteins that typically accompany chronic denervation in WT animals was attenuated in the absence of TFE3 in females. This was matched by a marked reduction in TFEB expression in female mice following chronic denervation, and a similar phenomenon was observed in a subset of lysosomal markers including v-ATPase and MCOLN1, both of which are integral to maintenance of lysosomal function[186,458,S23]. However,

while the denervation-induced expression of these lysosomal markers was not as great in males, the absence of TFE3 had no impact. Moreover, the denervation-induced elevation in ATG7 and Parkin were severely blunted in females lacking TFE3. Thus, our data suggest that TFE3 is dispensable basally, as well as in mediating denervation-induced increases in lysosomal and autophagy-related proteins in males. However, TFE3 appears to be more critical in the chronic denervation-induced lysosomal and autophagy responses in females, indicating a sexually dimorphic function of TFE3 in response to denervation-induced muscle atrophy.

Overall conclusion

Our findings contribute significantly to the emerging literature supporting a sexually dimorphic response of muscle to disuse conditions, as well as an important function for TFE3 in determining this divergent response. Females have a tendency to preserve muscle mass and mitochondria, perhaps at the expense of function by reducing mitochondrial clearance through mitophagy. This is not due to a limitation on lysosomes or autophagy machinery, as females exhibit an increased expression of lysosomal and autophagy proteins. On the other hand, males preferentially maintain mitochondrial function at the expense of content by maintaining high levels of mitophagy during denervation to help clear dysfunctional organelles. Autophagy and mitochondrial maintenance are key regulators of muscle mass, as the inhibition of autophagy leads to an accumulation of dysfunctional mitochondria that exert cytotoxic effects and promote nuclear decay[207,384,386,S22,S24], thereby exacerbating atrophy. It appears that despite having the lysosomal and autophagic capacity, females do not rely on these mechanisms to preserve muscle mass following 7 days of denervation since a decrease in mitophagy actually spared muscle mass in females while contributing to an accumulation of dysfunctional organelles. Our data underscore the value of further exploring the molecular underpinnings that regulate how males

and females respond to chronic muscle disuse such as denervation, and solidify the need to develop sex-specific strategies to combat muscle atrophy.

Acknowledgments:

J.M. Memme and J. Wong aided in tissue collection and mitochondrial isolations. J. Wong aided in western blotting experiments. A.N. Oliveira performed all surgical procedures, data collection, and data analysis. A.N. Oliveira and D.A. Hood conceived the experimental design and prepared the manuscript.

The authors of this manuscript certify that they comply with the ethical guidelines for authorship and publishing in the Journal of Cachexia, Sarcopenia and Muscle[459].

This work was supported by the Natural Sciences and Engineering Research Council of Canada and funding from the Canadian Institutes of Health Research. D.A. Hood is the holder of a Tier I Canada Research Chair in Cell Physiology. A.N. Oliveira is the recipient of the Natural Science and Engineering Research Council Doctoral Canada Graduate Scholarship.

Disclosure Statement:

All authors, A.N. Oliveira, J.M. Memme, J. Wong and D.A. Hood declare that they do not have any potential conflicts of interest.

Table 1: List of antibodies used for western blotting

Protein	**Concentration**	**Company**	**Catalogue Number**
ATG7	1:1000	Sigma-Aldrich	A2856
Beclin1	1:1000	Cell Signaling Technology	3738S
Citrate Synthase	1:1000	Abcam	AB96600
COX I	1:500	Abcam	AB14705
COX IV	1:500	Abcam	AB14744
Cathepsin B	1:1000	Cell Signaling Technology	31718S
Cathepsin D	1:1000	Santa Cruz Biotechnology	SC-377299
Lamp1	1:1000	Abcam	AB24170
LC3	1:500	Cell Signaling Technology	4108S
MCOLN1	1:1000	Invitrogen	PA1-46474
P62	1:1000	Cell Signaling Technology	5114S
Parkin	1:1000	Cell Signaling Technology	4211S
TFEB	1:500	MyBioSource	MBS120432
TFE3	1:500	Sigma-Aldrich	HPA023881
UQCRC2	1:500	Abcam	AB14734
v-ATPase	1:1000	Santa Cruz Biotechnology	SC-55544
VDAC	1:1000	Abcam	Ab14734
HRP-linked Anti-mouse	As per manufacturer's suggestions	Cell Signaling Technology	7074S
HRP-linked Anti-rabbit	As per manufacturer's suggestions	Cell Signaling Technology	7076S

Table 2: List of primer oligonucleotide sequences in real-time qPCR analysis for *Mus musculus*

Gene	**Forward Primer**	**Reverse Primer**
Tfeb	5'-AGCTCCAACCCGAGAAAGAGTTTG-3'	5'-CGTTCAGGTGGCTGCTAGAC-3'
Sqstm1	5'-TGTGGTGGGAACTCGCTATAA-3'	5'-CAGCGGCTATGAGAGAAGCTAT-3'
Map1lc3b	5'-GCTTGCAGCTCAATGCTAAC-3'	5'-CCTGCGAGGCATAAACCATGTA-3'
Beclin1	5'-AGGCTGAGGCGGAGAGATT-3'	5'-TCCACACTCTTGAGTTCGTCAT-3'
Park2	5'-GTCTGCAATTTGGTTTGGAGTA-3'	5'-GCATCATGGGATTGTCTCTTAAA-3'
Ctsb	5'-GAAGAAGCTGTGTGGCACTG-3'	5'-GTTCGGTCAGAAATGGCTTC-3'
Ctsd	5'-TTTGCCAATGCTGTCGTACT-3'	5'-AGCGAGTGTGACTATGTGTGA-3'
Lamp1	5'-CTAGTGGGAGTTGCGGTATCA-3'	5'-AGGGCATCAGGAAGAGTCATAT-3'
Lamp2	5'-GCTGAACAACAGCCAAATTA-3'	5'-CTGAGCCATTAGCCAAATACAT-3'
Mcoln1	5'-TTGCAGCCTACACACAGGAG-3'	5'-AGAGAGCCAAAGCTGATCCA-3'
Gapdh	5'-AACACTGAGCATCTCCCTCA-3'	5'-GTGGGTGCAGCGAACTTTAT-3'
Actb	5'-TGTGACGTTGACATCCGTAA-3'	5'-GCTAGGAGCCAGAGCAGTAA-3'

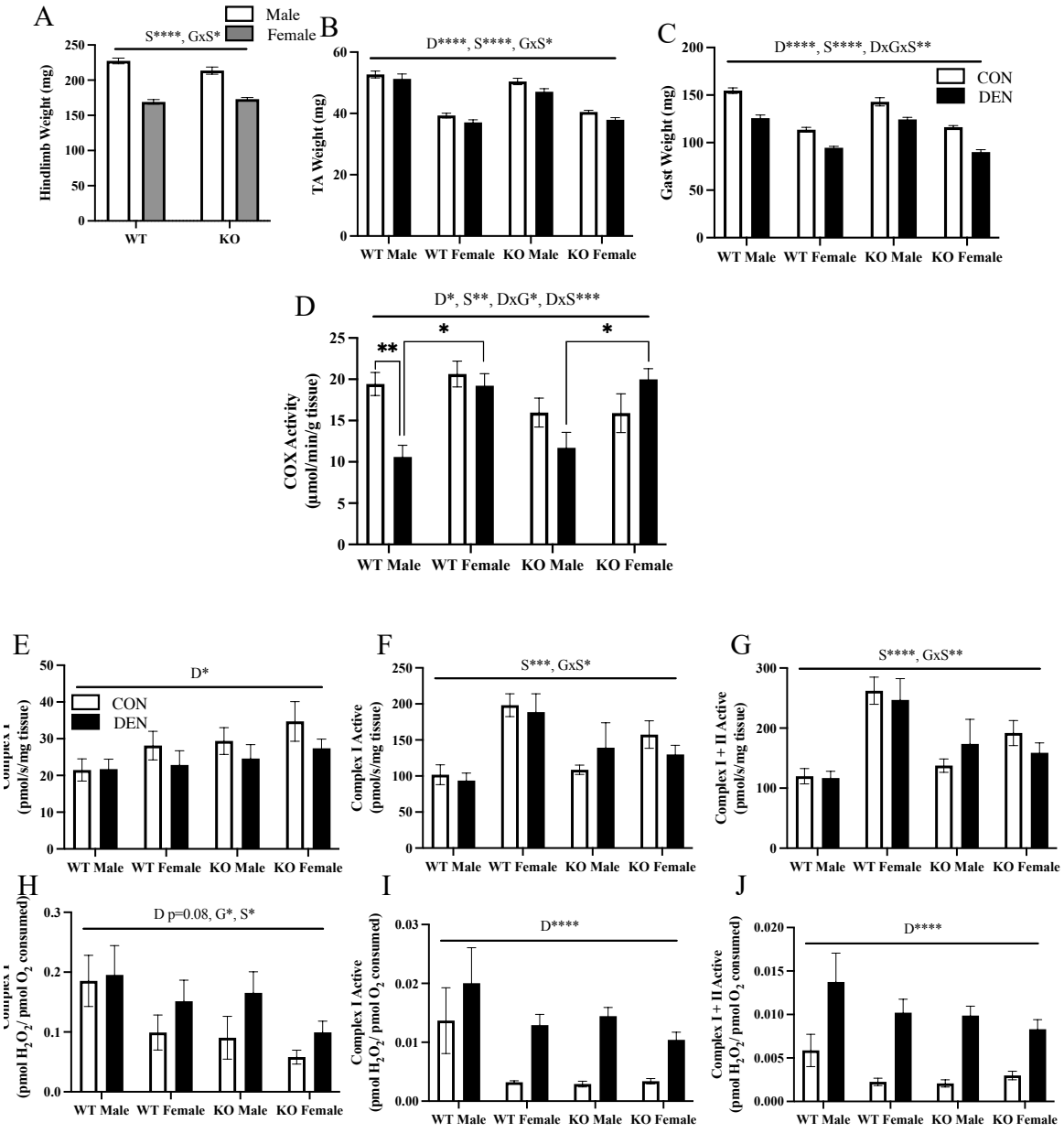

Supplemental Fig. 1 Expanded muscle weights, COX activity and mitochondrial function data. Basal differences in hindlimb muscle weights between males and females of WT and KO animals (A). Expanded TA (B) and gastrocnemius (C) weights following 7 days of denervation. Full graphical representation of cytochrome c oxidase (COX) activity following 7 days of denervation. Full graphical representation of oxygen consumption under complex I (E), complex I active (F) and complex I+II active (G) respiratory states following 7 days of denervation. Corresponding ROS emission under those states (H-J). G, represents a main effect of genotype; S, denotes a main effect of sex; D, indicates a main effect of denervation; GxS, represents an interaction between genotype and sex; DxG, interaction effect between denervation and genotype; DxGxS, denotes an interaction effect between denervation, genotype and sex; *, $p<0.05$; **, $p<0.01$; ***, $p<0.001$; ****, $p<0.0001$.

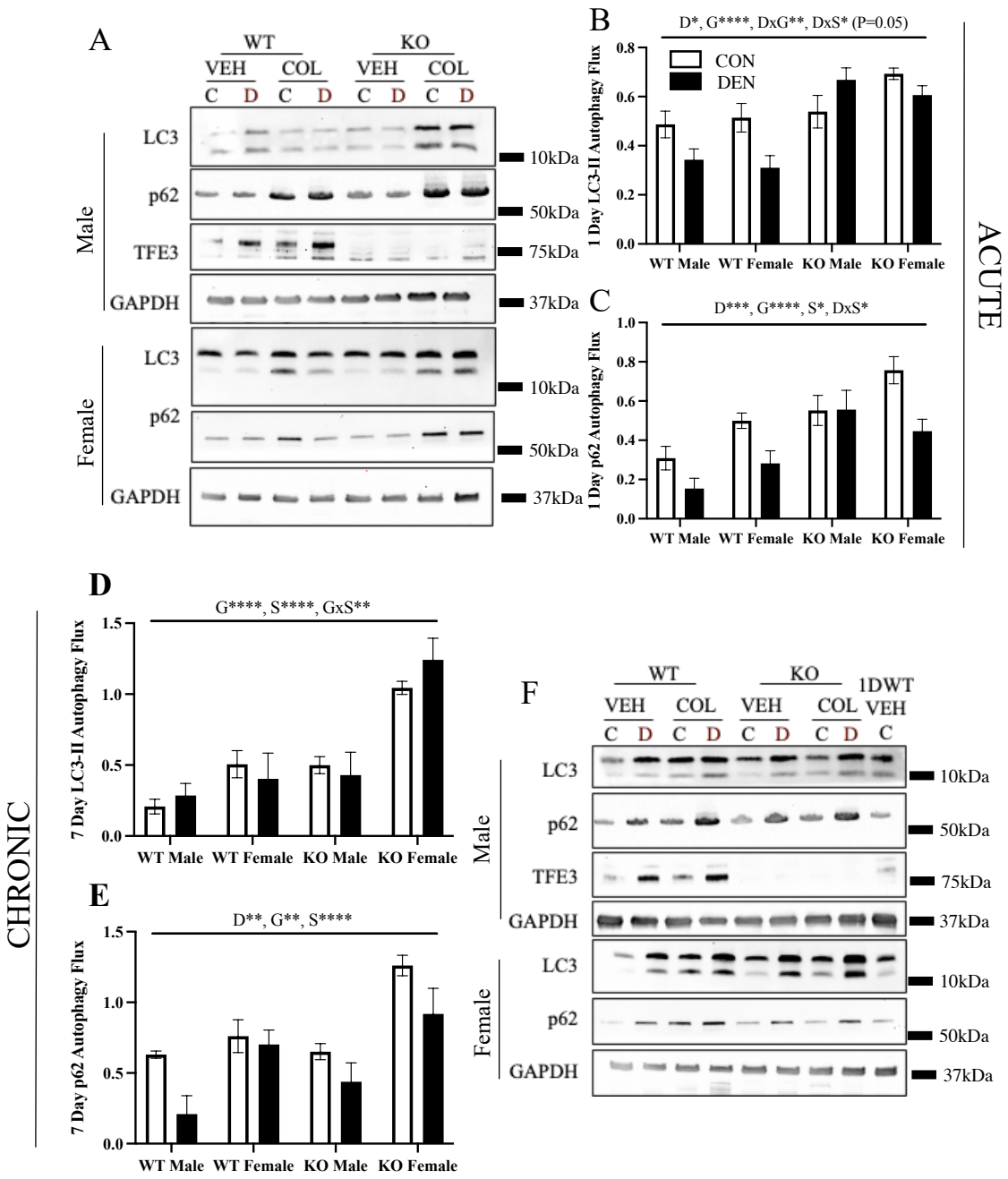

Supplemental Fig. 2 Autophagic response to denervation, acute and chronic. Representative blots of autophagy flux following 24 hr of denervation (A). Quantification of acute LC3-II (B) and p62 (C) autophagy flux, taken as the difference between colchicine- and vehicle-treated conditions. Quantification of LC3-II (D) and p62 (E) autophagy flux following 7 days of denervation, taken as the difference between colchicine- and vehicle-treated conditions. Representative blots of autophagy flux following 7 days of denervation (F). G, represents a main effect of genotype; S, denotes a main effect of sex; D, indicates a main effect of denervation; DxS, represents an interaction between denervation and sex; GxS, interaction effect between genotype and sex; *, $p<0.05$; **, $p<0.01$; ***, $p<0.001$; ****, $p<0.0001$.

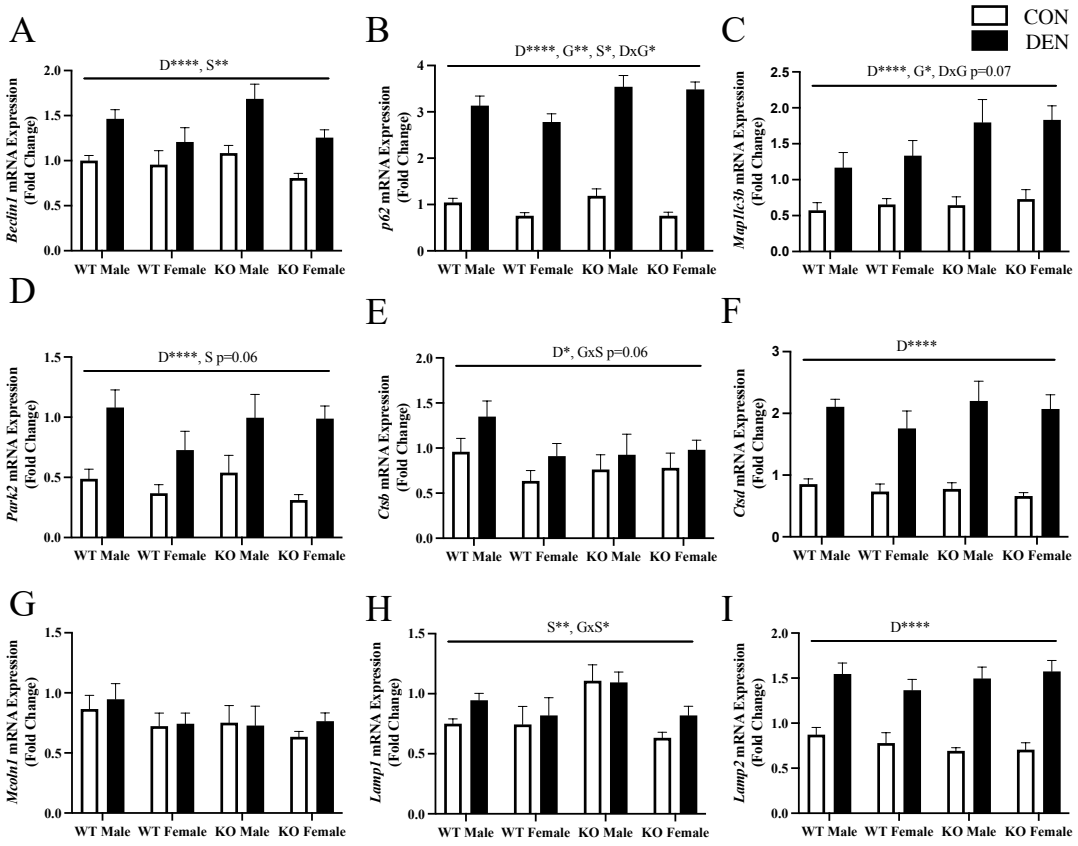

Supplemental Fig. 3 Lysosomal gene expression following chronic denervation. mRNA expression of *Beclin1* (A), *p62* (B), *Map1lc3b* (C), *Park2* (D), *Ctsb* (E), *Ctsd* (F), *Mcoln1* (G), *Lamp1* (H), and *Lamp2* (I) following 7 days of denervation normalized to *Gapdh* and *ActB*. G, represents a main effect of genotype; S, denotes a main effect of sex; D, indicates a main effect of denervation; DxG, represents an interaction between denervation and genotype; GxS, interaction effect between genotype and sex; *, $p<0.05$; **, $p<0.01$; ****, $p<0.0001$.

Fig. S4

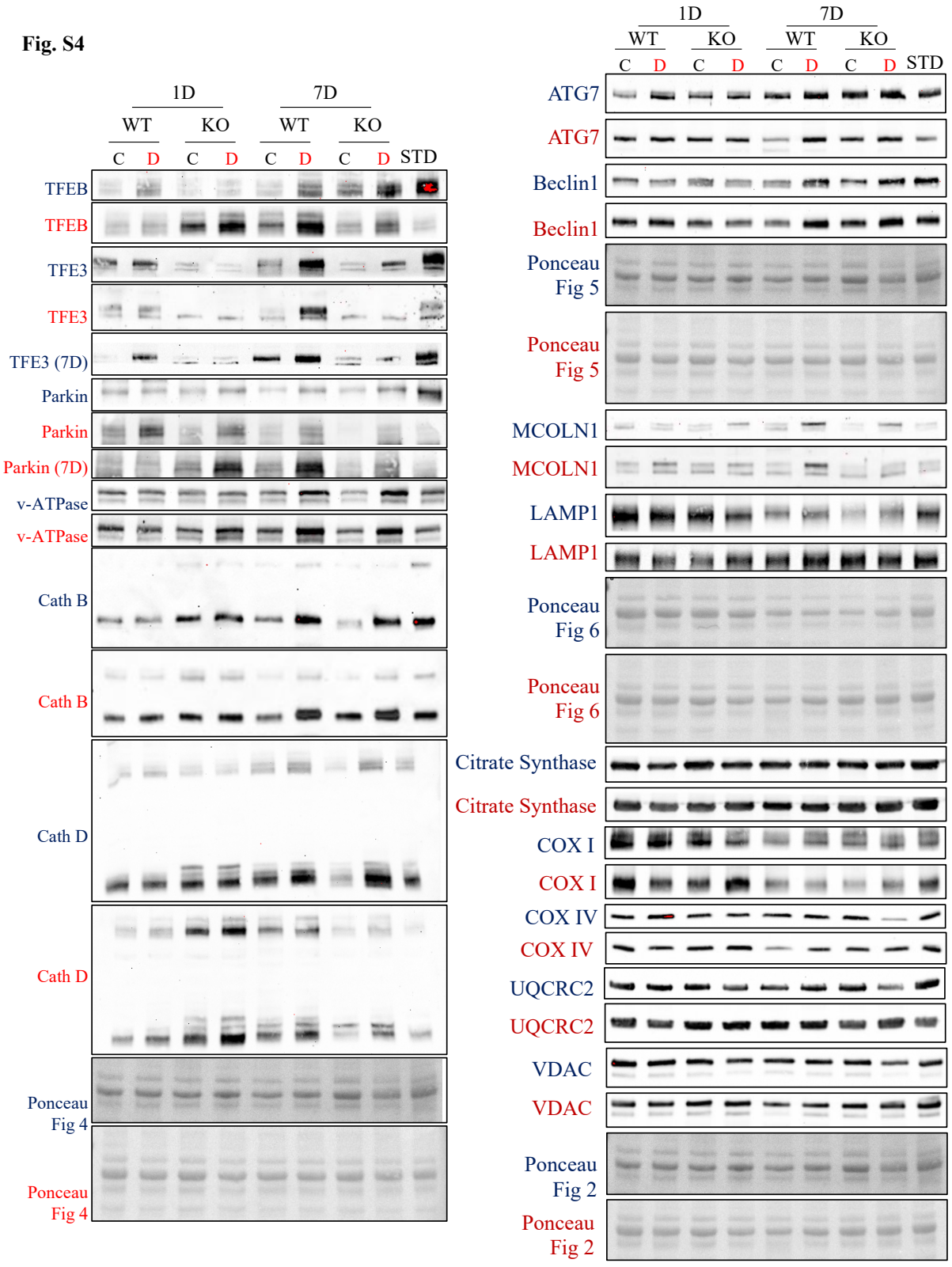

Supplemental Fig. 4 Full western blots expanded. Full blots from figures 2, 4, 5, including the standard that was used for quantification.

CHAPTER SIX:

SUMMARY & CONCLUSIONS

Skeletal muscle is a highly plastic tissue that can adapt to meet metabolic needs and demands imposed on it. The dynamic nature of skeletal muscle can be both positive and negative, as this allows stimuli such as exercise training to improve muscle performance and metabolism, but also allows negative stimuli such as disuse and aging to have severe consequences on muscle mass, function and metabolism. While the mechanisms that underlie the dynamic nature of muscle are multi-faceted, mitochondria are central to the maintenance and adaptability of skeletal muscle, as they too exhibit a high level of plasticity.

As a highly metabolic tissue, skeletal muscle relies heavily on mitochondria as the major production site of ATP through oxidative phosphorylation. However, mitochondria also participate in cellular signaling, oxidative stress, Ca^{2+} handling, and can initiate cell death or apoptosis. Thus, the maintenance of an optimal pool of mitochondria is essential for the overall health of skeletal muscle. Mitochondrial content and function are regulated through a collection of processes that support synthesis, proteostasis, and turnover. Through mitophagy, dysfunctional mitochondria are selectively recycled via the lysosomes. While reducing mitochondrial content is often considered a negative event, mitophagy is a pro-survival mechanism that helps optimize the reticulum and supports other cellular processes such as protein synthesis by supplying basic building blocks, like amino acids. As the degradative site for mitophagy, lysosomes are then inherently linked to mitochondrial maintenance, and recent

work suggests a high level of communication between the two organelles[111,265,267]. Appreciating the fact that both a single bout of exercise and acute periods of disuse can stimulate mitophagy and promote lysosomal biogenesis, but ultimately culminate in opposing phenotypes emphasizes the need to understand how lysosomes adapt and are maintained.

The microphthalmia (MiT) family of transcription factors, namely TFEB and TFE3, are key regulators of lysosomal biogenesis and autophagy[6]. These transcription factors are highly sensitive and responsive to cellular stresses including nutrient deprivation, oxidative stress, and energetic demands[167,169,189,190]. The overarching objective of this dissertation was to further characterize the role of these transcription factors in mediating lysosomal adaptations and the mitophagic responses to exercise and disuse and the resulting mitochondrial phenotype.

OBJECTIVE 1: Based on previous findings from our lab, it is clear that both mitochondria and lysosomes adapt to exercise training, and intriguingly lysosomal adaptations precede mitochondrial alterations[326]. Our first objective was to evaluate the involvement of the master regulators of lysosomal biogenesis, TFEB and TFE3, in mitochondrial and lysosomal adaptations to contractile activity.

Hypotheses:

1. Lysosomes will adapt to chronic contractile activity (CCA) both quantitatively and qualitatively. As redundant roles have been described for TFEB and TFE3, exercise-induced lysosomal adaptations will occur independent of either transcription factor;

2. Based on the literature, we hypothesize that mitochondrial impairments will be present in the absence of TFEB or TFE3, but CCA will rescue this defect;

3. In the absence of both TFEB and TFE3, exercise-induced mitochondrial and lysosomal adaptations will be abrogated due to declines in mitophagy flux.

Using an *in vitro* model of exercise, chronic contractile activity (CCA), we first recapitulated previous findings that an acute bout stimulates mitophagy flux and following repeated bouts, turnover is reduced[240,316]. This is likely due to the CCA-induced improvements in mitochondrial content and function that were observed after repeated bouts. The absence of TFEB or TFE3 alone did not impair mitophagy flux basally, which is in line with previous findings that have shown no changes in autophagy flux in the absence of TFEB or TFE3. Notably, this is the first study in which mitophagy flux was specifically assessed in the absence of these transcription factors in skeletal muscle. However, the absence of TFEB or TFE3 alone did negatively impact the acute mitophagic response to CA. Intriguingly, while the acute response was impaired, no differences were observed in mitophagy following CCA, and mitochondrial adaptations were comparable with or without the presence of the lysosomal regulators. Furthermore, contrary to our hypothesis we did not observe any impairments in mitochondrial function in the absence of either transcription factor basally. However, this can likely be attributed to experimental design which resulted in only a partial reduction in TFEB or TFE3 and only for a short duration. In line with our hypothesis, CCA elicited lysosomal adaptations, as increases in lysosomal content were observed, alongside reductions in lysosomal size and improved function. Enlarged lysosomes are often a sign of dysfunction, therefore smaller organelles may further demonstrate a functional adaptation. These lysosomal adaptations were observed independent of TFEB or TFE3, illustrating a level of redundancy between the MiT family members in mediating CCA-induced adaptations as we had speculated.

Due to the apparent redundancy between the transcription factors, we then sought to knockdown the expression of both TFEB and TFE3 together. In the absence of both TFEB and TFE3, mitophagy flux was significantly impaired basally, and the acute-CA induced mitophagic response was lost. Under these conditions, functional improvements in mitochondria were not observed and lysosomes did not adapt following CCA in line with our hypothesis, demonstrating that TFEB and TFE3 together are required for mediating mitochondrial adaptations to contractile activity. Intriguingly, our results also indicated that in the absence of TFEB and TFE3, dysfunctional lysosomes accumulated basally and following CCA. These data suggest that lysosomes undergo turnover themselves and that TFEB and TFE3 participate in these mechanisms. However, the means through which lysosomes are removed or degraded is still unclear. Taken together, these findings underscore the importance of functional lysosomes in mediating mitochondrial adaptations to contractile activity and highlight a level of interdependence or coordination between these organelles.

OBJECTIVE 2: It has long been known that contrary to exercise, disuse results in mitochondrial dysfunction. Recent work from our lab showed that mitophagy is elevated early on and then decreases with chronic disuse[334]. Furthermore, we also recently showed that lysosomes and autophagy machinery are disproportionate in males and females[218], whereby females have higher lysosomal content. However formal flux measurements were not made in this study. Thus, our objective was to further characterize sexual dimorphisms in lysosomes and mitophagy basally and in the context of atrophy, which has been largely overlooked.

Hypotheses:

1. Given the limited literature available, we hypothesize that females will have greater lysosomal content which would support increased mitophagy flux rates basally;
2. In response to denervation, both males and females will lose muscle mass, mitochondrial content and exhibit mitochondrial dysfunction;
3. In line with the previous hypothesis, given the postulated higher rates of flux, females will exhibit less mitochondrial dysfunction in comparison to males in response to denervation.

We first sought to characterize these differences between males and females basally. In line with previous literature[134,135,140,460], we observed improved mitochondrial function, both in oxygen consumption rates and in ROS emissions in females in comparison to males. Furthermore, in line with our hypothesis females exhibited increased lysosomal content basally, and elevated levels of mitophagy flux, which likely supports the superior mitochondrial phenotype. While reports from our lab and others have made inferences that support increased autophagy in females based on static measures, our study is the first to dynamically capture differences in mitophagy flux.

Our second aim was to evaluate sexual dimorphisms in the atrophy phenotype following denervation. Contrary to our hypothesis, females were modestly protected against muscle atrophy following 7 days of denervation in comparison to males. This phenomenon has not been observed in less severe models of disuse such as 7 days of hindlimb unloading[353], but has been reported with longer periods of disuse in rats[426]. A hallmark of the disuse-phenotype is a decline in mitochondrial content. To our surprise, females did not lose mitochondrial content following 7 days of denervation. However, this preservation in content is apparently at the cost of

mitochondrial function. While both males and females exhibited declines in oxygen consumption, and elevations in ROS emissions, the disuse-induced oxidative stress was more severe in females, contrary to our hypothesis. Following 24 hr of denervation, females actually reduced their mitophagy flux and this was maintained throughout the course of the 7 days. This inhibition of turnover likely supports the preservation of mitochondrial content, but also means that dysfunctional and long-lived mitochondria are not being cleared away. Intriguingly, this inhibition is not due to a lack of lysosomes or autophagy machinery. Denervation increased autophagy-related markers and lysosomal proteins in both males and females, however females exhibited an earlier and more profound response. Therefore, it is unclear how females inhibit their mitochondrial turnover in response to denervation, but it is evident that this contributes to the preservation of mitochondria.

OBJECTIVE 3: Our final aim was to evaluate the role of TFE3 in denervation-induced atrophy and mitochondrial impairments, again through the lens of biological sex differences.

Hypotheses:

1. Denervation will lead to increased lysosomal drive to support increased mitophagy flux to remove dysfunctional organelles;

2. The absence of TFE3 will impact lysosomal content and function following denervation, resulting in greater evidence of mitochondrial dysfunction;

3. Males lacking TFE3 will exhibit the most severe phenotype in response to denervation, as males are hypothesized to have less lysosomes in comparison to females, and the absence of TFE3 will exacerbate this deficit.

While the absence of TFE3 does not result in an overt phenotype basally, a reduction in muscle mass basally was observed in males but not females, indicating that TFE3 may regulate muscle mass maintenance in males. Loss of TFE3 resulted in a decline in mitochondrial content irrespective of sex, and the increased mitochondrial function seen in wildtype females in comparison to males was lost. To our surprise, in the absence of TFE3 mitophagy flux was increased in both males and females, but in contrast to wildtype animals, flux was equivalent between the sexes. This indicates that the sexual dimorphism seen in mitochondrial function is dependent on TFE3.

In response to denervation, the loss of TFE3 again displayed sexually dimorphic effects. While females were protected against muscle atrophy in WT animals, the loss of TFE3 reversed this sex-dependent effect whereby males preserved more muscle mass in comparison to females. Intriguingly, the loss of TFE3 conferred some level of protection against mitochondrial losses in both males and females. Furthermore, as mitochondrial content was preserved, mitochondrial dysfunction following denervation was intensified, a similar phenomenon seen in WT females. This is partially in line with our hypothesis that males lacking TFE3 would display a more severe mitochondrial phenotype in comparison to their WT counterparts although this cannot be attributed to impairments in the lysosomal response, as this was not affected in the males. Moreover, as WT females inhibited mitophagy flux in order to preserve mitochondria, in the absence of TFE3 the mitophagic response to denervation was disrupted in both males and females. Finally, as a robust lysosomal response was observed in WT females, this appears to be in part mediated by TFE3 as this was significantly blunted in KO females. Again, these findings partially support our initial hypotheses as lysosomes did adapt to denervation, however

TFE3 only impacted this response in females, but not in males. This indicates that the lysosomal adaptations observed in females following denervation are dependent on TFE3.

OVERALL CONCLUSION: As skeletal muscle adapts to external stimuli, mitochondria too exhibit the same level of plasticity to match metabolic demands. Mitochondria are maintained through a variety of mechanisms collectively known as mitochondrial quality control (MQC), including mitophagy which is the process through which dysfunctional organelles are recycled. As the degradative site of mitophagy, lysosomes are thereby inherently tied to the maintenance and adaptability of mitochondria. Despite opposing outcomes, exercise and disuse stimulate mitochondrial turnover and lysosomal biogenesis (Fig. 1). Based on the studies conducted in this dissertation, it is clear that lysosomal regulators TFEB and TFE3 are required for positive mitochondrial adaptations to contractile activity *in vitro.* It is also clear that TFE3 plays a significant role in mediating mitochondrial sexual dimorphisms basally. Furthermore, while biological sex imparts divergent approaches to disuse (Fig. 1), TFE3 may be implicated in these as loss of TFE3 disrupted the expected mitochondrial phenotype observed in males and was required for the lysosomal adaptations to disuse in females. Work from this dissertation highlights the role of lysosomes in mediating mitochondrial adaptations and also underscores the importance of studying biological sex, as males and females exhibit distinct mitochondrial and lysosomal phenotypes (Fig. 1). These observations contribute to our overall understanding of how muscle adapts to various stimuli and may provide insight into sex-specific approaches, such as targeting lysosomes for maintaining skeletal muscle health throughout age.

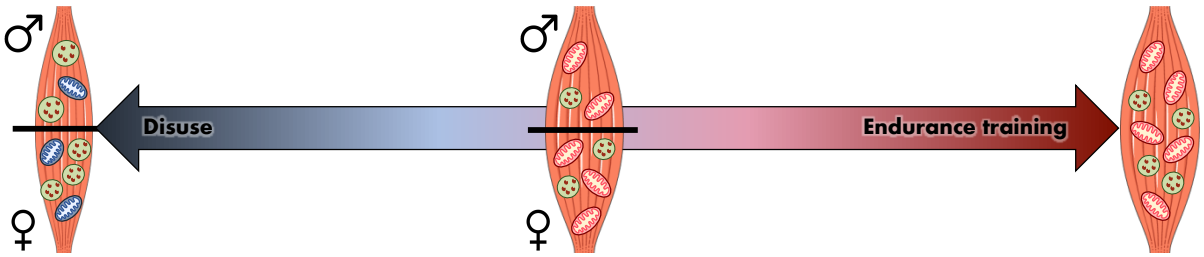

Figure 1: Mitochondrial and lysosomal adaptations in skeletal muscle. Exercise promotes a healthy skeletal muscle phenotype that is supported by mitochondrial and lysosomal adaptations. Increased mitochondrial and lysosomal content and function are observed in response to contractile activity. Furthermore, we elucidated differences between males and females in basal mitochondrial and lysosomal content in skeletal muscle whereby females exhibit higher mitochondrial content and function and greater lysosomal content, supporting elevated rates of mitochondrial turnover. Moreover, males and females respond differently to disuse as females preferentially maintain mitochondrial content at the expense of function. However, this cannot be attributed to lysosomal insufficiency as females exhibited a more robust lysosomal response in comparison to males. Taken together, our data underscore the importance of lysosomes in both positive and negative skeletal muscle adaptations, and the relevance of understanding the implications of sex.

CHAPTER SEVEN:

EXPERIMENTAL LIMITATIONS & FUTURE DIRECTIONS

Based on the findings presented in this dissertation, it is clear that lysosomes respond to both positive and negative stimuli and are heavily implicated in mitochondrial adaptations and overall skeletal muscle maintenance. Our findings support a high level of coordination between lysosomes and mitochondria, and highlight a role for lysosomal regulators in maintaining mitochondria and supporting adaptations. We have also identified that both mitochondrial and lysosomal phenotypes are heavily sex-dependent and even the level of mitophagy and autophagy flux varies between males and females. Our data also have begun to uncover a highly dimorphic response in the atrophy phenotype and this emphasizes the need for more sex stratified studies to understand how males and female skeletal muscle respond and adapt to external stimuli.

1. Uncovering the mechanisms of lysosomal turnover.

Based on findings presented in our first objective, it is clear that in the absence of key lysosomal regulators, dysfunctional lysosomes accumulate. While it is known that lysosomes do have a "lifespan", so to speak, and are degraded or removed from the cell, to limit cytotoxic effects, the mechanisms that underlie these processes remain unclear[158,448,449]. It is evident that TFEB and TFE3 contribute to these mechanisms as their absence caused this accumulation. Furthermore, others have suggested that lysosomes can undergo exocytosis to aid in membrane repair and this in turn also mitigates the accumulation of dysfunctional organelles. In line with our findings, TFEB and TFE3 are implicated in these processes. Thus, using a non-biased omics

approach to investigating potential key proteins and targets involved through RNA seq or proteomics would be warranted.

2. Evaluating the role of TFEB and TFE3 following exercise *in vivo.*

While using an *in vitro* model afforded a number of benefits, (i.e. ease of genetic manipulation), there are certain limitations of using a cell culture model especially in the context of exercise. While CCA elicits the same mitochondrial adaptations that are seen *in vivo*, this model cannot recapitulate the influence of circulating factors or the remodeling of surrounding tissues that in turn impacts skeletal muscle. However, Ballabio and colleagues have investigated the role of TFEB or TFE3 during exercise, and observed mitochondrial impairments but exercise was able to improve the phenotype[197,200]. As redundancy between the two transcription factors was observed in our hands, it would be interesting to generate an animal model that lacks both TFEB and TFE3, especially in an inducible and tissue-specific manner, as whole-body deletion of TFEB is embryonically lethal. This would be interesting as mitophagy flux has not yet been assessed *in vivo* in the absence of TFEB or TFE3, in the context of exercise.

3. Investigating the intersection of sex and TFE3 in exercise-induced adaptations.

Based on the findings from our second and third objective it was clear males and females exhibit dimorphic mitochondrial and lysosomal phenotypes basally and divergent responses in atrophic conditions. Understanding how females respond to positive stimuli such as exercise training with a specific focus on lysosomal adaptations and mitophagy would help elucidate the differences in with male and female skeletal muscle adapts. The implication here is that if males and females employ different approaches to mitochondrial and skeletal muscle remodeling, there is potential for sex-specific therapeutic interventions.

4. Developing assays to assess lysosomal function *in vivo.*

While there are a number of methodologies and strategies that can be employed to assess lysosomal function *in vitro*, which were employed in our first objective, these techniques have not yet been applied successfully to skeletal muscle. A clear limitation to our *in vivo* study was an inability to assess lysosomal function/status rigorously. Methodologies should be created that assess parameters such as lysosomal acidification, lysosomal membrane permeability, lysosomal hydrolysis and so forth. While assessments of autophagy and mitophagy flux offer an indication of lysosomal function, there are some limitations of the current methods available. Nonetheless, as autophagy and mitophagy rely heavily on complex signaling events, it is possible that impairments in flux may even occur as a result of impaired signaling independent of lysosomal function. Therefore, there is a need for assays that can be conducted in vivo to assess functional lysosomal parameters.

5. Activating lysosomes as a therapeutic target

Supporting previous literature, our results indicate that females have improved mitochondrial function and lower oxidative stress. Here we show for the first time that females also exhibit higher levels of mitophagy flux, and we argue that this elevated turnover may support the improved mitochondrial phenotype. Thus, it is possible that through the activation of lysosomes either through overexpression or pharmacologically, we can improve mitochondrial function. This can potentially be applied to models of disuse or aging in which mitochondrial function is impaired. However, this may be more of a viable therapeutic target in males rather than females, as females exhibited a robust lysosomal response to denervation, but seem to preferentially preserve mitochondrial content at the expense of function. Currently there are a number of pharmacological approaches to activating TFEB and TFE3 many of which rely

on the inhibition of mTOR such as rapamycin and Torin-1[6], although inhibiting mTORC1 will have a wide-range of cellular effects. Alternatives such as Trehalose[461] and curcumin analog C1[462] have been documented in the literature to activate TFEB and TFE3 independent of mTORC1.

CHAPTER EIGHT

REFERENCES

1. Canada S. Population Projections for Canada (2021 to 2068), Provinces and Territories (2021 to 2043): Technical Report on Methodology and Assumptions. 2022;Catalogue 91-620-X.
2. Statistics Canada. Health facts sheets: Overweight and obese adults, 2018. 2019;3–6.
3. Janssen I, Heymsfield SB, Wang Z, Ross R. Skeletal muscle mass and distribution in 468 men and women aged 18–88 yr. *J Appl Physiol* 2000;**89**:81–88.
4. Hargreaves M, Spriet LL. Skeletal muscle energy metabolism during exercise. *Nat Metab 2020 29* 2020;**2**:817–828.
5. Hood DA, Memme J. M, Oliveira AN, Triolo M. Maintenance of Skeletal Muscle Mitochondria in Health, Exercise, and Aging. *Annu Rev Physiol* 2019;**81**:19–41.
6. Napolitano G, Ballabio A. TFEB at a glance. *J Cell Sci* 2016;**129**:2475–2481.
7. Klionsky DJ, Abdelmohsen K, Abe A, Abedin MJ, Abeliovich H, Al E. Guidelines for the use and interpretation of assays for monitoring autophagy (3rd edition). *Autophagy* 2016;**12**:1.
8. Ballabio A, Bonifacino JS. Lysosomes as dynamic regulators of cell and organismal homeostasis. Nat. Rev. Mol. Cell Biol. 2020;**21**:101–118.
9. Argilés JM, Campos N, Lopez-Pedrosa JM, Rueda R, Rodriguez-Mañas L. Skeletal Muscle Regulates Metabolism via Interorgan Crosstalk: Roles in Health and Disease. *J Am Med Dir Assoc* 2016;**17**:789–796.
10. Oliveira AN, Hood DA. Exercise is mitochondrial medicine for muscle. *Sport Med Heal Sci* 2019;**1**:11–18.
11. Gotti C, Sensini A, Zucchelli A, Carloni R, Focarete ML. Hierarchical fibrous structures for muscle-inspired soft-actuators: A review. *Appl Mater Today* 2020;**20**:100772.
12. Willingham TB, Kim Y, Lindberg E, Bleck CKE, Glancy B. The unified myofibrillar matrix for force generation in muscle. *Nat Commun* 2020;**11**:1–10.
13. Ajayi PT, Katti P, Zhang Y, Willingham TB, Sun Y, Bleck CKE *et al.* Regulation of

the evolutionarily conserved muscle myofibrillar matrix by cell type dependent and independent mechanisms. *Nat Commun* 2022;**13**.

14. Shishmarev D. Excitation-contraction coupling in skeletal muscle: recent progress and unanswered questions. *Biophys Rev 2020 121* 2020;**12**:143–153.
15. Tupling AR. The decay phase of Ca2+ transients in skeletal muscle: regulation and physiology. *Appl Physiol Nutr Metab* 2009;**34**:373–376.
16. Mishra P, Varuzhanyan G, Pham AH, Chan DC. Mitochondrial dynamics is a distinguishing feature of skeletal muscle fiber types and regulates organellar compartmentalization HHS Public Access. *Cell Metab* 2015;**22**:1033–1044.
17. Schiaffino S, Reggiani C. FIBER TYPES IN MAMMALIAN SKELETAL MUSCLES. *Physiol Rev* 2011;**91**:1447–1531.
18. Nemeth PM, Pette D, Vrbová G. Comparison of enzyme activities among single muscle fibres within defined motor units. *J Physiol* 1981;**311**:489.
19. Mendell LM. The size principle: a rule describing the recruitment of motoneurons. *J Neurophysiol* 2005;**93**:3024–3026.
20. Bleck CKE, Kim Y, Willingham TB, Glancy B. Subcellular connectomic analyses of energy networks in striated muscle. *Nat Commun* 2018;**9**.
21. Ogata T, Yamasaki Y. No Title. *Cell Tissue Res* 1985http://link.springer.com/10.1007/BF00217168. Accessed 27 August 2018.
22. Ogata T, Yamasaki Y. Ultra-high-resolution scanning electron microscopy of mitochondria and sarcoplasmic reticulum arrangement in human red, white, and intermediate muscle fibers. *Anat Rec* 1997;**248**:214–23.
23. Cogswell AM, Stevens RJ, Hood DA. Properties of skeletal muscle mitochondria from subsarcolemmal and intermyofibrillar isolated regions. *Am J Physiol - Cell Physiol* 1993;**264**:C383-389.
24. Kirkwood SP, Munn EA, Brooks GA. Mitochondrial reticulum in limb skeletal muscle. *Am J Physiol - Cell Physiol* 1986;**251**:C395-402.
25. Picard M, White K, Turnbull DM. Mitochondrial morphology, topology, and membrane interactions in skeletal muscle: a quantitative three-dimensional electron microscopy study. *J Appl Physiol* 2013;**114**:161–171.
26. Vincent AE, White K, Davey T, Philips J, Ogden RT, Lawless C *et al.* Quantitative 3D

mapping of the human skeletal muscle mitochondrial network. *Cell Rep* 2019;**26**:996–1009.

27. Glancy B, Hsu LY, Dao L, Bakalar M, French S, Chess DJ *et al.* In Vivo microscopy reveals extensive embedding of capillaries within the sarcolemma of skeletal muscle fibers. *Microcirculation* 2014;**21**:131–147.
28. Mitchell P. Coupling of phosphorylation to electron and hydrogen transfer by a chemi-osmotic type of mechanism. *Nature* 1961;**191**:144–148.
29. Lambert AJ, Brand MD. Superoxide production by NADH:ubiquinone oxidoreductase (complex I) depends on the pH gradient across the mitochondrial inner membrane. *Biochem J* 2004;**382**:511–517.
30. Harbauer AB, Zahedi RP, Sickmann A, Pfanner N, Meisinger C. The protein import machinery of mitochondria - A regulatory hub in metabolism, stress, and disease. *Cell Metab* 2014;**19**:357–372.
31. Richards BJ, Slavin M, Oliveira AN, Sanfrancesco VC, Hood DA. Mitochondrial protein import and UPR mt in skeletal muscle remodeling and adaptation. *Semin Cell Dev Biol* 2022 doi:10.1016/J.SEMCDB.2022.01.002.
32. Silva AM, Oliveira PJ. Evaluation of respiration with clark type electrode in isolated mitochondria and permeabilized animal cells. *Methods Mol Biol* 2012;**810**:7–24.
33. Clark Jr LC, Wolf R, Granger D, Taylor Z. Continuous recording of blood oxygen tension by polarography. *J Appl Physiol* 1953;**6**:189–93.
34. Lowell BB, Spiegelman BM. Towards a molecular understanding of adaptive thermogenesis. *Nature* 2000;**404**:652–660.
35. Muller FL, Liu Y, Van Remmen H, Remmen H Van. Complex III Releases Superoxide to Both Sides of the Inner Mitochondrial Membrane *. *J Biol Chem* 2004;**279**:49064–49073.
36. Brand MD. Mitochondrial generation of superoxide and hydrogen peroxide as the source of mitochondrial redox signaling. *Free Radic Biol Med* 2016;**100**:14–31.
37. Williams MD, Van Remmen H, Conrad CC, Huang TT, Epstein CJ, Richardson A. Increased Oxidative Damage Is Correlated to Altered Mitochondrial Function in Heterozygous Manganese Superoxide Dismutase Knockout Mice. *J Biol Chem* 1998;**273**:28510–28515.

38. Mailloux RJ. Mitochondrial antioxidants and the maintenance of cellular hydrogen peroxide levels. *Oxid Med Cell Longev* 2018;**2018**.
39. Murphy MP. How mitochondria produce reactive oxygen species. *Biochem J* 2009;**417**:1.
40. Scarpulla RC. Metabolic control of mitochondrial biogenesis through the PGC-1 family regulatory network. *Biochim Biophys Acta* 2011;**1813**:1269–78.
41. Puigserver P, Wu Z, Park CW, Graves R, Wright M, Spiegelman BM. A Cold-Inducible Coactivator of Nuclear Receptors Linked to Adaptive Thermogenesis. *Cell* 1998;**92**:829–839.
42. Scarpulla RC. Nuclear activators and coactivators in mammalian mitochondrial biogenesis. *Biochim Biophys Acta - Gene Struct Expr* 2002;**1576**:1–14.
43. Pilegaard H, Saltin B, Neufer DP, Neufer PD. Exercise induces transient transcriptional activation of the PGC-1α gene in human skeletal muscle. *J Physiol* 2003;**546**:851–858.
44. Moulin C, Caumont-Sarcos A, Ieva R. Mitochondrial presequence import: Multiple regulatory knobs fine-tune mitochondrial biogenesis and homeostasis. *Biochim Biophys Acta - Mol Cell Res* 2019;**1866**:930–944.
45. Rath S, Sharma R, Gupta R, Ast T, Chan C, Durham TJ *et al.* MitoCarta3.0: an updated mitochondrial proteome now with sub-organelle localization and pathway annotations. *Nucleic Acids Res* 2020;**49**:1541–1547.
46. Wiedemann N, Pfanner N. Mitochondrial machineries for protein import and assembly. *Annu Rev Biochem* 2017;**86**:685–714.
47. Bonekamp NA, Jiang M, Motori E, Villegas RG, Koolmeister C, Atanassov I *et al.* High levels of TFAM repress mammalian mitochondrial DNA transcription in vivo. 2021 doi:10.26508/lsa.202101034.
48. Maniura-Weber K, Goffart S, Garstka HL, Montoya J, Wiesner RJ. Transient overexpression of mitochondrial transcription factor A (TFAM) is sufficient to stimulate mitochondrial DNA transcription, but not sufficient to increase mtDNA copy number in cultured cells. *Nucleic Acids Res* 2004;**32**:6015–6027.
49. Ngo HB, Lovely GA, Phillips R, Chan DC. Distinct structural features of TFAM drive mitochondrial DNA packaging versus transcriptional activation. *Nat Commun* 2014;**5**:3077.

50. Virbasius J V, Scarpulla RC. Activation of the human mitochondrial transcription factor A gene by nuclear respiratory factors: a potential regulatory link between nuclear and mitochondrial gene expression in organelle biogenesis. *Proc Natl Acad Sci U S A* 1994;**91**:1309–13.
51. Ngo HB, Kaiser JT, Chan DC. The mitochondrial transcription and packaging factor Tfam imposes a U-turn on mitochondrial DNA. *Nat Struct Mol Biol* 2011;**18**:1290–1296.
52. Gordon JW, Rungi AA, Inagaki H, Hood DA. Effects of contractile activity on mitochondrial transcription factor A expression in skeletal muscle. *J Appl Physiol* 2001;**90**:389–396.
53. Beyfuss K, Hood DA. A systematic review of p53 regulation of oxidative stress in skeletal muscle. *Redox Rep* 2018;**23**:100–117.
54. Achanta G, Sasaki R, Feng L, Carew JS, Lu W, Pelicano H *et al.* Novel role of p53 in maintaining mitochondrial genetic stability through interaction with DNA Pol gamma. *EMBO J* 2005;**24**:3482–92.
55. Matoba S, Kang J-G, Patino WD, Wragg A, Boehm M, Gavrilova O *et al.* p53 regulates mitochondrial metabolism. *Science (80-)* 2006;**312**:1650–1653.
56. Heyne K, Mannebach S, Wuertz E, Knaup KX, Mahyar-Roemer M, Roemer K. Identification of a putative p53 binding sequence within the human mitochondrial genome. *FEBS Lett* 2004;**578**:198–202.
57. Saleem A, Adhihetty PJ, Hood DA. Role of p53 in mitochondrial biogenesis and apoptosis in skeletal muscle. *Physiol Genomics* 2009;**3**:58–66.
58. Saleem A, Hood DA. Acute exercise induces tumour suppressor protein p53 translocation to the mitochondria and promotes a p53-Tfam-mitochondrial DNA complex in skeletal muscle. *J Physiol* 2013;**591**:3625–3636.
59. Memme JM, Oliveira AN, Hood DA. p53 regulates skeletal muscle mitophagy and mitochondrial quality control following denervation-induced muscle disuse. *J Biol Chem* 2021;101540.
60. Michel S, Canonne M, Arnould T, Renard P. Inhibition of mitochondrial genome expression triggers the activation of CHOP-10 by a cell signaling dependent on the integrated stress response but not the mitochondrial unfolded protein response.

Mitochondrion 2015;**21**:58–68.

61. Oliveira AN, Hood DA. Effect of Tim23 knockdown in vivo on mitochondrial protein import and retrograde signaling to the UPRmt in muscle. *Am J Physiol - Cell Physiol* 2018;**315**.
62. Jovaisaite V, Auwerx J. The mitochondrial unfolded protein response-synchronizing genomes. *Curr Opin Cell Biol* 2015;**33**:74–81.
63. Erlich AT, Tryon LD, Crilly MJ, Memme JM, Moosavi ZSM, Oliveira AN *et al.* Function of specialized regulatory proteins and signaling pathways in exercise-induced muscle mitochondrial biogenesis. *Integr Med Res* 2016;**5**:187–197.
64. Irrcher I, Ljubicic V, Hood DA. Interactions between ROS and AMP kinase activity in the regulation of PGC-1 transcription in skeletal muscle cells. *Am J Physiol - Cell Physiol* 2008;**296**:C116–C123.
65. Handschin C, Rhee J, Lin J, Tarr PT, Spiegelman BM. An autoregulatory loop controls peroxisome proliferator-activated receptor gamma coactivator 1alpha expression in muscle. *Proc Natl Acad Sci U S A* 2003;**100**:7111–6.
66. Zhang Y, Uguccioni G, Ljubicic V, Irrcher I, Iqbal S, Singh K *et al.* Multiple signaling pathways regulate contractile activity-mediated PGC-1 gene expression and activity in skeletal muscle cells. *Physiol Rep* 2014;**2**:e12008.
67. Combes A, Dekerle J, Webborn N, Watt P, Bougault V, Daussin FN. Exercise-induced metabolic fluctuations influence AMPK, p38-MAPK and CaMKII phosphorylation in human skeletal muscle. *Physiol Rep* 2015;**3**.
68. Jäger SS, Handschin CC, St-Pierre JJ, Spiegelman BMBM. AMP-activated protein kinase (AMPK) action in skeletal muscle via direct phosphorylation of PGC-1alpha. *Pnas* 2007;**104**:12017–12022.
69. Wright DC, Han D, Garcia-roves PM, Geiger PC, Jones TE, Holloszy JO. Exercise-induced Mitochondrial Biogenesis Begins before the Increase in Muscle PGC-1alpha Expression. *J Biol Chem* 2007;**282**:194–199.
70. Irrcher I, Ljubicic V, Kirwan AF, Hood DA. AMP-Activated Protein Kinase-Regulated Activation of the PGC-1α Promoter in Skeletal Muscle Cells. *PLoS One* 2008;**3**:e3614.
71. Russell RR, Bergeron R, Shulman GI, Young LH. Translocation of myocardial GLUT-4 and increased glucose uptake through activation of AMPK by AICAR. *Am J Physiol*

1999;**277**:H643–H649.

72. Winder WW, Holmes BF, Rubink DS, Jensen EB, Chen M, Holloszy JO. Activation of AMP-activated protein kinase increases mitochondrial enzymes in skeletal muscle. *J Appl Physiol* 2000;**88**:2219–2226.
73. Fan W, Evans RM. Exercise Mimetics: Impact on Health and Performance. *Cell Metab* 2017;**25**:242–247.
74. Wang Y, An H, Liu T, Qin C, Sesaki H, Guo S *et al.* Metformin improves mitochondrial respiratory activity through activation of AMPK. *Cell Rep* 2019;**29**:1511–1523.
75. Martin-montalvo A, Mercken EM, Mitchell SJ, Palacios HH, Mote PL, Scheibye-Knudsen M *et al.* Metformin improves healthspan and lifespan in mice. *Nat Commun* 2013;**4**.
76. Menzies KJ, Singh K, Saleem A, Hood DA. Sirtuin 1-mediated effects of exercise and resveratrol on mitochondrial biogenesis. *J Biol Chem* 2013;**288**:6968–6979.
77. Cantó C, Jiang LQ, Deshmukh AS, Mataki C, Coste A, Lagouge M *et al.* Interdependence of AMPK and SIRT1 for metabolic adaptation to fasting and exercise in skeletal muscle. *Cell Metab* 2010;**11**:213–9.
78. Gurd BJ, Yoshida Y, McFarlan JT, Holloway GP, Moyes CD, Heigenhauser GJF *et al.* Nuclear SIRT1 activity, but not protein content, regulates mitochondrial biogenesis in rat and human skeletal muscle. *Am J Physiol - Regul Integr Comp Physiol* 2011;**301**.
79. Fan W, Waizenegger W, Lin CS, Sorrentino V, He MX, Wall CE *et al.* PPARδ Promotes Running Endurance by Preserving Glucose. *Cell Metab* 2017;**25**:1186-1193.e4.
80. Cantó C, Houtkooper RH, Pirinen E, Youn DY, Oosterveer MH, Cen Y *et al.* The NAD+ precursor nicotinamide riboside enhances oxidative metabolism and protects against high-fat diet-induced obesity. *Cell Metab* 2012;**15**:838–847.
81. Price NL, Gomes AP, Ling AJY, Duarte F V, Martin-montalvo A, North BJ *et al.* SIRT1 is required for AMPK activation and the beneficial effects of resveratrol on mitochondrial function. *Cell Metab* 2012;**15**:675–690.
82. Fan M, Rhee J, St-Pierre J, Handschin C, Puigserver P, Lin J *et al.* Suppression of mitochondrial respiration through recruitment of p160 myb binding protein to PGC-1α:

Modulation by p38 MAPK. *Genes Dev* 2004;**18**:278–289.

83. Puigserver P, Rhee J, Lin J, Wu Z, Yoon JC, Zhang C *et al.* Cytokine stimulation of energy expenditure through p38 MAP kinase activation of PPARgamma coactivator-1. *Mol Cell* 2001;**8**:971–982.
84. Barger PM, Browning AC, Garner AN, Kelly DP. p38 mitogen-activated protein kinase activates peroxisome proliferator-activated receptor alpha: a potential role in the cardiac metabolic stress response. *J Biol Chem* 2001;**276**:44495–501.
85. Akimoto T, Pohnert SC, Li P, Zhang M, Gumbs C, Rosenberg PB *et al.* Exercise Stimulates Pgc-1α Transcription in Skeletal Muscle through Activation of the p38 MAPK Pathway. *J Biol Chem* 2005;**280**:19587–19593.
86. Ristow M, Zarse K, Oberbach A, Kloting N, Birringer M, Kiehntopf M *et al.* Antioxidants prevent health-promoting effects of physical exercise in humans. *Proc Natl Acad Sci* 2009;**106**:8665–8670.
87. Pastor R, Tur JA. Antioxidant Supplementation and Adaptive Response to Training: A Systematic Review. *Curr Pharm Des* 2019;**25**:1889–1912.
88. Wu H, Kanatous SB, Thurmond FA, Gallardo T, Isotani E, Bassel-Duby R *et al.* Regulation of mitochondrial biogenesis in skeletal muscle by CaMK. *Science (80-)* 2002;**296**:349–352.
89. Ojuka EO, Jones TE, Han D-H, Chen M, Wamhoff BR, Sturek M *et al.* Intermittent increases in cytosolic Ca $^{2+}$ stimulate mitochondrial biogenesis in muscle cells. *Am J Physiol Metab* 2002;**283**:E1040–E1045.
90. Freyssenet D, Irrcher I, Connor MK, Di Carlo M, Hood DA. Calcium-regulated changes in mitochondrial phenotype in skeletal muscle cells. *Am J Physiol Cell Physiol* 2004;**286**:C1053–C1061.
91. Rose AJ, Hargreaves M. Exercise increases Ca2+-calmodulin-dependent protein kinase II activity in human skeletal muscle. *J Physiol* 2003;**553**:303–309.
92. Carroll S, Nicotera P, Pette D. Calcium transients in single fibers of low-frequency stimulated fast- twitch muscle of rat. *Am J Physiol - Cell Physiol* 1999;**277**.
93. Handschin C, Chin S, Li P, Liu F, Maratos-Flier E, Lebrasseur NK *et al.* Skeletal muscle fiber-type switching, exercise intolerance, and myopathy in PGC-1alpha muscle-specific knock-out animals. *J Biol Chem* 2007;**282**:30014–21.

94. Vainshtein A, Tryon LD, Pauly M, Hood DA. Role of PGC-1α during acute exercise-induced autophagy and mitophagy in skeletal muscle. *Am J Physiol - Cell Physiol* 2015;**308**:710–719.
95. Rowe GC, El-Khoury R, Patten IS, Rustin P, Arany Z. PGC-1 a is dispensable for exercise-induced mitochondrial biogenesis in skeletal muscle. *PLoS One* 2012;**7**:e41817.
96. Leone TC, Lehman JJ, Finck BN, Schaeffer PJ, Wende AR, Boudina S *et al.* PGC-1alpha deficiency causes multi-system energy metabolic derangements: muscle dysfunction, abnormal weight control and hepatic steatosis. *PLoS Biol* 2005;**3**:e101.
97. Leick L, Wojtaszewski JFPP, Johansen STJ, Kiilerich K, Comes J, Hellsten Y *et al.* PGC-1α is not mandatory for exercise-and training-induced adaptive gene responses in mouse skeletal muscle. *Am J Physiol Endocrinol Metab* 2008;**294**:463–474.
98. Leick L, Lyngby SS, Wojtasewski JF, Pilegaard H. PGC-1α is required for training-induced prevention of age-associated decline in mitochondrial enzymes in mouse skeletal muscle. *Exp Gerontol* 2010;**45**:336–342.
99. Uguccioni G, Hood DA. The importance of PGC-1α in contractile activity-induced mitochondrial adaptations. *Am J Physiol Endocrinol Metab* 2011;**300**:E361--E371.
100. Giacomello M, Pyakurel A, Glytsou C, Scorrano L. The cell biology of mitochondrial membrane dynamics. *Nat Rev Mol Cell Biol 2020 214* 2020;**21**:204–224.
101. Cipolat S, De Brito OM, Dal Zilio B, Scorrano L. OPA1 requires mitofusin 1 to promote mitochondrial fusion. *Proc Natl Acad Sci U S A* 2004;**101**:15927–15932.
102. Glancy B, Hartnell LM, Malide D, Yu ZX, Combs CA, Connelly PS *et al.* Mitochondrial reticulum for cellular energy distribution in muscle. *Nature* 2015;**523**:617–620.
103. Glancy B, Hartnell LM, Combs CA, Fenmou A, Sun J, Murphy E *et al.* Power grid protection of the muscle mitochondrial reticulum. *Cell Rep* 2017;**19**:487–496.
104. Ono T, Isobe K, Nakada K, Hayashi J. Protection of human cells from mitochondrial dysfunction by exchange of mitochondrial DNA products between mitochondria. *Tara* 2001;**28**:1–4.
105. Gomes LC, Benedetto G Di, Scorrano L. During autophagy mitochondria elongate, are spared from degradation and sustain cell viability. *Nat Cell Biol* 2011;**13**:589–598.

106. Twig G, Elorza A, Molina AJA, Mohamed H, Wikstrom JD, Walzer G *et al.* Fission and selective fusion govern mitochondrial segregation and elimination by autophagy. *EMBO J* 2008;**27**:433–46.
107. Kleele T, Rey T, Winter J, Zaganelli S, Mahecic D, Perreten Lambert H *et al.* Distinct fission signatures predict mitochondrial degradation or biogenesis. *Nature* 2021;**593**:435–439.
108. Friedman JR, Lackner LL, West M, DiBenedetto JR, Nunnari J, Voeltz GK. ER tubules mark sites of mitochondrial division. *Science (80-)* 2011;**334**:358–362.
109. Korobova F, Ramabhadran V, Higgs HN. An Actin-Dependent Step in Mitochondrial Fission Mediated by the ER-Associated Formin INF2. *Science (80-)* 2013;**339**:464–467.
110. Lewis SC, Uchiyama LF, Nunnari J. ER-mitochondria contacts couple mtDNA synthesis with mitochondrial division in human cells. *Science (80-)* 2016;**353**:aaf5549.
111. Wong YC, Ysselstein D, Krainc D. Mitochondria-lysosome contacts regulate mitochondrial fission via RAB7 GTP hydrolysis. *Nature* 2018;**554**:382–386.
112. Burman JL, Pickles S, Wang C, Sekine S, Vargas JNS, Zhang Z *et al.* Mitochondrial fission facilitates the selective mitophagy of protein aggregates. *J Cell Biol* 2017;**216**:3231–3247.
113. Kang R, Zeh HJ, Lotze MT, Tang D. The Beclin 1 network regulates autophagy and apoptosis. *Cell Death Differ* 2011;**18**:571–580.
114. Russell RC, Tian Y, Yuan H, Park HW, Chang YY, Kim J *et al.* ULK1 induces autophagy by phosphorylating Beclin-1 and activating VPS34 lipid kinase. *Nat Cell Biol* 2013;**15**:741–750.
115. Park J-M, Seo M, Jung CH, Grunwald D, Stone M, Otto NM *et al.* ULK1 phosphorylates Ser30 of BECN1 in association with ATG14 to stimulate autophagy induction. *Autophagy* 2018;**14**:584.
116. Wei Y, Liu M, Li X, Liu J, Li H. Origin of the Autophagosome Membrane in Mammals. *Biomed Res Int* 2018;**2018**.
117. Kabeya Y, Mizushima N, Ueno T, Yamamoto A, Kirisako T, Noda T *et al.* LC3, a mammalian homologue of yeast Apg8p, is localized in autophagosome membranes after processing. *EMBO J* 2000;**19**:5720–5728.

118. Kabeya Y, Mizushima N, Yamamoto A, Oshitani-Okamoto S, Ohsumi Y, Yoshimori T. LC3, GABARAP and GATE16 localize to autophagosomal membrane depending on form-II formation. *J Cell Sci* 2004;**117**:2805–2812.
119. Weidberg H, Shvets E, Shpilka T, Shimron F, Shinder V, Elazar Z. LC3 and GATE-16/GABARAP subfamilies are both essential yet act differently in autophagosome biogenesis. *EMBO J* 2010;**29**:1792–1802.
120. Orsi A, Razi M, Dooley HC, Robinson D, Weston AE, Collinson LM *et al.* Dynamic and transient interactions of Atg9 with autophagosomes, but not membrane integration, are required for autophagy. *Mol Biol Cell* 2012;**23**:1860.
121. Handschin C, Cheol SC, Chin S, Kim S, Kawamori D, Kurpad AJ *et al.* Abnormal glucose homeostasis in skeletal muscle-specific PGC-1α knockout mice reveals skeletal muscle-pancreatic β cell crosstalk. *J Clin Invest* 2007;**117**:3463–3474.
122. Baines C. The molecular composition of the mitochondrial permeability transition pore. *J Mol Cell Cardiol* 2009;**46**:850–857.
123. Adhihetty PJ, Ljubicic V, Menzies KJ, Hood DA, Peter J, Ljubicic V *et al.* Differential susceptibility of subsarcolemmal and intermyofibrillar mitochondria to apoptotic stimuli. *Am J Physiol - Cell Physiol* 2005;**3**:994–1001.
124. Susin SA, Zamzami N, Castedo M, Hirsch T, Marchetti P, Macho A *et al.* Bcl-2 inhibits the mitochondrial release of an apoptogenic protease. *J Exp Med* 1996;**184**:1331–1341.
125. Liu X, Kim CN, Yang J, Jemmerson R, Wang X. Induction of apoptotic program in cell-free extracts: Requirement for dATP and cytochrome c. *Cell* 1996;**86**:147–157.
126. Wang C, Youle RJ. The role of mitochondria in apoptosis. *Annu Rev Genet* 2009;**43**:95–118.
127. Adhihetty PJ, O 'leary MFN, Chabi B, Wicks KL, Hood DA. Effect of denervation on mitochondrially mediated apoptosis in skeletal muscle. *J Appl Physiol (Bethesda, MD 1985)* 2007;**102**:1143–1151.
128. Cheema NJ, Herbst A, Mckenzie D, Aiken JM. Apoptosis and necrosis mediate skeletal muscle fiber loss in age-induced mitochondrial enzymatic abnormalities. *Aging Cell* 2015;**14**:1085–1093.
129. Romanello V, Sandri M. Mitochondrial quality control and muscle mass maintenance.

Front Physiol 2016;**6**:1–21.

130. Enns DL, Tiidus PM. The influence of estrogen on skeletal muscle: Sex matters. *Sport Med* 2010;**40**:41–58.
131. Ventura-Clapier R, Piquereau J, Veksler V, Garnier A. Estrogens, Estrogen Receptors Effects on Cardiac and Skeletal Muscle Mitochondria. *Front Endocrinol (Lausanne)* 2019;**10**.
132. Wüst RCI, Morse CI, De Haan A, Jones DA, Degens H. Sex differences in contractile properties and fatigue resistance of human skeletal muscle. *Exp Physiol* 2008;**93**:843–850.
133. Ikeda K, Horie-Inoue K, Inoue S. Functions of estrogen and estrogen receptor signaling on skeletal muscle. *J Steroid Biochem Mol Biol* 2019;**191**:105375.
134. Colom B, Alcolea M, Valle A, Oliver J, Roca P, García-Palmer F. Skeletal Muscle of Female Rats Exhibit Higher Mitochondrial Mass and Oxidative-Phosphorylative Capacities Compared to Males. *Cell Physiol Biochem* 2007;**19**:205–212.
135. Yasuda N, Glover EI, Phillips SM, Isfort RJ, Tarnopolsky MA. Sex-based differences in skeletal muscle function and morphology with short-term limb immobilization. *J Appl Physiol* 2005;**99**:1085–1092.
136. Maher AC, Fu MH, Isfort RJ, Varbanov AR, Qu XA, Tarnopolsky MA. Sex differences in global mRNA content of human skeletal muscle. *PLoS One* 2009;**4**.
137. Montero D, Madsen K, Meinild-Lundby A-K, Edin F, Lundby C. Sexual dimorphism of substrate utilization: Differences in skeletal muscle mitochondrial volume density and function. *Exp Physiol* 2018;**103**:851–859.
138. Watanabe D, Hatakeyama K, Ikegami R, Eshima H, Yagishita K, Poole DC *et al.* Sex differences in mitochondrial Ca2+ handling in mouse fast-twitch skeletal muscle in vivo. *J Appl Physiol* 2020;**128**:241–251.
139. Watanabe D, Ikegami R, Kano Y. Predominant cause of faster force recovery in females than males after intense eccentric contractions in mouse fast-twitch muscle. *J Physiol* 2021;**599**:4337–4356.
140. Tarnopolsky MA, Rennie CD, Robertshaw HA, Fedak-Tarnopolsky SN, Devries MC, Hamadeh MJ. Influence of endurance exercise training and sex on intramyocellular lipid and mitochondrial ultrastructure, substrate use, and mitochondrial enzyme

activity. *Am J Physiol - Regul Integr Comp Physiol* 2007;**292**:1271–1278.

141. Miotto PM, McGlory C, Holloway TM, Phillips SM, Holloway GP. Sex differences in mitochondrial respiratory function in human skeletal muscle. *Am J Physiol - Regul Integr Comp Physiol* 2018;**314**:R909–R915.
142. Monaco CMF, Bellissimo CA, Hughes MC, Ramos S V., Laham R, Perry CGR *et al.* Sexual dimorphism in human skeletal muscle mitochondrial bioenergetics in response to type 1 diabetes. *Am J Physiol - Endocrinol Metab* 2020;**318**:E44–E51.
143. Junker A, Wang J, Gouspillou G, Ehinger JK, Elmér E, Sjövall F *et al.* Human studies of mitochondrial biology demonstrate an overall lack of binary sex differences: A multivariate meta-analysis. *FASEB J* 2022;**36**:1–22.
144. Ribas V, Drew BG, Zhou Z, Phun J, Kalajian NY, Daraei P *et al.* Skeletal muscle action of estrogen receptor a is critical for the maintenance of mitochondrial function and metabolic homeostasis in females. *Sci Transl Med* 2016;**8**:334ra54.
145. Tower J, Pomatto LCD, Davies KJA. Sex differences in the response to oxidative and proteolytic stress. *Redox Biol* 2020;**31**.
146. Subbiah MT, Agrawal M, Rajan R, Abplanalp W, Rymaszewski Z. Antioxidant potential of specific estrogens on lipid peroxidation. *J Clin Endocrinol Metab* 1993;**77**:1095–1097.
147. Strehlow K, Rotter S, Wassmann S, Adam O, Grohé C, Laufs K *et al.* Modulation of antioxidant enzyme expression and function by estrogen. *Circ Res* 2003;**93**:170–177.
148. Chen JQ, Eshete M, Alworth WL, Yager JD. Binding of MCF-7 cell mitochondrial proteins and recombinant human estrogen receptors α and β to human mitochondrial DNA estrogen response elements. *J Cell Biochem* 2004;**93**:358–373.
149. Lejri I, Grimm A, Eckert A. Mitochondria, estrogen and female brain aging. *Front Aging Neurosci* 2018;**10**:1–12.
150. Razmara A, Sunday L, Stirone C, Wang XB, Krause DN, Sue P *et al.* Mitochondiral effexts of estrogen are mediated by ERalpha in endothelial cells. *J Pharmacol Exp Ther* 2008;**325**:782–790.
151. Whiting KP, Restall CJ, Brain PF. Steroid hormone-induced effects on membrane fluidity and their potential roles in non-genomic mechanisms. *Life Sci* 2000;**67**:743–757.

152. Torres MJ, Ryan TE, Lin C Te, Zeczycki TN, Neufer PD. Impact of 17β-estradiol on complex i kinetics and H2O2 production in liver and skeletal muscle mitochondria. *J Biol Chem* 2019;**293**:16889–16898.
153. Coffey JW, de Duve C. Digestive Activity of Lysosomes. *J Biol Chem* 1968;**243**:3255–3263.
154. Ohkuma S, Moriyama Y, Takano T. Identification and characterization of a proton pump on lysosomes by fluorescein isothiocyanate-dextran fluorescence. *Proc Natl Acad Sci U S A* 1982;**79**:2758–2762.
155. Mindell JA. Lysosomal Acidification Mechanisms. *Annu Rev Physiol* 2012;**74**:69–86.
156. Bechet D, Tassa A, Taillandier D, Combaret L, Attaix D. Lysosomal proteolysis in skeletal muscle. Int. J. Biochem. Cell Biol. 2005;**37**:2098–2114.
157. Lawrence RE, Zoncu R. The lysosome as a cellular centre for signalling, metabolism and quality control. Nat. Cell Biol. 2019;**21**:133–142.
158. Yang C, Wang X. Lysosome biogenesis: Regulation and functions. *J Cell Biol* 2021;**220**:1–15.
159. Luzio JP, Pryor PR, Bright NA. Lysosomes: Fusion and function. *Nat Rev Mol Cell Biol* 2007;**8**:622–632.
160. Bright NA, Gratian MJ, Luzio JP. Endocytic Delivery to Lysosomes Mediated by Concurrent Fusion and Kissing Events in Living Cells. *Curr Biol* 2005;**15**:360–365.
161. Pryor PR, Mullock BM, Bright NA, Gray SR, Luzio JP. The Role of Intraorganellar Ca 2 ⩽ in Late Endosome–Lysosome Heterotypic Fusion and in the Reformation of Lysosomes from Hybrid Organelles. *J Cell Biol* 2000;**149**:1053–1062.
162. Slade L, Pulinilkunnil T. The MiTF/TFE family of transcription factors: master regulators of organelle signaling, metabolism, and stress adaptation. *Mol Cancer Res* 2017;**15**:1637–1643.
163. Zhao GQ, Zhao Q, Zhou X, Mattei MG, de Crombrugghe B. TFEC, a basic helix-loop-helix protein, forms heterodimers with TFE3 and inhibits TFE3-dependent transcription activation. *Mol Cell Biol* 2015;**13**:4505–4512.
164. Palmieri M, Impey S, Kang H, Ronza A, Pelz C, Sardiello M *et al.* Characterization of the CLEAR network reveals an integrated control of cellular clearance pathways. *Hum Mol Genet* 2011;**20**:3852–3866.

165. Martina JA, Diab HI, Li H, Puertollano R. Novel roles for the MiTF/TFE family of transcription factors in organelle biogenesis, nutrient sensing, and energy homeostasis. *Cell Mol Life Sci* 2014;**71**:2483–97.
166. Sardiello M, Palmieri M, di Ronza A, Medina DL, Valenza M, Gennarino, Vincenzo Alessandro Chiara Di Malta FD *et al.* A Gene Network Regulating Lysosomal Biogenesis and Function. *Science* 2009;**325**:473–478.
167. Settembre C, Zoncu R, Medina DL, Vetrini F, Erdin SS, Erdin SS *et al.* A lysosome-to-nucleus signalling mechanism senses and regulates the lysosome via mTOR and TFEB. 2012;**31**:1095–108.
168. Martina JA, Diab HI, Brady OA, Puertollano R. TFEB and TFE3 are novel components of the integrated stress response. *EMBO J* 2016;**35**:479–495.
169. Martina JA, Diab HI, Lishu L, Jeong-A L, Patange S, Raben N *et al.* The nutrient-responsive transcription factor TFE3 promotes autophagy, lysosomal biogenesis, and clearance of cellular debris. *Sci Signal* 2014;**7**.
170. Ozturk DG, Kocak M, Akcay A, Kinoglu K, Kara E, Buyuk Y *et al.* MITF-MIR211 axis is a novel autophagy amplifier system during cellular stress. *Autophagy* 2019;**15**:375–390.
171. Kuiper RP, Schepens M, Thijssen J, Schoenmakers EFPM, van Kessel AG. Regulation of the MiTF/TFE bHLH-LZ transcription factors through restricted spatial expression and alternative splicing of functional domains. *Nucleic Acids Res* 2004;**32**:2315–2322.
172. Yang X, Xue P, Liu X, Xu X, Chen Z. HMGB1/autophagy pathway mediates the atrophic effect of TGF-β1 in denervated skeletal muscle. *Cell Commun Signal* 2018;**16**:97.
173. Ploper D, De Robertis EM. The MITF family of transcription factors: Role in endolysosomal biogenesis, Wnt signaling, and oncogenesis. *Pharmacol Res* 2015;**99**:36–43.
174. Martina JA, Chen Y, Gucek M, Puertollano R. MTORC1 functions as a transcriptional regulator of autophagy by preventing nuclear transport of TFEB. *Autophagy* 2012;**8**:903–14.
175. Roczniak-ferguson A, Petit CS, Froehlich F, Qian S, Ky J, Angarola B *et al.* The transcription factor TFEB links mTORC1 signaling to transcriptional control of

lysosome homeostasis. *Sci Signal* 2012;**5**:ra42.

176. Pena-Llopis S, Vega-Rubin-de-Celis S, Schwartz JC, Wolff NC, Tran TAT, Zou L *et al.* Regulation of TFEB and V-ATPases by mTORC1. *EMBO Journalzon* 2011;**30**:3242–3258.
177. Sancak Y, Bar-Peled L, Zoncu R, Markhard AL, Nada S, Sabatini DM. Ragulator-rag complex targets mTORC1 to the lysosomal surface and is necessary for its activation by amino acids. *Cell* 2010;**141**:290–303.
178. Sancak Y, Peterson TR, Shaul YD, Lindquist RA, Thoreen CC, Bar-peled L *et al.* The Rag GTPases bind raptor and mediate amino acid signaling to mTORC1. 2008;**320**:1496–1501.
179. Zoncu R, Bar-Peled L, Efeyan A, Wang S, Sancak Y, Sabatini DM. mTORC1 senses lysosomal amino acids through an inside-out mechanism that requires the Vacuolar H+ ATPase. *Science (80-)* 2011;**334**:678–683.
180. Vega-Rubin-de-Celis S, Peña-Llopis S, Konda M, Brugarolas J. Multistep regulation of TFEB by MTORC1. *Autophagy* 2017;**13**:464–472.
181. Bar-Peled L, Schweitzer LD, Zoncu R, Sabatini DM. Ragulator is a GEF for the rag GTPases that signal amino acid levels to mTORC1. *Cell* 2012;**150**:1196–1208.
182. Martina JA, Puertollano R. Rag GTPases mediate amino acid-dependent recruitment of TFEB and MITF to lysosomes. *J Cell Biol* 2013;**200**:475–491.
183. Settembre C, Cegli R De, Mansueto G, Saha PK, Vetrini F, Visvikis O *et al.* TFEB controls cellular lipid metabolism through a starvation-induced autoregulatory loop. *Nat Cell Biol* 2013;**15**:647–658.
184. Ferron M, Settembre C, Shimazu J, Lacombe J, Kato S, Rawlings DJ *et al.* A RANKL-PKCβ-TFEB signaling cascade is necessary for lysosomal biogenesis in osteoclasts. *Genes Dev* 2013;**27**:955–969.
185. Medina DL, Di Paola S, Peluso I, Armani A, De Stefani D, Venditti R *et al.* Lysosomal calcium signalling regulates autophagy through calcineurin and TFEB. *Nat Cell Biol* 2015;**17**:288–299.
186. Zhang X, Cheng X, Yu L, Yang J, Calvo R, Patnaik S *et al.* MCOLN1 is a ROS sensor in lysosomes that regulates autophagy. *Nat Commun* 2016;**7**:12109.
187. Scotto Rosato A, Montefusco S, Soldati C, Di Paola S, Capuozzo A, Monfregola J *et*

al. TRPML1 links lysosomal calcium to autophagosome biogenesis through the activation of the CaMKKβ/VPS34 pathway. *Nat Commun* 2019;**10**:1–16.

188. Andersson DC, Betzenhauser MJ, Reiken S, Meli AC, Umanskaya A, Xie W *et al.* Ryanodine receptor oxidation causes intracellular calcium leak and muscle weakness in aging. *Cell Metab* 2011;**14**:196–207.
189. Wang H, Wang N, Xu D, Ma Q, Chen Y, Xu S *et al.* Oxidation of multiple MiT/TFE transcription factors links oxidative stress to transcriptional control of autophagy and lysosome biogenesis. *Autophagy* 2020;**16**:1683–1696.
190. Paquette M, El-Houjeiri L, Zirden LC, Puustinen P, Blanchette P, Jeong H *et al.* AMPK-dependent phosphorylation is required for transcriptional activation of TFEB and TFE3. *Autophagy* 2021;**Epub**:1–19.
191. Shin HJR, Kim H, Oh S, Lee JG, Kee M, Ko HJ *et al.* AMPK-SKP2-CARM1 signalling cascade in transcriptional regulation of autophagy. *Nature* 2016;**534**:553–557.
192. Park JY, Sohn HY, Koh YH, Jo C. A splicing variant of TFEB negatively regulates the TFEB-autophagy pathway. *Sci Rep* 2021;**11**:1–11.
193. Steingrímsson E, Tessarollo L, Reid SW, Jenkins NA, Copeland NG. The bHLH-Zip transcription factor Tfeb is essential for placental vascularization. *Development* 1998;**125**:4607–4616.
194. Betschinger J, Nichols J, Dietmann S, Corrin PD, Paddison PJ, Smith A. Exit from pluripotency is gated by intracellular redistribution of the bHLH transcription factor Tfe3. *Cell* 2013;**153**:335–347.
195. Naka A, Iida KT, Nakagawa Y, Iwasaki H, Takeuchi Y, Satoh A *et al.* TFE3 inhibits myoblast differentiation in C2C12 cells via down-regulating gene expression of myogenin. *Biochem Biophys Res Commun* 2013;**430**:664–669.
196. Tassabehjil M, Newton VE, Read AP. Waardenburg syndrome type 2 caused by mutations in the human microphthalmia (MITF) gene. *Nat Gen* 1994;**8**:251–255.
197. Pastore N, Vainshtein A, Klisch TJ, Armani A, Huynh T, Herz NJ *et al.* TFE3 regulates whole-body energy metabolism in cooperation with TFEB. *EMBO Mol Med* 2017;**9**:605–621.
198. Fujimoto Y, Nakagawa Y, Satoh A, Okuda K, Shingyouchi A, Naka A *et al.* TFE3

controls lipid metabolism in adipose tissue of male mice by suppressing lipolysis and thermogenesis. *Endocrinology* 2013;**154**:3577–3588.

199. Salma N, Song JS, Kawakami A, Devi SP. Tfe3 and Tfeb transcriptionally regulate peroxisome proliferator-activated receptor gamma2 expression in adipocytes and mediate adiponectin and glucose levels in mice. *Mol Cell Biol* 2017;**37**:1–23.
200. Mansueto G, Armani A, Viscomi C, D'Orsi L, De Cegli R, Polishchuk E V *et al.* Transcription factor EB controls metabolic flexibility during exercise. *Cell Metab* 2017;**25**:182–196.
201. Iwasaki H, Naka A, Iida KT, Nakagawa Y, Matsuzaka T, Ishii K *et al.* TFE3 regulates muscle metabolic gene expression, increases glycogen stores, and enhances insulin sensitivity in mice. *Am J Physiol Metab* 2012;**302**:E896–E902.
202. Salma N, Song JS, Arany Z, Fisher DE. Transcription factor Tfe3 directly regulates Pgc-1alpha in muscle. *J Cell Physiol* 2015;**230**:2330–2336.
203. Reed SA, Sandesara PB, Senf SM, Judge AR. Inhibition of FoxO transcriptional activity prevents muscle fiber atrophy during cachexia and induces hypertrophy. *FASEB J* 2012;**26**:987.
204. Sandri M, Sandri C, Gilbert A, Skurk C, Calabria E, Picard A *et al.* Foxo transcription factors induce the atrophy-related ubiquitin ligase atrogin-1 and cause skeletal muscle atrophy. *Cell* 2004;**117**:399–412.
205. Lee D, Goldberg AL. SIRT1 protein, by blocking the activities of transcription factors FoxO1 and FoxO3, inhibits muscle atrophy and promotes muscle growth. *J Biol Chem* 2013;**288**:30515–30526.
206. Tang H, Inoki K, Lee M, Wright E, Khuong AA, Khuong AA *et al.* MTORC1 promotes denervation-induced muscle atrophy through a mechanism involving the activation of FoxO and E3 ubiquitin ligases. *Sci Signal* 2014;**7**.
207. Mammucari C, Milan G, Romanello V, Masiero E, Rudolf R, Del Piccolo P *et al.* FoxO3 Controls Autophagy in Skeletal Muscle In Vivo. *Cell Metab* 2007;**6**:458–471.
208. Zhao J, Brault JJ, Schild A, Cao P, Sandri M, Schiaffino S *et al.* FoxO3 Coordinately Activates Protein Degradation by the Autophagic/Lysosomal and Proteasomal Pathways in Atrophying Muscle Cells. *Cell Metab* 2007;**6**:472–483.
209. Liu Y, Li J, Shang Y, Guo Y, Li Z. CARM1 contributes to skeletal muscle wasting by

mediating FoxO3 activity and promoting myofiber autophagy. *Exp Cell Res* 2019;**374**:198–209.

210. Sanchez AMJ, Candau RB, Bernardi H. FoxO transcription factors: their roles in the maintenance of skeletal muscle homeostasis. *Cell Mol Life Sci 2013 719* 2013;**71**:1657–1671.
211. Martínez-Fábregas J, Prescott A, van Kasteren S, Pedrioli DL, McLean I, Moles A *et al.* Lysosomal protease deficiency or substrate overload induces an oxidative-stress mediated STAT3-dependent pathway of lysosomal homeostasis. *Nat Commun* 2018;**9**:1–16.
212. Liu B, Palmfeldt J, Lin L, Colaço A, Clemmensen KKB, Huang J *et al.* STAT3 associates with vacuolar H+-ATPase and regulates cytosolic and lysosomal pH. *Cell Res* 2018;**28**:996–1012.
213. Shang D, Wang L, Klionsky DJ, Cheng H, Zhou R. Sex differences in autophagy-mediated diseases: toward precision medicine. *Autophagy* 2021;**17**:1065–1076.
214. Congdon EE. Sex differences in autophagy contribute to female vulnerability in Alzheimer's disease. *Front Neurosci* 2018;**12**:1–16.
215. Li XZ, Sui CY, Chen Q, Chen XP, Zhang H, Zhou XP. Upregulation of cell surface estrogen receptor alpha is associated with the mitogen-activated protein kinase/extracellular signal-regulated kinase activity and promotes autophagy maturation. *Int J Clin Exp Pathol* 2015;**8**:8832–8841.
216. Blessing AM, Rajapakshe K, Reddy Bollu L, Shi Y, White MA, Pham AH *et al.* Transcriptional regulation of core autophagy and lysosomal genes by the androgen receptor promotes prostate cancer progression. *Autophagy* 2017;**13**:506–521.
217. Augereau P, Miralles F, Cavaillès V, Gaudelet C, Parker M, Rochefort H. Characterization of the proximal estrogen-responsive element of human cathepsin D gene. *Mol Endocrinol* 1994;**8**:693–703.
218. Triolo M, Oliveira AN, Kumari R, Hood DA. The influence of age, sex, and exercise on autophagy, mitophagy, and lysosome biogenesis in skeletal muscle. *Skelet Muscle* 2022;**12**:1–18.
219. Rosa-Caldwell ME, Lim S, Haynie WS, Jansen LT, Westervelt LC, Amos MG *et al.* Altering aspects of mitochondrial quality to improve musculoskeletal outcomes in

disuse atrophy. *J Appl Physiol* 2020;**129**:1290–1303.

220. Rosa-Caldwell ME, Lim S, Haynie WS, Brown JL, Lee DE, Dunlap KR *et al.* Mitochondrial aberrations during the progression of disuse atrophy differentially affect male and female mice. *J Cachexia Sarcopenia Muscle* 2021;**12**:2056.
221. Luk HY, Appell C, Levitt DE, Jiwan NC, Vingren JL. Differential Autophagy Response in Men and Women After Muscle Damage. *Front Physiol* 2021;**12**:1–10.
222. Oliván S, Calvo AC, Manzano R, Zaragoza P, Osta R. Sex Differences in Constitutive Autophagy. *Biomed Res Int* 2014;**2014**.
223. Demarest TG, Waite EL, Kristian T, Puche AC, Waddell J, Mckenna MC *et al.* Sex-dependent mitophagy and neuronal death following rat neonatal hypoxia-ischemia. *Neuroscience* 2016;**29**:103–113.
224. Campesi I, Straface E, Occhioni S, Montella A, Franconi F. Protein oxidation seems to be linked to constitutive autophagy: A sex study. *Life Sci* 2013;**93**:145–152.
225. Costa AJ, Oliveira RB, Wachilewski P, Nishino MS, Bassani TB, Stilhano RS *et al.* Membrane estrogen receptor ERα activation improves tau clearance via autophagy induction in a tauopathy cell model. *Brain Res* 2022;**1795**:148079.
226. Noh B, McCullough L, Moruno-Manchon J. Sex-biased autophagy as a potential mechanism mediating sex differences in ischemic stroke outcome. *Neural Regen Res* 2023;**18**:31.
227. Thomas RE, Andrews LA, Burman JL, Lin W-Y, Pallanck LJ. PINK1-Parkin Pathway Activity Is Regulated by Degradation of PINK1 in the Mitochondrial Matrix. *PLoS Genet* 2014;**10**:e1004279.
228. Greene AW, Grenier K, Aguileta MA, Muise S, Farazifard R, Haque ME *et al.* Mitochondrial processing peptidase regulates PINK1 processing, import and Parkin recruitment. *EMBO Rep* 2012;**13**:378–385.
229. Matsuda N, Sato S, Shiba K, Okatsu K, Saisho K, Gautier CA *et al.* PINK1 stabilized by mitochondrial depolarization recruits Parkin to damaged mitochondria and activates latent Parkin for mitophagy. *J Cell Biol* 2010;**189**:211–221.
230. Narendra DP, Jin SM, Tanaka A, Suen D-FF, Gautier CA, Shen J *et al.* PINK1 is selectively stabilized on impaired mitochondria to activate Parkin. *PLoS Biol* 2010;**8**:e1000298.

231. Kondapalli C, Kazlauskaite A, Zhang N, Woodroof HI, Campbell DG, Gourlay R *et al.* PINK1 is activated by mitochondrial membrane potential depolarization and stimulates Parkin E3 ligase activity by phosphorylating Serine 65. *Open Biol* 2012;**2**:120080.
232. Killackey SA, Bi Y, Soares F, Hammi I, Winsor NJ, Abdul-Sater AA *et al.* Mitochondrial protein import stress regulates the LC3 lipidation step of mitophagy through NLRX1 and RRBP1. *Mol Cell* 2022;1–17.
233. Jin SM, Youle RJ. The accumulation of misfolded proteins in the mitochondrial matrix is sensed by PINK1 to induce PARK2/Parkin-mediated mitophagy of polarized mitochondria. *Autophagy* 2013;**9**:1750–1757.
234. Michaelis JB, Brunstein ME, Bozkurt S, Alves L, Wegner M, Kaulich M *et al.* Protein import motor complex reacts to mitochondrial misfolding by reducing protein import and activating mitophagy. *Nat Commun* 2022;**13**:5164.
235. Kane LA, Lazarou M, Fogel AI, Li Y, Yamano K, Sarraf SA *et al.* PINK1 phosphorylates ubiquitin to activate Parkin E3 ubiquitin ligase activity. *J Cell Biol* 2014;**205**:143–53.
236. Okatsu K, Oka T, Iguchi M, Imamura K, Kosako H, Tani N *et al.* PINK1 autophosphorylation upon membrane potential dissipation is essential for Parkin recruitment to damaged mitochondria. *Nat Commun* 2012;**3**:1–10.
237. Koyano F, Okatsu K, Kosako H, Tamura Y, Go E, Kimura M *et al.* Ubiquitin is phosphorylated by PINK1 to activate parkin. *Nature* 2014;**510**:162–166.
238. Kazlauskaite A, Kondapalli C, Gourlay R, Campbell DG, Ritorto MS, Hofmann K *et al.* Parkin is activated by PINK1-dependent phosphorylation of ubiquitin at Ser65. *Biochem J* 2014;**460**:127–39.
239. Shiba-Fukushima K, Imai Y, Yoshida S, Ishihama Y, Kanao T, Sato S *et al.* PINK1-mediated phosphorylation of the Parkin ubiquitin-like domain primes mitochondrial translocation of Parkin and regulates mitophagy. *Sci Rep* 2012;**2**:1002.
240. Chen CCCW, Erlich AT, Hood DA. Role of Parkin and endurance training on mitochondrial turnover in skeletal muscle. *Skelet Muscle* 2018;**8**:1–14.
241. Chen CCW, Erlich AT, Crilly MJ, Hood DA. Parkin is required for exercise-induced mitophagy in muscle: impact of aging. *Am J Physiol Metab* 2018;**315**:E404–E415.
242. Lokireddy S, Wijesoma IW, Teng S, Bonala S, Gluckman PD, McFarlane C *et al.* The

ubiquitin ligase Mul1 induces mitophagy in skeletal muscle in response to muscle-wasting stimuli. *Cell Metab* 2012;**16**:613–624.

243. Fu M, St-pierre P, Shankar J, Wang PTC, Joshi B, Nabi IR *et al.* Regulation of mitophagy by the Gp78 E3 ubiquitin ligase. 2013;**24**:1153–1162.
244. Di Rita A, Peschiaroli A, D′Acunzo P, Strobbe D, Hu Z, Gruber J *et al.* HUWE1 E3 ligase promotes PINK1/PARKIN-independent mitophagy by regulating AMBRA1 activation via IKKα. *Nat Commun* 2018;**9**.
245. Lazarou M, Sliter DA, Kane LA, Sarraf SA, Wang C, Burman JL *et al.* The ubiquitin kinase PINK1 recruits autophagy receptors to induce mitophagy. *Nat 2015 5247565* 2015;**524**:309–314.
246. Geisler S, Holmström KM, Skujat D, Fiesel FC, Rothfuss OC, Kahle PJ *et al.* PINK1/Parkin-mediated mitophagy is dependent on VDAC1 and p62/SQSTM1. *Nat Cell Biol* 2010;**12**:119–131.
247. Wong YC, Holzbaur ELF. Optineurin is an autophagy receptor for damaged mitochondria in parkin-mediated mitophagy that is disrupted by an ALS-linked mutation. *Proc Natl Acad Sci U S A* 2014;**111**:E4439-48.
248. Gao J, Yu L, Wang Z, Wang R, Liu X. Induction of mitophagy in C2C12 cells by electrical pulse stimulation involves increasing the level of the mitochondrial receptor FUNDC1 through the AMPK-ULK1 pathway. *Am J Transl Res* 2020;**12**:6879–6894.
249. Liu L, Feng D, Chen G, Chen M, Zheng Q, Song P *et al.* Mitochondrial outer-membrane protein FUNDC1 mediates hypoxia-induced mitophagy in mammalian cells. *Nat Cell Biol* 2012;**14**:177–185.
250. Wu W, Tian W, Hu Z, Chen G, Huang L, Li W *et al.* ULK1 translocates to mitochondria and phosphorylates FUNDC1 to regulate mitophagy. *EMBO Rep* 2014;**15**:566–575.
251. Novak I, Kirkin V, McEwan DG, Zhang J, Wild P, Rozenknop A *et al.* Nix is a selective autophagy receptor for mitochondrial clearance. *EMBO Rep* 2010;**11**:45–51.
252. Schwarten M, Mohrlüder J, Ma P, Stoldt M, Thielmann Y, Stangler T *et al.* Nix directly binds to GABARAP: a possible crosstalk between apoptosis and autophagy. *Autophagy* 2009;**5**:690–8.
253. Ding W-X, Ni H-M, Li M, Liao Y, Chen X, Stolz DB *et al.* Nix is critical to two

distinct phases of mitophagy, reactive oxygen species-mediated autophagy induction and Parkin-ubiquitin-p62-mediated mitochondrial priming. *J Biol Chem* 2010;**285**:27879–90.

254. Kanki T. Nix, a receptor protein for mitophagy in mammals. *Autophagy* 2010;**6**:433–5.
255. Rogov V V., Suzuki H, Marinković M, Lang V, Kato R, Kawasaki M *et al.* Phosphorylation of the mitochondrial autophagy receptor Nix enhances its interaction with LC3 proteins. *Sci Reports 2017 71* 2017;**7**:1–12.
256. Chu CT, Ji J, Dagda RK, Jiang JF, Tyurina YY, Kapralov AA *et al.* Cardiolipin externalization to the outer mitochondrial membrane acts as an elimination signal for mitophagy in neuronal cells. *Nat Cell Biol* 2013;**15**:1197–1205.
257. Rikka S, Quinsay MN, Thomas RL, Kubli DA, Zhang X, Murphy AN *et al.* Bnip3 impairs mitochondrial bioenergetics and stimulates mitochondrial turnover. *Cell Death Differ* 2011;**18**:721–31.
258. Quinsay MN, Thomas RL, Lee Y, Gustafsson AB. Bnip3-mediated mitochondrial autophagy is independent of the mitochondrial permeability transition pore. *Autophagy* 2010;**6**:855–62.
259. Luk HY, Jiwan NC, Appell CR, Levitt DE, Vingren JL. Sex-specific mitochondrial dynamics and mitophagy response to muscle damage. *Physiol Rep* 2022;**10**:1–12.
260. Nilsson MI, MacNeil LG, Kitaoka Y, Suri R, Young SP, Kaczor JJ *et al.* Combined aerobic exercise and enzyme replacement therapy rejuvenates the mitochondrial–lysosomal axis and alleviates autophagic blockage in Pompe disease. *Free Radic Biol Med* 2015;**87**:98–112.
261. Parenti G, Andria G, Ballabio A. Lysosomal Storage Diseases: From Pathophysiology to Therapy. *Annu Rev Med* 2015;**66**:471–486.
262. Parousis A, Carter HN, Tran C, Erlich AT, Mesbah Moosavi ZS, Pauly M *et al.* Contractile activity attenuates autophagy suppression and reverses mitochondrial defects in skeletal muscle cells. *Autophagy* 2018;**14**:1886–1897.
263. Demers-Lamarche J, Guillebaud G, Tlili M, Todkar K, Bélanger N, Grondin M *et al.* Loss of Mitochondrial Function Impairs Lysosomes. *J Biol Chem* 2016;**291**:10263.
264. Fernandez-mosquera L, Yambire KF, Couto R, Pabis K, Ponsford AH, Diogo C V *et al.* Mitochondrial respiratory chain deficiency inhibits lysosomal hydrolysis. *Autophagy*

2019;**15**:1572–1591.

265. Fernández-Mosquera L, DIogo C V., Yambire KF, Santos GL, Luna Sánchez M, Bénit P *et al.* Acute and chronic mitochondrial respiratory chain deficiency differentially regulate lysosomal biogenesis. *Sci Rep* 2017;**7**:1–11.
266. Melser S, Chatelain EH, Lavie J, Mahfouf W, Jose C, Obre E *et al.* Rheb regulates mitophagy induced by mitochondrial energetic status. *Cell Metab* 2013;**17**:719–730.
267. Peng W, Wong YC, Krainc D. Mitochondria-lysosome contacts regulate mitochondrial Ca2+ dynamics via lysosomal TRPML1. *Proc Natl Acad Sci U S A* 2020;**117**:19266–19275.
268. Holloszy JO. Biochemical Adaptations in Muscle. *J Biol Chem* 1967;**242**:2278–2282.
269. Holloszy JO, Booth FW. Biochemical adaptations to endurance exercise in muscle. *Annu Rev Physiol* 1976;**38**:273–291.
270. Kirkwood SP, Packer L, Brooks GA. Effects of Endurance Training on a Mitochondrial Reticulum in Limb Skeletal Muscle. *Arch Biochem Biophys* 1987;**255**:80–88.
271. Hoppeler H. Exercise-induced uItrastructural changes in skeletal muscle. *Integr J Sport Med* 1986;**7**:187–204.
272. Perry CGR, Lally J, Holloway GP, Heigenhauser GJF, Bonen A, Spriet LL. Repeated transient mRNA bursts precede increases in transcriptional and mitochondrial proteins during training in human skeletal muscle. *J Physiol* 2010;**588**:4795–4810.
273. Hood D a, Parent G. Metabolic and contractile responses of rat fast-twitch muscle to 10-Hz stimulation. *Am J Physiol* 1991;**260**:C832-40.
274. Gowans GJ, Hawley SA, Ross FA, Hardie DG. AMP is a true physiological regulator of amp-activated protein kinase by both allosteric activation and enhancing net phosphorylation. *Cell Metab* 2013;**18**:556–566.
275. Garcia-Roves PM, Osler ME, Holmström MH, Zierath JR. Gain-of-function R225Q mutation in AMP-activated protein kinase γ3 subunit increases mitochondrial biogenesis in glycolytic skeletal muscle. *J Biol Chem* 2008;**283**:35724–35734.
276. Amat R, Planavila A, Chen SL, Iglesias R, Giralt M, Villarroya F. SIRT1 controls the transcription of the peroxisome proliferator-activated receptor-gamma Co-activator-1alpha (PGC-1alpha) gene in skeletal muscle through the PGC-1alpha autoregulatory loop and interaction with MyoD. *J Biol Chem* 2009;**284**:21872–80.

277. Gerhart-Hines Z, Rodgers JT, Bare O, Lerin C, Kim S-H, Mostoslavsky R *et al.* Metabolic control of muscle mitochondrial function and fatty acid oxidation through SIRT1/PGC-1alpha. *EMBO J* 2007;**26**:1913–23.
278. Ojuka EO, Jones TE, Han D-H, Chen M, Holloszy JO. Raising Ca2+ in L6 myotubes mimics effects of exercise on mitochondrial biogenesis in muscle. *Fed Am Soc Exp Biol* 2003;**17**:675–681.
279. Freyssenet D, Di Carlo M, Hood DA. Calcium-dependent regulation of cytochrome c gene expression in skeletal muscle cells. Identification of a protein kinase c-dependent pathway. 1999;**274**:9305–9311.
280. Sakellariou GK, Vasilaki A, Palomero J, Kayani A, Zibrik L, McArdle A *et al.* Studies of mitochondrial and nonmitochondrial sources implicate nicotinamide adenine dinucleotide phosphate oxidase(s) in the increased skeletal muscle superoxide generation that occurs during contractile activity. *Antioxidants Redox Signal* 2013;**18**:603–621.
281. Sakellariou GK, Jackson MJ, Vasilaki A. Redefining the major contributors to superoxide production in contracting skeletal muscle. The role of NAD(P)H oxidases. *Free Radic Res* 2014;**48**:12–29.
282. Olesen J, Ringholm S, Nielsen MM, Brandt CT, Pedersen JT, Halling JF *et al.* Role of PGC-1α in exercise training- and resveratrol-induced prevention of age-associated inflammation. *Exp Gerontol* 2013;**48**:1274–1284.
283. Granata C, Oliveira RSF, Little JP, Renner K, Bishop DJ. Sprint-interval but not continuous exercise increases PGC-1α protein content and p53 phosphorylation in nuclear fractions of human skeletal muscle. *Sci Rep* 2017;**7**:44227.
284. Bartlett JD, Louhelainen J, Iqbal Z, Cochran AJ, Gibala MJ, Gregson W *et al.* Reduced carbohydrate availability enhances exercise-induced p53 signaling in human skeletal muscle: implications for mitochondrial biogenesis. *Am J Physiol Regul Integr Comp Physiol* 2013;**304**:R450--R458.
285. Park J-Y, Wang P-Y, Matsumoto T, Sung HJ, Ma W, Choi JW *et al.* p53 Improves Aerobic Exercise Capacity and Augments Skeletal Muscle Mitochondrial DNA Content. *Circ Res* 2009;**105**:705–712.
286. Donahue RJ, Razmara M, HOEK JB, Knudsen TB. Direct influence of the p53 tumor

suppressor on mitochondrial biogenesis and function. *FASEB J* 2001;**15**:635–644.

287. Beyfuss K, Erlich ATAT, Triolo M, Hood DADA. The role of p53 in determining mitochondrial adaptations to endurance training in skeletal muscle. *Sci Rep* 2018;**8**:14710.
288. Yoshida Y, Izumi H, Torigoe T, Ishiguchi H, Itoh H, Kang D *et al.* p53 physically interacts with mitochondrial transcription factor A and differentially regulates binding to damaged DNA. *Cancer Res* 2003;**63**:3729–3734.
289. Takahashi M, Chesley A, Freyssenet D, Hood DA. Contractile activity-induced adaptations in the mitochondrial protein import system. *Am J Physiol* 1998;**274**:C1380-7.
290. Joseph A, Hood DA. Plasticity of TOM complex assembly in skeletal muscle mitochondria in response to chronic contractile activity. *Mitochondrion* 2012;**12**:305–312.
291. Mottis A, Jovaisaite V, Auwerx J. The mitochondrial unfolded protein response in mammalian physiology. *Mamm Genome* 2014;**25**:424–433.
292. Ogborn DI, McKay BR, Crane JD, Parise G, Tarnopolsky MA. The unfolded protein response is triggered following a single, unaccustomed resistance-exercise bout. *Am J Physiol Regul Integr Comp Physiol* 2014;**2100**:R664-9.
293. Memme JM, Oliveira AN, Hood DA. Chronology of UPR activation in skeletal muscle adaptations to chronic contractile activity. *Am J Physiol - Cell Physiol* 2016;**310**:C1024--C1036.
294. Mesbah Moosavi ZS, Hood DA. The unfolded protein response in relation to mitochondrial biogenesis in skeletal muscle cells. *Am J Physiol - Cell Physiol* 2017;**312**:C583–C594.
295. Wu J, Ruas JL, Estall JL, Rasbach KA, Choi JH, Ye L *et al.* The unfolded protein response mediates adaptation to exercise in skeletal muscle through a PGC-1α/ATF6α complex. *Cell Metab* 2011;**13**:160–169.
296. Shenton D, Smirnova JB, Selley JN, Carroll K, Hubbard SJ, Pavitt GD *et al.* Global translational responses to oxidative stress impact upon multiple levels of protein synthesis. *J Biol Chem* 2006;**281**:29011–29021.
297. Baker BM, Nargund AM, Sun T, Haynes CM. Protective coupling of mitochondrial

function and protein synthesis via the eIF2α kinase GCN-2. *PLoS Genet* 2012;**8**.

298. Fiorese CJ, Schulz AM, Lin Y-FF, Rosin N, Pellegrino MW, Haynes CM. The transcription factor ATF5 mediates a mammalian mitochondrial UPR. *Curr Biol* 2016;**26**:2037–2043.
299. Melber A, Haynes CM. UPRmt regulation and output: a stress response mediated by mitochondrial-nuclear communication. *Cell Res* 2018;1–15.
300. Pirinen E, Cantó C, Jo YS, Morato L, Zhang H, Menzies KJ *et al.* Pharmacological inhibition of poly(ADP-ribose) polymerases improves fitness and mitochondrial function in skeletal muscle. *Cell Metab* 2014;**19**:1034–1041.
301. Quiros PM, Prado MA, Zamboni N, D'Amico D, Williams RW, Finley D *et al.* Multi-omics analysis identifies ATF4 as a key regulator of the mitochondrial stress response in mammals. *J Cell Biol* 2017;**216**:2027–2045.
302. Nargund AM, Pellegrino MW, Fiorese CJ, Baker BM, Haynes CM. Mitochondrial import efficiency of ATFS-1 regulates mitochondrial UPR activation. *Science* 2012;**337**:587–590.
303. Haynes CM, Petrova K, Benedetti C, Yang Y, Ron D. ClpP mediates activation of a mitochondrial unfolded protein response in C. elegans. *Dev Cell* 2007;**13**:467–480.
304. Haynes CM, Yang Y, Blais SP, Neubert TA. The matrix peptide exporter HAF-1 signals a mitochondrial unfolded protein response by activating the transcription factor ZC376.7 in C. elegans. *Mol Cell* 2010;**37**:529–540.
305. Dahl R, Larsen S, Dohlmann TL, Qvortrup K, Helge JW, Dela F *et al.* Three-dimensional reconstruction of the human skeletal muscle mitochondrial network as a tool to assess mitochondrial content and structural organization. *Acta Physiol* 2015;**213**:145–155.
306. Mishra P, Chan DC. Metabolic regulation of mitochondrial dynamics. *J Cell Biol* 2016;**212**:379–387.
307. Iqbal S, Ostojic O, Singh K, Joseph A-M, Hood DA. Expression of mitochondrial fission and fusion regulatory proteins in skeletal muscle during chronic use and disuse. *Muscle Nerve* 2013;**48**:963–970.
308. Bell MB, Bush Z, McGinnis GR, Rowe GC. Adult skeletal muscle deletion of Mitofusin 1 and 2 impedes exercise performance and training capacity. *J Appl Physiol*

2019;**126**:341–353.

309. Picard M, Gentil BJ, McManus MJ, White K, St. Louis K, Gartside SE *et al.* Acute exercise remodels mitochondrial membrane interactions in mouse skeletal muscle. *J Appl Physiol* 2013 doi:10.1152/japplphysiol.00819.2013.
310. Picard M, McManus MJ, Csordás G, Várnai P, Dorn GW, Williams D *et al.* Trans-mitochondrial coordination of cristae at regulated membrane junctions. *Nat Commun* 2015 doi:10.1038/ncomms7259.
311. Nielsen J, Gejl KD, Hey-Mogensen M, Holmberg H-C, Suetta C, Krustrup P *et al.* Plasticity in mitochondrial cristae density allows metabolic capacity modulation in human skeletal muscle. *J Physiol J Physiol J Physiol* 2017;**5959**:2839–2847.
312. Lira VA, Okutsu M, Zhang M, Greene NP, Laker RC, Breen DS *et al.* Autophagy is required for exercise training-induced skeletal muscle adaptation and improvement of physical performance. *FASEB J* 2013;**27**:4184–4193.
313. Kim Y, Triolo MM, Erlich ATAT, Hood DADA. Regulation of autophagic and mitophagic flux during chronic contractile activity-induced muscle adaptations. *Pflugers Arch* 2019;**471**:431–440.
314. Laker RC, Xu P, Ryall KA, Sujkowski A, Kenwood BM, Chain KH *et al.* A novel MitoTimer reporter gene for mitochondrial content, structure, stress, and damage in vivo. *J Biol Chem* 2014;**289**:12005–15.
315. Laker RC, Drake JC, Wilson RJ, Lira VA, Lewellen BM, Ryall KA *et al.* Ampk phosphorylation of Ulk1 is required for targeting of mitochondria to lysosomes in exercise-induced mitophagy. *Nat Commun* 2017;**8**:548.
316. Carter HN, Kim Y, Erlich AT, Zarrin-khat D, Hood DA. Autophagy and mitophagy flux in young and aged skeletal muscle following chronic contractile activity. 2018;**596**.
317. Ljubicic V, Hood DA. Specific attenuation of protein kinase phosphorylation in muscle with a high mitochondrial content. 2009;**297**.
318. Dudley GA, Tullsons PC, Terjung RL. Influence of Mitochondrial Content on the Sensitivity of Respiratory Control. *J Biol Chem* 1987;**262**:9109–9114.
319. Dun Y, Liu S, Zhang W, Xie M, Qiu L. Exercise combined with rhodiolasacra supplementation improves exercise capacity and ameliorates exhaustive exercise-induced muscle damage through enhancement of mitochondrial quality control. *Oxid*

Med Cell Longev 2017;**2017**:8024857.

320. Hernandez G, Thornton C, Stotland A, Lui D, Sin J, Ramil J *et al.* MitoTimer: A novel tool for monitoring mitochondrial turnover. *Autophagy* 2013;**9**:1852–1861.
321. Sun N, Yun J, Liu J, Malide D, Liu C, Rovira II *et al.* Measuring in vivo mitophagy. *Mol Cell* 2015;**60**:685–696.
322. Williams JA, Zhao K, Jin S, Ding WX. New methods for monitoring mitochondrial biogenesis and mitophagy in vitro and in vivo. *Exp Biol Med* 2017;**242**:781–787.
323. McWilliams TG, Prescott AR, Allen GFG, Tamjar J, Munson MJ, Thomson C *et al.* Mito-QC illuminates mitophagy and mitochondrial architecture in vivo. *J Cell Biol* 2016;**214**:333–345.
324. Erlich AT, Brownlee DM, Beyfuss K, Hood DA. Exercise induces TFEB expression and activity in skeletal muscle in a PGC-1α-dependent manner. *Am J Physiol - Cell Physiol* 2017;**314**:C62–C72.
325. Mansueto G, Armani A, Viscomi C, Zeviani M, Sandri M, Ballabio A *et al.* Transcription factor EB controls metabolic flexibility during exercise. *Cell Metab* 2017;**25**:182–196.
326. Kim Y, Hood DA. Regulation of the autophagy system during chronic contractile activity-induced muscle adaptations. *Physiol Rep* 2017;**5**:e13307.
327. Memme JM, Slavin M, Moradi N, Hood DA. Mitochondrial Bioenergetics and Turnover during Chronic Muscle Disuse. *Int J Mol Sci 2021, Vol 22, Page 5179* 2021;**22**:5179.
328. Morey-Holton ER, Globus RK. Hindlimb unloading rodent model: Technical aspects. *J Appl Physiol* 2002;**92**:1367–1377.
329. Madaro L, Smeriglio P, Molinaro M, Bouché M. Unilateral immobilization : a simple model of limb atrophy in mice. *Basic Appl Myol* 2008;**149**–**153**:5.
330. Caron AZ, Drouin G, Desrosiers J, Trensz F, Grenier G. A novel hindlimb immobilization procedure for studying skeletal muscle atrophy and recovery in mouse. *J Appl Physiol* 2009;**106**:2049–2059.
331. Marmonti E, Busquets S, Toledo M, Ricci M, Beltrà M, Gudiño V *et al.* A rat immobilization model based on cage volume reduction: A physiological model for bed rest? *Front Physiol* 2017;**8**:1–11.

332. Musacchia XJ, Steffen JM, Fell RD. Disuse atrophy of skeletal muscle: Animal models. Exerc. Sport Sci. Rev. 1988;**16**:61–87.
333. Memme JM, Oliveira AN, Hood DA. p53 regulates skeletal muscle mitophagy and mitochondrial quality control following denervation-induced muscle disuse. *J Biol Chem* 2022;**298**:101540.
334. Triolo M, Slavin M, Moradi N, Hood DA. Time-dependent changes in autophagy, mitophagy and lysosomes in skeletal muscle during denervation-induced disuse. *J Physiol* 2022 doi:10.1113/JP282173.
335. Groswald DE, Dettbarn WD. Nerve crush induced changes in molecular forms of acetylcholinesterase in soleus and extensor digitorum muscles. *Exp Neurol* 1983;**79**:519–531.
336. Buffelli M, Pasino E, Cangiano A. Paralysis of rat skeletal muscle equally affects contractile properties as does permanent denervation. *J Muscle Res Cell Motil* 1997;**18**:683–695.
337. Triolo M, Hood DA. Mitochondrial breakdown in skeletal muscle and the emerging role of the lysosomes. *Arch Biochem Biophys* 2019;**661**:66–73.
338. Wang Y, Pessin JE. Mechanisms for fiber-type specificity of skeletal muscle atrophy. *Curr Opin Clin Nutr Metab Care* 2013;**16**:243.
339. Macpherson PCD, Wang X, Goldman D. Myogenin Regulates Denervation-Dependent Muscle Atrophy in Mouse Soleus Muscle. *J Cell Biochem* 2011;**112**:2149.
340. Kilroe SP, Fulford J, Jackman SR, Van Loon LJC, Wall BT. Temporal Muscle-specific Disuse Atrophy during One Week of Leg Immobilization. *Med Sci Sports Exerc* 2020;**52**:944–954.
341. Eley HL, Tisdale MJ. Skeletal Muscle Atrophy, a Link between Depression of Protein Synthesis and Increase in Degradation. *J Biol Chem* 2007;**282**:7087–7097.
342. Schiaffino S, Mammucari C. Regulation of skeletal muscle growth by the IGF1-Akt/PKB pathway: insights from genetic models. *Skelet Muscle 2011 11* 2011;**1**:1–14.
343. Gordon BS, Kelleher AR, Kimball SR. Regulation of muscle protein synthesis and the effects of catabolic states. *Int J Biochem Cell Biol* 2013;**45**:2147–2157.
344. Reynolds IV TH, Bodine SC, Lawrence JC. Control of Ser2448 phosphorylation in the mammalian target of rapamycin by insulin and skeletal muscle load. *J Biol Chem*

2002;**277**:17657–17662.

345. Bodine SC, Stitt TN, Gonzalez M, Kline WO, Stover GL, Bauerlein R *et al.* Akt/mTOR pathway is a crucial regulator of skeletal muscle hypertrophy and can prevent muscle atrophy in vivo. *Nat Cell Biol* 2001;**3**:1014–1019.
346. Argadine HM, Hellyer NJ, Mantilla CB, Zhan W-Z, Sieck GC. The effect of denervation on protein synthesis and degradation in adult rat diaphragm muscle. *J Appl Physiol* 2009;**107**:438.
347. Kline WO, Panaro FJ, Yang H, Bodine SC. Rapamycin inhibits the growth and muscle-sparing effects of clenbuterol. *J Appl Physiol* 2007;**102**:740–747.
348. Goldspink DF. The effects of denervation on protein turnover of rat skeletal muscle. *Biochem J* 1976;**156**:71.
349. Booth FW, Seider MJ. Early change in skeletal muscle protein synthesis after limb immobilization of rats. *J Appl Physiol Respir Env Exerc Physiol* 1979;**47**:974–7.
350. Glover EI, Phillips SM, Oates BR, Tang JE, Tarnopolsky MA, Selby A *et al.* Immobilization induces anabolic resistance in human myofibrillar protein synthesis with low and high dose amino acid infusion. *J Physiol* 2008;**586**:6049–6061.
351. Wall BT, Snijders T, Senden JMG, Ottenbros CLP, Gijsen AP, Verdijk LB *et al.* Disuse Impairs the Muscle Protein Synthetic Response to Protein Ingestion in Healthy Men. *J Clin Endocrinol Metab* 2013;**98**:4872–4881.
352. Kelleher AR, Kimball SR, Dennis MD, Schilder RJ, Jefferson LS. The mTORC1 signaling repressors REDD1/2 are rapidly induced and activation of p70S6K1 by leucine is defective in skeletal muscle of an immobilized rat hindlimb. *Am J Physiol - Endocrinol Metab* 2013;**304**:229–236.
353. Rosa-Caldwell ME, Lim S, Haynie WA, Brown JL, Deaver JW, Silva FM Da *et al.* Female mice may have exacerbated catabolic signalling response compared to male mice during development and progression of disuse atrophy. *J Cachexia Sarcopenia Muscle* 2021;**12**:717–730.
354. Richter EA, Kiens B, Mizuno M, Strange S. Insulin action in human thighs after one-legged immobilization. *J Appl Physiol* 1989;**67**:19–23.
355. Allen DL, Linderman JK, Roy RR, Grindeland RE, Mukku V, Edgerton VR. Growth hormone/IGF-I and/or resistive exercise maintains myonuclear number in hindlimb

unweighted muscles. *J Appl Physiol* 1997;**83**:1857–1861.

356. O'Keefe MP, Perez FR, Sloniger JA, Tischler ME, Henriksen EJ. Enhanced insulin action on glucose transport and insulin signaling in 7-day unweighted rat soleus muscle. *J Appl Physiol* 2004;**97**:63–71.
357. Ji CH, Kwon YT. Crosstalk and Interplay between the Ubiquitin-Proteasome System and Autophagy. *Mol Cells* 2017;**40**:441.
358. Kitajima Y, Tashiro Y, Suzuki N, Warita H, Kato M, Tateyama M *et al.* Proteasome dysfunction induces muscle growth defects and protein aggregation. *J Cell Sci* 2014;**127**:5204–5217.
359. Kitajima Y, Suzuki N, Yoshioka K, Izumi R, Tateyama M, Tashiro Y *et al.* Inducible Rpt3, a Proteasome Component, Knockout in Adult Skeletal Muscle Results in Muscle Atrophy. *Front Cell Dev Biol* 2020;**8**:1–11.
360. Hughes DC, Baehr LM, Waddell DS, Sharples AP, Bodine SC. Ubiquitin Ligases in Longevity and Aging Skeletal Muscle. *Int J Mol Sci* 2022;**23**:1–23.
361. Taillandier D, Polge C. Skeletal muscle atrogenes: From rodent models to human pathologies. *Biochimie* 2019;**166**:251–269.
362. Egerman MA, Glass DJ. Signaling pathways controlling skeletal muscle mass. *Crit Rev Biochem Mol Biol* 2014;**49**:59.
363. Bodine SC, Latres E, Baumhueter S, Lai VKM, Nunez L, Clarke BA *et al.* Identification of ubiquitin ligases required for skeletal Muscle Atrophy. *Science (80-)* 2001;**294**:1704–1708.
364. Sacheck JM, Hyatt J-PK, Raffaello A, Jagoe RT, Roy RR, Edgerton VR *et al.* Rapid disuse and denervation atrophy involve transcriptional changes similar to those of muscle wasting during systemic diseases. *FASEB J* 2007;**21**:140–155.
365. Cadena SM, Zhang Y, Fang J, Brachat S, Kuss P, Giorgetti E *et al.* Skeletal muscle in MuRF1 null mice is not spared in low-gravity conditions, indicating atrophy proceeds by unique mechanisms in space. *Sci Reports 2019 91* 2019;**9**:1–11.
366. Furlow JD, Watson ML, Waddell DS, Neff ES, Baehr LM, Ross AP *et al.* Altered gene expression patterns in muscle ring finger 1 null mice during denervation- and dexamethasone-induced muscle atrophy. *Physiol Genomics* 2013;**45**:1168–1185.
367. Baehr LM, Hughes DC, Lynch SA, Van Haver D, Maia TM, Marshall AG *et al.*

Identification of the MuRF1 Skeletal Muscle Ubiquitylome Through Quantitative Proteomics. *Function* 2021;**2**:1–18.

368. Huang Z, Fang Q, Ma W, Zhang Q, Qiu J, Gu X *et al.* Skeletal muscle atrophy was alleviated by salidroside through suppressing oxidative stress and inflammation during denervation. *Front Pharmacol* 2019;**10**:997.
369. Ruohonen S, Khademi M, Jagodic M, Taskinen H-S, Olsson T, Röyttä M. Cytokine responses during chronic denervation. *J Neuroinflammation 2005 21* 2005;**2**:1–11.
370. Bryndina IG, Ovchinina NG, Protopopov VA, Shalagina MN, Ovchinina NN, Sekunov A V. TNFa is Involved in the Development of Disuse Muscle Atrophy Through the Acid Sphingomyelinase/ Ceramide Up-Regulation and Pro-Oxidant Signaling. *Res Sq* 2020;**1**.
371. Dodd SL, Gagnon BJ, Senf SM, Hain BA, Judge AR. ROS-mediated activation of NF-κB and Foxo during muscle disuse. *Muscle Nerve* 2010;**41**:110.
372. Stuart CA, Shangraw RE, Prince MJ, Peters EJ, Wolfe RR. Bed-rest-induced insulin resistance occurs primarily in muscle. *Metab - Clin Exp* 1988;**37**:802–806.
373. Wilkes JJ, Bonen A. Reduced insulin-stimulated glucose transport in denervated muscle is associated with impaired Akt-α activation. *Am J Physiol - Endocrinol Metab* 2000;**279**:42.
374. Stitt TN, Drujan D, Clarke BA, Panaro F, Timofeyva Y, Kline WO *et al.* The IGF-1/PI3K/Akt pathway prevents expression of muscle atrophy-induced ubiquitin ligases by inhibiting FOXO transcription factors. *Mol Cell* 2004;**14**:395–403.
375. Sandri M, Lin J, Handschin C, Yang W, Arany ZP, Lecker SH *et al.* PGC-1alpha protects skeletal muscle from atrophy by suppressing FoxO3 action and atrophy-specific gene transcription. *Proc Natl Acad Sci U S A* 2006;**103**:16260–16265.
376. Milan G, Romanello V, Pescatore F, Armani A, Paik J-H, Frasson L *et al.* Regulation of autophagy and the ubiquitin–proteasome system by the FoxO transcriptional network during muscle atrophy. *Nat Commun 2015 61* 2015;**6**:1–14.
377. Waddell DS, Baehr LM, Van Den Brandt J, Johnsen SA, Reichardt HM, Furlow JD *et al.* The glucocorticoid receptor and FOXO1 synergistically activate the skeletal muscle atrophy-associated MuRF1 gene. *Am J Physiol - Endocrinol Metab* 2008;**295**:785–797.
378. Hyatt HW, Powers SK. The Role of Calpains in Skeletal Muscle Remodeling with

Exercise and Inactivity-induced Atrophy. *Int J Sports Med* 2020;**41**:994–1008.

379. Talbert EE, Smuder AJ, Min K, Kwon OS, Powers SK. Calpain and caspase-3 play required roles in immobilization-induced limb muscle atrophy. *J Appl Physiol* 2013;**114**:1482–1489.
380. Du J, Wang X, Miereles C, Bailey JL, Debigare R, Zheng B *et al.* Activation of caspase-3 is an initial step triggering accelerated muscle proteolysis in catabolic conditions. *J Clin Invest* 2004;**113**:115.
381. Plant PJ, Bain JR, Correa JE, Woo M, Batt J. Absence of caspase-3 protects against denervation-induced skeletal muscle atrophy. *J Appl Physiol* 2009;**107**:224–234.
382. Dobrowolny G, Aucello M, Rizzuto E, Beccafico S, Mammucari C, Boncompagni S *et al.* Skeletal Muscle Is a Primary Target of SOD1G93A-Mediated Toxicity. *Cell Metab* 2008;**8**:425–436.
383. Yu Z, Wang AM, Adachi H, Katsuno M, Sobue G, Yue Z *et al.* Macroautophagy is regulated by the UPR-mediator CHOP and accentuates the phenotype of SBMA mice. *PLoS Genet* 2011;**7**.
384. Masiero E, Agatea L, Mammucari C, Blaauw B, Loro E, Komatsu M *et al.* Autophagy Is Required to Maintain Muscle Mass. *Cell Metab* 2009;**10**:507–515.
385. Castets P, Lin S, Rion N, Di Fulvio S, Romanino K, Guridi M *et al.* Sustained Activation of mTORC1 in Skeletal Muscle Inhibits Constitutive and Starvation-Induced Autophagy and Causes a Severe, Late-Onset Myopathy. *Cell Metab* 2013;**17**:731–744.
386. Irazoki A, Martinez-Vicente M, Aparicio P, Aris C, Alibakhshi E, Rubio-Valera M *et al.* Coordination of mitochondrial and lysosomal homeostasis mitigates inflammation and muscle atrophy during aging. *Aging Cell* 2022;**21**:1–16.
387. MacDonald EM, Andres-Mateos E, Mejias R, Simmers JL, Mi R, Park JS *et al.* Denervation atrophy is independent from Akt and mTOR activation and is not rescued by myostatin inhibition. *DMM Dis Model Mech* 2014;**7**:471–481.
388. Sugiura T, Abe N, Nagano M, Goto K, Sakuma K, Naito H *et al.* Changes in PKB/Akt and calcineurin signaling during recovery in atrophied soleus muscle induced by unloading. *Am J Physiol - Regul Integr Comp Physiol* 2005;**288**:1273–1278.
389. Castets P, Rion N, Théodore M, Falcetta D, Lin S, Reischl M *et al.* mTORC1 and PKB/Akt control the muscle response to denervation by regulating autophagy and

HDAC4. *Nat Commun* 2019;**10**:1–16.

390. Belova SP, Vilchinskaya NA, Mochalova EP, Mirzoev TM, Nemirovskaya TL, Shenkman BS. Elevated p70S6K phosphorylation in rat soleus muscle during the early stage of unloading: Causes and consequences. *Arch Biochem Biophys* 2019;**674**:108105.
391. Senf SM, Dodd SL, McClung JM, Judge AR. Hsp70 overexpression inhibits NF-κB and Foxo3a transcriptional activities and prevents skeletal muscle atrophy. *FASEB J* 2008;**22**:3836.
392. Beharry AW, Sandesara PB, Roberts BM, Ferreira LF, Senf SM, Judge AR. HDAC1 activates FoxO and is both sufficient and required for skeletal muscle atrophy. *J Cell Sci* 2014;**127**:1441–1453.
393. Senf SM, Dodd SL, Judge AR. FOXO signaling is required for disuse muscle atrophy and is directly regulated by Hsp70. *Am J Physiol - Cell Physiol* 2010;**298**:C38.
394. Smuder AJ, Sollanek KJ, Min K, Nelson WB, Powers SK. Inhibition of forkhead BoxO-specific transcription prevents mechanical ventilation-induced diaphragm dysfunction. *Crit Care Med* 2015;**43**:e133–e142.
395. Guo Y, Meng J, Tang Y, Wang T, Wei B, Feng R *et al.* AMP-activated kinase α2 deficiency protects mice from denervation-induced skeletal muscle atrophy. *Arch Biochem Biophys* 2016;**600**:56–60.
396. Stouth DW, Manta A, Ljubicic V. Protein arginine methyltransferase expression, localization, and activity during disuse-induced skeletal muscle plasticity. *Am J Physiol - Cell Physiol* 2018;**314**:C177–C190.
397. Tamura Y, Kitaoka Y, Matsunaga Y, Hoshino D, Hatta H. Daily heat stress treatment rescues denervation-activated mitochondrial clearance and atrophy in skeletal muscle. *J Physiol* 2015;**593**:2707–20.
398. Graham ZA, Harlow L, Bauman WA, Cardozo CP. Alterations in mitochondrial fission, fusion, and mitophagic protein expression in the gastrocnemius of mice after a sciatic nerve transection. *Muscle Nerve* 2018;**58**:592–599.
399. Stouth DW, vanLieshout TL, Ng SY, Webb EK, Manta A, Moll Z *et al.* CARM1 Regulates AMPK Signaling in Skeletal Muscle. *iScience* 2020;**23**:101755.
400. Kim J, Kundu M, Viollet B, Guan K-LL, Kim Joungmok, Kundu Mondira, Viollet

Benoit GK-L, Kim J *et al.* AMPK and mTOR regulate autophagy through direct phosphorylation of Ulk1. *Nat Cell Biol* 2011;**13**:132–141.

401. Mihaylova MM, Shaw RJ. The AMPK signalling pathway coordinates cell growth, autophagy and metabolism. *Nat Cell Biol* 2011;**13**:1016–1023.
402. Gwinn DM, Shackelford DB, Egan DF, Mihaylova MM, Mery A, Vasquez DS *et al.* AMPK Phosphorylation of Raptor Mediates a Metabolic Checkpoint. *Mol Cell* 2008;**30**:214–226.
403. Vainshtein A, Desjardins EM, Armani A, Sandri M, Hood DA. PGC-1α modulates denervation-induced mitophagy in skeletal muscle. *Skelet Muscle* 2015;**5**:9.
404. Weinstein RB, Slentz MJ, Webster K, Takeuchi JA, Tischler ME. Lysosomal proteolysis in distally or proximally denervated rat soleus muscle. *Am J Physiol - Regul Integr Comp Physiol* 1997;**273**.
405. Max SR, Mayer RF, Vogelsang L. Lysosomes and disuse atrophy of skeletal muscle. *Arch Biochem Biophys* 1971;**146**:227–232.
406. Taillandier D, Aurousseau E, Meynial-Denis D, Bechet D, Ferrara M, Cottin P *et al.* Coordinate activation of lysosomal, Ca2+-activated and ATP-ubiquitin-dependent proteinases in the unweighted rat soleus muscle. *Biochem J* 1996;**316**:65–72.
407. O'Leary MF, Vainshtein A, Iqbal S, Ostojic O, Hood DA. Adaptive plasticity of autophagic proteins to denervation in aging skeletal muscle. *Am J Physiol Cell Physiol* 2013;**304**:C422--30.
408. Wang F, Gómez-Sintes R, Boya P. Lysosomal membrane permeabilization and cell death. *Traffic* 2018;**19**:918–931.
409. Adhihetty PJ, O 'leary MFN, Chabi B, Wicks KL, Hood DA, O'Leary MFNN *et al.* Effect of denervation on mitochondrially mediated apoptosis in skeletal muscle. *J Appl Physiol* 2007;**102**:1143–1151.
410. Min K, Smuder AJ, Kwon O, Kavazis AN, Szeto HH, Powers SK. Mitochondrial-targeted antioxidants protect skeletal muscle against immobilization-induced muscle atrophy. *J Appl Physiol* 2011;**111**:1459–1466.
411. Muller FL, Song W, Jang YC, Liu Y, Sabia M, Richardson A *et al.* Denervation-induced skeletal muscle atrophy is associated with increased mitochondrial ROS production. *Am J Physiol Regul Integr Comp Physiol* 2007;**293**:R1159--68.

412. Yang X, Xue P, Chen H, Yuan M, Kang Y, Duscher D *et al.* Denervation drives skeletal muscle atrophy and induces mitochondrial dysfunction, mitophagy and apoptosis via miR-142a-5p/MFN1 axis. *Theranostics* 2020;**10**:1415.
413. Romanello V, Guadagnin E, Gomes L, Roder I, Sandri C, Petersen Y *et al.* Mitochondrial fission and remodelling contributes to muscle atrophy. *EMBO J* 2010;**29**:1774–1785.
414. Csukly K, Ascah A, Matas J, Gardiner PF, Fontaine E, Burelle Y. Muscle denervation promotes opening of the permeability transition pore and increases the expression of cyclophilin D. *J Physiol* 2006;**574**:319–327.
415. Davies KJ. Protein damage and degradation by oxygen radicals. I. general aspects. *J Biol Chem* 1987;**262**:9895–9901.
416. Siu PM, Alway SE. Mitochondria-associated apoptotic signalling in denervated rat skeletal muscle. *J Physiol* 2005;**565**:309–323.
417. Siu PM, Alway SE. Deficiency of the Bax gene attenuates denervation-induced apoptosis. *Apoptosis* 2006;**11**:967.
418. Talbert EE, Smuder AJ, Min K, Kwon OS, Szeto HH, Powers SK. Immobilization-induced activation of key proteolytic systems in skeletal muscles is prevented by a mitochondria-targeted antioxidant. *J Appl Physiol* 2013;**115**:529–538.
419. Frank M, Duvezin-Caubet S, Koob S, Occhipinti A, Jagasia R, Petcherski A *et al.* Mitophagy is triggered by mild oxidative stress in a mitochondrial fission dependent manner. *Biochim Biophys Acta - Mol Cell Res* 2012;**1823**:2297–2310.
420. Wan Q, Zhang L, Huang Z, Zhang H, Gu J, Xu H *et al.* Aspirin alleviates denervation-induced muscle atrophy via regulating the Sirt1/PGC-1α axis and STAT3 signaling. *Ann Transl Med* 2020;**8**:1524–1524.
421. Haizlip KM, Harrison BC, Leinwand LA. Sex-Based Differences in Skeletal Muscle Kinetics and Fiber-Type Composition. *Physiology* 2015;**30**:30.
422. Sugiura T, Ito N, Goto K, Naito H, Yoshioka T, Powers SK. Estrogen administration attenuates immobilization-induced skeletal muscle atrophy in male rats. *J Physiol Sci* 2006;**56**:393–399.
423. Rosa-Caldwell ME, Greene NP. Muscle metabolism and atrophy: let's talk about sex. *Biol Sex Differ 2019 101* 2019;**10**:1–14.

424. Lipes J, Mardini L, Jayaraman D. Sex and Mortality of Hospitalization Admission to an Intensive Care. *Am J Crit Care* 2013;**22**:314–319.
425. Yoshihara T, Natsume T, Tsuzuki T, Chang S, Kakigi R, Sugiura T *et al.* Sex differences in forkhead box O3a signaling response to hindlimb unloading in rat soleus muscle. *J Physiol Sci 2018 692* 2018;**69**:235–244.
426. Mortreux M, Rosa-Caldwell ME, Stiehl ID, Sung DM, Thomas NT, Fry CS *et al.* Hindlimb suspension in Wistar rats: Sex-based differences in muscle response. *Physiol Rep* 2021;**9**:1–15.
427. Iqbal S, Thomas A, Bunyan K, Tiidus PM. Progesterone and estrogen influence postexercise leukocyte infiltration in overiectomized female rats. *Appl Physiol Nutr Metab* 2008;**33**:1207–1212.
428. Tiidus PM, Holden D, Bombardier E, Zajchowski S, Enns D, Belcastro A. Estrogen effect on post-exercise skeletal muscle neutrophil infiltration and calpain activity. *Can J Physiol Pharmacol* 2001;**79**:400–6.
429. Raj DA, Booker TS, Belcastro AN. Striated muscle calcium-stimulated cysteine protease (calpain-like) activity promotes myeloperoxidase activity with exercise. *Pflugers Arch Eur J Physiol* 1998;**435**:804–809.
430. Belcastro AN, Shewchuk LD, Raj DA. Exercise-induced muscle injury: A calpain hypothesis. *Mol Cell Biochem* 1998;**179**:135–145.
431. Youle RJ, Narendra DP. Mechanisms of mitophagy. *Nat Rev Mol Cell Biol* 2011;**12**:9–14.
432. Jin SM, Lazarou M, Wang C, Kane LA, Narendra DP, Youle RJ. Mitochondrial membrane potential regulates PINK1 import and proteolytic destabilization by PARL. *J Cell Biol* 2010;**191**:933–42.
433. Kravic B, Harbauer AB, Romanello V, Simeone L, Vögtle F-N, Kaiser T *et al.* In mammalian skeletal muscle, phosphorylation of TOMM22 by protein kinase CSNK2/CK2 controls mitophagy. *Autophagy* 2017;**8627**:01–65.
434. Wang Y, Nartiss Y, Steipe B, McQuibban GA, Kim PK. ROS-induced mitochondrial depolarization initiates PARK2/PARKIN-dependent mitochondrial degradation by autophagy. *Autophagy* 2012;**8**:1462–1476.
435. Matsumoto G, Wada K, Okuno M, Kurosawa M, Nukina N. Serine 403

Phosphorylation of p62/SQSTM1 Regulates Selective Autophagic Clearance of Ubiquitinated Proteins. *Mol Cell* 2011;**44**:279–289.

436. Lee Y, Lee H-Y, Hanna R, Gustafsson A. Mitochondrial autophagy by Bnip3 involves Drp1-mediated mitochondrial fission and recruitment of Parkin in cardiac myocytes. *AJP Hear Circ Physiol* 2011;**301**:H1924–H1931.
437. Di Bartolomeo S, Corazzari M, Nazio F, Oliverio S, Lisi G, Antonioli M *et al.* The dynamic interaction of AMBRA1 with the dynein motor complex regulates mammalian autophagy. *J Cell Biol* 2010;**191**:155–168.
438. Wei Y, Chiang WC, Sumpter R, Mishra P, Levine B. Prohibitin 2 Is an Inner Mitochondrial Membrane Mitophagy Receptor. *Cell* 2017;**168**:224-238.e10.
439. Medina DL, Di Paola S, Peluso I, Armani A, De Stefani D, Venditti R *et al.* Lysosomal calcium signalling regulates autophagy through calcineurin and TFEB. *Nat Cell Biol* 2015;**17**:288–99.
440. Medina DL, Ballabio A. Lysosomal calcium regulates autophagy. *Nature* 2015;**11**:970–971.
441. Vainshtein A, Hood DA. The regulation of autophagy during exercise in skeletal muscle. *J Appl Physiol* 2016;**120**:664–673.
442. Demers-Lamarche J, Guillebaud G, Tlili M, Todkar K, Bélanger N, Grondin M *et al.* Loss of mitochondrial function impairs Lysosomes∗. *J Biol Chem* 2016;**291**:10263–10276.
443. Connor MK, Irrcher I, Hood DA. Contractile activity-induced transcriptional activation of cytochrome C involves Sp1 and is proportional to mitochondrial ATP synthesis in C2C12 muscle cells. *J Biol Chem* 2001;**276**:15898–15904.
444. Irrcher I, Adhihetty PJ, Sheehan T, Joseph A-MM, Hood DA. PPARγ coactivator-1α expression during thyroid hormone- and contractile activity-induced mitochondrial adaptations. 2003;**284**:C1669–C1677.
445. Settembre C, Polito VA, Garcia M, Vetrini F, Erdin SSU, Erdin SSU *et al.* TFEB links autophagy to lysosomal biogenesis. *Science* 2011;**332**:1429–33.
446. Nezich CL, Wang C, Fogel AI, Youle RJ. MiT / TFE transcription factors are activated during mitophagy downstream of Parkin and Atg5. *J Cell Biol* 2015;**210**:435–450.
447. de Araujo MEG, Liebscher G, Hess MW, Huber LA. Lysosomal size matters. *Traffic*

2020;**21**:60–75.

448. McGrath MJ, Eramo MJ, Gurung R, Sriratana A, Gehrig SM, Lynch GS *et al.* Defective lysosome reformation during autophagy causes skeletal muscle disease. *J Clin Invest* 2021;**131**:1–16.
449. Medina DL, Fraldi A, Bouche V, Annunziata F, Mansueto G, Spampanato C *et al.* Transcriptional activation of lysosomal exocytosis promotes cellular clearance. *Dev Cell* 2011;**21**:421–430.
450. Metter EJ, Talbot LA, Schrager M, Conwit R. Skeletal muscle strength as a predictor of all-cause mortality in healthy men. *Journals Gerontol - Ser A Biol Sci Med Sci* 2002;**57**:B359–B365.
451. Powers SK, Wiggs MP, Duarte JA, Murat Zergeroglu A, Demirel HA, Zergeroglu AM *et al.* Mitochondrial signaling contributes to disuse muscle atrophy. *Am J Physiol Endocrinol Metab* 2012;**303**:E31--9.
452. Carafoli E, Margreth A, Buffa P. Early biochemical changes in mitochondria from denervated muscle and their relation to the onset of atrophy. *Exp Mol Pathol* 1964;**3**:171–181.
453. Kang C, Goodman C a, Hornberger T a, Ji LL. PGC-1$α$ overexpression by in vivo transfection attenuates mitochondrial deterioration of skeletal muscle caused by immobilization. *FASEB J* 2015 doi:10.1096/fj.14-266619.
454. Smuder AJ, Sollanek KJ, Nelson WB, Min K, Talbert EE, Kavazis AN *et al.* Crosstalk between autophagy and oxidative stress regulates proteolysis in the diaphragm during mechanical ventilation. *Free Radic Biol Med* 2018;**115**:179–190.
455. Rosa-Caldwell ME, Brown JL, Perry RA, Shimkus KL, Shirazi-Fard Y, Brown LA *et al.* Regulation of mitochondrial quality following repeated bouts of hindlimb unloading. *Appl Physiol Nutr Metab* 2020;**45**:264–274.
456. Kang C, Yeo D, Ji LL. Muscle immobilization activates mitophagy and disrupts mitochondrial dynamics in mice. *Acta Physiol* 2016;**218**:188–197.
457. O′Leary MFN, Vainshtein A, Carter HN, Zhang Y, Hood DA. Denervation-induced mitochondrial dysfunction and autophagy in skeletal muscle of apoptosis-deficient animals. *Am J Physiol Physiol* 2012;**303**:C447–C454.
458. Kissing S, Hermsen C, Repnik U, Nesset CK, Von Bargen K, Griffiths G *et al.*

Vacuolar ATPase in phagosome-lysosome fusion. *J Biol Chem* 2015;**290**:14166–14180.

459. von Haehling S, Morley JE, Coats AJS, Anker SD. Ethical guidelines for publishing in the journal of cachexia, sarcopenia and muscle: update 2017. *J Cachexia Sarcopenia Muscle* 2017;**8**:1081–1083.
460. Montero D, Madsen K, Meinild-Lundby AK, Edin F, Lundby C. Sexual dimorphism of substrate utilization: Differences in skeletal muscle mitochondrial volume density and function. *Exp Physiol* 2018;**103**:851–859.
461. Palmieri M, Pal R, Nelvagal HR, Lotfi P, Stinnett GR, Seymour ML *et al.* mTORC1-independent TFEB activation via Akt inhibition promotes cellular clearance in neurodegenerative storage diseases. *Nat Commun 2017 81* 2017;**8**:1–19.
462. Song J, Malampati S, Zeng Y, Durairajan SSK, Yang C, Tong BC *et al.* A small molecule transcription factor EB activator ameliorates beta-amyloid precursor protein and Tau pathology in Alzheimer's disease models. *Aging Cell* 2020;**19**.
463. Crilly MJ, Tryon LD, Erlich AT, Hood DA. The role of Nrf2 in skeletal muscle contractile and mitochondrial function. *J Appl Physiol* 2016;**121**:730–740.

APPENDIX A

ADDITIONAL DATA PERTAINING TO CHAPTER FOUR

A.1 Gene expression following contractile activity in the absence of TFEB or TFE3.

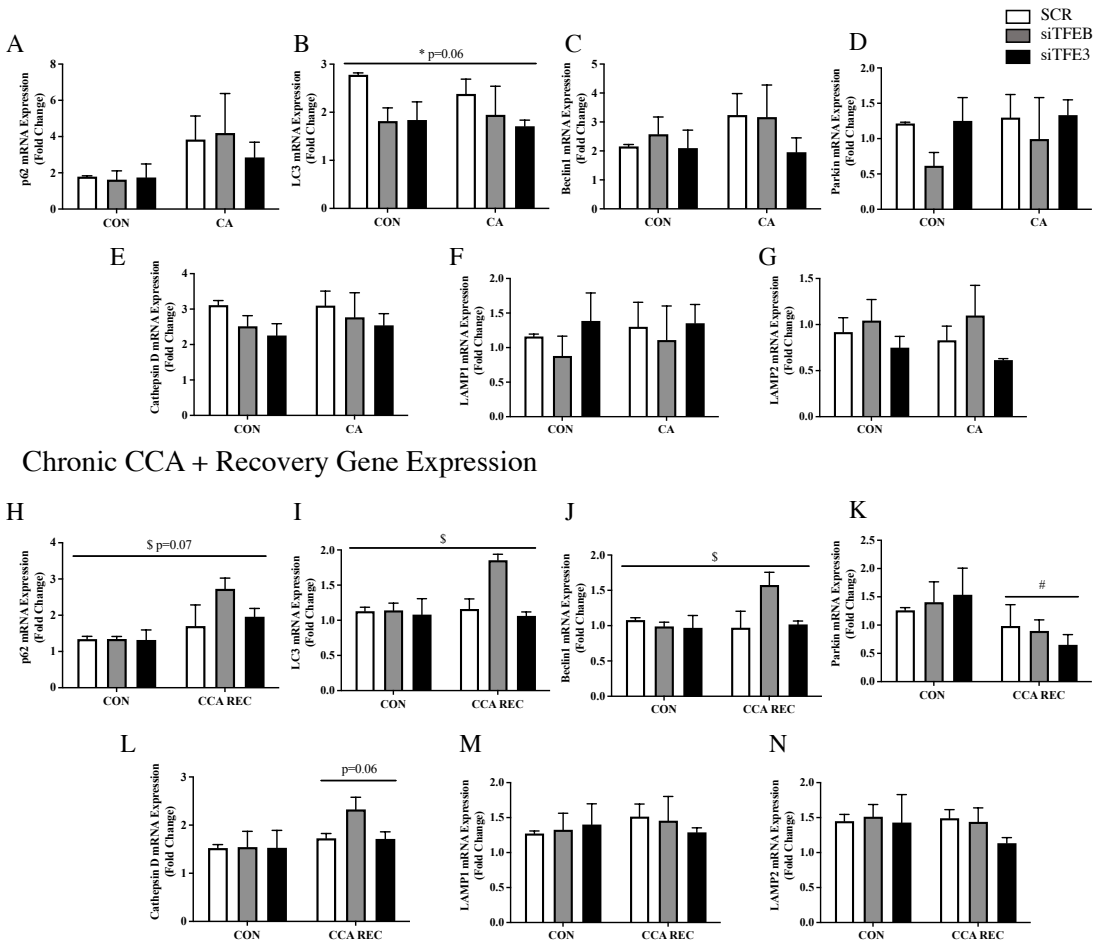

Fig. A1: Gene expression following contractile activity in the absence of TFEB or TFE3. *P62* or *Sqstm1* (A), *Lc3* or *Map1lcb* (B), *Beclin1* (C), *Parkin* (D), *Cathepsin D* (E), *LAMP1* (F), *LAMP2*(G) mRNA expression was assessed following an acute bout of contractile activity in the absence of TFEB or TFE3. No differences were observed. *P62* or *Sqstm1* (H), *LC3* or *Map1lcb* (I), *Beclin1* (J), *Parkin* (K), *Cathepsin D* (L), *LAMP1* (M), *LAMP2*(N) mRNA expression was assessed following a chronic contractile activity and a 21hr recovery period. Similar to the data presented following CCA, an interaction effect was observed for *Lc3, Beclin1,* and *Cathepsin D* with the greatest change occurring in the absence of TFEB, likely due to a compensatory increase in TFE3. Furthermore, *Parkin* mRNA was also reduced following CCA and recovery, in line with the data presented following CCA. #, denotes a main effect of CCA+REC, $p<0.05$; $, indicates an interaction effect, $p<0.05$.

A.2 Gene expression following contractile activity and recovery in the absence of TFEB and TFE3.

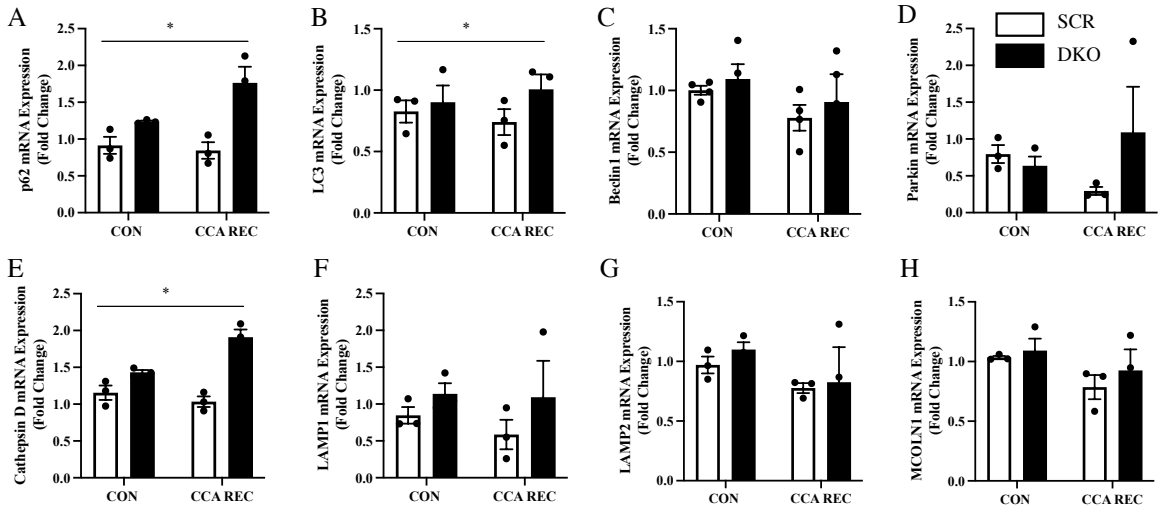

Fig. A2: Gene expression following contractile activity and recovery in the absence of TFEB and TFE3. *P62* or *Sqstm1* (A), *Lc3* or *Map1lcb* (B), *Beclin1* (C), *Parkin* (D), *Cathepsin D* (E), *LAMP1* (F), *LAMP2*(G) and *Mcoln1* (H) mRNA expression was assessed following chronic contractile activity and a 21 hr recovery period in the absence of TFEB and TFE3 (DKO). Increased *p62, Lc3* and *Cathepsin D* transcripts were observed in the absence of TFEB and TFE3 in line with the CA and CCA data presented. *, denotes a main effect of DKO, $p<0.05$.

A.3 Lysosomal adaptations to CCA

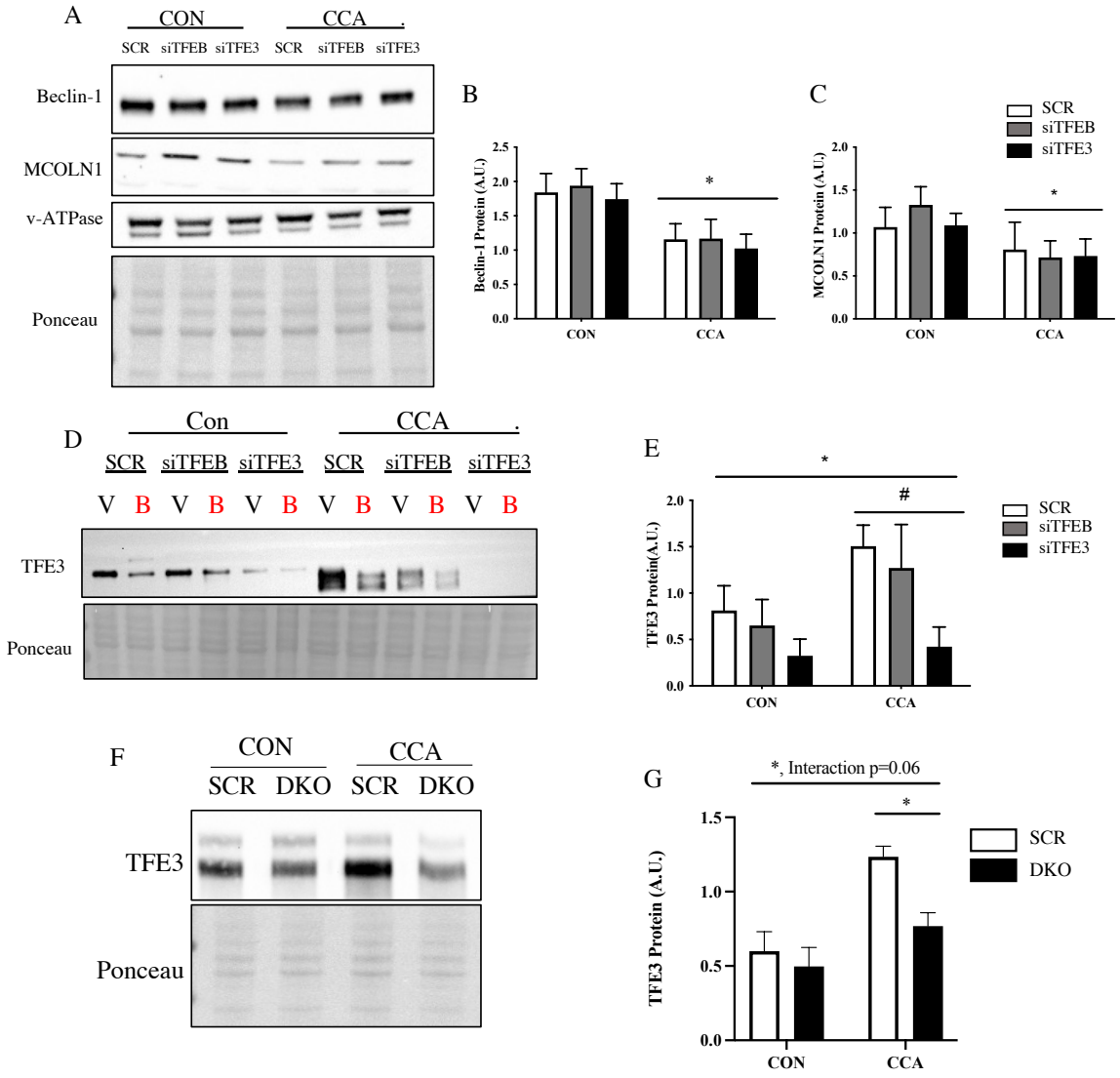

Fig. A3: Lysosomal adaptations to CCA. Representative western blots of lysosomal markers following chronic contractile activity in the absence of TFEB or TFE3 (A). Beclin1 protein content (B) was reduced following CCA across all conditions supporting the finding that CCA improves the mitochondrial pool, decreasing the need for mitophagy. Contrary to the findings of increased lysosomal content following CCA, a decrease in MCOLN1 protein content (C) was observed following CCA potentially indicating a compositional change in lysosomes following CCA. No changes were observed for v-ATPase, another lysosomal marker. TFE3 protein content was increased dramatically following CCA in SCR conditions (D, E), but was significantly reduced in siTFE3 (E) and DKO conditions (F, G). *, denotes a main effect of siRNA or DKO, $p<0.05$; #, indicates a main effect of CCA, $p<0.05$.

APPENDIX B

ADDITIONAL DATA PERTAINING TO CHAPTER FIVE

Supplemental References

S1. Memme JM, Slavin M, Moradi N, Hood DA. Mitochondrial Bioenergetics and Turnover during Chronic Muscle Disuse. *Int J Mol Sci 2021, Vol 22, Page 5179* 2021;**22**:5179.

S2. Hyatt H, Deminice R, Yoshihara T, Powers SK. Mitochondrial dysfunction induces muscle atrophy during prolonged inactivity: A review of the causes and effects. *Arch Biochem Biophys* 2019;**662**:49–60.

S3. Vainshtein A, Desjardins EM, Armani A, Sandri M, Hood DA. PGC-1α modulates denervation-induced mitophagy in skeletal muscle. *Skelet Muscle* 2015;**5**:9.

S4. Hood DA, Memme J. M, Oliveira AN, Triolo M. Maintenance of Skeletal Muscle Mitochondria in Health, Exercise, and Aging. *Annu Rev Physiol* 2019;**81**:19–41.

S5. Adhihetty PJ, O 'leary MFN, Chabi B, Wicks KL, Hood DA, O'Leary MFNN *et al.* Effect of denervation on mitochondrially mediated apoptosis in skeletal muscle. *J Appl Physiol* 2007;**102**:1143–1151.

S6. Wicks KL, Hood DA. Mitochondrial adaptations in denervated muscle: relationship to muscle performance. *Am J Physiol - Cell Physiol* 1991;**260**:C841–C850.

S7. Trevino MB, Zhang X, Standley RA, Wang M, Han X, Reis FCG *et al.* Loss of mitochondrial energetics is associated with poor recovery of muscle function but not mass following disuse atrophy. *Am J Physiol - Endocrinol Metab* 2019;**317**:E899–E910.

S8. Zhang X, Trevino MB, Wang M, Gardell SJ, Ayala JE, Han X *et al.* Impaired Mitochondrial Energetics Characterize Poor Early Recovery of Muscle Mass Following Hind Limb Unloading in Old Mice - PubMed. *Journals Gerontol A Biol Sci Med Sci* 2018;**10**:1313–1322.

S9. Hyatt HW, Powers SK. The Role of Calpains in Skeletal Muscle Remodeling with Exercise and Inactivity-induced Atrophy. *Int J Sports Med* 2020;**41**:994–1008.

S10. O'Leary MF, Vainshtein A, Iqbal S, Ostojic O, Hood DA. Adaptive plasticity of autophagic proteins to denervation in aging skeletal muscle. *Am J Physiol Cell Physiol* 2013;**304**:C422--30.

S11. Wang Y, Nartiss Y, Steipe B, McQuibban GA, Kim PK. ROS-induced mitochondrial depolarization initiates PARK2/PARKIN-dependent mitochondrial degradation by autophagy. *Autophagy* 2012;**8**:1462–1476.

S12. Killackey SA, Bi Y, Soares F, Hammi I, Winsor NJ, Abdul-Sater AA *et al.* Mitochondrial protein import stress regulates the LC3 lipidation step of mitophagy through NLRX1 and RRBP1. *Mol Cell* 2022;1–17.

S13. Kondapalli C, Kazlauskaite A, Zhang N, Woodroof HI, Campbell DG, Gourlay R *et al.*

PINK1 is activated by mitochondrial membrane potential depolarization and stimulates Parkin E3 ligase activity by phosphorylating Serine 65. *Open Biol* 2012;**2**:120080.

S14. Settembre C, Fraldi A, Medina DL, Ballabio A. Signals from the lysosome: A control centre for cellular clearance and energy metabolism. *Nat Rev Mol Cell Biol* 2013;**14**:283–296.

S15. Napolitano G, Ballabio A. TFEB at a glance. *J Cell Sci* 2016;**129**:2475–2481.

S16. Sardiello M, Palmieri M, di Ronza A, Medina DL, Valenza M, Gennarino, Vincenzo Alessandro Chiara Di Malta FD *et al.* A Gene Network Regulating Lysosomal Biogenesis and Function. *Science* 2009;**325**:473–478.

S17. Oliván S, Calvo AC, Manzano R, Zaragoza P, Osta R. Sex Differences in Constitutive Autophagy. *Biomed Res Int* 2014;**2014**.

S18. Chen CCCW, Erlich AT, Hood DA. Role of Parkin and endurance training on mitochondrial turnover in skeletal muscle. *Skelet Muscle* 2018;**8**:1–14.

S19. Tower J, Pomatto LCD, Davies KJA. Sex differences in the response to oxidative and proteolytic stress. *Redox Biol* 2020;**31**.

S20. Zhao J, Brault JJ, Schild A, Cao P, Sandri M, Schiaffino S *et al.* FoxO3 Coordinately Activates Protein Degradation by the Autophagic/Lysosomal and Proteasomal Pathways in Atrophying Muscle Cells. *Cell Metab* 2007;**6**:472–483.

S21. Singh K, Hood DA. Effect of denervation-induced muscle disuse on mitochondrial protein import. *Am J Physiol - Cell Physiol* 2011;**300**:C138-145.

S22. Castets P, Lin S, Rion N, Di Fulvio S, Romanino K, Guridi M *et al.* Sustained Activation of mTORC1 in Skeletal Muscle Inhibits Constitutive and Starvation-Induced Autophagy and Causes a Severe, Late-Onset Myopathy. *Cell Metab* 2013;**17**:731–744.

S23. Xu H, Ren D. Lysosomal physiology. *Annu Rev Physiol* 2015;**77**:57–80.

S24. Romanello V, Sandri M. Mitochondrial quality control and muscle mass maintenance. *Front Physiol* 2016;**6**:1–21.

B.1 Oxygen consumption and ROS emissions following 24hrs of denervation

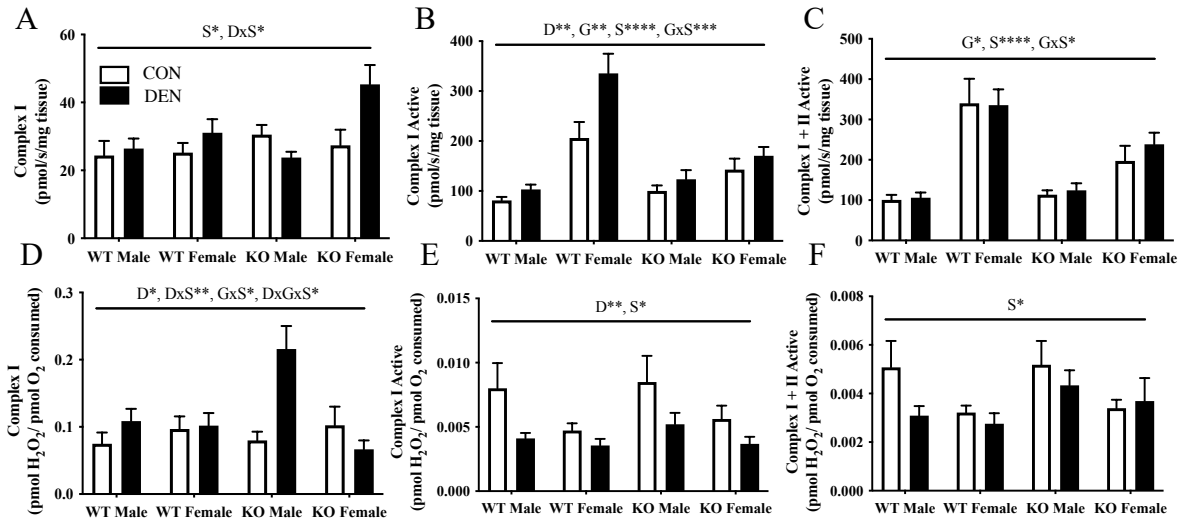

Fig. B.1: Oxygen consumption and ROS emissions following 24hrs of denervation. Oxygen consumption was assessed in permeabilized fibers of WT and TFE3 KO animals following 24hr denervation. In line with the findings presented, increased oxygen consumption during active respiratory states (A-C) was observed in females irrespective of genotype in comparison to male counterparts, however the absence of TFE3 reduced oxygen consumption in females. Furthermore, decreased ROS emission were observed in both WT and KO females in comparison to males (D-F). Acute denervation induced an increase in ROS emissions during complex I supported respiration primarily in males (D), however this was not observed during active respiratory states (E, F). D, indicates a main effect of denervation; G, denotes a main effect of genotype; S, represents a main effect of sex; DxS, interaction effect of denervation and sex; GxS, interaction effect of genotype and sex; DxGxS, interaction effect of denervation, genotype and sex; *, $p<0.05$; **, $p<0.01$; ***, $p<0.001$; ****, $p<0.0001$.

B.2 Gene expression following acute denervation in WT and TFE3 KO males and females.

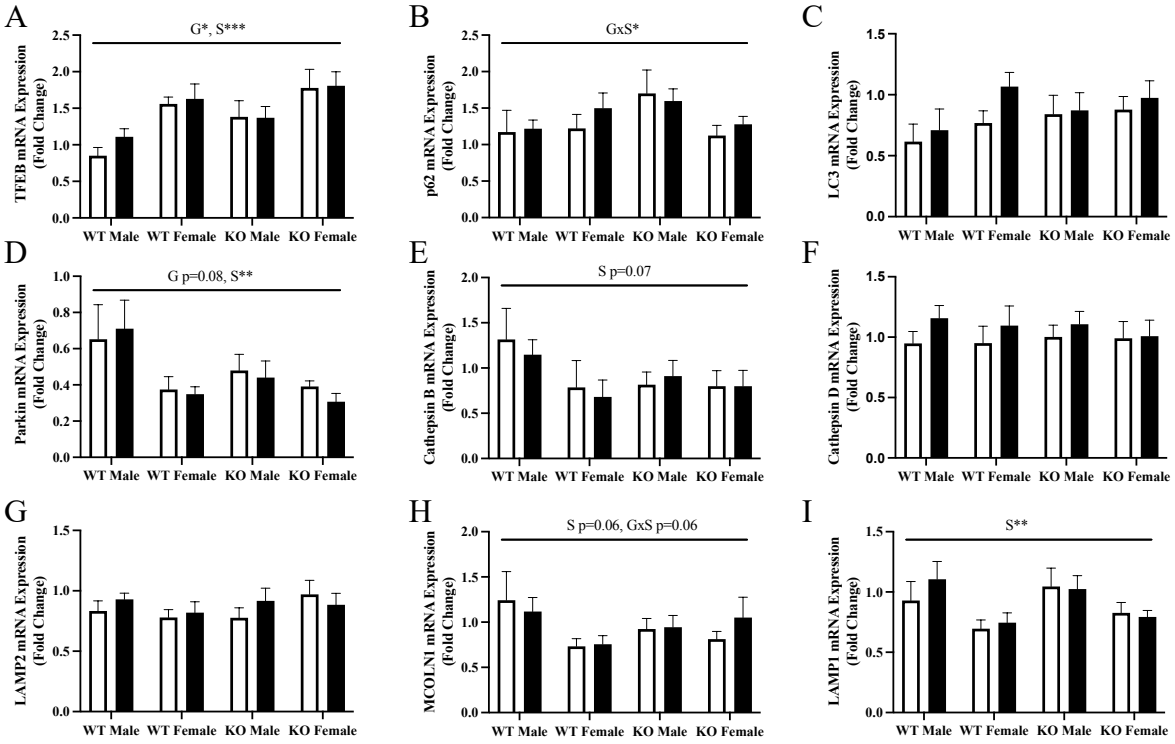

Fig. B.2 Gene expression following acute denervation in WT and TFE3 KO males and females. *Tfeb* (A), *p62* (B), *Lc3* (C), *Parkin* (D), *Cathepsin B* (E), *Cathepsin D* (F), *LAMP2* (G), *MCOLN1* (H), and *Lamp1* (I) mRNA expression following 24 hr of denervation in WT and TFE3 KO animals. In line with the chronic data presented, increased Tfeb mRNA was observed in females irrespective of genotype (A). Trends for decreased expression of *Parkin, Cathepsin B, Mcoln1* and *Lamp1* were observed in females supporting the data presented. Acute denervation had no effect on the expression of these autophagy and lysosomal genes. G, main effect of genotype; S, main effect of sex; GxS, interaction of genotype and sex; *, $p<0.05$; **, $p<0.01$.

APPENDIX C

ADDITIONAL DATA

C.1 Attempted TFEB knockdown via CRISPR-Cas9

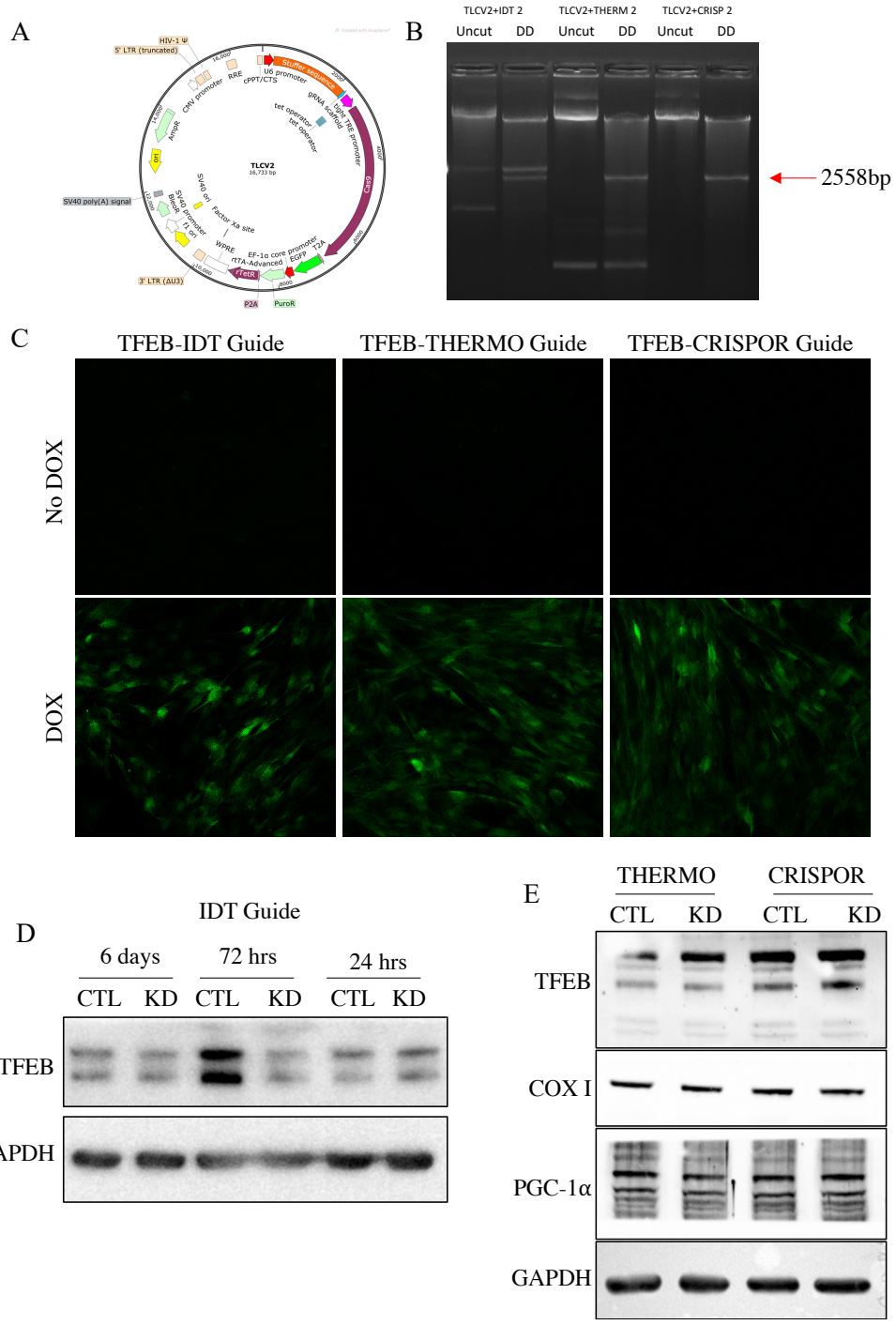

Fig. C.1: Attempted TFEB knockdown via CRISPR-Cas9. TLCV2 plasmid contains a constitutively active U6 promoter, space for guide insertion, followed by a doxycycline-inducible promoter and Cas9 gene with EGFP tag. This plasmid allows the inducible knockdown of any gene with a positive control. Three separate guides were purchased to target TFEB expression (denoted as IDT, THERMO, and CRISPOR). Guides were inserted and then plasmids were cut with Kpn1 and EcoRV to produce a 2558bp fragment. Cas9 expression was induced with doxycycline treatment at 1ug/ml for 72hrs, at which point cells were imaged to detect GFP (note laser power and gain were significantly higher for control wells [laser power 4.0, gain 125 vs laser power 2.0, gain 100]). A timecourse was attempted with the IDT guide and cells were harvested 6 days, 72hr, and 24hr following dox treatment, no knockdown of TFEB was observed. THERMO and CRISPOR guides were attempted and cells were harvested immediately following dox treatment but again no TFEB knockdown was observed. FurtHermore, no changes were observed in COX I or PGC-1 α.

Table C1: Distance run during acute exhaustive test.

Endurance capacities of TFE3 KO animals were assessed in a small pilot study, however in the absence of sufficient WT animals, a heterozygous female was used as a comparison. Average WT running distances were used as a reference from published work from our lab as a comparison. Animals were acclimatized for 3 days prior to exhaustive test. While distance to exhaustion was highly variable among the 3 KO animals (grey), no differences were observed in comparison to HT animal in current pilot or previously published data[287].

Acute Exhaustive Test		193 HT	174 KO	200 KO	207 KO
		Female	Male	Male	Male
5m/min	5 min	-	-	-	-
10m/min	10 min	-	-	-	-
15m/min	15 min	-	-	-	-
20m/min	20 min	-	-	-	-
21m/min	3 min	-	-	-	-
22m/min	3 min	-	-	-	-
23m/min	3 min	-	STOP	-	-
24m/min	3 min	-		-	-
25m/min	3 min	-		-	-
26m/min	3 min	-		STOP	-
27m/min	3 min	-			-
28m/min	3 min	-			-
29m/min	3 min	-			-
30m/min	3 min	STOP			-
31m/min	3 min				-
32m/min	3 min				STOP
Lactate		12.4	3.6	9.1	3.5
Time (min)		77min	56min	65min	83min
Distance (m)		1,515	948	1,173	1,704

Table C2: Distances run during 6 weeks of voluntary wheel running.

A small cohort of TFE3 KO animals were subjected to 6 weeks of voluntary wheel running (VWR), however in the absence of sufficient WT animals, heterozygous females were used as a comparison. Total distances run are presented as weekly totals in km. Animals lacking TFE3 display a resistance to run in comparison heterozygous females and in comparison to previously published data[240].

VWR Training	187 HT Female-VEH	188 HT Female-COL	184 KO Male	192 KO Male-VEH	199 KO Male-COL
Week 1	21.8	20.5	0.32	6.5	16.2
Week 2	27.2	41.6	3.6	19.6	38
Week 3	73.9	73.4	14.6	20.4	45.8
Week 4	91.5	62	22.4	16.4	27.1
Week 5	74.5	55.5	11.2	11.8	9.4
Week 6	42.4	29.7	9	10.2	2.9
Total Distance	331.3	282.7	61.12	84.9	139.4

C2: In-situ force production in WT animals.

A

In-Situ Protocol:
-Find appropriate length/tension
-Test voltage dependence

-3 single twitches
-1 tetanic contraction
-Short rest/recovery (not even 1 min)

-0.25 TPS 3 mins
-0.5 TPS 3 mins
-1 TPS 3 mins

-Harvest tissue immediately

B

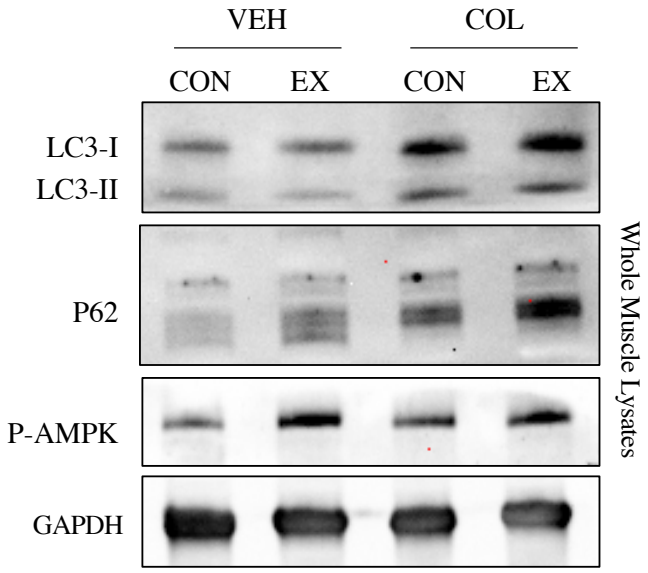

C

In-Situ Protocol:
-Find appropriate length/tension
-Test voltage dependence

-3 single twitches
-1 tetanic contraction
-Short rest/recovery (not even 1 min)

-0.10 TPS 30 mins
-0.25 TPS 3 mins
-0.5 TPS 3 mins
-1 TPS 3 mins
-2 TPS 3 mins
-3 TPS 2-3 mins **until no force produced

-Harvest tissue immediately:

D

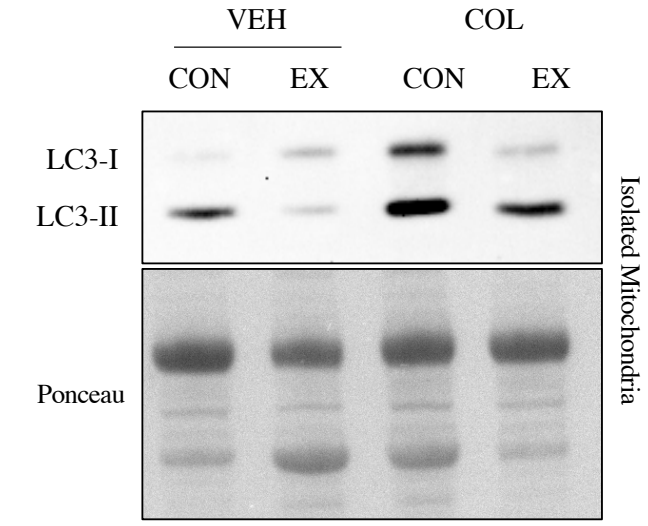

E

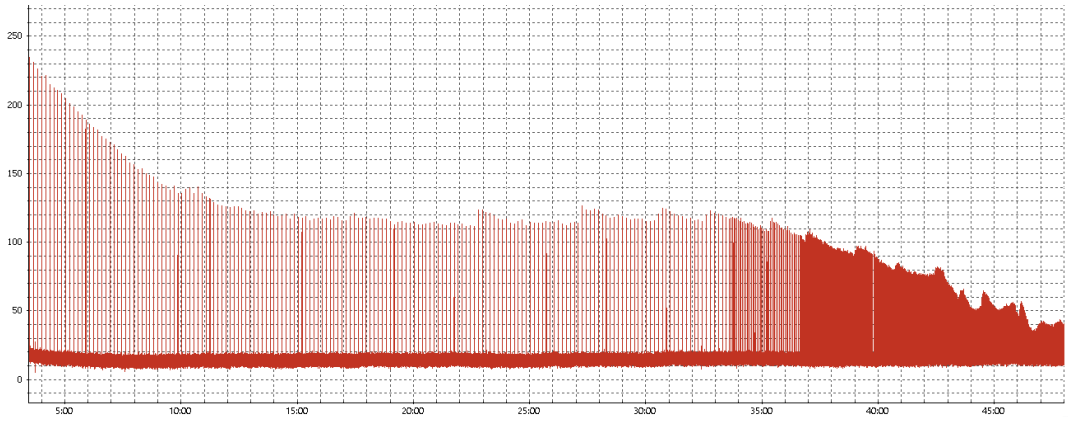

Fig C2: In-situ force muscle stimulation in WT animals. In-situ muscle stimulation was performed in a small cohort of animals to assess whether or not an acute bout of contractile activity *in vivo* stimulates mitophagy flux. Mice were treated with colchicine (0.4mg/kg/day for 3 days) in order to capture flux. Briefly, the gastrocnemius muscle was exposed, the tendon was attached to a force transducer, and the sciatic nerve was isolated and directed stimulated to induce contraction of the gastrocnemius. We first started with a short stimulation protocol as has been used previously[463], that progressively increases the trains per second (TPS) from 0.25 to 1 (A). Based on a preliminary assessment, LC3-II and p62 autophagy flux were not increased following this acute contractile bout, despite observing increases in the phosphorylation of AMPK (B). Thus, we then attempted to modify the protocol to mimic an endurance-style exhaustive exercise, starting at 0.1 TPS for 30 min and then gradually increasing intensity every 3 minutes from 0.25 TPS to 3 TPS or until no force was produced (C). This protocol was success in eliciting mitophagy flux as assessed by LC3-II in mitochondrial fractions (D). A sample force tracing of the extended protocol is provided (E). To our surprise, despite the low intensity there is a significant initial drop-off in force production which is then maintained throughout 30 min period, fatigue becomes evident as the incremental phase of the protocol ensues, and is most rapid from 1 TPS onwards. These pilot data were used to inform a training study which is currently underway.

APPENDIX D

OTHER SCIENTIFIC CONTRIBUTIONS

1.0 PEER REVIEWED ARTICLES:

1. Vainshtein A, Slavin MB, Cheng AJ, Memme JM, **Oliveira AN**, Perry CGR, Abdul-Sater AA, Belcastro AN, Riddell M, Triolo M, Haas TL, Roudier E, Hood DA. Scientific meeting report: International Biochemistry of Exercise 2022. *J Appl Physiol* 2022; Submitted & Accepted.
2. Triolo M, **Oliveira AN**, Kumari R, Hood DA. The influence of age, sex and exercise on autophagy, mitophagy and lysosomal biogenesis in skeletal muscle. *Skeletal Muscle* 2022;12(1):13.
3. Slavin MB, Memme JM, **Oliveira AN**, Moradi N, Hood DA. Regulatory networks controlling mitochondrial quality control in skeletal muscle. *Am J Physiol Cell Physiol* 2022; 322(5):C913-926.
4. Memme JM, **Oliveira AN**, Hood DA. P53 regulates skeletal muscle mitophagy and mitochondrial quality control following denervation-induced muscle disuse. *J Biol Chem* 2022; 298(2):101540.
5. Richards BJ, Slavin M, **Oliveira AN**, Hood DA. Mitochondrial protein import and UPR^{mt} in skeletal muscle remodeling and adaptation. *Semin Cell Develop Biol* 2022; S1084-9521(22).
6. **Oliveira AN**, Richards BJ, Hood DA. Measurement of protein import capacity of skeletal muscle mitochondria. *J Vis Exp* 2021; 179.

7. **Oliveira AN**, Yanagawa B, Verma S, Hood DA. Blunted stress response with age in human right atrial tissue following ischemia-reperfusion. *J Card Surg* 2021; 36(10):3643-3651.
8. **Oliveira AN**, Richards BJ, Slavin M, Hood DA. Exercise is muscle mitochondrial medicine. *Exerc Sport Sci Rev* 2021; 49(2):67-76.
9. Zhang Y, **Oliveira AN**, Hood DA. The intersection of exercise and aging on mitochondrial protein quality control. *Exp Gerontol* 2020; 131: 110824.
10. **Oliveira AN**, & Hood DA. Exercise is mitochondrial medicine for muscle. *Sport Med Health Sci* 2019; 1(1): 11-18
11. Hood DA, Memme JM, **Oliveira AN**, Triolo M. Maintenance of skeletal muscle mitochondria in health, exercise and aging. *Annu Rev Physiol* 2019; 81: 19-41

2.0 NON-PEER REVIEWED ARTICLES:

1. Memme JM, **Oliveira AN**, Hood DA. The importance of p53 in regulating the mitophagy-lysosomal machinery in muscle following disuse. *Autophagy Rep*. 2022; doi: 10.1080/27694127.2022.2047265

3.0 ORAL & Poster Presentations:

1. Wong J, **Oliveira AN**, Hood DA. The role of TFE3 in endurance training-induced skeletal muscle adaptations. *Canadian Society of Exercise Physiology.* Fredericton, NB, Canada. November 2022 (Poster presentation- presented by Wong).

2. **Oliveira AN**, Memme JM, Wong J, Hood DA. Intersection of TFE3 and sex in mediating disuse-induced muscle atrophy. *International Biochemistry of Exercise Conference.* Toronto, ON, Canada. May 2022 (Poster presentation).
3. **Oliveira AN,** Memme JM, Wong J, Hood DA. Role of TFE3 in Mitochondrial Adaptations to Skeletal Muscle Disuse. *Experimental Biology.* Philadelphia, PA, USA. April 2022 (Poster presentation).
4. Richards BJ, **Oliveira AN**, Hood DA. A Reduction in Tafazzin Decreases Mitochondrial Function in C2C12 Myotubes. *Experimental Biology.* April 2022 (Poster presentation-presented by Richards).
5. **Oliveira AN,** Memme JM, Tamura Y, Hood DA. TFEB, an important mitochondrial regulator in skeletal muscle cells. *Canadian Society of Exercise Physiology*. Virtual Meeting 2020 (Poster presentation).
6. **Oliveira AN,** Memme JM, Tamura Y, Hood DA. Absence of TFEB or TFE3 results in divergent mitochondrial phenotypes that are rescued by exercise. *Integrative Physiology of Exercise.* Virtual Meeting 2020. (Poster presentation).
7. **Oliveira AN**, Karmanova L, Murugavel S, Yanagawa B, Hood DA. Enhanced mitochondrial turnover in aged human right atrial tissue. *Experimental Biology*. San Diego, CA, USA. 2020-Meeting canceled; abstracts published.
8. **Oliveira AN**, Murugavel S, Yanagawa B, Hood DA. Mitochondrial maintenance in aged human right atrial tissue following ischemia-reperfusion injury. *MHRC Muscle Health Awareness Day 11*. Virtual meeting 2020 (Poster presentation).

9. **Oliveira AN**, Memme JM, Tamura Y, Hood DA. (2019). TFEB and TFE3 exert distinct roles in mitochondrial adaptations in skeletal muscle cells. *MitoNET Conference*. Toronto, ON, Canada. 2019. (Poster presentation).
10. Memme JM, **Oliveira AN,** Hood DA. (2019) Regulation of skeletal muscle mitochondrial quality by p53 in denervated skeletal muscle. *MitoNET Conference.* Toronto, ON, Canada. 2019 (Poster presentation- presented by Memme).
11. **Oliveira AN,** Memme JM, Hood DA. Differential roles of TFEB and TFE3 in mediating exercise-induced mitochondrial adaptations. NHLBI Mitochondrial Biology Symposium on Mitochondrial Networks and Energetics. Bethesda, MD, USA. 2019 (Poster presentation).
12. Memme JM, **Oliveira AN**, Hood DA. Regulation of skeletal muscle mitochondrial quality control by p53 following 7 days of hindlimb disuse. NHLBI Mitochondrial Biology Symposium on Mitochondrial Networks and Energetics. Bethesda, MD, USA. 2019 (Poster presentation- presented by Memme).
13. **Oliveira AN**, Karmanova L, Murugavel S, Yanagawa B, Hood DA. Effect of age on mitochondrial turnover in human atrial tissue. *Southern Ontario Cardiovascular Research Association.* Toronto, ON, Canada. 2019 (Poster presentation).
14. **Oliveira AN**, Memme JM, Tamura Y, Hood DA. Microphthalmia family of transcription factors and their role in contractile activity-induced adaptation in skeletal muscle cells. *Canadian Physiological Society Symposium*. Toronto, Ontario, Canada. 2019. (Poster presentation)

15. Memme JM, **Oliveira AN**, Hood DA. The role of p53 in regulating mitochondria quality during denervation-induced skeletal muscle disuse. Canadian Physiological Society Symposium: Toronto, ON, Canada. 2019 (Poster presentation).
16. **Oliveira AN**, Memme JM, Tamura Y, Hood DA. Importance of TFEB and TFE3 in mediating lysosomal and mitochondrial adaptations. *Experimental Biology*. Orlando, Fl, USA 2019 (Poster presentation).
17. Memme JM, **Oliveira AN**, Hood DA. Mitochondrial quality control regulation by p53 during disuse-induced atrophy. *Experimental Biology*. Orlando, FL, USA. 2019 (Poster presentation- presented by Memme).
18. Triolo M, **Oliveira AN**, Hood DA. The effects of age and acute endurance exercise on skeletal muscle mitochondria and lysosomal biogenesis. *Muscle Health Awareness Day*. Toronto, ON, Canada. 2018. (Poster presentation- presented by Triolo).
19. **Oliveira AN**, Memme JM, Tamura Y, Hood DA. Role of TFEB and TFE3 in mediating stimulation-induced adaptations in C2C12 myotubes. *Ontario Exercise Physiology*. Barrie, ON, Canada. 2018 (Oral presentation).
20. Memme JM, **Oliveira AN**, Hood DA. Denervation-induced hindlimb atrophy in skeletal muscle-specific p53 KO mice. *Ontario Exercise Physiology*. Barrie, ON, Canada. 2018 (Oral presentation- presented by Memme).
21. Triolo M, **Oliveira AN**, Hood DA. The effect of aging and exercise on muscle mitochondria function and signaling towards mitophagy. *Ontario Exercise Physiology*. Barrie, ON, Canada. 2018 (Oral presentation- presented by Triolo).

4.0 JUNIOR REVIEWER:

Frontiers in Medicine (2022)

Nature Communications (2021)

Physiology International (2020)

Frontiers in Cell and Developmental Biology (2020)

Biomedicine and Pharmacotherapy (2020)

Aging and Disease (2020)

Autophagy (2018)

Frontiers in Cardiovascular Medicine (2018)

General Physiology and Biophysics (2018)